UNIVERSIDADE FEDERAL DO RIO DE JANEIRO
CENTRO DE CIÊNCIAS MATEMÁTICAS E DA NATUREZA - CCMN
INSTITUTO DE QUÍMICA - IQ
DEPARTAMENTO DE BIOQUÍMICA

Avaliação da função metabólica da oncoproteína NSD3s de humano e da Pdp3 de levedura.

Germana Breves Rona
RIO DE JANEIRO 2018

UNIVERSIDADE FEDERAL DO RIO DE JANEIRO
CENTRO DE CIÊNCIAS MATEMÁTICAS E DA NATUREZA – CCMN
INSTITUTO DE QUÍMICA - IQ
DEPARTAMENTO DE BIOQUÍMICA

Avaliação da função metabólica da oncoproteína NSD3s de humano e da Pdp3 de levedura.

Germana Breves Rona

Tese de doutorado apresentada ao Programa de Pós-graduação em Bioquímica, Instituto de Química, da Universidade Federal do Rio de Janeiro, como parte dos requisitos necessários à obtenção do título de Mestre em Ciências – Bioquímica.

Orientadora: Elis Cristina Araújo Eleutherio

Coorientador: Anderson de Sá Pinheiro

RIO DE JANEIRO
SETEMBRO/2018

Avaliação da função metabólica da oncoproteína NSD3s de humano e da Pdp3 de levedura.

Germana Breves Rona

Orientadora: Elis Cristina Araujo Eleutherio

Coorientador: Anderson de Sá Pinheiro

Tese de Doutorado submetida ao Programa de Pós-Graduação em Bioquímica, Instituto de Química, da Universidade Federal do Rio de Janeiro - UFRJ, como parte dos requisitos necessários à obtenção do título de Mestre em Ciências - Bioquímica.

Aprovada por:

_____
Presidente, Dr.ª Elis Cristina Araujo Eleutherio
Instituto de Química - UFRJ

_____
Dra. Luzineide Wanderley Tinoco
Instituto de Pesquisa de Produtos Naturais – UFRJ

_____
Dr. Francisco Meirelles Bastos de Oliveira
Instituto de Biofísica Carlos Chagas Filho- UFRJ

_____
Dra. Luisa Ketzer
Pólo de Xerém – UFRJ

_____
Dra. Luciana Pizzatti Barboza
Instituto de Química - UFRJ

Rio de Janeiro
Setembro 2018

R768a

Rona, Germana

Avaliação da função metabólica da oncoproteína NSD3s de humano e da Pdp3 de levedura. / Germana Rona. -- Rio de Janeiro, 2018. 104 f.

Orientadora: Elis Eleutherio. Coorientador: Anderson Pinheiro. Tese (doutorado) - Universidade Federal do Rio de Janeiro, Instituto de Química, Programa de Pós Graduação em Bioquímica, 2018.

1. NSD3. 2. Pdp3. 3. Câncer. 4. S. cerevisiae. 5. PWWP. I. Eleutherio, Elis, orient. II. Pinheiro, Anderson, coorient. III. Título.

Aos meus pais Vania Breves Rona

e Antonio Moreira Rona

AGRADECIMENTOS

Primeiramente agradeço a Deus, pela saúde, força e oportunidade para desenvolver este trabalho.

Em especial a minha tia, Maria do Socorro Moreira, aos meus primos Julio André Moreira Neto e Ivan Moreira Júnior,e suas esposas, Josilene Moreira e Maria Alice Mussallam Moreira; e ao meu padrinho Mário Zilberberg, por todo apoio, amor e carinho, que me foram dados, por confiarem nas minhas escolhas e incentivarem a seguir o caminho desejado.

Aos meus afilhados e sobrinhos, Leonardo Jansen Moreira, e os meus sobrinhos Maria Luiza Mussallam Moreira, João Pedro Mussallam Moreira e Daniel Cruz, pela alegria, leveza e bagunça que eles proporcionam.

Ao meu marido João Vitor Couto da Cruz pela paciência, apoio, compreensão, força, carinho, incentivo, amor, comidas gostosas, surpresas, e momentos de alegria e descontração.

Aos meus sogros Zizalda Couto da Cruz e Christovão Cruz pelo apoio e carinho.

As minhas "tias novas" Catarina Guzzatti e Luisa Rona por aumentar a minha família, deveríamos escrever um livro.

A minha orientadora Elis Cristina Araujo Eleutherio por me acompanhar por tantos anos e acreditar na minha capacidade, pelo apoio, carinho, "puxões de orelha", ensinamentos, paciência, atenção, e confiança.

Ao meu orientador Anderson de Sa Pinheiro por acreditar e me fazer acreditar que sou capaz, pelos ensinamentos, apoios, risadas, confiança e atenção.

Aos meus orientadores anteriores, que nunca deixaram de me orientar, Daniel Vidal Perez, Sarai de Alcantara, Rodrigo Volcan e Sérgio Cantú por me orientarem nas pesquisas e fora dos laboratórios, pelo apoio e pela confiança.

Aos amigos, colegas e companheiros de bancada do LIFE, LaBMol e LABEP por me acolherem de braços abertos, por toda ajuda recebida ao longo dos experimentos e pelos momentos de alegria. É muito bom trabalhar dentro de um grupo tão unido e receptivo. Faria outro doutorado só para poder passar mais quatro anos abraçando Mariana Castela que diz não gostar de abraços (mentira!), sentar ao lado da querida Aline Brasil na hora do almoço e poder escutar os melhores comentários, poder desabafar com a minha mexicana preferida Rayne Magalhães, discutir sobre séries, entre um PCR e outro, com a Fernanda Boechat, escutar as risadas da Carol Matos e os conselhos da Carol Lixa.

Aos meus alunos Diego Seixas, Natalia Pinto, Daniel Costa e Nathalia Lins que tive o prazer de orientar, tenho vontade de guardar vocês em um chaveiro para poder carregar para todos os lugares que eu vou.

A todos os meus amigos que estiveram ao meu lado me apoiando em todos os momentos.

Ao Colégio Teresiano pela contribuição a minha formação acadêmica e pessoal.

Aos professores Reginaldo Ramos de Menezes e Roberto Salgado Amado pelos ensinamentos sobre o eletrodo de Clark.

Ao professor Cláudio Masuda pelas cepas cedidas.

Ao Gilson Santos e Tatiana Fidalgo pelos ensinamentos de metabolômica.

Ao suporte financeiro da CAPES e da FAPERJ.

Ao Instituto de Química da Universidade Federal do Rio de Janeiro, agradeço pelo incentivo e por todas as oportunidades.

RESUMO

Avaliação da função metabólica da oncoproteína NSD3s de humano e da Pdp3 de levedura.

.

Germana Breves Rona

Elis Cristina Araujo Eleutherio

Anderson de Sá Pinheiro

Resumo da Tese de Doutorado submetida ao Programa de Pós-graduação em Bioquímica, Instituto de Química, da Universidade Federal do Rio de Janeiro – UFRJ, como parte dos requisitos necessários à obtenção do título de Mestre em Ciências – Bioquímica.

O câncer é definido como um conjunto de doenças caracterizadas pelo crescimento celular desordenado. Atualmente, é conhecida a existência de diferentes tipos de câncer, sendo o de mama o mais incidente entre as mulheres. A amplificação da região 11-12 do braço curto do cromossomo 8 consiste em uma das principais modificações genômicas ocorridas no câncer de mama, estando presente em aproximadamente 15% dos casos. Dentre os genes que formam esta região, o gene *WHSC1L1/NSD3*, que codifica uma histona metil-transferase, destaca-se como principal candidato a oncogene líder. NSD3s, a isoforma curta de NSD3, contendo apenas o domínio PWWP (Pro-Trp-Trp-Pro) amino-terminal, apresenta elevada capacidade transformante. O domínio PWWP de NSD3s apresenta semelhança estrutural com o domínio PWWP da proteína Pdp3 de *Saccharomyces cerevisiae*. A superexpressão de NSD3s ou de Pdp3 induz alterações metabólicas similares na levedura, como o aumento da taxa de crescimento, aumento da sensibilidade ao estresse oxidativo e diminuição do consumo de oxigênio. Além disso, o domínio PWWP de NSD3s é capaz de substituir funcionalmente o domínio PWWP de Pdp3. Utilizando a metabolômica por RMN ^{1}H, analisamos a as alterações no metaboloma da levedura em resposta à superexpressão de NS3s ou Pdp3. Foi possível observar um aumento nos níveis de aspartato e alanina, juntamente com uma diminuição nos níveis de arginina, em função da superexpressão de NSD3s ou Pdp3, sugerindo um aumento na taxa de glutaminólise. Além disso, certos metabólitos, como glutamato, valina e fosfocolina, foram específicos para NSD3s ou Pdp3, indicando que vias metabólicas adicionais são adaptadas de maneira dependente da proteína. A observação de que certas vias metabólicas são reguladas diferencialmente por NSD3s e Pdp3 sugere que, apesar da similaridade estrutural entre seus domínios PWWP, as duas proteínas atuam por mecanismos únicos e podem recrutar diferentes complexos de sinalização. Este trabalho estabelece, pela primeira vez, um elo funcional entre a oncoproteína humana NSD3s e a reprogramação metabólica no câncer.

Palavras Chaves: NSD3s, Pdp3, *Saccharomyces cerevisiae*, PWWP, Efeito Warburg, RMN e metabolômica.

ABSTRACT

Evaluation of the metabolic function of human oncoprotein NSD3s and yeast Pdp3.

Germana Breves Rona

Elis Cristina Araujo Eleutherio

Anderson de Sá Pinheiro

Abstract da Tese de Doutorado submetida ao Programa de Pós-graduação em Bioquímica, Instituto de Química, da Universidade Federal do Rio de Janeiro – UFRJ, como parte dos requisitos necessários à obtenção do título de Mestre em Ciências – Bioquímica.

Cancer is defined as a set of diseases characterized by disordered cell growth. Currently, different types of cancer are known, being breast cancer the most frequent among women. Amplification of the 11-12 region of the short arm of chromosome 8 consists in one of the major genomic changes occurred in breast cancer, being present in approximately 15% of the cases. Among the genes forming this region, *WHSC1L1/NSD3* gene, which encodes a histone methyl-transferase, stands out as the main candidate for leading oncogene. NSD3s, the short isoform of NSD3, containing only an amino-terminal PWWP (Pro-Trp-Trp-Pro) domain displays high transformation properties. The PWWP domain of NSD3s shows structural similarity to that of the Saccharomyces cerevisiae protein, Pdp3. Overexpression of NSD3s or Pdp3 induces similar metabolic changes in yeast, such as increased growth rate, increased sensitivity to oxidative stress, and decreased oxygen consumption. In addition, NSD3s PWWP domain functionally substitutes that of Pdp3. Using 1H NMR metabolomics, we analyzed the changes in yeast metabolome in response NS3s or Pdp3 overexpression. We observed an increase in aspartate and alanine levels, together with a decrease in arginine levels, upon overexpression of NSD3s or Pdp3, suggesting an increase in the rate of glutaminolysis. Moreover, certain metabolites, including glutamate, valine and phosphocholine, were specific for NSD3s or Pdp3, indicating that additional metabolic pathways are adapted in a protein-dependent manner. The observation that certain metabolic pathways are differentially regulated by NSD3s and Pdp3 suggests that, despite the structural similarity between their PWWP domains, the two proteins act by single mechanisms and can recruit different downstream signaling complexes. This work establishes, for the first time, a functional link between the human oncoprotein NSD3s cancer metabolic reprogramming.

Keywords: NSD3s, Pdp3, *Saccharomyces cerevisiae*, PWWP, Warburg effect, NMR and metabolomics.

Lista de abreviações

ACLY	ATP-Citrato Liase
Akt	Protein Kinase B
ASS1	Argininosuccinato Sintase 1
ATP	Adenosina Trifosfato
BCAA	Aminoácidos de Cadeia Ramificada
BCAT1	*Branched-Chain Amino Acid Transaminase 1*
BMRB	*Biological Magnetic Data Resonance Bank*
BRD4	*Bromodomain-Containing Protein 4*
BRDs	*Bromodomains*
CDC6	*Cell Division Cicle 6*
CDK2	*Cyclin Dependent Kinase 2*
CHD8	*Chromodomain-helicase-DNA-binding protein 8*
CK	Colina Quinase
CLAE	Cromatografia Líquida de Alta Eficiência
CPMG	*Carr-Purcell-Meiboom-Gill*
CTE	Cadeia de Transporte de Elétrons
DDHD2	DDHD domain containing 2
DNA	Ácido Desoxirribonucleico
DTT	Ditiotreitol
EGFR	*Epidermal Growth Factor Receptor*
ENO1	Enolase 1
ERLIN2	ER Lipid Raft Associated 2
ERO	Espécie Reativa de Oxigênio
ERα	*Estrogen Receptor Alpha*
ESR1	*Estrogen Receptor 1*
ET	*Extra Terminal*
GFP	Proteína Verde Fluorescente
GLS	Glutaminase
GLUD	Glutamato Desidrogenase

GLUT	Transportador de Glicose
GOT	Glutamato Oxaloacetato Transaminase
GPT	Glutamato Piruvato Transaminase
HAT	Histona Acetil-Transferase
HDAC	Histonas Deacetilase
HIF-1α	*Hypoxia-Inducible Factor 1*-alpha
HKII	Hexoquinase II
HMDB	*Human Metabolomic Database*
HMTases	Histona metil-transferase
Hxk2	Hexoquinase 2
IARC	*International Agency for Research on Cancer*
INCA	Instituto Nacional de Câncer José Alencar Gomes da Silva
IPTG	isopropil-b-D-galactosídeo
LDHA	Lactato Desidrogenase A
LMA	Leucemia Mielóide Aguda
MBT	*Malignant Brain Tumor*
Mig1	*Multicopy Inhibitor of GAL gene expression*
MMSET	*Multiple Myeloma SET Domain*
mTOR	Mammalian Target of Rapamycin
MYC	MYC proto-oncegene
NEAA	Aminoácido Não Essencial
NF-kB	*Nuclear Factor Kappa B*
NK	*Natural Killer*
NSD	*Nuclear Receptor SET Domain*
NSD1	*Nuclear Receptor Binding SET Domain Protein 1*
NSD2	*Nuclear Receptor Binding SET Domain Protein 2*
NSD3	Nuclear Receptor Binding SET Domain Protein 3
NSD3l	Isoforma Longa da NSD3
NSD3s	Isoforma Curta NSD3
NUP98	*Nuclear Pore Complex Protein Nup98*
NUT	*Nuclear Protein of the Testis*

ORFs	*Open Reading Frames*
OXPHOS	Fosforilação Oxidativa
PCA	Análise de Componentes Principais
PDK1	Piruvato Desidrogenase Quinase 1
PET	Tomografia por Emissão de Pósitrons
PFKM	Fosfofrutoquinase
pH	potencial Hidrogeniônico
PHD	*Plant Homeodomain Zinc Fingers*
PI3K	Phosphoinositide 3-Kinase
PKM2	Piruvato Quinase M1/2
PSAT	Fosfoserina Transaminase
PTM	Modificação Pós-Traducional
PWWP	Prolina-Triptofano-Triptofano-Prolina
RAS	RAt Sarcoma Vírus
RMN	Ressonância Magnética Nuclear
RMSD	Root Mean Square Deviation
SCCHN	*Squamous Cell Carcinoma of the Head/Neck*
SET	Su(var)3-9,Enhancer-of-zeste andTrithorax
Snf1	*Sucrose NonFermenting*
TCA	Ácido Tricarboxílico
TEV	*Tobacco Etch Virus nuclear-inclusion-a endopeptidase*
VDAC	*Voltage-Dependent Anion Channels*
WHSC1	*Wolf–Hirschhorn Syndrome Candidate 1*
WHSC1L1	Wolf-Hirschhorn Syndrome Candidate 1-Like 1

Sumário

Lista de Figuras

Lista de tabelas

1 INTRODUÇÃO

1.1 CÂNCER

Atualmente, o câncer é considerado um caso de saúde pública, principalmente em países em desenvolvimento, onde espera-se cerca de 80% de novos casos em 2025 (INCA, 2015). Segundo a estatística mundial realizada no projeto GLOBOCAN 2012 pela IARC (*International Agency for Research on Cancer)*, ocorreram 14,1 milhões de casos novos de câncer e 8,2 milhões de mortes por câncer no mundo, em 2012 (INCA, 2015; LINDSEY A. TORRE; FREDDIE BRAY; REBECCA L. SIEGEL; JACQUES FERLAY; JOANNIE LORTET-TIEULENT; AHMEDIN JEMAL, 2015). As maiores taxas de câncer são observadas em países desenvolvidos e os principais tipos de câncer dessas regiões são relacionados a urbanização e desenvolvimento (INCA, 2018). Os tipos de câncer mais incidentes no mundo são, respectivamente: pulmão, mama, intestino e próstata (INCA, 2015; LINDSEY A. TORRE; FREDDIE BRAY; REBECCA L. SIEGEL; JACQUES FERLAY; JOANNIE LORTET-TIEULENT; AHMEDIN JEMAL, 2015). Para o biênio 2018-2019, o INCA (Instituto Nacional de Câncer José Alencar Gomes da Silva) estima a ocorrência de cerca de mais de 600 mil novos casos de câncer no Brasil, sendo os mais incidentes próstata (31,7%) para homens e mama (29,5%) para mulheres, exceto os casos de câncer de pele não melanoma (INCA, 2018).

O câncer é um grupo de doenças caracterizado por um padrão aberrante da expressão gênica (ALBERT; HELIN, 2010). Sua evolução ocorre devido a alterações genéticas e epigenéticas, necessárias para a homeostase celular, levando a ativação de oncogenes e a inativação de genes supressores de tumor (ALBERT; HELIN, 2010; LUCIO-ETEROVIC; CARPENTER, 2011). As alterações genômicas podem ocorrer devido a pequenas variações, como a mudança de um único nucleotídeo, ou grandes variações, como rearranjos cromossomais (YI; JU, 2018). As variações estruturais podem ser divididas em quatro tipos: deleções, duplicações (amplificações), translocações e inversões (YI; JU, 2018). As alterações epigenéticas incluem variações nos padrões de metilação do DNA (Ácido Desoxirribonucleico), modificação pós-translacional de histonas e remodelação da cromatina (SOGABE et al., 2018). Um crescente corpo de evidências aponta para o fato de que as alterações epigenéticas parecem desempenhar um papel fundamental na iniciação e progressão do câncer,

bem como no desenvolvimento de quimiorresistência (HAJJI et al., 2018). Apenas as mudanças epigenéticas podem ser reversíveis, logo uma população celular com fenótipo maligno, resultante de uma alteração epigenética, pode ser convertido em uma com fenótipo benigno. Com isso, a terapia epigenética surge como uma ferramenta efetiva e valiosa contra o câncer (MORISHITA; DI LUCCIO, 2011a). Isto resultou em uma série de ensaios clínicos envolvendo medicamentos com alvos epigenéticos, epi-droga, como tratamento único ou combinado com drogas convencionais anticâncer, com objetivo de aumentar a eficácia do tratamento (HAJJI et al., 2018; SHIN; BAYARSAIHAN, 2017). Entre os candidatos a fármacos, os inibidores de BRDs *(Bromodomains)*, domínio de reconhecimento de lisinas acetiladas, demonstraram efeitos positivos em neoplasias sólidas e hematológicas, incluindo tumores cerebrais (SHIN; BAYARSAIHAN, 2017). Um exemplo de epi-droga é o UVI5008, este apresenta atividades anticancerígenas inibindo três enzimas: HDACs (Histonas Deacetilase) (em particular HDAC1-4), sirtuínas e DNA metil-transferases. O UVI5008 possui um efeito apoptótico em vários cânceres, como leucemia, osteossarcoma, melanoma e carcinoma de mama, próstata e cólon (BENEDETTI et al., 2015).

Além da genética e epigenética, o microambiente é um regulador muito importante da progressão tumoral (SHEN; KANG, 2018). O microambiente tumoral pode ser subdividido em microambiente químico (baixo oxigênio, baixo pH e baixa nutrição) e microambiente celular (células tumorais, células estromais, matriz extracelular, e células imunes inflamatórias) (SHAO et al., 2018). A composição e a função do microambiente tumoral pode ser diferente nos diversos tipos de câncer e seus estágios (SHEN; KANG, 2018). Muitas terapias contra o câncer, como radioterapia, quimioterapia e hormonioterapia, afetam não apenas a célula tumoral, mas também o seu microambiente, podendo modulá-lo positiva ou negativamente (SHEN; KANG, 2018).

Apesar do câncer ser um grupo complexo e heterogêneo de doenças que pode afetar uma grande variedade de grupos celulares, existem algumas alterações essenciais que são comuns a todos os tipos de células tumorais, como: manutenção de sinais proliferativos, insensibilidade a sinalizações inibidoras de crescimento, evasão da morte celular programada (apoptose), potencial explicativo ilimitado,

manutenção de vascularização (angiogênese), invasão de tecidos/metástase (HANAHAN; WEINBERG, 2000) e reprogramação metabólica/energética celular (HANAHAN; WEINBERG, 2011). Com a finalidade de dar suporte a intensa proliferação celular, a célula tumoral necessita aumentar o seu consumo de glicose, aminoácidos e lipídeos. Os transportadores de aminoácidos, glicose, monocarboxilatos, ácidos graxos e lipoproteínas são regulados em todos os tipos de câncer, e o aumento da expressão desses transportadores está relacionado com a agressividade e estágio tumoral (FINICLE; JAYASHANKAR; EDINGER, 2018). Com o objetivo de produzir ATP (Adenosina Trifosfato) e/ou realizar anabolismo, a célula tumoral supre a sua alta demanda por nutrientes adquirindo nutrientes da corrente sanguínea e consumindo macromoléculas produzidas por outras células do seu microambiente (FINICLE; JAYASHANKAR; EDINGER, 2018).

1.2 METABOLISMO DA CÉLULA TUMORAL

Otto Heinrich Warburg foi um fisiologista e bioquímico alemão. Em 1931, Warburg foi agraciado com o Prêmio Nobel de Fisiologia pela sua “descoberta sobre a natureza e modo de ação da enzima respiratória” (ZHOU; LIOTTA; PETRICOIN, 2017). Essa observação abriu novas frentes para estudar e entender o metabolismo celular. Em 1956, Otto Warburg publicou o artigo “*On the Origin of Cancer Cells*”, o qual relata danos irreversíveis à respiração mitocondrial de células tumorais (WARBURG, 1956a). A maior parte do metabolismo de células tumorais muda da fosforilação oxidativa para a glicólise aeróbica, mesmo sob condições normais de oxigênio, esse fenômeno foi chamado de efeito Warburg (CHEN et al., 2018; ZHOU; LIOTTA; PETRICOIN, 2017). O efeito Warburg foi observado pela primeira vez em células tumorais, as quais apresentaram maior consumo de glicose, menor consumo de oxigênio e aumento da produção de L-lactato (WARBURG, 1956b). Há uma forte associação entre câncer e o efeito Warburg (BURNS; MANDA, 2017), onde a intensa glicólise assegura as altas taxas de proliferação das células tumorais (YU et al., 2017). O aumento da glicólise aeróbica pode ser observada em pacientes com tumores malignos usando o PET *scan* (Tomografia por Emissão de Pósitrons) (CHEN et al., 2016). O efeito Warburg já foi descrito em diversos tipos de câncer, como colorretal, mama, pulmão e glioblastoma (POTTER; NEWPORT; MORTEN, 2016).

As bases moleculares do efeito Warburg foram recentemente reconsideradas. De fato, muitas mitocôndrias de células tumorais não são deficientes, mas passam por uma reprogramação metabólica, alterando a regulação da glicólise e dos processos mitocondriais (BURNS; MANDA, 2017; GUARAGNELLA et al., 2013). Atualmente, relaciona-se a taxa glicolítica de um tumor a sua agressividade. Quanto mais invasivo é o tumor, maior a taxa de glicólise aeróbica (OCAÑA et al., 2018).

Existem algumas hipóteses que tentam explicar as bases moleculares do efeito Warburg, porém ainda não existe nenhuma teoria concreta. (ZHOU; LIOTTA; PETRICOIN, 2017). Algumas hipóteses relacionadas a esse efeito, são: aumento da expressão de GLUTs (Transportador de Glicose) (BURNS; MANDA, 2017; DIAZ-RUIZ; RIGOULET; DEVIN, 2011a) e *HKII* (Hexoquinase II) (DIAZ-RUIZ; RIGOULET; DEVIN, 2011a), altos níveis de piruvato desidrogenase quinase (BURNS; MANDA, 2017), alta expressão de *PKM2* (Piruvato Quinase M1/2) e *NF-kB (*Nuclear Factor Kappa B**)** (BURNS; MANDA, 2017).

A elevada expressão de diferentes GLUTs, por exemplo, já foi descrita em diferentes tipos de câncer. Foi observado que os GLUTs são epigeneticamente regulados para acelerar o transporte de glicose através da membrana celular. Foi relatado que a inibição de HDAC é responsável pela expressão aumentada de GLUTs (GLUT1, GLUT3 e GLUT4) em câncer (TEKADE; SUN, 2017). A expressão de HKII é controlada por vários fatores de transcrição e alterações epigenéticas (TEKADE; SUN, 2017). O aumento de sua expressão está relacionado com a metástase de vários tipos de câncer. Muitos agentes anticâncer (2-DG, lonidamina, 3-BP, metformina, MJ, oroxilina A, casiopeina II-gly, NA, prosapogenina A, clotrimazol, bifonazol e anti-HKII shRNA) realizam inibição dirigida da HKII ou do complexo HKII-VDAC (*Voltage-Dependent Anion Channels*) (ZHONG; ZHOU, 2017). Células saudáveis exibem baixa afinidade para HKIV, que é alterada para a isoforma HKII durante a oncogênese (TEKADE; SUN, 2017).

Já foi relatado o envolvimento de algumas oncoproteínas e supressores de tumor, incluindo a via de sinalização PI3K (phosphoinositide 3-Kinase)/Akt (Protein Kinase B)/mTOR (Mammalian Target of Rapamycin), *MYC* (MYC proto-oncegene), *HIF-1α (*Hypoxia-inducible factor 1-alpha*)* e p53, na adaptação metabólica favorecendo o crescimento tumoral, proliferação celular, angiogênese e resistência ao

estresse (CHEN et al., 2016). A via de sinalização PI3K/Akt está envolvida em muitos processos, como inflamação, autofagia e progressão do câncer (CHEN et al., 2016). A ativação do oncogene *AKT* em células tumorais aumenta o transporte de glicose, estimulando a glicólise aeróbica. Além disso, AKT pode ativar a HKII a fim de melhorar a taxa glicolítica (CHEN et al., 2016). O oncogene *MYC* é um fator de transcrição que controla o processo de crescimento e o metabolismo celular. A sua ativação regula muitos genes que codificam enzimas do metabolismo da glicose, como GLUT1, HK-II, PFKM (Fosfofrutoquinase), ENO1 (Enolase 1), LDHA (Lactato Desidrogenase A) e PDK1 (Piruvato Desidrogenase Quinase 1), estimulando assim o efeito Warburg (CHEN et al., 2016). O gene *HIF-1* se torna ativo em ambientes com baixa concentração de oxigênio (hipóxia), mas já foi observado que também pode ser ativado por um oncogene ou por estresse oxidativo (GENTRIC; MIEULET; MECHTA-GRIGORIOU, 2017). *HIF-1* aumenta a expressão dos transportadores de glicose e de enzimas glicolíticas, e inibe o ciclo do TCA (Ácido Tricarboxílico) (GENTRIC; MIEULET; MECHTA-GRIGORIOU, 2017). O supressor tumoral p53 pode regular negativamente o crescimento celular induzindo transcricionalmente inibidores de mTOR. p53 pode reduzir a glicólise aumentando a atividade da frutose-2,6-bisfosfatase e inibindo os transportadores de glicose. Frequentemente, esse supressor tumoral encontra-se mutado em tumores humanos, levando a redução ou perda da sua função, o que pode estar associado ao efeito Warburg (CHEN et al., 2016).

Apesar do baixo rendimento de ATP por molécula de glicose, células tumorais são capazes de obter o mesmo rendimento energético por glicólise aeróbica e por fosforilação oxidativa (OCAÑA et al., 2018). Devido à alta taxa de proliferação celular, células tumorais possuem uma elevada demanda de precursores, como nucleotídeos, lipídeos e aminoácidos, para a geração de células filhas (OCAÑA et al., 2018). A glicose pode ser desviada e utilizada como fonte de carbono para a síntese de acetil-CoA (lipídeos), produção de aminoácidos não essenciais e ribose (nucleotídeos), requeridos pela alta taxa proliferativa (GENTRIC; MIEULET; MECHTA-GRIGORIOU, 2017; OCAÑA et al., 2018). Contudo, não se pode afirmar que todos os tumores são exclusivamente glicogênicos. Já foram identificados alguns linfomas e melanomas que possuem alta atividade de OXPHOS (Fosforilação Oxidativa) e muitos tumores

apresentam os dois metabolismos, tanto o glicolítico quanto o oxidativo (GENTRIC; MIEULET; MECHTA-GRIGORIOU, 2017; OCAÑA et al., 2018). Células cancerosas podem exibir um fenótipo glicolítico sob condições regulares, mas podem mudar para um fenótipo não-glicolítico sob acidose láctica. Quando a oferta de glicose é suficiente, as células tumorais podem ser inicialmente glicolíticas e, conforme o piruvato é transformado em lactato, ocorre um acúmulo deste, levando a acidose láctica. A acidose láctica, por usa vez, é uma consequência inevitável do efeito Warburg e é comum na maioria dos tumores sólidos. A acidose láctica acidifica o citosol, baixando o seu pH, diminuindo o fluxo glicolítico e suprimindo as atividades das enzimas glicolíticas, eventualmente comprometendo a glicólise. A acidose láctica pode promover a transição do efeito Warburg para um fenótipo não-glicolítico (CHEN et al., 2016).

Um novo tipo de metabolismo em câncer chamado de “Efeito Warburg reverso” ou “acoplamento metabólico” tem sido identificado. Este efeito pode explicar os fenômenos contraditórios observados em certos tipos de tumor que apresentam alta taxa de respiração mitocondrial e baixo nível de glicólise. Este conceito implica em uma simbiose entre células tumorais e fibroblastos glicolíticos (CHEN et al., 2016). Células cancerosas secretam espécies reativas de oxigênio induzindo estresse oxidativo em fibroblastos associados ao câncer, levando-os à glicólise aeróbica. O lactato produzido serve como combustível para OXPHOs mitocondriais de células tumorais, produzindo altos níveis de ATP e protegendo estas células contra a apoptose (CHEN et al., 2016; FU et al., 2017; PAVLIDES et al., 2009; XU et al., 2015). O efeito Warburg e o efeito Warburg reverso podem ser considerados processos cooperativos (FU et al., 2017).

As células que sofrem o efeito Warburg remodulam seu metabolismo para glicólise e glutaminólise produzindo níveis aumentados de substratos, como lactato, proveniente da glicólise, além de succinato, alanina e aspartato, provenientes da degradação de glutamina e outros aminoácidos (TIDWELL; SØREIDE; HAGLAND, 2017).Células tumorais são capazes de utilizar outros substratos além da glicose. A glutamina, aminoácido mais abundante na corrente sanguínea, também possui um papel importante no crescimento tumoral, visto que é uma grande fonte de nitrogênio (OCAÑA et al., 2018). Transportadores de glutamina são superexpressos em vários

tipos de câncer. Já foi descrito em células tumorais que o proto-oncogene c-MYC se liga transcricionalmente às regiões promotoras de transportadores de glutamina de alta afinidade, levando a maior captação de glutamina (YANG; VENNETI; NAGRATH, 2017a). A glutaminólise é o processo pelo qual as células convertem glutamina em metabólitos do ciclo do TCA através da atividade de múltiplas enzimas. A glutamina é convertida a glutamato por uma GLS (Glutaminase). O glutamato é então convertido em α-cetoglutarato através de duas vias. A primeira ocorre através da atividade da GLUD (Glutamato Desidrogenase). A segunda se dá através da atividade de um grupo de transaminases, incluindo GOT (Glutamato Oxaloacetato Transaminase), GPT (Glutamato Piruvato Transaminase) e PSAT (Fosfoserina Transaminase) (YANG; VENNETI; NAGRATH, 2017a). As transaminases promovem a geração de NEAAs (Aminoácidos Não Essenciais), incluindo aspartato, alanina e fosfoserina. O α-cetoglutarato gerado pode servir como substrato anaplerótico para o ciclo do TCA, gerando ATP através de OXPHOS. O citrato é gerado quando o α-cetoglutarato derivado da glutamina se condensa com acetil-CoA. O citrato conecta o metabolismo mitocondrial à lipogênese através da ACLY (ATP-Citrato Liase) e ácido graxo sintetase, levando à síntese de lipídeos (CHENG et al., 2018; YANG; VENNETI; NAGRATH, 2017a).

A via serina/glicina modula a capacidade antioxidante e está envolvida na homeostase redox da célula, além de ser necessária para a síntese de proteínas, purinas e para a metilação de DNA e histonas (GENTRIC; MIEULET; MECHTA-GRIGORIOU, 2017). Quando não é possível repor os intermediários do ciclo do TCA via glutamina, a biossíntese de serina se torna o maior contribuidor para o suprimento do ciclo do TCA, levando a uma maior proliferação da célula tumoral (GENTRIC; MIEULET; MECHTA-GRIGORIOU, 2017).

Muitas evidências mostram que há uma reprogramação do metabolismo de lipídeos em células tumorais (CHENG et al., 2018). Tumores apresentam maior lipogênese devido ao aumento da biogênese de membrana plasmática (CHENG et al., 2018). A glicose é o maior precursor da síntese de lipídeos. Esta é convertida a piruvato que entra na mitocôndria, produzindo citrato. Já no citoplasma, o citrato pode ser convertido em ácido graxo e colesterol (CHENG et al., 2018).

Os substratos metabólicos e os metabólitos resultantes da alteração do metabolismo sofrida por uma célula tumoral sinalizam processos de transcrição baseado na disponibilidade nutricional e na necessidade de crescimento, esse processo ocorre devido a um controle epigenético. Assim, a transição metabólica que ocorre em células cancerígenas podem regular a expressão gênica epigeneticamente (TIDWELL; SØREIDE; HAGLAND, 2017).

1.3 REGULAÇÃO GÊNICA E EPIGENÉTICA

O DNA eucariótico está empacotado dentro do núcleo através da sua associação com proteínas histonas, formando a fibra de cromatina. O nucleossomo, a unidade fundamental da cromatina, é constituído por 146 pb de DNA envolto em torno de um octâmero de histonas composto por duas cópias de H2A, H2B, H3 e H4 (Figura 1) (ALBERT; HELIN, 2010; VÖLKEL; ANGRAND, 2007). O nucleossomo desempenha papel importante na regulação de muitos processos dependentes do DNA genômico, como transcrição, reparo e apoptose (VERMEULEN et al., 2010).

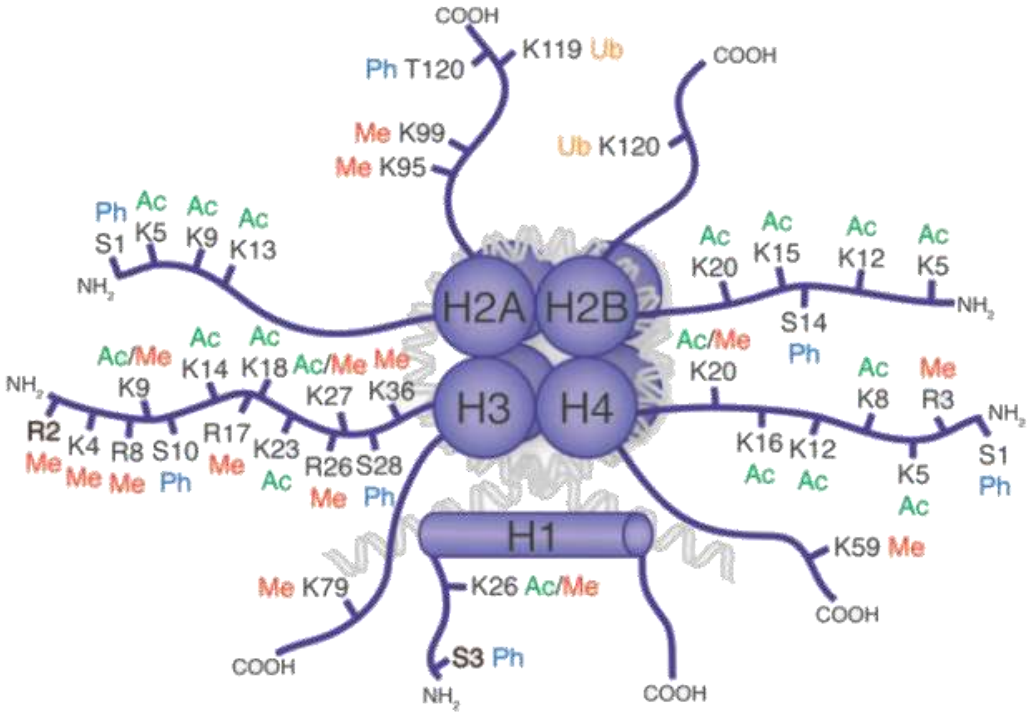

Figura 1. Representação esquemática do nucleossomo eucariótico. O nucleossomo, a unidade fundamental da cromatina, é formado por um octâmero de histonas, formado por quatro dímeros de H2A, H2B, H3 e H4 (azul) envolvido por 146 pb de DNA eucariótico (dupla hélice cinza).As caudas amino-terminais da histonas podem sofrer modificações pós-traducionais, como metilação (Me- vermelho), acetilação (Ac- verde) e fosforilação (Ph- azul).

Cada célula de um indivíduo possui a mesma sequência genômica, ainda que presente em tecidos diferentes, podendo apresentar fenótipos amplamente diferentes. Essa variação surge porque cada célula expressa um subconjunto específico de genes, alguns genes são ativados enquanto outros são reprimidos, resultando em um padrão de expressão gênica que caracteriza a identidade de uma célula (HAWKINS; AL-ATTAR; STOREY, 2018). O padrão de expressão gênica é direcionado por fatores de transcrição que se ligam a um promotor específico. A cromatina sofre mudanças estruturais que facilita os processos biológicos de replicação, reparo do DNA, recombinação, progressão do ciclo celular e transcrição, apresentando um papel importante neste último processo (ALBERT; HELIN, 2010; HUEN et al., 2010; SLATER; ALLEN; BYCROFT, 2003). Logo, a acessibilidade do DNA às proteínas que participam desses processos é largamente afetada pelo grau de condensação da cromatina (Figura 1) (VÖLKEL; ANGRAND, 2007).

Em 1942, Conrad Waddington criou o termo epigenética para descrever as mudanças herdadas em fenótipo sem alterações no genótipo (NEBBIOSO et al., 2018). A capacidade de armazenar informações através de alterações no nucleossomo e na estrutura da cromatina sem alterar a sequência de DNA é definida como epigenética (ALBERT; HELIN, 2010). A informação gênica é passada de geração para geração através da replicação do DNA e, da mesma forma, os mecanismos epigenéticos podem ser transmitidos as células filhas e através de gerações (HAWKINS; AL-ATTAR; STOREY, 2018). As modificações em caudas de histonas e a metilação de DNA são os eventos epigenéticos mais conhecidos (ALBERT; HELIN, 2010).

A condensação da cromatina é controlada, entre outros fatores, pelas PTMs (Modificação Pós-Traducional) em histonas. As caudas das histonas desempenham papel importante no processo de enovelamento da cromatina (VÖLKEL; ANGRAND, 2007). O enovelamento e a condensação dos nucleossomos resultam em uma mudança no estado funcional da cromatina, impedindo as atividades que requerem acesso ao material genético. As células possuem vários mecanismos de modificação da estrutura da cromatina, incluindo a modificação de histonas e o recrutamento de fatores responsáveis pelo remodelamento da cromatina (HUEN et al., 2010). A estrutura da cromatina pode ser modificada de diversas maneiras. Vários complexos

multi-proteicos modulam as interações DNA-histona de maneira ATP-dependente. Outras proteínas modificam aminoácidos da região amino-terminal das histonas por meio de acetilação, metilação, fosforilação (SLATER; ALLEN; BYCROFT, 2003; WANG; QIU; WU, 2018), ubiquitinação, sumoilação, ribosilação de difosfato de adenosina (ADP), isomerização de prolina, biotinilação, citrulinação e suas várias combinações (WANG; QIU; WU, 2018) (Figura 1). Essas modificações podem alterar a interação de histonas com o DNA nucleossomal, além de fornecerem sítios de ligação para proteínas regulatórias (SLATER; ALLEN; BYCROFT, 2003). Esses mecanismos trabalham juntos para permitir a regulação espaço- temporal do acesso ao material genético, facilitando e controlando todos os processos dependentes do DNA genômico, incluindo a expressão gênica (HUEN et al., 2010).

As modificações covalentes que ocorrem com alta especificidade nas caudas das histonas podem implicar em resultados distintos em termos de funções dependentes da cromatina, como a expressão gênica. Esta ideia foi formalmente proposta como o “Código de Histonas”. De acordo com esta hipótese, as histonas atuam como plataformas de sinalização, integrando vias que induzem respostas nucleares adequadas, tais como a ativação ou a repressão da transcrição (VÖLKEL; ANGRAND, 2007). Existem inúmeras modificações que podem ocorrer nas caudas das histonas e, a cada ano, novas modificações são descobertas. Atualmente, as modificações melhor caracterizadas são acetilação e metilação de lisinas em histonas. Os resíduos de lisina são acetilados por HATs (Histona Acetil-Transferase) e desacetilados por HDACs. A acetilação de histonas pode criar sítios de ligação para fatores envolvidos na regulação transcricional ou neutralizar a carga positiva da histona, diminuindo a interação histona-DNA. A metilação de lisinas em histonas é reconhecida por proteínas efetoras que agem positiva ou negativamente sobre a transcrição (HAWKINS; AL-ATTAR; STOREY, 2018).

As anomalias presentes nos padrões de expressão gênica, relacionadas com diversos tipos de câncer e doenças ligadas ao desenvolvimento e diferenciação, não estão envolvidas apenas com mutações no DNA, mas também as mudanças epigenéticas (ALBERT; HELIN, 2010; MORISHITA; DI LUCCIO, 2011b). Alterações epigenéticas não afetam apenas a compactação do DNA, mas também possuem um papel regulatório importante em quase todos os aspectos referentes ao metabolismo

do DNA, incluindo transcrição, replicação, recombinação e reparo (WANG et al., 2009). Alterações genéticas e epigenéticas são responsáveis pela iniciação e propagação do câncer, porém, apenas as aberrações epigenéticas são reversíveis (ALBERT; HELIN, 2010; MORISHITA; DI LUCCIO, 2011a). As aberrações epigenéticas relacionadas ao câncer podem ocorrer devido a mutações genéticas de modificadores e remodeladores da cromatina. Modificadores da cromatina geralmente utilizam metabólitos como cofatores e, portanto, são sensíveis a pequenas alterações no seu equilíbrio. O estado nutricional e metabólico, a interação com o microambiente tumoral e o envelhecimento representam exemplos de processos biológicos que decorrem de alterações epigenéticas tumorais (NEBBIOSO et al., 2018).

A terapia epigenética vem crescendo como uma abordagem efetiva e valiosa na terapia e prevenção do câncer (ALBERT; HELIN, 2010; MORISHITA; DI LUCCIO, 2011a). A metilação de DNA e modificações nas caudas das histonas são os fenômenos epigenéticos mais estudados e muitas drogas estão sendo desenvolvidas para atuar nestes processos (ALBERT; HELIN, 2010; MORISHITA; DI LUCCIO, 2011a). Inibidores de desacetilases e metil transferases estão sendo desenvolvidos para quimioterapia e quimioprevenção do câncer (ALBERT; HELIN, 2010; MORISHITA; DI LUCCIO, 2011b). O uso desses inibidores já foi aprovado em alguns tratamentos de cânceres hematológicos e estão em processo de testes clínicos para outros tipos de câncer (ALBERT; HELIN, 2010).

Os inibidores de HDAC demonstraram ser agentes terapêuticos anticâncer eficazes através de múltiplos mecanismos, como: indução de parada do ciclo celular, mecanismos apoptóticos intrínsecos e extrínsecos, morte celular autofágica, espécies reativas de oxigênio, inibição da angiogênese e melhora da imunidade tumoral mediada por células NK (*Natural Killer)* (HAJJI et al., 2018). Estudos recentes mostram que moduladores da metilação de DNA são capazes de sensibilizar células tumorais multirresistentes ao tratamento convencional. No entanto, o uso de agentes de regulação da metilação do DNA pode ativar genes indesejáveis, incluindo novos genes de resistência a drogas e outros que induzem a progressão tumoral (HAJJI et al., 2018). Esses moduladores podem ser considerados como biomarcadores de resistência a drogas e como potencial alvo terapêutico para o combate a resistência aos tratamentos convencionais. No entanto, uma compreensão mais profunda dos

mecanismos epigenéticos na resistência a drogas contra o câncer, poderia aumentar a eficácia terapêutica contra as células tumorais (HAJJI et al., 2018).

1.4 AMPLICON 8p11-12

A amplificação cromossomal está entre as principais alterações genéticas ocorridas no câncer (SPRINGER et al., 2015). A amplificação da região 11-12 do braço curto do cromossomo 8 (8p11-12) ocorre em cerca de 15% dos casos de câncer de mama (LUCIO-ETEROVIC; CARPENTER, 2011; SPRINGER et al., 2015; YANG et al., 2010), principalmente no subtipo positivo para receptor de estrogênio (SPRINGER et al., 2015). Além do câncer de mama, a amplificação da região 8p11-12 já foi descrita em câncer de pulmão, bexiga e pâncreas (MAHMOOD et al., 2013). Moelans e colaboradores mostraram que não só a amplificação, mas também a perda da região 8p11-12, se correlaciona com um fenótipo mais agressivo de tumor de mama (MOELANS et al., 2018). Foram identificados 23 genes relacionados à progressão tumoral no amplicon 8p11-12. Os genes *WHSC1L1 (Wolf-Hirschhorn Syndrome Candidate 1-Like 1*)*, DDHD2 (DDHD Domain Containing 2*) *e ERLIN2* (*ER Lipid Raft Associated 2*) são considerados os oncogenes mais expressivos e com maior capacidade de transformação de células saudáveis em células com fenótipos tumorais (YANG et al., 2010). *WHSC1L1* e *DDHD2* desempenham papéis relacionados a proliferação e sobrevivência celular (LUO et al., 2017). Dentre esses candidatos, o gene *WHSC1L1*, referente à síndrome de Wolf-Hirschhorn, também conhecido como NSD3 (*Nuclear Receptor Binding SET Domain Protein* 3), foi apontado como um dos principais candidatos a oncogene líder dessa região, capaz de dirigir a expressão de outros oncogenes presentes na região 8p11-12. A superexpressão de *WHSC1L1* em células MCF-10A apresentou a maior eficiência de transformação de células saudáveis de mama em células com características tumorais (YANG et al., 2010).

1.5 FAMÍLIA NSD

NSD (*Nuclear Receptor SET Domain*) é uma família composta por 3 proteínas HMTases (Histona metil-transferase), NSD1 *(Nuclear Receptor Binding SET Domain Protein 1)* (*loci* 5q35), NSD2/MMSET/WHSC1 (*Nuclear Receptor Binding SET Domain Protein 2/ Multiple Myeloma SET Domain/ Wolf–Hirschhorn Syndrome Candidate 1*)

(*loci* 4p16) e NSD3/WHSC1L1 (*loci* 8p12) (MORISHITA; DI LUCCIO, 2011a, 2011b). As NSDs são proteínas multi-domínios, compostas por um domínio catalítico SET *(Su(var)3-9,Enhancer-of-zeste and Trithorax)*, subdividido em pré-SET, SET e pós-SET, dois domínios PWWP (Prolina-Triptofano-Triptofano-Prolina) e cinco domínios PHD (*Plant Homeodomain Zinc Fingers*) (Figura 2). Os domínios PWWP e PHD são considerados leitores de marcas epigenéticas (BENNETT et al., 2017). As três proteínas dessa família estão envolvidas em diversas patologias, incluindo vários tipos de câncer, devido a alterações nos *loci* e nos seus níveis de expressão. NSD1 está associada a leucemia mieloide aguda, mieloma múltiplo e câncer de pulmão (LUCIO-ETEROVIC; CARPENTER, 2011; MORISHITA; DI LUCCIO, 2011a); NSD2 com mieloma múltiplo e câncer de pulmão; NSD3 com leucemia mieloide aguda, câncer de mama, pulmão entre outros (LUCIO-ETEROVIC; CARPENTER, 2011; MORISHITA; DI LUCCIO, 2011a).

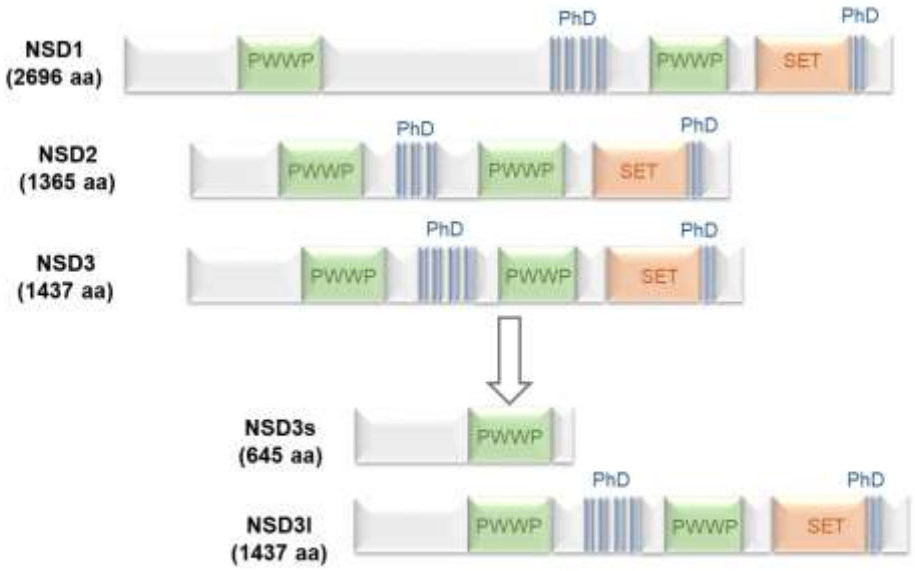

Figura 2. Representação esquemática dos membros da família NSD. A família NSD é composta por 3 proteínas: NSD1(2696 aa), NSD2 (1365 aa) e NSD3 (1437 aa). As NSDs são compostas pelos mesmos domínios: dois PWWP, cinco PHD e um SET. NSD3 sofre *splicing* alternativo resultando em uma isoforma curta (645 aa), que possui apenas o primeiro domínio PWWP, e uma isoforma longa (1437 aa).

Suspeita-se que a diversidade funcional das três proteínas NSDs pode se originar a partir de diferentes substratos devido as especificidades de seus domínios

SET. As NSDs desempenham atividade de histona mono- e di-metilases, sendo altamente específicas para o resíduo de lisina 36 na histona H3 (HE et al., 2013).

Estudos indicam que NSD1 medeia especificamente a transferência de grupos metila (mono ou di) para a lisina K36 na histona H3 (H3K36). Esta marca epigenética atua como promotora da transcrição e é essencial para o crescimento e desenvolvimento normais. NSD1 é normalmente expressa em cérebro, rim, baço, timo e músculo esquelético de indivíduos adultos (VOUGIOUKLAKIS et al., 2015). A expressão aberrante de NSD1 leva a determinados tipos de câncer, além das síndromes de Soto, desordem genética definida pelo demasiado crescimento nos primeiros anos de vida acompanhada de retardo; e Beckwith-Wiedeman, caracterizada pelo sobre crescimento e predisposição tumoral. (BENNETT et al., 2017; PAPPAS, 2015; SHETH et al., 2015; VOUGIOUKLAKIS et al., 2015). NSD1 é uma proteína de 2696 aminoácidos que contém cinco domínios PHD, dois domínios PWWP e um domínio SET, responsável pela sua atividade HMTásica. NSD2 possui 1365 aminoácidos, apresenta os mesmo domínios funcionais que NSD1 e também catalisa a mono- e di-metilação (preferencialmente) de H3K36. NSD2 é amplamente expressa no desenvolvimento inicial, e desempenha papel fundamental no crescimento. A deficiência de NSD2 está envolvida na síndrome de Wolf-Hirschhorn, caracterizada por defeitos cerebrais associados ao atraso no desenvolvimento e epilepsia. NSD2 está envolvida no sistema de reparo de DNA e provavelmente desempenha papel importante nos mecanismos de quimioresistência em tumores (BATTAGLIA; CAREY; SOUTH, 2015; BENNETT et al., 2017). NSD3 possui 1437 aminoácidos e sua superexpressão está relacionada a diversos tipos de câncer. Algumas evidências sugerem que NSD3 ativa a sinalização das vias de progressão do ciclo celular e proliferação (BENNETT et al., 2017; MORISHITA; DI LUCCIO, 2011a, 2011b).

Um número crescente de estudos vincula a desregulação da expressão das proteínas NSD a vários tipos de câncer. Em muitos casos, a diminuição da quantidade das proteínas dessa família pode suprimir o desenvolvimento do câncer. A família NSD pode ser utilizada como modelo para o desenvolvimento racional de drogas anticâncer através do desenho de inibidores específicos e seletivos. No entanto, pouco se sabe sobre o mecanismo de ação dessas proteínas e poucos compostos

foram descritos até hoje como inibidores seletivos de HMTases. Até o momento, nenhum dos inibidores de HMTases é capaz de inibir seletivamente as proteínas NSD. Isto ocorre principalmente devido a carência de estudos sobre as estruturas das HMTases, em particular a família NSD (MORISHITA; DI LUCCIO, 2011a, 2011b).

1.6 NSD3

NSD3, também conhecida como WHSC1L1, é o terceiro membro da família NSD de HMTases. Três isoformas de NSD3 foram relatadas. A isoforma mais longa, NSD3l, codifica uma proteína de 1437 aminoácidos. NSD3l inclui dois domínios PWWP, cinco domínios PHD e um domínio catalítico SET. O domínio SET de NSD3l tem especificidade pelos resíduos de lisina H3K4, H3K27 e H3K36 (HE et al., 2013; ZHOU et al., 2010). NSD3l possui maior grau de similaridade de sequência com NSD1 do que com NSD2. NSD3l é expressa em elevados níveis no cérebro, coração, músculo esquelético e placenta e, em níveis mais baixos, no pâncreas, fígado, pulmão e rim (ZHOU et al., 2010). O produto do *splicing* alternativo do exon 10 resulta em um transcrito que codifica uma proteína de 645 aminoácidos, a isoforma curta de NSD3 (NSD3s). Os 619 aminoácidos que formam a NSD3s são idênticos à porção amino-terminal de NSD3l e, dos domínios proteicos presentes na NSD3l, somente o primeiro domínio PWWP está incluso em NSD3s (YANG et al., 2010). Como as duas isoformas são coexpressas em tecidos tumorais, elas competem pela interação com proteínas através dos seus domínios PWWP (HAN et al., 2018). A terceira isoforma de NSD3, WHISTLE, é expressa em baixos níveis em comparação com as demais isoformas. WHISTLE possui 506 aminoácidos e contém apenas o segundo domínio PWWP, o domínio SET e o domínio pós-SET (HAN et al., 2018; ZHOU et al., 2010). Esta isoforma possui a capacidade de reprimir a transcrição gênica, facilitando atividades específicas de desmetilação nas histonas H3K4 e H3K27 (HAN et al., 2018).

NSD3 está envolvida em diversos processos biológicos, como modificação da cromatina, regulação transcricional e reparo de DNA, tanto por regulação da metilação de histonas quanto por interação proteína-proteína através de seus domínios (LIU et al., 2017). Além de histonas, NSD3 também é capaz de metilar proteínas não histonas. NSD3 mono-metila o fator de transcrição IRF3 (*interferon regulatory factor 3*) no resíduo de lisina 366, mantendo-o fosforilado, aumentando a sua atividade

transcricional e promovendo a resposta imune antiviral (MINO; TAKEUCHI, 2017; WANG et al., 2017).

NSD3 está associada ao câncer por dois mecanismos. Esta encontra-se frequentemente amplificada, como ocorre no câncer de mama, pulmão, bexiga, pâncreas, pulmão, hematológico, cabeça e pescoço, e osteorsarcoma, sugerindo um papel importante no controle do crescimento e diferenciação celular (HAN et al., 2018; SALOURA et al., 2017; ZHOU et al., 2010). Ainda, NSD3 pode encontrar-se fusionada a outra proteína, como na leucemia mieloide aguda, NUT (*Nuclear Protein of the Testis*)-carcinoma medular e em alguns carcinomas pélvicos (HAN et al., 2018).

NSD3 é capaz de interagir com o domínio ET (*Extra Terminal*) da proteína BRD4 *(Bromodomain-Containing Protein 4)* através da sua porção amino-terminal (KONUMA et al., 2017; ZHANG et al., 2016), presente tanto na isoforma longa quanto na curta. Essa interação é característica de LMA (Leucemia Mielóide Aguda) e pode estar relacionada à patogênese da doença (ZHANG et al., 2016). Em LMA, NSD3s desempenha sua função regulatória através de quatro interfaces de interação: (*i*) um sítio de ligação a BRD4, (*ii*) um sítio de ligação a CHD8 *(Chromodomain-Helicase-DNA-Binding Protein 8)*, (*iii*) um domínio PWWP que reconhece histonas metiladas no nucleossomo e (*iv*) um domínio ácido de ativação transcricional (aminoácidos 1-100) (SHEN et al., 2015). NSD3s se apresenta como um adaptador multifuncional de proteínas em LMA, e provavelmente em outros tipos de câncer, através da ligação a BRD4 e CHD8, sustentando a transcrição oncogênica (SHEN et al., 2015). NSD3s é essencial para a proliferação celular em LMA (SHEN et al., 2015). Em pacientes de LMA e LLA (Leucemia Linfocítica Aguda), os níveis de expressão de NSD3 são maiores do que o controle (ZHOU et al., 2010). NSD3 é encontrada fusionada a NUP98 *(Nuclear pore complex protein Nup98)* em casos de LMA (ALBERT; HELIN, 2010). Apesar da sua importância, ainda não se sabe ao certo como a NSD3 atua, pouco é sabido sobre seu mecanismo de ação e alvos moleculares (ALBERT; HELIN, 2010; LUCIO-ETEROVIC; CARPENTER, 2011).

NSD3s se liga a MYC regulando seu acesso à cromatina (LI et al., 2017). A região carboxi-terminal de MYC interage com o domínio PWWP de NSD3s e essa ligação estabiliza e aumenta os níveis transcricionais de MYC (LI et al., 2017). O complexo NSD3s-MYC foi detectado em câncer de pulmão (LI et al., 2017). Esses

resultados levaram a hipótese de que NSD3s estimula a atividade oncogênica de MYC, pois faz uma ponte entre MYC e BRD4, permitindo a regulação da função de MYC em resposta a moduladores epigenéticos (LI et al., 2017).

A amplificação do gene *NSD3* ocorre em 9,3% dos casos de câncer de cabeça e pescoço (SALOURA et al., 2016). O *knockdown* dessa oncoproteína resultou em supressão do crescimento e viabilidade, bem como na redução dos níveis de H3K36me2 em células de câncer de cabeça e pescoço (SALOURA et al., 2016, 2017). *NSD3* é um oncogene que regula transcricionalmente os genes *CDC6* (*Cell Division Cicle 6*) e *CDK2* (*Cyclin Dependent Kinase 2*) através da di-metilação de H3K36 em SCCHN (*Squamous Cell* Carcinoma *of the Head/Neck*) (SALOURA et al., 2016, 2017). A marca epigenética H3K36me2, produto da atividade de NSD3, é essencial para a transição da fase G1 para a fase S em células de SCCHN (SALOURA et al., 2016). NSD3 é capaz de metilar substratos diferentes de histonas, como a lisina 721 do domínio EGFR (*Epidermal Growth Factor Receptor*). Essa mono-metilação pode levar ao aumento da síntese de DNA e a progressão da fase S, por exemplo. Sendo assim, NSD3 pode ser um potencial alvo para o desenvolvimento de drogas antitumorais para pacientes com câncer de cabeça e pescoço (SALOURA et al., 2016, 2017).

NSD3 é amplificada em alguns casos de câncer de mama, apresentando alto potencial transformante (ALBERT; HELIN, 2010; YANG et al., 2010). Em células de câncer de mama, o silenciamento de NSD3 leva a diminuição da proliferação e crescimento celular (YANG et al., 2010). A isoforma curta é suficiente para transformar uma célula saudável em uma célula com características tumorais (YANG et al., 2010). A superexpressão de NSD3 está conectada a superexpressão de ERα (*Estrogen Receptor Alpha*) em células de câncer de mama SUM-44 e em células de câncer de mama primário. O *knockdown* de NSD3, principalmente da isoforma curta (NSD3s), tem um efeito profundo nos níveis de RNAm de *ESR1* (*Estrogen Receptor 1*) e *ERα*. Muitos genes relacionados a câncer de mama (*ESR1, ERBB3, ERBB4, CD44, CD24, MYB*) tem a sua expressão reduzida em reflexo ao *knockdown* de *NSD3* (IRISH et al., 2016). A isoforma curta NSD3s possui maiores níveis de expressão do que a isoforma longa em células de linhagens de câncer de mama, assim como em células de câncer primário (IRISH et al., 2016). A isoforma curta se tornou muito importante, visto que foi observado que, em alguns tumores de mama, apenas os éxons que codificam a

NSD3s são amplificados, levando a superexpressão apenas da isoforma curta, e não da longa (IRISH et al., 2016). O *knockdown* apenas da isoforma curta tem um efeito mais drástico do que o *knockdown* ambas as isoformas sobre a expressão de *ESR1* e na proliferação celular. Esses resultados mostram que NSD3, principalmente NSD3s, possui um papel na superexpressão de *ERα* (IRISH et al., 2016). Essas evidências mostram um papel importante da NSD3s na epigenômica, apesar de não possuir o domínio catalítico SET (IRISH et al., 2016). A figura 3 resume esquematicamente o envolvimento de NSD3 com os diferentes tipos de câncer.

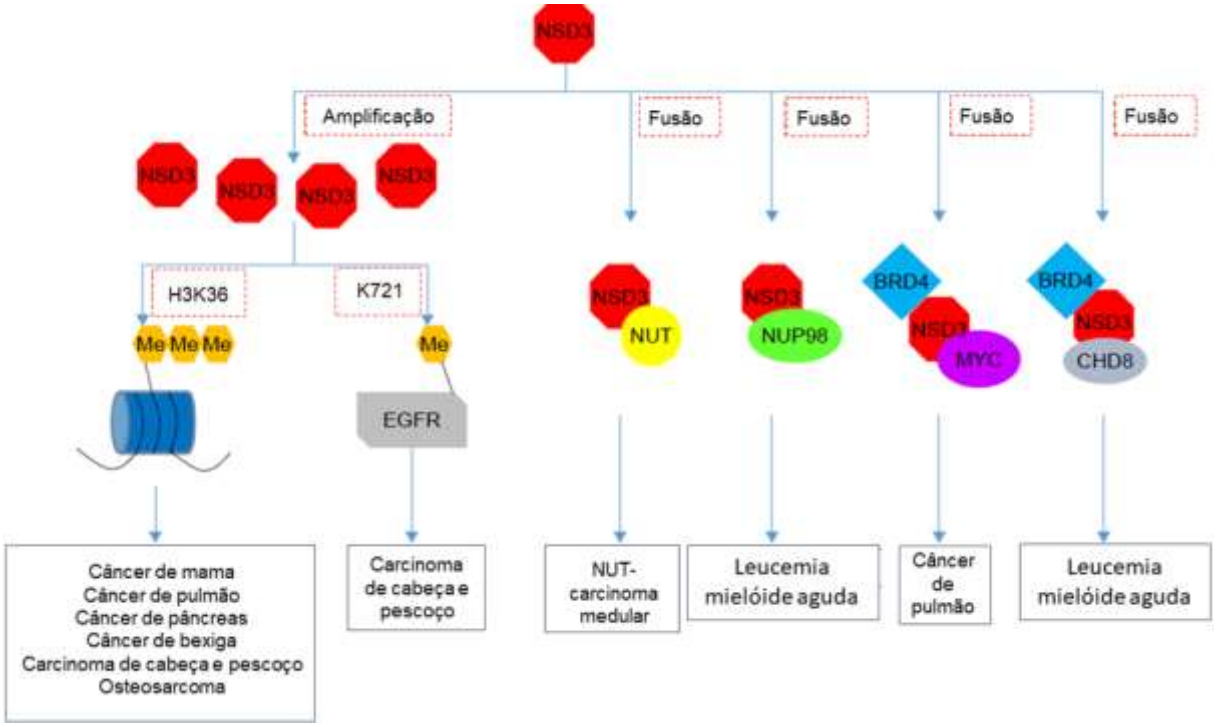

Figura 3. Esquema dos diversos tipos de câncer desencadeados pela NSD3. (Figura adaptada de (HAN et al., 2018)).

1.7 O DOMÍNIO PWWP

O domínio PWWP foi primeiramente descrito no gene *WHSC1* e é encontrado apenas em organismos eucarióticos. Este domínio é caracterizado pelo motivo de sequência Pro-Trp-Trp-Pro conservado (ALVAREZ-VENEGAS; AVRAMOVA, 2012; WU et al., 2011). Apesar da conservação, variações no motivo PWWP podem ocorrer em determinadas proteínas. Por exemplo, a proteína metil-transferase de DNA, DNMT2a/b, contém o motivo SWWP, enquanto o fator de crescimento derivado de hepatoma, HDGF, possui o motivo PHWP (RONA; ELEUTHERIO; PINHEIRO, 2016).

O domínio PWWP é encontrado em mais 60 proteínas eucarióticas implicadas na regulação da transcrição e organização da cromatina (ALVAREZ-VENEGAS; AVRAMOVA, 2012). As proteínas que possuem este domínio normalmente apresentam outros domínios, como: bromo, cromo, PHD e SET. Esse domínio apresenta entre 90 a 130 aminoácidos e está presente em proteínas nucleares relacionadas ao crescimento, divisão e diferenciação celular (ALVAREZ-VENEGAS; AVRAMOVA, 2012; RONA; ELEUTHERIO; PINHEIRO, 2016; STEC et al., 2000).

O domínio PWWP pertence a superfamília *Royal*, a qual também pertencem os domínios: Tudor, cromo e MBT *(Malignant Brain Tumor)* (ALVAREZ-VENEGAS; AVRAMOVA, 2012; WANG et al., 2009; WU et al., 2011). Esse domínio contém uma cavidade hidrofóbica formada por resíduos aromáticos capaz de reconhecer resíduos de lisina metilados em histonas. Além da gaiola hidrofóbica, o domínio PWWP também possui uma grande número de resíduos básicos, como lisina e arginina, o que aumenta o ponto isoelétrico da cadeia peptídica. Esses aminoácidos formam uma superfície carregada positivamente que funciona como uma interface favorável a ligação eletrostática, não específica, com o esqueleto de fosfato do DNA (RONA; ELEUTHERIO; PINHEIRO, 2016). O domínio PWWP pode interagir simultaneamente com histona e DNA, contribuindo para a manutenção da habilidade de reconhecimento do nucleossomo como um todo (QIN; MIN, 2014; WANG et al., 2009; WU et al., 2011). Desta forma, o domínio PWWP é descrito como um motivo de reconhecimento lisinas metiladas em histonas (WU et al., 2011), desempenhando um papel importante na regulação epigenética (YANG et al., 2010).

A porção amino terminal do domínio PWWP exibe uma estrutura em barril-β, enquanto a porção carboxi-terminal é constituída por um feixe de α-hélices (Figura 4). As estruturas tridimensionais determinadas para complexos de domínios da superfamília *Royal* com peptídeos derivados de histona mostraram que o reconhecimento de lisinas metiladas é desempenhado pela estrutura em barril-β.

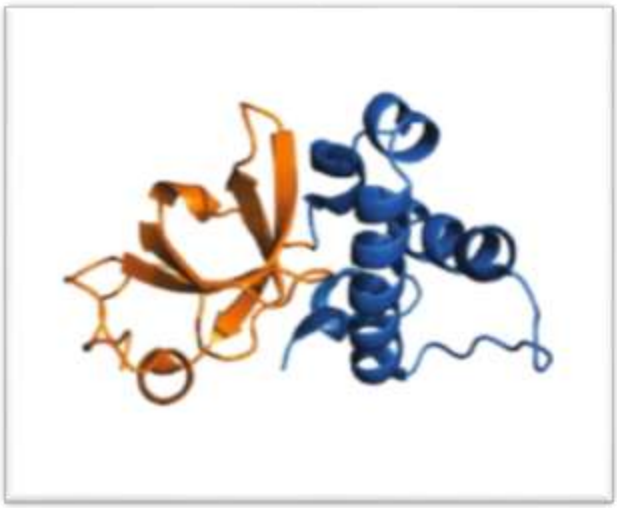

Figura 4. Diagrama tridimensional do domínio PWWP de DNMT3b O β-barril da região N-terminal é representado em laranja, enquanto o feixe helicoidal da região C-terminal está representado em azul em azul (RONA et al., 2017).

1.8 Saccharomyces cerevisisae

A levedura *Saccharomyces cerevisiae* é um microrganismo utilizado como modelo de estudo para células eucarióticas. Devido a facilidade de manipulação genética, a semelhança bioquímica com células animais e a disponibilidade de recursos em genômica funcional e análise ômicas, este eucarioto unicelular foi estabelecido como uma ferramenta valiosa para a investigação bioquímica (GUARAGNELLA et al., 2013). Além disso, uma grande quantidade de proteínas de levedura pode ser substituída por proteínas ortólogas humanas (MANNARINO et al., 2011). Para genes que não possuem ortólogos,a levedura geralmente apresenta uma via de ação análoga à via de ação do gene humano, de modo que o gene pode ser expresso de forma heteróloga em *S. cerevisiae* e o fenótipo resultante pode ser estudado (TOSATO et al., 2013). Recentemente, Kachroo e colaboradores (2015) substituíram 414 genes da levedura por seus ortólogos humanos equivalentes, observando que aproximadamente 43% destes genes foram capazes de manter a sobrevivência da levedura e manutenção das vias metabólicas (KACHROO et al., 2015). *S. cerevisiae* também tem sido utilizada para estudos de mutações no mtDNA, incluindo componentes dos complexos de cadeia respiratória III e IV (MALINA; LARSSON; NIELSEN, 2018).

Diversas instituições de pesquisa de câncer em todo o mundo fazem uso da genética de leveduras como parte de sua estratégia de investigação simulando nesse

modelo as alterações patológicas observadas nas células cancerígenas e, em seguida, manipulando-o para tentar reverter tais alterações. Pelo menos dois grupos são (ou foram), liderados por prêmios Nobel que atingiram os seus títulos importantes utilizando leveduras como modelo. Leland H. Hartwell e Paul Nurse, que junto com Tim Hunt foram agraciados com o Prêmio Nobel de 2001 em Fisiologia ou Medicina por seu trabalho sobre o ciclo celular em eucarioto. O ponto chave é mimetizar, se possível, as alterações patológicas observadas em células cancerosas em células de levedura e, em seguida, manipular esse modelo, a fim de tentar reduzir os efeitos dessas mudanças. A previsão de que cerca de metade de todos os genes de levedura que têm homólogos estruturais ou funcionais do genoma humano, levou a muitos estudos comparativos entre leveduras e células de mamíferos (TOSATO et al., 2013).

A *S. cerevisiae* tem sido amplamente utilizada em pesquisa básica devido a uma série de vantagens frente a outros organismos eucarióticos, como pequeno ciclo celular, rápido crescimento celular, fácil manipulação e o fato de utilizar diversos mecanismos genéticos que são semelhantes aos de organismos multicelulares (TOSATO et al., 2013). Atualmente, bancos de dados contendo coleções completas de deleções de todas as ORFs (*Open Reading Frames*) de *S. cerevisiae* encontram-se disponíveis comercialmente. Além disso, bibliotecas de ORFs fusionadas a *tags* de expressão também estão disponíveis, o que facilita a realização de estudos de imunoprecipitação e interação proteica. Alguns dos exemplos mais importantes incluem ORFs fusionadas à GFP (Proteína Verde Fluorescente) o que permite a determinação de sua localização celular em diferentes condições (BOTSTEIN; FINK, 2011).

S. cerevisiae é um modelo interessante para estudar respostas ao oxigênio, pois é um organismo anaeróbio facultativo, podendo crescer em ambiente sem a presença de oxigênio (SAMANFAR et al., 2013). Segundo Louis Pasteur, o oxigênio tem efeito inibitório da fermentação da glicose em células capazes de realizar tanto anaerobiose quanto aerobiose. Em 1929, Herbert Crabtree observou que algumas células tumorais sob alta concentração de glicose mudam para o metabolismo fermentativo por mecanismos de curto prazo, mesmo na presença de oxigênio (CRABTREE, 1928, 1929; DE DEKEN, 1966; DIAZ-RUIZ et al., 2009). Esse fenômeno era conhecido como Efeito Contrário de Pasteur, Efeito Crabtree (DE DEKEN, 1966), ou efeito de

repressão catabólica. Deken analisou um grupo de leveduras e classificou em Crabtree positivo ou negativo. Foi demonstrado que *Saccharomyces cerevisiae, S. chevalieri, S. italicus, S. oviforme, S. pasteurianus, S. turbidans, S. carlsbergensis, Schixosaccharomyces pombe, Debaryomyces globosus, Brettanomyces lambicus, Torulopsis dattila, T. glabrata, T. colliculosa , Nematospora coryli, Nadsonia fulvescens* são positivas para Crabtree (DE DEKEN, 1966).

A glicose e a frutose são as principais fontes de energia consumidas pela *S. cerevisiae*, mas outras fontes de carbono também podem ser usadas (CARLSON, 1999; KIM et al., 2013). Células de levedura se adaptam a diferentes fontes de carbono por um controle transcricional, a transcrição gênica é diferente de acordo com os níveis de glicose. Quando a concentração de glicose é alta no ambiente, há repressão da expressão de genes envolvidos no ciclo de Krebs e na cadeia de transporte de elétrons (KIM et al., 2013; THEVELEIN, 1994).

Em relação ao metabolismo energético, há semelhanças entre a repressão do metabolismo oxidativo induzida pela glicose (repressão catabólica) em levedura e a glicólise aeróbica de células tumorais. Em ambos os tipos de células, a regulação negativa do metabolismo oxidativo é observada juntamente com um aumento da fermentação independente da presença de oxigênio. Isso aponta *S. cerevisiae* como um modelo metabólico favorável para a triagem de drogas para a terapia antitumoral cujo alvo é o metabolismo. Por exemplo, assim como em células tumorais, na fermentação de levedura há a superexpressão das enzimas da glicólise (DIAZ-RUIZ; RIGOULET; DEVIN, 2011b).

Existem alguns importantes oncogenes humanos que apresentam genes ortólogos em *S. cerevisiae*. O RAS (RAt Sarcoma Vírus) é um proto-oncogene humano que leva à sobrevivência, crescimento e diferenciação celular. Em levedura, RAS1 e RAS2 controlam a via de sinalização cAMP/PKA (DIAZ-RUIZ; RIGOULET; DEVIN, 2011b). SCH9 é um ortólogo de levedura do oncogene humano *AKT1*. Sch9 está envolvida nas vias de sinalização da glicose (DIAZ-RUIZ; RIGOULET; DEVIN, 2011b). O *mTOR* (Target Of Rapamycin), também possui ortólogo em levedura, é capaz de ativar o efeito Warburg, uma vez que promove a expressão de enzimas glicolíticas (YU et al., 2017).

1.9 REPRESSÃO CATABÓLICA

Quando há elevada quantidade de glicose no meio, a levedura fermenta, mesmo em presença de oxigênio, num processo denominado repressão catabólica. Há uma grande semelhança entre a repressão catabólica da levedura e o efeito Warburg da célula tumoral. Em ambos os casos ocorre uma regulação negativa do metabolismo oxidativo respiratório associado a um aumento da fermentação, independente da presença de oxigênio. Desta forma, a levedura em fase de crescimento em meio contendo excesso de glicose apresenta um metabolismo energético semelhante ao da célula tumoral.

As principais proteínas envolvidas na via de repressão catabólica são a Hxk2 (Hexoquinase 2) , Snf1 (*Sucrose NonFermenting*) e Mig1 (*Multicopy Inhibitor of GAL gene expression*). Os genes envolvidos na via de repressão catabólica pela glicose são de dois tipos: genes requeridos para a repressão, como o *HXK2*, e genes necessários à desrepressão, como *CAT1*/*SNF1* (THEVELEIN, 1994). O gene *HXK2* codifica a hexoquinase 2, uma enzima responsável por catalisar a fosforilação da glicose no citosol e por regular a repressão catabólica (CARLSON, 1999; THEVELEIN, 1994). O alvo primário da Hxk2 é a proteína quinase Cat1/Snf1; o alvo secundário é o complexo transcricional Mig1-Ssn6/Cyc8-Tup1, que está envolvido na repressão da respiração mitocondrial, gliconeogênese, ciclo do glioxilato e no uso de fontes de carbono alternativas. A inibição é mantida enquanto a concentração de glicose se mantém alta no meio (THEVELEIN, 1994). De modo geral, na presença de glicose em concentrações elevadas, a Hxk2 impede a fosforilação de Mig1 pela Snf1, permitindo a Mig1 exercer seu efeito repressor sobre os genes envolvidos no ciclo de Krebs e na cadeia transportadora de elétrons. Hxk2 também interage com Reg1, facilitando a ação da fosfatase Glc7 sobre Snf1 para mantê-la em sua forma desfosforilada e inativa, contribuindo, desta forma, para o baixo nível de fosforilação de Mig1. Na ausência de glicose, Snf1 é fosforilado por qualquer uma das quinases Elm1, Tos3 e Sak1; sob esta forma, Snf1 fosforila Mig1, que migra para o citosol e lá se mantém junto à Hxk2, de modo que a expressão gênica pode finalmente ocorrer (Figura 5) (GANCEDO; FLORES, 2008).

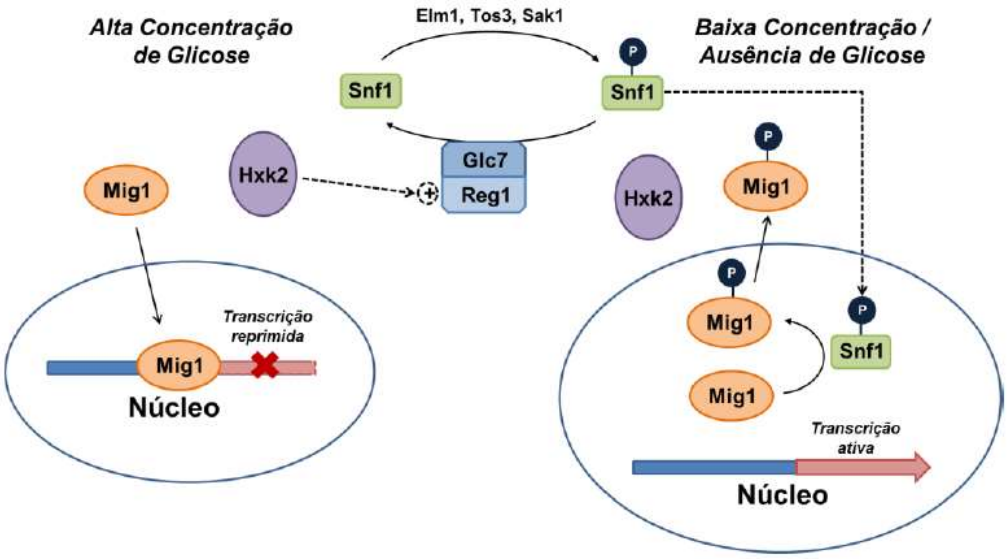

Figura 5. Mecanismo de repressão catabólica em levedura. As principais proteínas envolvidas na via de repressão catabólica são a Hxk2, Snf1 e Mig1 (adaptado de Gancedo e Flores, 2008).

Existe uma alta similaridade entre a repressão por glicose da levedura e o efeito Warburg em mamíferos (DIAZ-RUIZ; RIGOULET; DEVIN, 2011b), ambos os efeitos redirecionam o fluxo metabólico para a fermentação (DIAZ-RUIZ et al., 2009). Assim como células tumorais, a levedura apresenta um aumento na expressão de enzimas chaves da via glicolítica, em resposta a presença de glicose, e diminuição na atividade e expressão de enzimas que participam do metabolismo oxidativo (DIAZ-RUIZ; RIGOULET; DEVIN, 2011a). A expressão de outros genes também são afetados, como os envolvidos na utilização de outras fontes de carbono e na gliconeogênese (CARLSON, 1999). Durante a repressão catabólica ou efeito Warburg, há uma diminuição de expressão das enzimas do ciclo do ácido cítrico, resultando em um mau funcionamento desta via (Figura 6). Os dois efeitos exibem superexpressão de HxkII e piruvato desidrogenase quinase. No efeito Warburg, a isocitrato desidrogenase apresenta um defeito; já em *S. cerevisiae* sob repressão catabólica, essa enzima é inativa. O complexo II da cadeia de transporte de elétrons apresenta baixa expressão no efeito Warburg e é reprimido no efeito Crabtree. Em ambos os processos, há uma diminuição na atividade da ATP sintase (DIAZ-RUIZ et al., 2009). Apesar de o efeito Warburg e a repressão catabólica apresentarem diversas semelhanças, o efeito observado em leveduras é reversível, enquanto o efeito Warburg é irreversível.

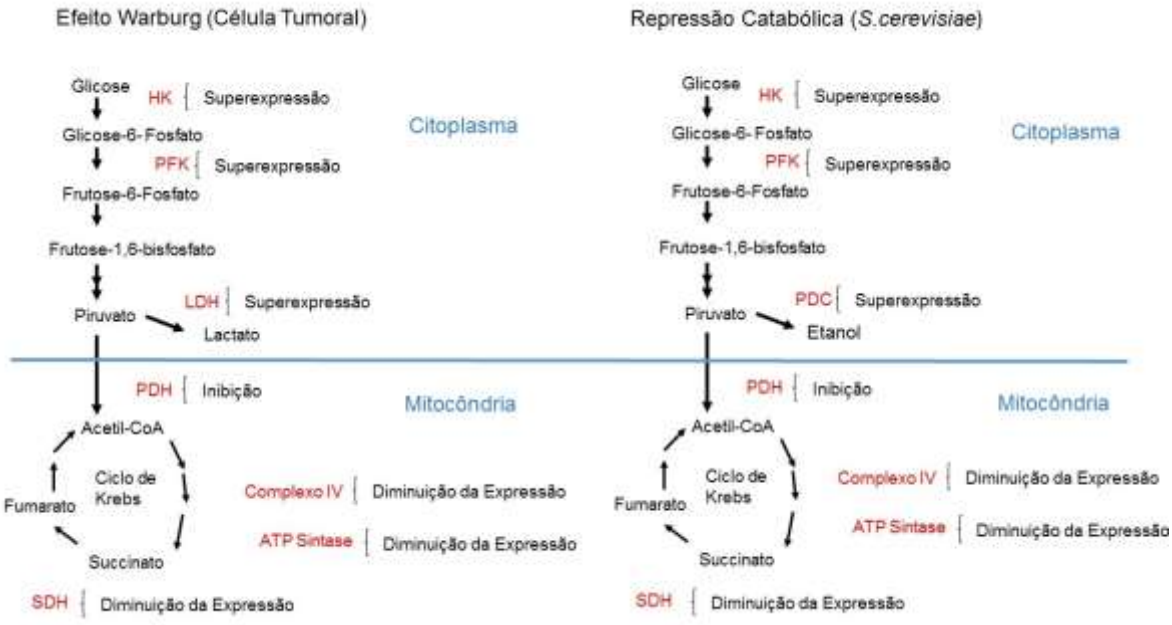

Figura 6. Semelhança entre Células tumorais e Repressão Catabólica. Comparação entre o efeito Warburg (célula tumoral) e a repressão catabólica (*S. cerevisiae*). Os dois efeitos são muito semelhantes: há a superexpressão das enzimas que participam da glicólise e uma diminuição da atividade das enzimas que participam da via oxidativa (Figura adaptada de Diaz-Ruiz et al. 2011).

1.10 ESPÉCIES REATIVAS DE OXIGÊNIO (ERO)

A maioria da produção de EROs ocorre na CTE (Cadeia de Transporte de Elétrons) das mitocôndrias, durante a respiração mitocondrial. Nesse processo, uma molécula de oxigênio recebe quatro elétrons sendo reduzida a água; no entanto, ao longo desse processo, alguns dos elétrons vazam prematuramente durante seu transporte para o oxigênio, produzindo EROs. Como os elétrons são sequencialmente transferidos do complexo I ou complexo II para o complexo III e depois para o complexo IV, os prótons são translocados da matriz mitocondrial para o espaço intermembrana, criando um gradiente eletroquímico que é usado como energia para a síntese de ATP pela ATP sintase (ELEUTHERIO et al., 2017). Durante a respiração celular o aceptor final de elétrons é o oxigênio molecular, que é reduzido a H_2O ao final da via respiratória (ABBOTT et al., 2009). O complexo I, de mamíferos, é o principal ponto de entrada de elétrons na CTE e desempenha um papel crucial na produção de EROs. Os elétrons podem vazar do complexo I e reagir com o oxigênio, resultando na produção de ânion superóxido (O_2^-) (BACCOLO et al., 2018). Em *S. cerevisiae*, o complexo I é substituído por Ndi1, uma NADH desidrogenase, que não bombeia prótons na membrana interna. Já foi observado que a superexpressão de

Ndi1 na levedura leva a um aumento dos níveis de EROs (BACCOLO et al., 2018). O complexo III é uma das principais fontes de ânion peróxido (O_2^{2-}) na CTE (BACCOLO et al., 2018). O superóxido, o peróxido de hidrogênio e os compostos gerados a partir destes, como o radical hidroxila (·OH), são definidos como EROs. Para atenuar as EROs, ocorre a expressão e atuação de enzimas responsáveis por neutralizar e regularizar os níveis destas espécies e manter a homeostase fisiológica durante o processo de respiração celular. Assim como outros organismos eucarióticos, a levedura *S. cerevisiae* possui mecanismos de defesa antioxidantes enzimáticos, como a catalase e a superóxido dismutase (ABBOTT et al., 2009), e não enzimáticos, como a glutationa (GSH) (FRANÇA; PANEK; ELEUTHERIO, 2007). A enzima superóxido dismutase (Sod) remove o radical superóxido, convertendo-o a oxigênio e H_2O_2. O peróxido por sua vez, pode atravessar a membrana e ser completamente reduzido pela ação das enzimas catalase e peroxidase, produzindo água e oxigênio (ABBOTT et al., 2009; MANNARINO et al., 2008). O superóxido também pode sofrer dismutação espontânea, embora a uma taxa muito mais lenta (ELEUTHERIO et al., 2017).

Na inibição da cadeia respiratória, a atuação das enzimas de defesa antioxidante é baixa e a célula acumula EROs, o que resulta em danos oxidativos, definindo o estresse oxidativo. A regulação negativa do metabolismo oxidativo ocorre tanto no efeito Warburg (células tumorais) quanto no efeito Crabtree (células de levedura), de modo que tais células não desenvolvem uma defesa antioxidante eficiente contra EROs, que são capazes de danificar todos os principais blocos de construção da célula, incluindo DNA, lipídios e proteínas. Estes danos levam à morte celular, acelerando o processo de envelhecimento e induzem doenças relacionadas à idade. Tanto a redução das defesas antioxidantes quanto o aumento da produção de EROs, ou ambos, levam ao aumento do estresse oxidativo que reduz a longevidade celular (ABBOTT et al., 2009; MOSKOVITZ et al., 2001).

1.11 METABOLISMO DE GLICEROL

Glicerol pode ser utilizado como fonte de carbono e energia por diversos tipos de levedura (HIMMS-HAGEN, 1968). O glicerol é fosforilado por uma glicerol quinase (Gut1), gerando glicerol-3-fosfato. A seguir, glicerol-3-fosfato é oxidado a DHAP (Di-Hidroxiacetona Fosfato) pela enzima glicerol fosfato ubiquinona oxirredutase (Gut2),

localizada na superfície da membrana mitocondrial interna. Os elétrons desta oxidação são transferidos para a ubiquinona, entrando na cadeia respiratória (FLORES et al., 2000; NEVOIGT; STAHL, 1997). DHAP entra na via glicolítica, gerando NADH (no citoplasma) e piruvato, que segue para a via respiratória. Glicerol-3-fosfato desidrogenase (Gpd1/2) auxilia na re-oxidação do NADH (Dinucleotídeo de Nicotinamida e Adenina - reduzido) citoplasmático (HERRERO et al., 2008). Logo, quando a fonte de carbono utilizada é o glicerol, a levedura apresenta uma elevação no nível de EROs, característica do metabolismo oxidativo e, portanto, ocorre um estímulo no desenvolvimento da defesa oxidante. Com um sistema de defesa antioxidante presente, a célula tem maior resistência a EROs, apesar de a produção de tais espécies ser maior durante o processo respiratório do que no processo fermentativo. Esse balanço entre a produção de EROs e recrutamento da defesa antioxidante durante o processo respiratório deve ser equilibrado para evitar danos moleculares demasiados à célula.

O processo de fermentação da glicose também tem como subproduto o glicerol (HIMMS-HAGEN, 1968). A produção de glicerol ocorre primeiramente devido a redução da dihidroacetona fosfato, oriunda da via glicolítica, produzindo glicerol-3-fosfato pela enzima G3P desidrogenase citosólica (ctGDP). A enzima glicerol 3-fosfatase catalisa a desfosforilação do G3P em glicerol. A produção de glicerol tem papel fundamental na manutenção do balanço redox citosólico. A enzima GPP tem sua atividade aumentada em presença de glicose, porém, a ctGDP é reprimida nessas condições. Acredita-se que um aumento da atividade da enzima ctGDP durante crescimento em fontes de carbono não repressoras está associado a uma necessidade de balanceamento dos níveis intracelulares de G3P para síntese de glicerídeos necessária para produção de membrana celular. (NEVOIGT; STAHL, 1997).

1.12 PDP3

Pdp3 é uma proteína de *S. cerevisiae* primariamente localizada no núcleo, porém migra para o citoplasma em resposta a condições de estresse, como hipóxia (DASTIDAR et al., 2012). Composta por 304 aminoácidos, possui um único domínio PWWP similar ao da NSD3s (25% de identidade de sequência) (RONA, 2014) cuja

estrutura tridimensional ainda não foi determinada. Pdp3 faz parte do complexo NuA3b que possui uma função de histona acetil-transferase e está envolvido no prolongamento da transcrição. Pdp3 é responsável pelo reconhecimento da trimetilação da lisina 36 da histona 3 (H3K36me3), recrutando a proteína Sas3 para que ocorra a acetilação de histonas (Figura 7) (GILBERT et al., 2014; VICENTE-MUÑOZ et al., 2014). O complexo NuA3 existe sob duas formas diferentes: NuA3a, que se liga especificamente a H3K4me1/2/3 através do domínio PHD da proteína Yng1 que, em seguida, acetila H3K14, dando início ao processo de transcrição; e o complexo NuA3b, no qual o domínio PWWP da proteína Pdp3 se liga a H3K36me3 atuando como um regulador positivo para o alongamento da transcrição (Figura 7) (GILBERT et al., 2014; MARTIN et al., 2017). A presença de uma gaiola aromático no domínio PWWP de Pdp3 é necessária para a interação com a lisina trimetilada na posição lisina 36 (H3K36me3). Os resíduos aromáticos F18, W21 e F48, presentes em Pdp3, são conservados e mutações independentes nestes resíduos são capazes de abolir a interação de Pdp3 com o peptídeo H3K36me3, sugerindo que Pdp3 requer uma gaiola aromática para ligar-se à cromatina (GILBERT et al., 2014). Gilbert e colaboradores demonstraram que segmento amino-terminal formado pelos aminoácidos 1-150 de Pdp3 são essenciais para o reconhecimento de H3K36me3. Estes dados sugerem que Pdp3, e outras proteínas contendo o domínio PWWP, requerem uma região carboxi-terminal α-helicoidal para a estabilidade e função da cavidade aromática (GILBERT et al., 2014).

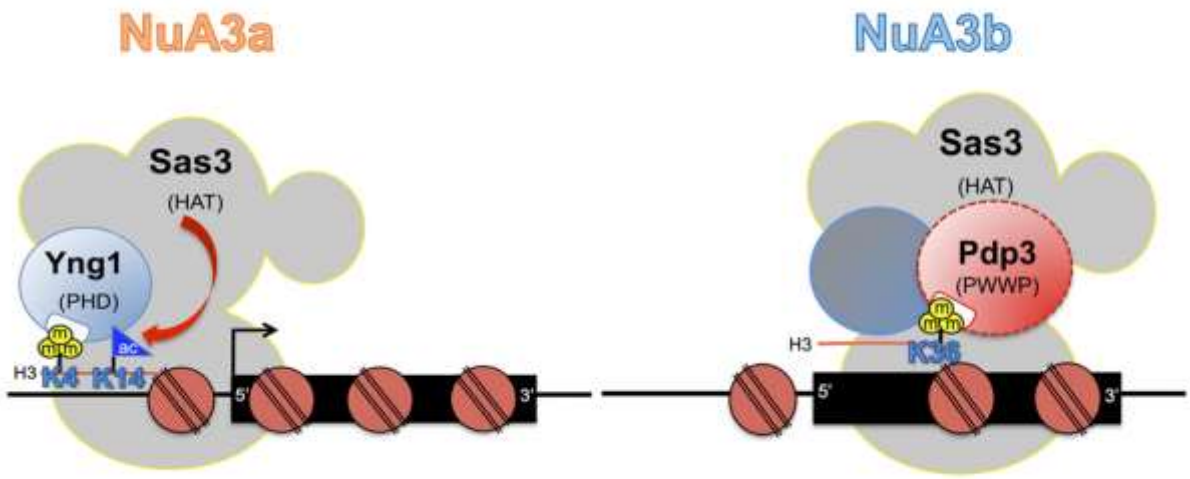

Figura 7. Representação esquemática dos complexos NuA3. NuA3a: Yng1 se liga através de seu domínio PHD a H3K4me3 (resíduo de lisina 4 da histona H3 trimetilado), recrutando o complexo NuA3a para a região promotora de genes transcricionalmente ativos. Em seguida, Sas3 acetila H3K14 (resíduo de lisina 14 na histona H3), dando início ao processo de transcrição gênica. NuA3b: Pdp3 se liga através de seu domínio PWWP a H3K36me3 (resíduo de lisina 36 na histona H3 trimetilada), recrutando o complexo NuA3b para a região codificadora de genes transcricionalmente ativos (Gilbert et al., 2014).

2 JUSTIFICATIVA

Segundo a Organização mundial da saúde, cerca de dois terços das mortes no mundo são causadas por doenças não-transmissíveis, como doenças cardíacas, diabetes e câncer. O câncer é responsável por cerca de 13% de casos de mortes no mundo. O aumento dessa porcentagem está relacionado com o envelhecimento da população e o tempo de exposição a fatores ambientais como cigarro, sol e alimentação. Ao ser diagnosticado tardiamente, o câncer pode se espalhar para outros tecidos (metástase) podendo levar a morte.

O tratamento contra o câncer consiste em cirurgia, quimioterapia, radioterapia e/ou tratamentos hormonais. Esses tratamentos apresentam uma série de limitações visto que não há como separar, a nível molecular, uma célula saudável de uma cancerosa. Com isso, células saudáveis acabam sendo prejudicadas e, muitas vezes, células tumorais permanecem, podendo dar início a um novo foco da doença.

Muitos estudos nessa área mostram que genes específicos são superexpressos em determinados tipos de câncer. Atualmente, novas linhas de pesquisa são baseadas na investigação do mecanismo, a nível molecular, das proteínas traduzidas por esses genes. Uma nova forma de tratamento seria a inibição da atividade dessas proteínas. Com isso, o tratamento atingiria apenas as células cancerosas, diminuindo a sua toxidade e, por conseguinte, os efeitos colaterais sofridos pelo paciente.

Diversos estudos mostram que o *amplicon* 8p11-12 é superexpresso em 15 % dos casos de câncer de mama, além de estar envolvido em câncer de pulmão, bexiga e pâncreas. Essa região cromossomal possui alguns candidatos a oncogene líder, dentre eles o gene *WHSC1L1/NSD3*. *NSD3* está envolvido em diferentes tipos de câncer, tais como mama, pulmão, ovário, leucemia e cabeça e pescoço. NSD3 apresenta similaridade de sequência com a proteína Pdp3 de *S. cerevisiae*. Essa levedura é um bom modelo celular para a investigação das alterações bioquímica na tumorigênese, visto que apresenta um metabolismo primariamente fermentativo na presença de glicose, devido ao fenômeno da repressão catabólica, assim como ocorre na célula tumoral que sofre o efeito Warburg. A *S. cerevisiae* apresenta grande semelhança com células animais, podendo apresentar genes ortólogos, além da possibilidade de expressar proteínas humanas de maneira heteróloga.

Tanto Pdp3 quanto a isoforma curta de NSD3 apresentam um único domínio conhecido como PWWP. A estrutura tridimensional e o mecanismo de ação dessas

proteínas não são conhecidos, além disso pouco se sabe sobre o papel regulatório que desempenham no metabolismo celular. Portanto, torna-se necessário estudar a função metabólica de NSD3s humana e Pdp3 de *S. cerevisiae*, a fim de estabelecer uma conexão evolutiva entre as proteínas. No futuro, este conhecimento poderá ser empregado no desenvolvimento racional de novas estratégias anticâncer que visem a inibição de vias metabólicas ativadas pela oncoproteína NSD3s.

3 OBJETIVOS

Objetivo Geral:

O presente trabalho experimental de tese teve como objetivo principal avaliar a função metabólica da isoforma curta da oncoproteína humana NSD3 e da proteína ortóloga Pdp3 de *Saccharomyces cerevisiae*.

Objetivos específicos:

- Avaliar o efeito da superexpressão de NSD3s e da Pdp3 no fenótipo de *S. cerevisiae*.
- Avaliar a semelhança funcional entre os domínios PWWP de NSD3s e Pdp3
- Avaliar a importância da integridade da gaiola aromática na função metabólica de Pdp3.
- Avaliar a relação entre Pdp3 e Set 2.
- Avaliar a dependência da Pdp3 do complexo NuA3b.
- Determinar os metabólitos significantemente alterados pela superexpressão da NSD3s e da Pdp3.

4 MATERIAIS E MÉTODOS

4.1 ANÁLISE FENOTÍPICA

4.1.1 Cepas e condições de cultivo de S. cerevisiae

A cepa BY4741 de *Saccharomyces cerevisiae (MATa; his3; leu2; met15; ura3*) e suas mutantes isogênicas *Δpdp3, Δset2, Δsas3,* contendo os genes *PDP3*, *SET2* ou *SAS3*, respectivamente, interrompidos pelo gene *KanMX4,* conferindo resistência a geneticina. A cepa *Δpdp3* foi adquirida da Euroscarf, Frankfurt, Alemanha. As cepas *Δset2* e *Δsas3* foram gentilmente cedidas pelo professor Claudio Akio Masuda, do Instituto de Bioquímica Médica da UFRJ, previamente adquiridas da Euroscarf. Os estoques das cepas foram mantidos em meio sólido YPD 2% (1% extrato de lêvedo, 2% glicose, 2% peptona e 2% ágar) em condições apropriadas para evitar a seleção de petites ou supressores. No caso da cepa mutante, este meio de cultivo também continha 0,002% de geneticina.

As cepas mutantes que superexpressam NSD3s ou Pdp3 foram construídas a partir da inserção do plasmídeo pECUh6 (Figura 8), adquirido da empresa Enzimax (EUA), contendo o gene que codifica NSD3s ou Pdp3, respectivamente, na cepa BY4741 ($NSD3s^+$ ou $Pdp3^+$, respectivamente). A cepa que superexpressa o mutante Pdp3 W21A, onde o resíduo de triptofano na posição 21 de Pdp3 foi substituído por alanina, ou a quimera molecular Pdp3 (PWWP-NSD3s), onde o domínio PWWP de Pdp3 foi substituído pelo de NSD3s, foram construídas a partir da inserção do plasmídeo pECUh6, contendo as sequências gênicas que codificam cada construção, na cepa *Δpdp3* ($W21A^+$ ou $Pdp3(PWWP\text{-}NSD3s)^+$, respectivamente). O plasmídeo pECUh6 contendo a sequência gênica que codifica Pdp3 também foi inserido nas cepas *Δset2* (*Δset2*$(Pdp3)^+$) e *Δsas3* (*Δsas3*$(Pdp3)^+$). pECUh6 é um plasmídeo de cópias múltiplas com promotor forte *CUP1* (induzido pela presença de Cu^{+2}), marcador de resistência a ampicilina e marcador nutricional para uracila. A subclonagem da sequência gênica referente a NSD3s foi realizada utilizando as enzimas de restrição 5'-*EcoR*I e 3'-*Hind*III. A subclonagem da sequência gênica referente a Pdp3 foi realizada utilizando as enzimas de restrição 5'-*XhoI* e 3'-*HindIII*. A subclonagem da sequência referente ao mutante Pdp3 W21A foi realizada utilizando as enzimas de restriçãoo 5'-*XhoI* e 3'-*HindIII*. A subclonagem da sequência referente a quimera Pdp3-PWWPNSD3s foi realizada utilizando as enzimas de restrição 5'-*XhoI* e 3'-

HindIII. Os plasmídeos recombinantes, contendo os genes de interesse, foram obtidos comercialmente da empresa Genscript (EUA). Para uso como controle, foi inserido nas cepas BY4741, *Δpdp3, Δset2* e *Δsas3* o vetor pECUh6 sem nenhuma sequência gênica (WT, *Δpdp3, Δset2* e *Δsas3* respectivamente). As cepas utilizadas estão apresentadas na Tabela 1.

Tabela 1. Cepas utilizadas.

Cepa	Genótipo (Fenótipo)	Nome
BY4741	MATa *his3Δ1 leu2Δ0 met15Δ0 ura3Δ0*	
Δ*pdp3*	Isogênica da BY4741 exceto *PDP3 :: KanMX4* (Sem expressão de Pdp3)	**Δ*pdp3***
BY4741 pECUh6	Isogênica da BY4741 com pECUh6 (Controle com plasmídeo vazio)	**WT**
BY4741 pECUh6 PDP3	Isogênica da BY4741 com pECUh6-*PDP3* (Superexpressão da proteína Pdp3)	**Pdp3^{+}**
BY4741 pECUh6 NSD3s	Isogênica da BY4741 com pECUh6-*NSD3s* (Superexpressão da NSD3s)	**NSD3s^{+}**
Δpdp3 pECUh6 PDP3$_{W21A}$	Isogênica da BY4741 exceto *PDP3 :: KanMX4* com pECUh6 *PDP3$_{W21A}$* (Sem expressão de *PDP3*, superexpressão vetor *PDP3$_{W21A}$*)	**W21A^{+}**
Δpdp3 pECUh6 PDP3$_{PWWPNSD3s}$	Isogênica da BY4741 exceto *PDP3 :: KanMX4* com pECUh6 *PDP3$_{PWWPNSD3s}$* (Sem expressão de *PDP3*, Superexpressão vetor *PDP3$_{PWWPNSD3s}$*)	**Pdp3(PWWP-NSD3s)$^{+}$**
Δset2	Isogênica da BY4741 exceto *SET2 :: KanMX4* (Sem expressão de Set2)	**Δ*set2***
Δset2 pECUh6 *PDP3*	Isogênica da BY4741 exceto *SET2 :: KanMX4* com pECUh6 *PDP3* (Sem expressão de *SET2*, Superexpressão da Pdp3)	**Δ*set2* Pdp3^{+}**
Δsas3	Isogênica da BY4741 exceto *SAS3 :: KanMX4* (Sem expressão de Sas3)	**Δ*sas3***
Δset2 pECUh6 *PDP3*	Isogênica da BY4741 exceto *SAS3 :: KanMX4* com pECUh6 *PDP3* (Sem expressão de *SAS3*, Superexpressão da Pdp3)	**Δ*sas3* Pdp3^{+}**

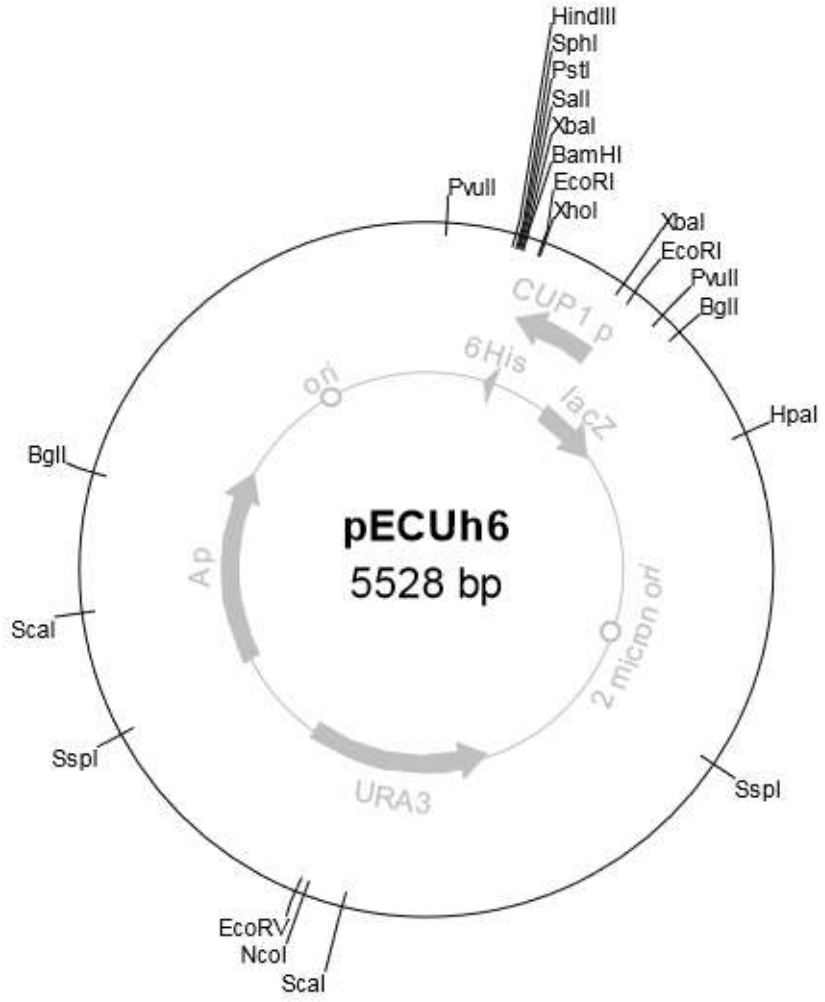

Figura 8. Mapa de restrição do vetor plasmidial pECUh6.

Os estoques das cepas superexpressando NSD3s, Pdp3, W21A, a quimera Pdp3 (PWWP-NSD3s) e seus controles foram mantidos em meio *drop out* sólido sem uracila. Todos os experimentos foram conduzidos em meio *drop out* líquido. A cepas foram cultivadas em meio *drop out* sem uracila e suplementado com sulfato de cobre 50µM para respectiva indução dos genes e controle. Os cultivos foram realizados a 28ºC, 160 rpm, em *erlenmeyers* preenchidos com 1/5 do seu volume com meio de cultura. A seguir é descrita a composição do meio de cultivo ***drop out*:**

Base nitrogenada sem aminoácidos – 0,67%
Fonte de Carbono: Glicose – 2% (fermentação) ou Glicerol 4% (Respiração)
Mistura Drop out – 0,2%
OBS: Para o meio sólido acrescentar ágar - 2%

Mistura *Drop out*:

Ácido aspártico 2,0g	Glutamina 2,0g	Serina 2,0g
Ácido glutâmico 2,0g	Histidina 2,0g	Tirosina 2,0g
Adenina 0,5g	Inositol 2,0g	Treonina 2,0g
Arginina 2,0g	Isoleucina 2,0g	Triptofano 2,0g
Asparagina 2,0g	Leucina 10,0g	Uracila 2,0g
Fenilalanina 2,0g	Lisina 2,0g	Valina 2,0g
Glicina 2,0g	Metionina 2,0g	

4.1.2 Meios de cultura e condições de crescimento de bactérias

Os meios de cultura utilizados para o crescimento de bactérias foram: meio LB (Luria-Bertani) e meio mínimo M9. Com a finalidade de selecionar as cepas com resistência à ampicilina ou canamicina foi adicionado ao meio 100 µg/mL ampicilina ou canamicina, respectivamente. Para crescimento em meio sólido, foi adicionado aos meios 2,0% (p/v) de ágar. Os crescimentos ocorreram a 37ºC e, para crescimento em meio líquido, utilizou-se agitação de 300 rpm em agitador rotatório.

Meio LB

1% (p/v) Triptona

0,5% (p/v) Extrato de levedura

1% (p/v) NaCl

Acertar o pH a 7.5 com NaOH 1N

Meio Mínimo M9

3 g/L KH_2PO_4

6 g/L Na_2HPO_4

0,5 g/L NaCl

2 mM $MgSO_4$

0,4% Glicose (^{13}C)

100 µM $CaCl_2$

10 µg/mL Tiamina

10 µg/mL Biotina

1g/L NH_4Cl

4.1.3 Preparação de DNA plasmidial bacteriano em pequena escala (miniprep)

Para o isolamento rápido e em pequena escala de DNA plasmidial da E. coli foi utilizado o kit QIAprep Spin Miniprep, da Qiagen. A extração de DNA plasmidial através do kit foi efetuada de acordo com as recomendações do fabricante descritas no respectivo protocolo. A solução de DNA plasmidial foi armazenada em água ultrapura estéril a -20ºC.

4.1.4 Transformação de levedura em fase estacionária

Primeiramente, as cepas de levedura foram cultivadas a 28ºC em meio rico YPD2%, durante a noite e sob agitação a 160 rpm, até atingir a saturação (fase estacionária). O volume de 200 µL de células foi coletado em micro tubo de 1,5 e centrifugado por 5000 rpm, temperatura ambiente por 5 s. Após o descarte do sobrenadante, as células foram ressuspendidas em tampão *One Step* (0,2 N acetato de lítio, 40% (p/v) PEG4000 e 100 mM ditiotreitol (DTT). Posteriormente, foi adicionado 50-1000 ng de plasmídeo em um volume final de 100 µL. Após esta etapa, as células foram incubadas a 45ºC por 1 hora e plaqueadas em meio mínimo SD 2% (2% glicose, 0,67% base nitrogenada sem aminoácido, 0,001% requerimentos nutricionais e 2% ágar) na ausência de uracila com a finalidade de selecionar as transformantes.

4.1.5 Determinação da taxa específica de crescimento (µ)

A avaliação do crescimento celular foi determinada por espectrofotometria, através da medida da absorvância a 570 nm de uma suspensão de células, e convertida em concentração de células (mg de peso seco de células/mL). O fator de conversão em peso seco foi calculado a partir da filtração de um volume adequado da suspensão de células em filtro Millipore (45 µm) que, posteriormente, foi colocado sob luz de infravermelho até peso constante.

Para a determinação da velocidade específica de crescimento (µ), foram realizadas medidas da absorvância a 570 nm em intervalos regulares até as células atingirem a fase estacionária. O µ destas células foi determinado na primeira fase de crescimento exponencial pela expressão $\ln X/X0 = \mu t$. Sendo que X0 corresponde a massa de células (mg de peso seco/mL) inicial e X, a massa de células (mg de peso seco/ mL) após um tempo de crescimento t.

4.1.6 Consumo de oxigênio

O consumo de O_2 pelas células crescidas em meio *drop out* foi obtido através de polarografia computadorizada utilizando um eletrodo de Clark em câmara de consumo projetada e construída para este fim (MANNARINO et al., 2008). As células foram separadas do meio de cultivo por centrifugação 3000 g, por 5 min, a temperatura ambiente e colocadas na câmara de consumo na proporção: 3,5 mL tampão (50 mM fosfato de potássio pH 6,0, 100 mM glicose) e 50 µL da suspensão celular contendo 100 µg de células (massa úmida)/100 µL de água destilada. O consumo de oxigênio foi avaliado durante 10 min.

4.1.7 Consumo de glicose

A taxa de consumo de glicose foi avaliada por dosagem da glicose residual no meio por cromatografia líquida de alta eficiência (CLAE). As células foram cultivadas em meio *drop out* e coletadas durante a primeira fase exponencial de crescimento. A suspensão celular foi centrifugada a 3000 g, a temperatura ambiente por 5 min. O sobrenadante foi descartado e o *pellet* foi ressuspendido em tampão (50 mM fosfato de sódio pH 6,0, 20 mM glicose) a uma concentração final de 3 mg peso seco/mL. Foi retirada uma alíquota (ponto zero, 0 min) e centrifugada imediatamente a 14500 g por 5 min, a temperatura ambiente. O sobrenadante foi armazenado para posterior análise por CLAE. Em seguida, a suspensão celular foi incubada a 28ºC, 160 rpm, e alíquotas de 1mL foram retiradas nos pontos referentes a 20, 40 e 60min. Após a retirada das alíquotas, as amostras foram centrifugadas e armazenadas para posterior análise por CLAE.

A glicose residual foi analisada utilizando um sistema de CLAE equipado com um detector de índice de refração RI- 2031 Plus (JASCO, Japão). A glicose foi quantificada em uma coluna Aminex HPX-87H (7.8 mm I.D. × 30 cm, BioRad, EUA), com a temperatura igual a 60 °C utilizando 0,004 mM de ácido sulfúrico como eluente a um fluxo de 0,6 mL/min.

Após a determinação da concentração de glicose residual no sobrenadante em cada uma das alíquotas coletadas ao longo do tempo, foi feita uma curva de ajuste cujo coeficiente angular corresponde à taxa de consumo de glicose ($g.L^{-1}.min^{-1}$).

4.1.8 Estresse com peróxido de hidrogênio

As células, cultivadas até metade da primeira fase exponencial, foram tratadas com 3 mM de peróxido de hidrogênio durante 1 h a 28ºC, 160 rpm. Em seguida, as células foram lavadas duas vezes com água, a fim de interromper o estresse, e utilizadas nos experimentos de viabilidade e peroxidação lipídica. Já quando a fonte de carbono utilizada foi glicerol, a concentração de peróxido de hidrogênio utilizada no experimento foi de 20 mM, tanto para a viabilidade quanto para a peroxidação lipídica.

4.1.9 Viabilidade celular

A viabilidade celular foi analisada por plaqueamento em meio sólido YPD2% antes e após o estresse com peróxido de hidrogênio. O plaqueamento foi feito após diluições seriadas apropriadas para a contagem das colônias em triplicata. As placas foram incubadas a 28ºC por 72 h e o número de colônias contado. A taxa de sobrevivência foi calculada a partir da relação entre o número de colônias obtido antes e após o estresse.

4.1.10 Peroxidação lipídica

Cerca de 50 mg de célula foram centrifugados e lavados duas vezes com água milliQ gelada. Após as lavagens, o *pellet* foi ressuspendido em 500 µL de solução 10% (p/v) ácido tricloroacético, adicionando-se, a seguir, 1,5 g de pérolas de vidro. As células foram rompidas por seis ciclos de agitação violenta em vórtex por 20 s, intercalados com 20 s em banho de gelo. O sobrenadante foi obtido após a centrifugação a 2000 *g* por 5 min, temperatura ambiente. O nível de peroxidação lipídica foi determinado pelo método TBARS (*Tiobarbithuric Acid Reagents Species*) (STEELS; LEARMONTH; WATSON, 1994). O ensaio foi feito com 150 µL de extrato, 150 µL de 10% (p/v) ácido tricloroacético, 100 µL de 0,1 M EDTA e 600 µL de 1% (p/v) ácido tiobarbitúrico em 0,05 M NaOH, para um volume final de 1 mL. A mistura reacional foi incubada em tubos de micro centrífuga a 100ºC por 15 min. A seguir, os tubos foram resfriados e a absorvância determinada por espectrofotometria a 532 nm. Cada ensaio foi realizado em duplicata e os resultados expressos em picomoles de malonaldialdeído, um produto da peroxidação lipídica, por miligrama de célula (pmoles MDA/mg célula). O resultado final, expresso em vezes de aumento, foi calculado

através da razão entre a peroxidação após o estresse com peróxido de hidrogênio e o controle (antes do estresse).

4.1.11 Analise de dados e análise estatística

Os resultados de todos os experimentos representam a média ± desvio padrão de no mínimo 3 experimentos independentes para cada condição e cepa testada. Para a análise dos resultados, foi feito primeiramente o teste F para a análise das variâncias e, posteriormente, os resultados foram analisados utilizando o teste *t* de Student. As barras marcadas com asteriscos representam resultados estatisticamente diferentes para um p abaixo de 0,05 dentro de cada condição ou cepa estudada.

4.1.12 Análise de bioinformática

As sequências dos domínios PWWP de NSD3s (UniProt #Q9BZ95-3) e Pdp3 (UniProt #Q06188) foram coletados a partir do banco de dados UniProt (THE UNIPROT CONSORTIUM, 2013). As sequências foram alinhadas utilizando o programa T-coffee (NOTREDAME; HIGGINS; HERINGA, 2000). O servidor *ITasser* foi usado para a modelagem *ab initio* dos domínios PWWP de NSD3s e Pdp3 (ROY; KUCUKURAL; ZHANG, 2011). Os *TM-scores* e desvios quadráticos médios (RMSDs) dos modelos tridimensionais foram calculados utilizando o programa *TM-Align* (ZHANG; SKOLNICK, 2005).

4.2 METABOLÔMICA

4.2.1 Cepas e condições de cultivo de S. cerevisiae

As cepas NSD3s^{+} e Pdp3^{+} foram cultivadas em meio *drop out* com glicerol 4% como fonte de carbono até metade da fase exponencial.

4.2.2 Extração dos metabólitos polares

As cepas NSD3s^{+} e Pdp3^{+} foram cultivadas em meio *drop out* com glicerol 4% como fonte de carbono até metade da fase exponencial. Alíquotas de células referentes a 100 O.D.$_{600}$ foram recolhidas, centrifugadas a 7224 *g* por 5 min a 4 °C, lavadas três vezes com água milliQ gelada e congeladas a -80 °C. Em seguida, as

células foram vortexadas em 3 mL de solução 75% (v/v) etanol, utilizando 2 mL de pérolas de vidro de 450-600 µm de diâmetro. As células foram rompidas por doze ciclos de agitação violenta em vórtex por 30 s, intercalados com 30 s em banho de gelo. Os extratos celulares foram centrifugados a 2000 *g* por 5 min a 4 ^{o}C. Uma alíquota de 1,6 mL de sobrenadante foi coletada e evaporada utilizando *speedvac* (AIROLDI ET AL, 2015). Em seguida, as amostras foram armazenadas a -80^{o}C para posterior análise por RMN (Ressonância Magnética Nuclear). Os extratos foram ressuspendidos em 600 µL de tampão 50 mM fosfato de sódio, pH 7,4, 10% (v/v) D_2O e 0,1 mM ácido 4,4-dimetil-4-silapentano-1-sulfónico (DSS). O DSS foi usado como referência interna de deslocamento químico do ^{1}H (δ^{1}H = 0 ppm).

4.2.3 Espectroscopia de RMN

Os espectros de RMN foram coletados a 25^{o}C em um espectrômetro Bruker Avance III operando na frequência de 500,13 MHz para ^{1}H. Os espectros 1D ^{1}H RMN foram adquiridos com a sequência de pulsos *excitation sculpture* para supressão do sinal da água, largura espectral de 20 ppm, tempo de relaxação de 1,74 s, 65536 pontos e 1024 de acumulações. Foi utilizado um filtro de CPMG (*Carr-Purcell-Meiboom-Gill*) (atraso spin-eco de 500 µs, loop 64 vezes) para suprimir os sinais indesejados de moléculas de alto peso molecular. Além disso, espectros 2D [^{1}H-^{13}C] HSQC, 2D [^{1}H-^{1}H] TOCSY e 2D pJRES foram utilizados para a atribuição das ressonâncias. Para os assinalamentos, foram utilizados os bancos de dados HMDB (*Human Metabolomic Database*) 3.0 (WISHART et al., 2013) e BMRB (*Biological Magnetic Data Resonance Bank*) (ULRICH et al., 2008), além do próprio programa COLMARm (ROBINETTE et al., 2008). Os espectros foram processados com o programa TopSpin 3.2 (Bruker-Biospin). Os espectros cujas correção de fase e/ou ajuste de linha base não foram considerados satisfatórios foram excluídos da análise. Os espectros processados foram fracionados em intervalos (*buckets*) de 0,03 ppm após a eliminação da região da água (4,6-4,9 ppm), etanol (1,15-1,18 ppm e 3,64-3,66 ppm) e sinais de 8,19-8,26 ppm, e exportados para o programa AMIX (Bruker-Biospin) para a análise multivariada.

4.2.4 Análise estatística

Para a análise estatística, foram utilizados conjuntos de dados independentes coletados para 6 extratos polares de células WT, 5 de células que superexpressavam de NSD3s e 4 de células que superexpressavam Pdp3. Utilizou-se análise multivariada para discriminar o efeito da superexpressão de NSD3s ou Pdp3 sobre o perfil metabólico das células de levedura. Todos os espectros foram processados utilizando o programa TopSpin 3.2 (Bruker-Biospin). Os espectros processados foram fracionados em intervalos (*buckets*) de 0,03 ppm, normalizamos pela soma das intensidades e escala de Pareto. Em seguida, o método de análise de componentes principais (PCA) foi utilizado (RAMADAN et al., 2006). A separação dos *buckets* foi realizada com o programa AMIX (Bruker-Biospin), enquanto a análise multivariada foi realizada com o programa MetaboAnalyst 3.0 (XIA; WISHART, 2016).

A análise univariada foi realizada através do múltiplo teste t, usando a correção para comparações múltiplas pelo método de Holm-sidak. A análise foi feita no programa GraphPad Prism 6.0, com nível de confiança de 95%.

5 RESULTADOS

5.1 ANÁLISE FENOTÍPICA

NSD3s codifica uma proteína de 645 aminoácidos que possui um único domínio PWWP (YANG et al., 2010; ZHOU et al., 2010). O domínio PWWP é encontrado em uma diversidade de proteínas que desempenham papel central na divisão, crescimento e diferenciação celular. Várias dessas proteínas estão ligadas ao câncer e a outras patologias (SLATER; ALLEN; BYCROFT, 2003) ou agem como fatores de crescimento. A *S. cerevisiae* possui uma proteína, Pdp3, que contém um domínio PWWP e mais nenhum outro domínio enovelado (STEC et al., 2000). Pdp3 é um membro do complexo NuA3. Esse complexo apresenta uma atividade de histona acetil-transferase envolvida na transcrição do DNA. A maioria dos genes controlados pelo complexo NuA3 estão envolvidos na replicação do DNA (GILBERT et al., 2014).

Através de alinhamento de sequência, foi mostrado que o domínio PWWP de Pdp3 apresenta 25% de identidade com o domínio PWWP de NSD3s de humanos (RONA, 2014). Foi realizada a modelagem estrutural *ab initio* dos domínios PWWP de NSD3s e Pdp3 utilizando o servidor *I-TASSER* (Figura 9) (ROY; KUCUKURAL; ZHANG, 2011). Os modelos estruturais mostraram que ambas as proteínas são compostas por um subdomínio amino-terminal que adota um enovelamento em β-barril, implicado no reconhecimento de lisinas metiladas em histonas (YANG et al., 2010), e um subdomínio carboxi-terminal α-helicoidal (Figura 9). Foi realizado o alinhamento entre os modelos estruturais dos domínios PWWP de NSD3s e Pdp3 utilizando a ferramenta TM-Align (ZHANG; SKOLNICK, 2005). O TM-score foi utilizado para avaliar a similaridade topológica entre as estruturas tridimensionais, enquanto o RMSD mediu a distância média entre os átomos das proteínas sobrepostas. Tais parâmetros foram utilizados para analisar a topologia e a similaridade estrutural entre os modelos (DE CARVALHO; DE MESQUITA, 2013; JIMENEZ-LOPEZ et al., 2010). O valor de RMSD entre os modelos calculados para Pdp3-PWWP e NSD3s-PWWP foi de 3,8 Å. Esta diferença de RMSD é consistente com estruturas tridimensionais semelhantes (ROY; KUCUKURAL; ZHANG, 2011). O TM-score encontrado ao alinhar os dois domínios foi de 0,5, sugerindo um enovelamento similar (STRAHL et al., 2002). Apesar da baixa similaridade de sequência, a análise de bioinformática indicou que os domínios PWWP de Pdp3 e NSD3s são altamente similares em termos

conformacionais (Figura 9) e, portanto, possivelmente guardam uma relação funcional.

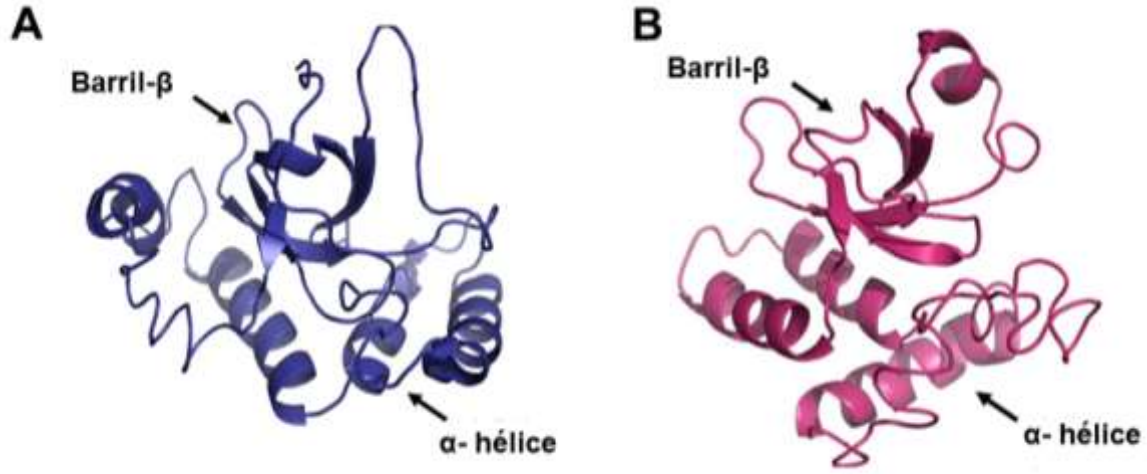

Figura 9. Modelos estruturais dos domínios PWWP de NSD3s e Pdp3. (A) Modelo estrutural de NSD3s-PWWP(azul). (B) Modelo estrutural de Pdp3-PWWP(rosa). O subdomínio amino-terminal em barril-β e o subdomínio carboxi-terminal em α-hélice estão indicados.

Os domínios PWWP possuem uma gaiola aromática capaz de interagir com lisinas metiladas específicas em histonas. Os resíduos aromáticos que compõem esse sítio de interação são frequentemente conservados em domínios PWWP e ocupam as posições F18, W21 e F48 na sequência de Pdp3 (GILBERT et al., 2014). Gilbert e colaboradores (2014), mostraram *in vitro*, que a mutação nesses sítios abole a interação com a histona, sendo crucial para o reconhecimento de H3K36 (GILBERT et al., 2014). Para avaliar a importância da integridade da gaiola aromática na função metabólica de Pdp3, foi construído o mutante Pdp3 W21A, onde o resíduo de triptofano na posição 21 foi substituído por alanina. Esse mutante foi superexpresso em uma cepa de levedura onde a Pdp3 endógena foi excluída (*Δpdp3*). As células foram cultivadas em glicose, uma fonte de carbono que favorece o metabolismo fermentativo, logo o fenótipo metabólico se assemelha ao de uma célula com características tumorais. Tanto a cepa *Δpdp3* (RONA, 2014) quanto a W21A^{+} apresentaram características fenotípicas semelhantes quando comparadas ao controle. Ambas as linhagens de levedura apresentaram taxa de crescimento específica menores em relação a cepa controle (Figura 10A). Além disso, células WT apresentaram taxas de consumo de glicose significativamente mais elevadas do que

as mutantes (Figura 10B).

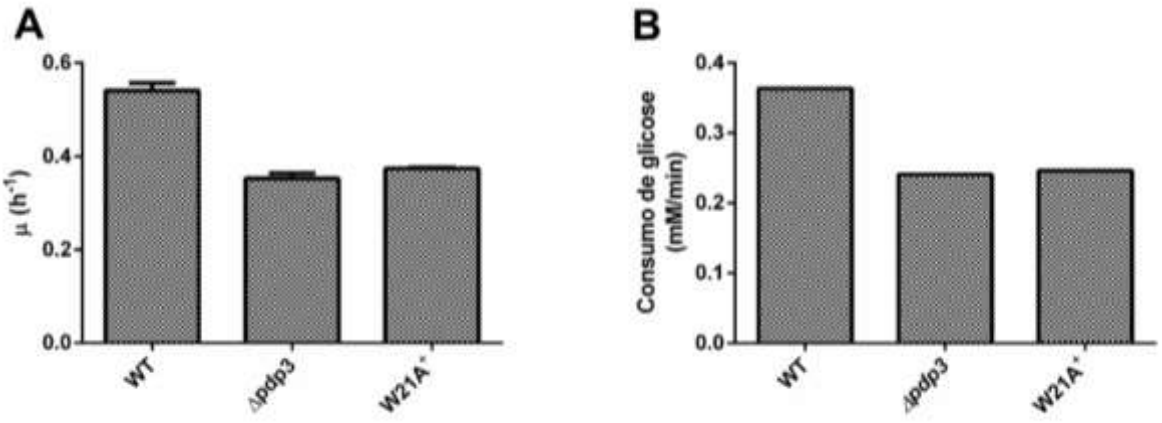

Figura 10. A mutação W21A, assim como a deleção de Pdp3, muda o metabolismo de fermentativo para oxidativo. As cepas WT, ***Δpdp3*** e W21A$^+$ foram cultivadas em meio contendo glicose 2% até o meio da 1ª fase de crescimento exponencial. (A) Taxa de crescimento específico. As medidas de absorvância a 570 nm foram realizadas em intervalos regulares até as células atingirem a fase estacionária. O μ destas células foi determinado na fase de crescimento exponencial pela expressão ln $X/X_0 = \mu t$. (B) Taxa de consumo de glicose. A taxa do consumo de glicose residual foi determinada utilizando CLAE. Os resultados representam a média ± desvio padrão de pelo menos três experimentos independentes e * ou ** significam resultados diferentes em WT *vos* ***Δpdp3*** * p <0,05 e WT *v*s W21A$^+$ ** p <0,05.

Em relação à sensibilidade a espécies reativas de oxigênio, tanto a deficiente em Pdp3 quanto a W21A$^+$ apresentaram maior tolerância a EROs (Figura 11). Após estresse com peróxido de hidrogênio por uma hora, as cepas ***Δpdp3*** e W21A$^+$ apresentaram maior viabilidade e menor nível de peroxidação lipídica quando comparadas a controle (Figura 11). Estes resultados corroboram os de Gilbert e colaboradores que demonstraram que todas as três mutações (F18, W21 e F48) são capazes de abolir, de forma independente, a interação entre Pdp3 e um peptídeo derivado de histona contendo a marca epigenética H3K36me3, sugerindo que Pdp3-PWWP requer a gaiola hidrofóbica conservada para ligar-se à cromatina (GILBERT et al., 2014). Como as cepas W21A$^+$ e ***Δpdp3*** apresentaram o mesmo fenótipo quando comparados com a cepa controle, concluímos que a gaiola hidrofóbica do domínio PWWP de Pdp3 é essencial para a sua função metabólica.

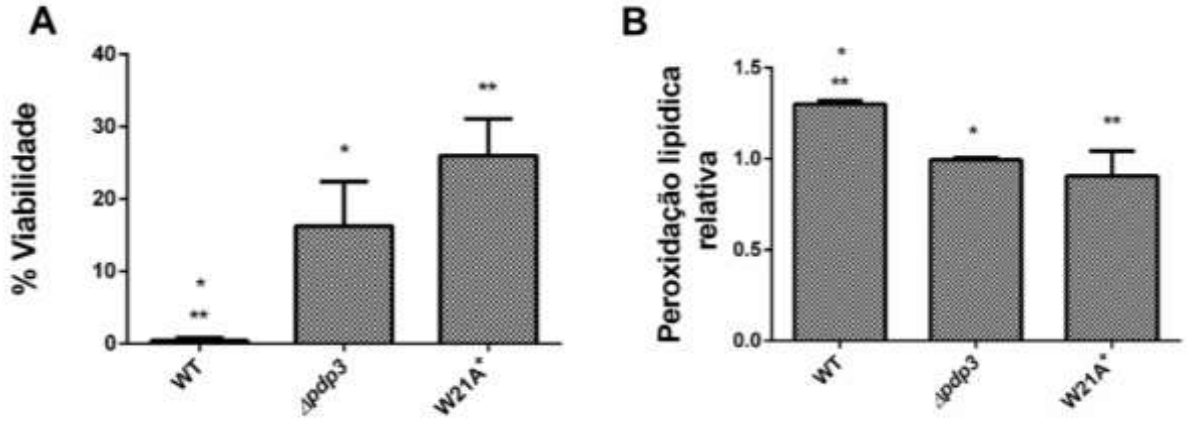

Figura 11. Efeito da mutação W21A na tolerância ao estresse oxidativo. As cepas WT, *Δpdp3* e W21A^{+} foram cultivadas em meio contendo glicose 2% até o meio da 1ª fase de crescimento exponencial. Os danos oxidativos foram analisados após estresse com 3 mM H_2O_2/1 h/28 ºC/160 rpm. (A) Viabilidade celular. A viabilidade celular foi medida através de plaqueamento das células em meio rico YPD2% sólido. (B) Peroxidação lipídica. Os níveis de peroxidação lipídica foram determinados pelo método de TBARS. Os resultados representam a média ± desvio padrão de pelo menos três experimentos independentes e * ou ** significam resultados diferentes em WT *vs Δpdp3* * p <0,05 e WT *vs* W21A + ** p <0,05.

Posteriormente, foi analisado o efeito da superexpressão de Pdp3 sobre os mesmos fenótipos. Foi observado que a superexpressão de Pdp3 induziu um efeito sobre o metabolismo celular semelhante à superexpressão de NSD3s (RONA, 2014). A superexpressão de NSD3s em *S. cerevisae*, em metabolismo oxidativo, leva ao aumento da taxa de crescimento específica (μ) e a diminuição no consumo de oxigênio, indicando que a superexpressão de NSD3s é capaz de diminuir a capacidade respiratória das células para uma proliferação mais rápida. Além disso, a superexpressão de NSD3s torna a célula de levedura mais sensível a exposição a espécies reativas de oxigênio (RONA, 2014). A NSD3s é capaz de alterar o metabolismo celular de aeróbico (respiração) para anaeróbico (fermentação) sugerindo que as células de levedura superexpressando NSD3s exibem um fenótipo semelhante a células tumorigênicas, sob condições que estimulam a respiração (RONA, 2014). Quando cultivadas em glicerol, as células de levedura superexpressando Pdp3 exibiram taxa de crescimento específico aumentado (Figura 12A), diminuição da taxa de consumo de oxigênio (Figura 12B) e maior sensibilidade a EROs em relação a WT (Figura 13). A Figura 13A mostra que as cepas Pdp3^{+} de levedura foram menos viáveis do que a controle quando submetidas a condições de estresse oxidativo. Além disso, as mutantes Pdp3^{+} apresentaram maiores níveis de

peroxidação lipídica após uma hora de exposição a peróxido de hidrogênio (20 mM) (Figura 13B). A superexpressão de Pdp3 foi capaz de induzir uma mudança no metabolismo em direção a fermentação, semelhante à superexpressão do oncogene NSD3s.

Com a finalidade de avaliar a semelhança funcional entre os domínios PWWP de NSD3s e Pdp3, foi construída uma forma quimérica de Pdp3, onde domínio PWWP de Pdp3 foi substituído pelo domínio PWWP de NSD3s. Com isso, foi possível analisar se o domínio PWWP de NSD3s é capaz de substituir funcionalmente o domínio PWWP da Pdp3 de levedura. Quando cultivadas em glicerol, as células que expressaram a quimera apresentaram maior taxa de crescimento específico (Figura 12A), menor consumo de oxigênio (Figura 12B) e aumento da sensibilidade a EROs (Figura 13) do que a WT, assim como a superexpressão de NSD3s ou de Pdp3. Esses resultados mostram que o domínio PWWP da proteína NSD3s humana foi capaz de substituir funcionalmente o da proteína de levedura Pdp3 no metabolismo respiratório.

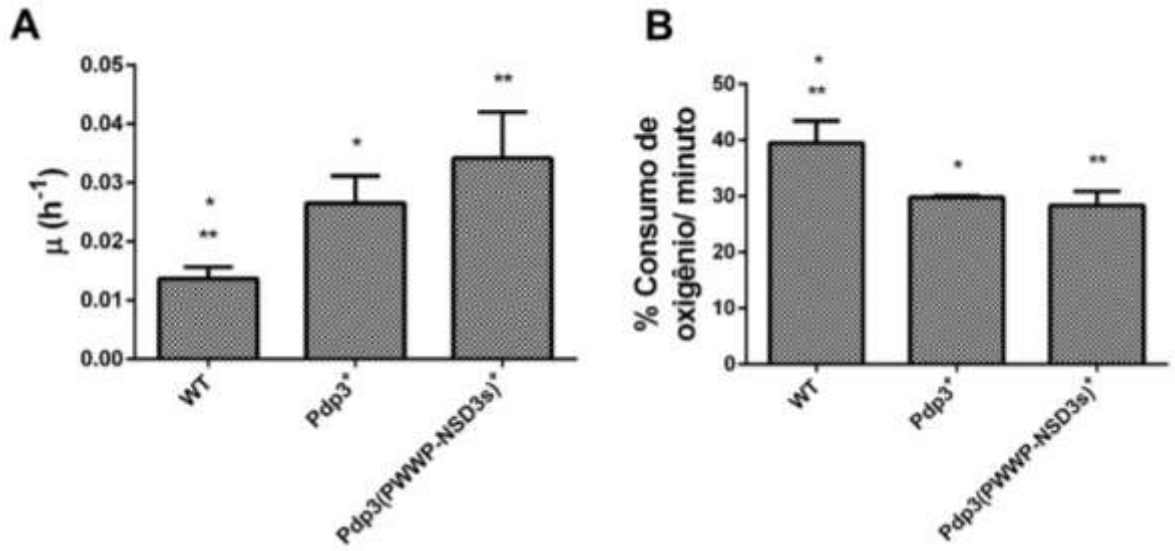

Figura 12. O domínio PWWP de NSD3s substitui funcionalmente o de Pdp3. As cepas WT, Pdp3^{+} e Pdp3 (PWWP-NSD3s)$^{+}$ foram cultivadas em meio *drop out* glicerol 4% até o meio da fase de crescimento exponencial. (A) Taxa de crescimento específico. As medidas da absorvância a 570 nm foram realizadas em intervalos regulares até as células atingirem a fase estacionária. O μ destas células foi determinado na fase de crescimento exponencial pela expressão ln $X/X_0 = \mu t$. (B) Consumo de oxigênio. O consumo de oxigênio foi dosado utilizando um eletrodo de Clark. Os resultados representam a média ± desvio padrão de pelo menos três experimentos independentes e * ou** significa resultados diferentes em WT *vs* Pdp3+ * p <0,05 e WT *vs* Pdp3 (PWWP-NSD3s)$^{+}$ ** p <0,05.

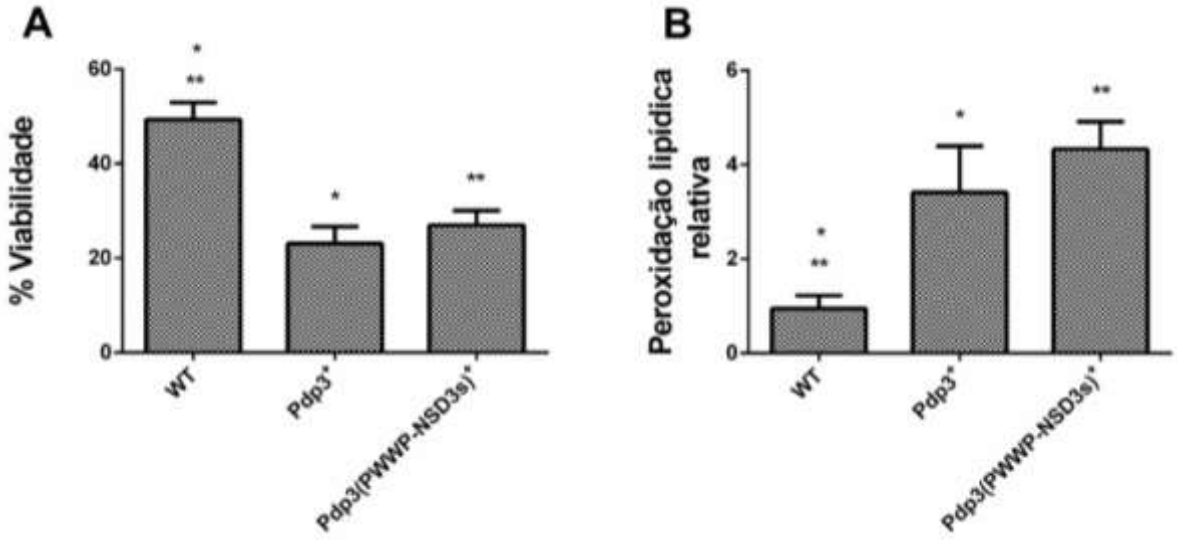

Figura 13. Efeito da superexpressão de Pdp3 e da quimera (Pdp3 (PWWP-NSD3s)) na tolerância ao estresse oxidativo. As cepas WT, Pdp3$^+$ e (Pdp3 (PWWP-NSD3s)$^+$ foram cultivadas em meio *drop out* glicerol 4% até o meio da fase de crescimento exponencial. Os danos oxidativos foram analisados após estresse com 20 mM H_2O_2/1 h/28 ^oC/160 rpm. (A) Viabilidade celular. A viabilidade celular foi medida através de plaqueamento das células em meio rico YPD2% sólido. (B) Peroxidação lipídica. Os níveis de peroxidação lipídica foram determinados pelo método de TBARS. Os resultados representam a média ± padrão desvio de pelo menos três experimentos independentes e * ou ** resultados diferentes no WT *vs* PDP3$^+$ * p <0,05 e WT *vs* Pdp3 (PWWPNSD3s)$^+$ ** p <0,05.

Para confirmar que o domínio PWWP regula a mudança metabólica através de um mecanismo depende da capacidade de Pdp3 de se ligar à cromatina metilada, Pdp3 foi superexpressa em uma cepa *Δset2*. A proteína Set2 de *S. cerevisiae* é uma histona (H3) metil-transferase altamente seletiva para lisina 36 (H3K36) (STRAHL et al., 2002). Como mostrado na Figura 14, a superexpressão de Pdp3 não causou qualquer alteração no comportamento metabólico da cepa *Δset2*. Ambos *Δset2* e *Δset2*(Pdp3)$^+$ exibiram a mesma taxa de crescimento específico (Figura 14A) e de consumo de oxigênio (Figura 14B). Além disso, a tolerância ao estresse oxidativo permaneceu inalterado, na qual a viabilidade e peroxidação lipídica foram estatisticamente iguais entre as cepas (Figura 14C e 14D). Esses resultados indicam que o fenótipo metabólico induzido pela superexpressão de Pdp3 depende da metilação específica de H3K36, que é realizado por Set2. Estes resultados corroboram os obtidos com a cepa mutante W21A$^+$, sugerindo que o efeito da superexpressão de Pdp3 nas alterações metabólicas depende da capacidade do seu domínio PWWP de reconhecer e se ligar a H3K36 metilada.

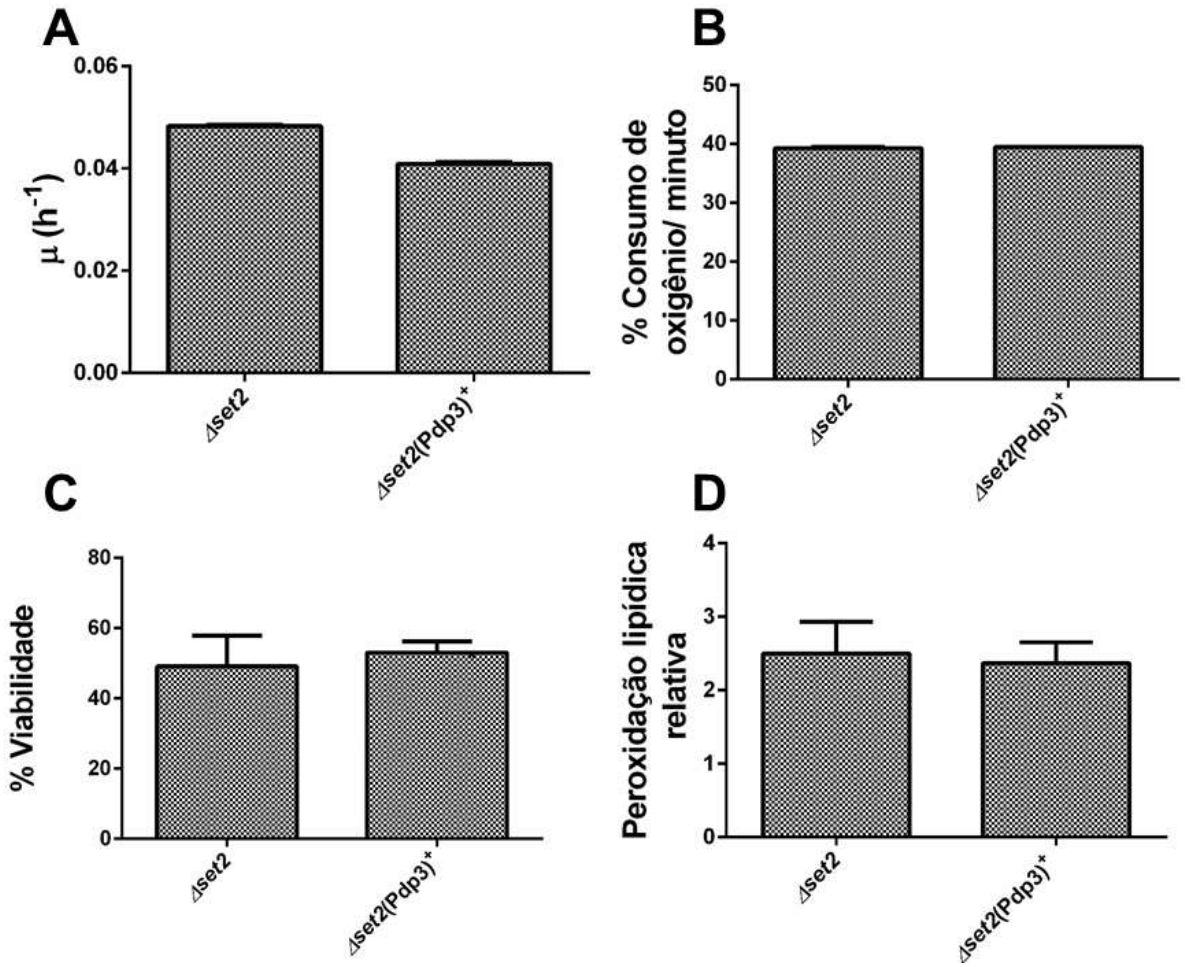

Figura 14. Set2 é essencial para o reconhecimento de H3K36me3 por Pdp3. As cepas *Δset2* e *Δset2Pdp3*$^{+}$ foram cultivadas em meio *drop out* glicerol 4% até o meio da fase de crescimento exponencial. Os danos oxidativos foram analisados após estresse com 20 mM H_2O_2/1 h/28 ^{o}C/160 rpm. (A) Taxa de crescimento específico. As medidas da absorvância a 570 nm foram realizadas em intervalos regulares até as células atingirem a fase estacionária. O μ destas células foi determinado na fase de crescimento exponencial pela expressão ln $X/X_0 = \mu t$. (B) Consumo de oxigênio. O consumo de oxigênio foi dosado utilizando um eletrodo de Clark. (C) Viabilidade (D) Peroxidação lipídica. Os níveis de peroxidação lipídica foram determinados pelo método de TBARS. Os resultados representam a média ± desvio padrão de pelo menos três experimentos independentes.

Ao interagir com H3K36me3, Pdp3 recruta o complexo NuA3b para regiões codificantes de genes ativamente transcritos (GILBERT et al., 2014). Sas3, uma subunidade do complexo NuA3b, é uma histona acetil-transferase que acetila H4, H3 e H2A (TAKECHI; NAKAYAMA, 1999). No entanto, ainda não se sabe a função completa do complexo NuA3b e o alvo específico de acetilação de Sas3 [43]. Para verificar se a função metabólica de Pdp3 é dependente do complexo NuA3b, Pdp3 foi superexpressa em uma cepa *Δsas3*. A superexpressão de Pdp3 não leva a qualquer mudança no comportamento metabólico de *Δsas3* (Figura 15), sugerindo que, sob

condições respiratórias, o complexo NuA3b é responsável por mediar o desvio metabólico induzido por Pdp3.

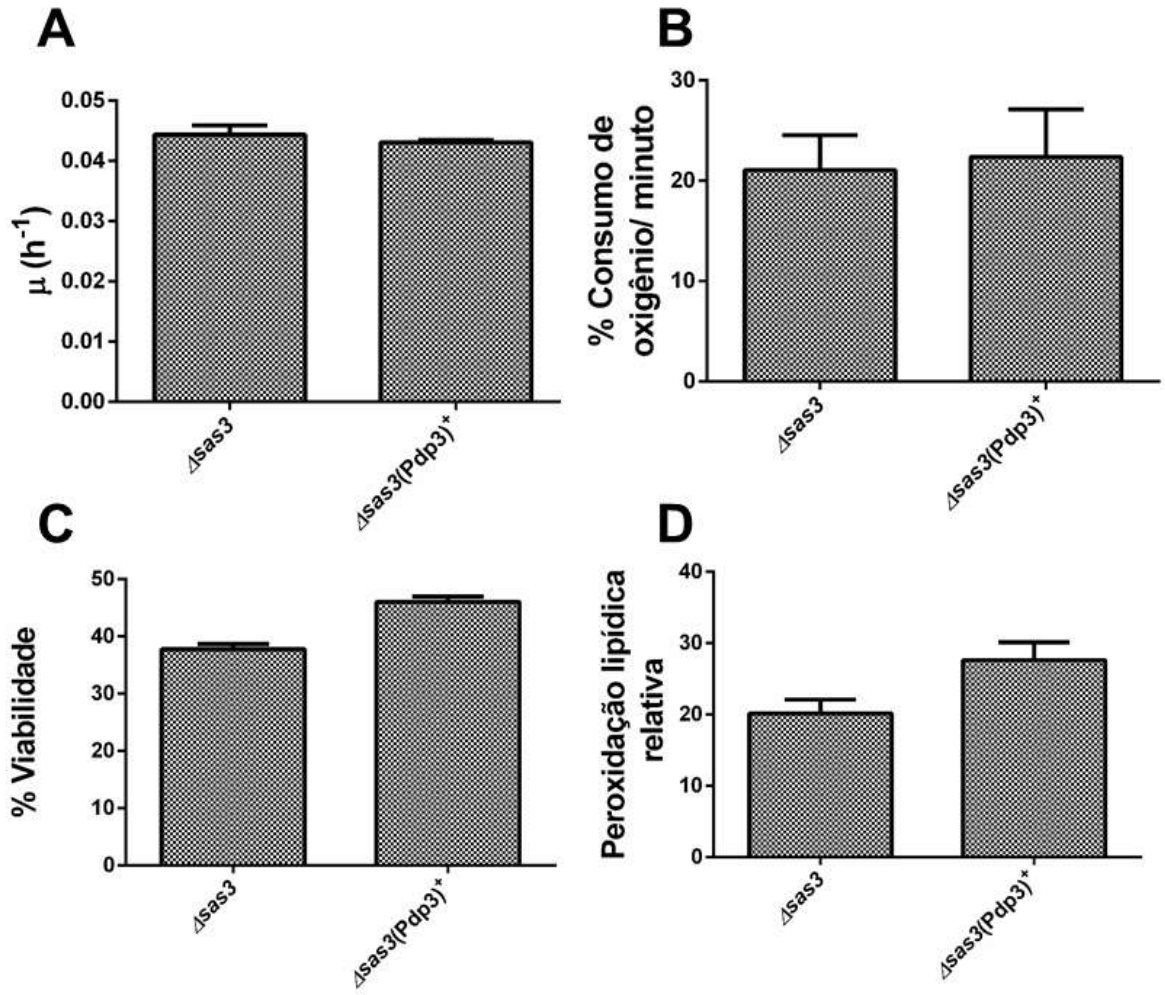

Figura 15. Sas3 é essencial para o desvio metabólico induzido por Pdp3. As cepas *Δsas3* e *Δsas3* Pdp3⁺ foram cultivadas em meio *drop out* glicerol 4% até o meio da fase de crescimento exponencial. Os danos oxidativos foram analisados após estresse com 20 mM H_2O_2/1 h/28 ^oC/160 rpm. (A) Taxa de crescimento específico. As medidas da absorvância a 570 nm foram realizadas em intervalos regulares até as células atingirem a fase estacionária. O μ destas células foi determinado na fase de crescimento exponencial pela expressão $\ln X/X_0 = \mu t$. (B) Consumo de oxigênio. O consumo de oxigênio foi dosado utilizando um eletrodo de Clark. (C) Viabilidade celular. A viabilidade celular foi medida através de plaqueamento das células em meio rico YPD2% sólido. (D) Peroxidação lipídica. Os níveis de peroxidação lipídica foram determinados pelo método de TBARS. Os resultados representam a média ± desvio padrão de pelo menos três experimentos independentes.

5.2 ANÁLISE METABOLÔMICA

No item 5.1 deste documento foi demonstrado que a superexpressão de Pdp3 ou NSD3s em *S. cerevisiae*, cultivadas sob metabolismo oxidativo, levou a um aumento na taxa de crescimento e sensibilidade a espécies reativas de oxigênio,

enquanto diminuiu o consumo de oxigênio. Para obter mais informações sobre os mecanismos moleculares que resultaram nesse fenótipo resultante, foram analisados os metabólitos mais relevantes produzidos em resultado a superexpressão de NSD3s ou Pdp3 em meio oxidativo. A cepa WT, usada como controle, assim como as linhagens $Pdp3^{+}$ e $NSD3s^{+}$ foram cultivadas em glicerol até a metade da fase exponencial. Os metabólitos polares foram submetidos à análise metabolômica por RMN, e os espectros ^{1}H 1D NMR foram atribuídos para determinar os metabólitos mais relevantes (Figura 16).

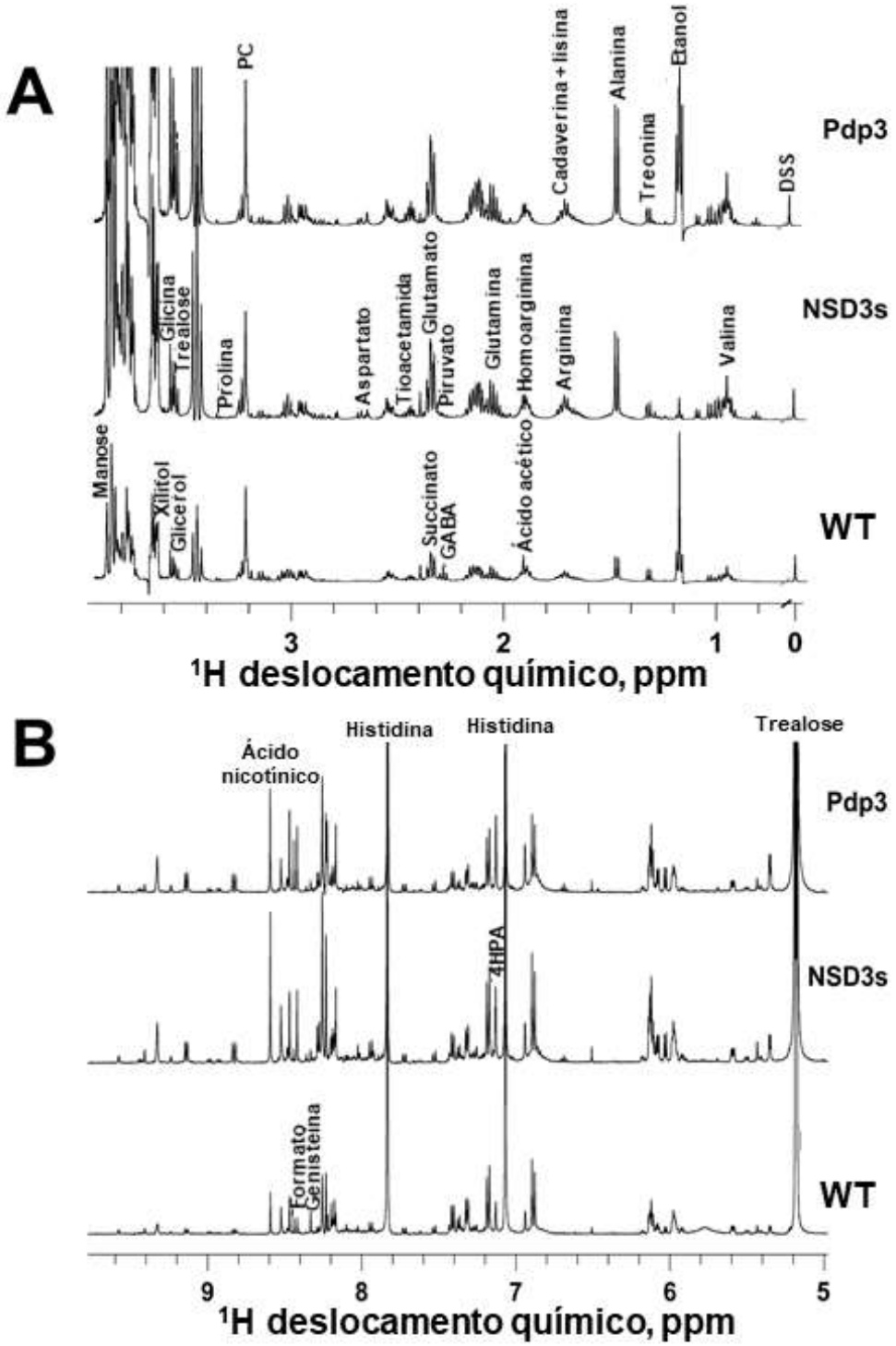

Figura 16. Espectros de ^{1}H-RMN de 1D a partir de extracto polar de culas de levedura. Região alifática (A) e aromática (B). PC-fosfocolina; Ácido DSS-4,4-dimetil-4-silapentano-1-sulfónico; GABA-gama amibutirato.

As Figuras 17A e 17B mostram os gráficos de PCA (Análise da Componente Principal) para NSD3s^{+} x WT e Pdp3^{+} x WT, respectivamente. Os gráficos de PCA mostraram forte discriminação de classe entre o controle e as células que superexpressam NSD3s/Pdp3 (Figura 17A e 17B). Ao analisar o efeito da superexpressão de NSD3s em relação a WT, observou-se um aumento no conteúdo de alanina, piruvato, valina, glutamato e aspartato. Por outro lado, o conteúdo de homoarginina, histidina, prolina e arginina foi diminuído (Tabela 2, Figura 18A). Ao analisar o efeito da superexpressão de Pdp3 em relação a WT, observou-se um aumento no conteúdo de alanina, fosfocolina e aspartato. Além disso, foi detectado uma diminuição de arginina, histidina, homoarginina, aspartato, treonina, aspartato + manose e cadaverina + lisina (Tabela 3, Figura 18B). Comparando o perfil metabólico de NSD3s^{+} e Pdp3^{+}, foram observadas mudanças similares nos metabólitos mais relevantes, tais como um aumento nos níveis de alanina e aspartato, acompanhado de uma diminuição em histidina e arginina (Figura 18C). Além disso, certos metabólitos exibiram um perfil específico para cada proteína, incluindo um aumento nos níveis de glutamato e valina em NSD3s^{+} e um aumento no teor de fosfocolina em Pdp3^{+} (Figura 18C). Apesar de suas particularidades, as adaptações metabólicas em resposta a superexpressão de NSD3s ou Pdp3 são similares àquelas observadas em células tumorais, como aumento da glutaminólise.

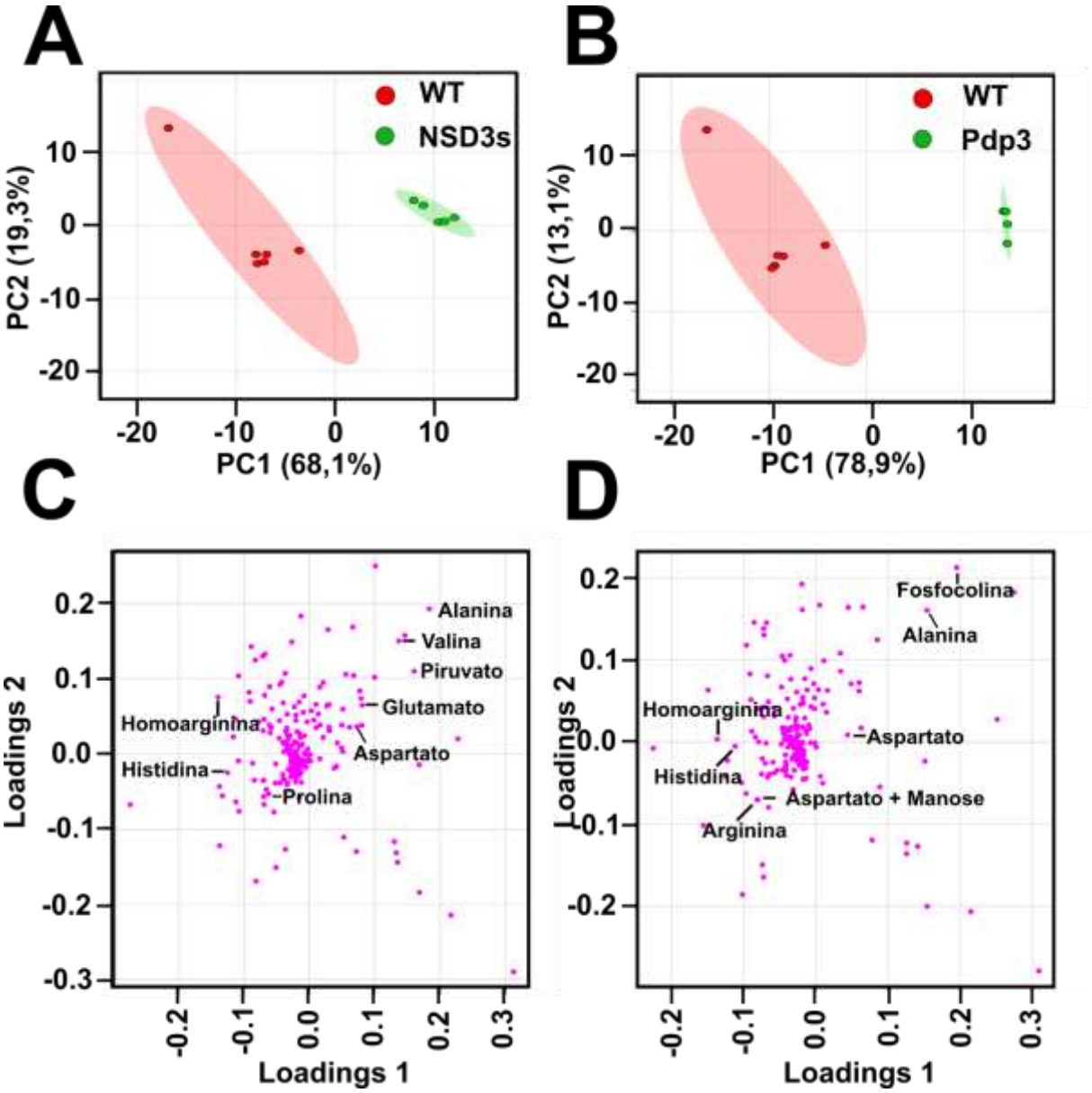

Figura 17. A superexpressão de NSD3s ou Pdp3 promove uma alteração similar no metaboloma celular. Gráficos de PCA mostram uma forte discriminação de classe entre replicatas do controle (WT) (vermelho) e superexpressão de NSD3s (verde) (A) e entre replicatas do controle (WT) (vermelho) e superexpressão de Pdp3 (verde) (B). Os *loadings plots* do PCA destacam metabólitos importantes para a discriminação de classes entre NSD3s^{+} e WT, como glutamato, aspartato e alanina (C), e entre Pdp3^{+} e WT, como fosfocolina, aspartato e alanina (D).

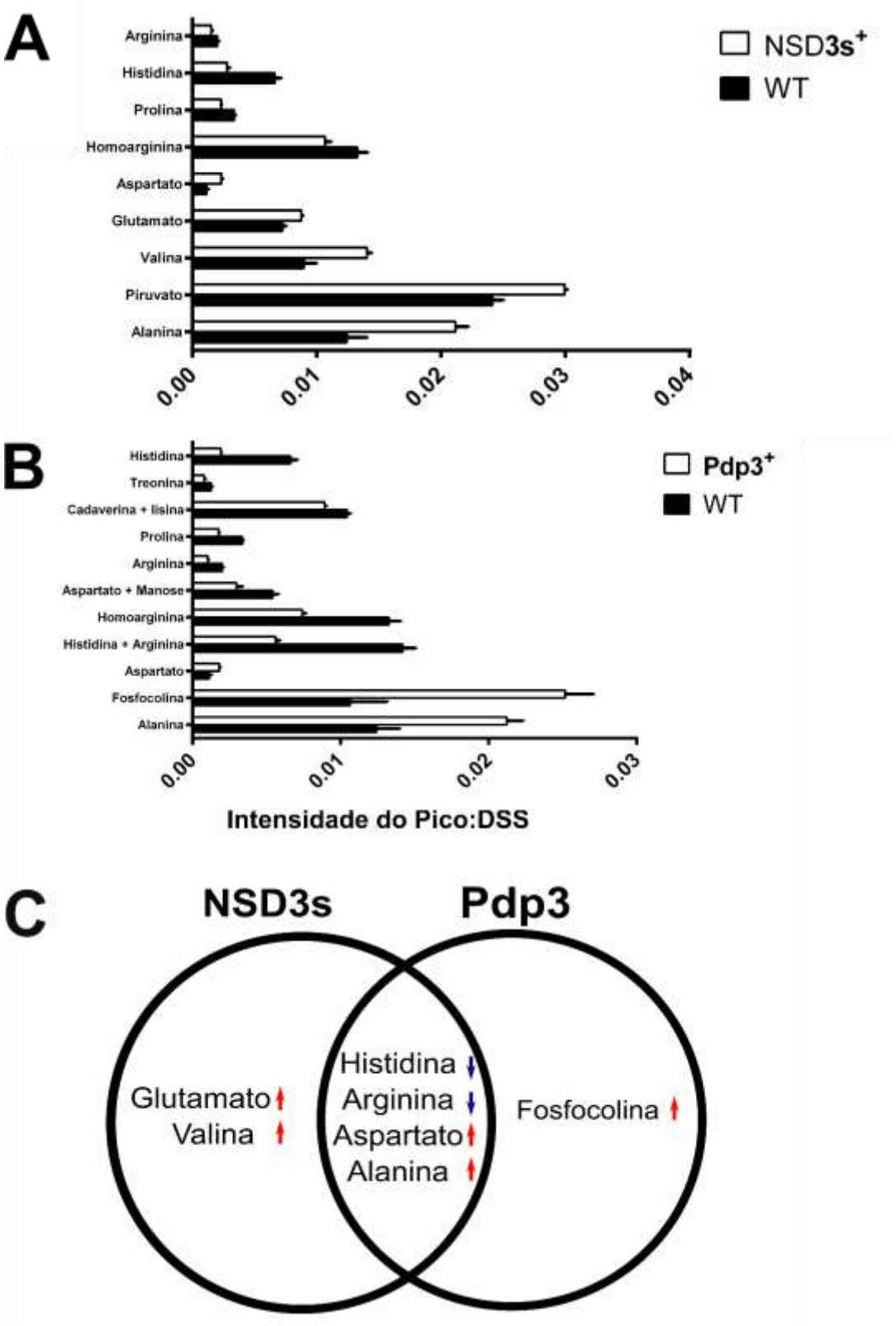

Figura 18. Metabólitos alterados pela superexpressão de NSD3s ou Pdp3. O efeito da superexpressão de NSD3s (branco) contra WT (preto) (A). O efeito da superexpressão de Pdp3 (branco) contra WT (preto) (B). Diagrama representativo dos principais metabólitos detectados na superexpressão de NSD3s ou Pdp3. Setas azuis representam a diminuição e setas vermelhas representam o aumento (C).

Tabela 2. Metabólitos alterados pela superexpressão de NSD3s. A tabela mostra características importantes dos metabólitos identificados: estado em função da superexpressão de NSD3s (↑ aumentado e ↓ diminuído), deslocamento químico de próton, coeficientes de regressão do PCA nos componentes 1 e 2 (comp1 e comp2) e valor de p (p <0,05).

Metabólito	Estado	**δH (ppm)**	Comp1	Comp2	p value
Alanina	↑	1.46	0,18323	0,19269	0,000573
Piruvato	↑	2.34	0,16026	0,10985	0,000039
Valina	↑	0.96	0,13661	0,14995	0,000489
Histidina	↓	7.06	-0,13746	-0,043354	0,000017
Arginina	↓	1.61	-0,044987	-0,038565	0,000965
Homoarginina	↓	1.88	-0,11615	0,022653	0,029446
Prolina	↓	3.32	-0,069595	-0,03496	<0,000001
Aspartato	↑	2.66	0,07268	0,035966	0,000033
Glutamato	↑	2.36	0,080825	0,064629	0,000609

Tabela 3. Metabólitos alterados pela superexpressão de Pdp3. A tabela mostra características importantes dos metabólitos identificados: estado em função da superexpressão de NSD3s (↑ aumentado e ↓ diminuído), deslocamento químico de próton, coeficientes de regressão do PCA nos componentes 1 e 2 (comp1 e comp2) e valor de p (p <0,05).

Metabólito	Estado	**δH (ppm)**	Comp1	Comp2	p value
Alanina	↑	1.46	0,15438	0,16036	0,002973
Fosfocolina	↑	3.20	0,19552	0,2124	0,002663
Histidina	↓	7.06	-0,12284	-0,02251	0,000017
Arginina	↓	1.61	-0,053594	-0,034463	0,000017
Homoarginina	↓	1.88	-0,13699	0,0033875	0,000164
Prolina	↓	3.32	-0,070288	-0,026126	<0,000001
Aspartato	↑	2.66	0,044151	0,0085807	0,008473
Aspartato +manose	↓	3.89	-0,081661	-0,070484	0,003189
Cadaverina + lisina	↓	1.70	-0,069145	-0,0014328	0,000504
Treonina	↓	4.22	-0,038901	-0,0062421	0,003414

6 DISCUSSÃO

6.1 ANÁLISE FENOTÍPICA

A glicose é a principal fonte de carbono consumida pela *S. cerevisiae*, mas a levedura também faz uso de outras fontes (CARLSON, 1999; KIM et al., 2013). O cultivo de levedura em meio rico em glicose é seguido por um rápido crescimento, impulsionando a fermentação e, posteriormente, a produção de etanol (DERISI; IYER; BROWN, 1997). Através da análise da expressão gênica, descobriu-se que muitos genes são transcritos diferencialmente em resposta a diferentes níveis de glicose. Um conjunto de genes é induzido pela glicose, codificando transportadores de glicose de baixa afinidade, enzimas glicolíticas e proteínas ribossômicas. Outro conjunto de genes é reprimido pela glicose, incluindo aqueles envolvidos em utilização de fontes alternativas de carbono, gliconeogênese, respiração e funções peroxissômicas (CARLSON, 1999; DERISI; IYER; BROWN, 1997; KIM et al., 2013; THEVELEIN, 1994). Genes envolvidos na via de repressão catabólica da glicose são de dois tipos: genes necessários para a repressão, como o *HXK2* e *MIG1*, e genes necessários para a desrepressão, como *SNF1* (DEVIT; WADDLE; JOHNSTON, 1997; THEVELEIN, 1994). Snf1, é uma proteína quinase que apresenta um papel central na via de repressão catabólica sofrida pela *S. cerevisiae*. Sua síntese é requerida quando os níveis de glicose são baixos. Hexoquinase II fosforila a glicose e regula a repressão catabólica ocorrida pelo alto nível de glicose, logo regula a função da Snf1. Mig 1 é um repressor de transcrição que se liga ao DNA, localiza-se no núcleo na presença de alta concentração de glicose e migra para o citoplasma em baixas concentrações de glicose. A principal função de Snf1 é inibir a repressão por Mig1 quando a concentração de glicose é limitante. Snf1 regula a localização de Mig1 de acordo com a concentração de glicose (CARLSON, 1999).

A substituição de glicose por glicerol como fonte de carbono força a levedura a obter energia através da respiração. Quando o metabolismo respiratório é adotado pela levedura, o glicerol é fosforilado pela glicerol quinase a glicerol 3-fosfato. Então, o glicerol 3-fosfato é oxidado a di-hidroxiacetona-fosfato pela glicerol fosfato ubiquinona oxidoredutase, localizado na superfície da membrana interna da mitocôndria. Os elétrons referentes a essa oxidação são transferidos para a ubiquinona, entrando na cadeia respiratória (FLORES et al., 2000; NEVOIGT; STAHL, 1997). A DHAP entra na via glicolítica, gerando NADH (citoplasma) e piruvato,

dirigindo-se para a cadeia respiratória. Glicerol-3-fosfato desidrogenase ajuda na reoxidação do NADH citoplasmático (HERRERO et al., 2008).

Células saudáveis utilizam a fosforilação oxidativa mitocondrial para produção de energia (SANTIDRIAN et al., 2013), enquanto células tumorais apresentam um aumento significativo na glicólise e na expressão de enzimas glicolíticas, convertendo a maior parte de glicose em L-lactato, mesmo sob níveis normais de oxigênio (DEBERARDINIS et al., 2008b; LÓPEZ-LÁZARO, 2008). Este fenômeno é conhecido como efeito Warburg e representa uma marca metabólica de células tumorais, estabelecendo a ideia de que o câncer também é uma doença com características metabólicas (WARBURG, 1956b). Foi mostrado que algumas células cancerígenas podem alternar reversivelmente entre fermentação e respiração, dependendo da ausência ou presença de glicose e das condições ambientais (JOSE; BELLANCE; ROSSIGNOL, 2011). Esta propriedade representa uma vantagem das células tumorais *in vivo*, uma vez que podem adaptar o seu metabolismo a microambientes heterogêneos, apresentando crescimento rápido em tumores sólidos malignos (ZHOU et al., 2010).

O efeito Warburg, além de aumentar a taxa de proliferação, diminuir a atividade mitocondrial e aumentar os níveis de glicólise, também apresenta como característica um aumento da sensibilidade das células tumorais a espécies reativas de oxigênio. Como há uma diminuição da via oxidativa, a célula não produz as enzimas envolvidas no processo de resposta ao estresse oxidativo (Ruckenstuhl et al. 2009).

NSD3s é uma oncoproteína de 645 aminoácidos que contém um único domínio PWWP (YANG et al., 2010; ZHOU et al., 2010). A superexpressão de NSD3s em *S. cerevisiae*, cultivada na presença de glicerol, uma fonte de carbono oxidativa, promoveu uma mudança no metabolismo celular de respiratório para fermentativo (RONA, 2014). Essa hipótese foi confirmada pelo aumento da taxa de crescimento específico e diminuição no consumo de oxigênio, levando a uma menor tolerância a EROs na levedura (RONA, 2014). Em células de mamíferos, a superexpressão de NSD3 induziu a formação de colônias em expansão em meio isento de insulina. Estas células foram capazes de crescer continuamente na ausência de fatores de crescimento semelhantes à insulina, apresentaram maior taxa de proliferação e formaram colônias tridimensionais em meio de cultura semissólido (YANG et al.,

2010). Com base no número de fenótipos alterados adquiridos por células de mamíferos superexpressando NSD3, Yang e colaboradores concluíram que NSD3 é um importante oncogene transformante da região 8p11-12 (YANG et al., 2010). As células de levedura superexpressando NSD3s passaram a exibir um fenótipo metabólico semelhante às células tumorigênicas, sob condições que estimulam a respiração (RONA, 2014).

Foi observado uma semelhança estrutural, *in silico*, entre o domínio PWWP de NSD3s e de Pdp3. Pdp3 é uma proteína de *S. cerevisiae* que possui um único domínio PWWP (STEC et al., 2000). O domínio PWWP de Pdp3 possui uma gaiola aromática conservada necessária para a ligação com H3K36me3. Os resíduos aromáticos são conservados no domínio PWWP de Pdp3 nas posições F18, W21 e F48 (GILBERT et al., 2014). Foi observado que a integridade da gaiola hidrofóbica é essencial para a função metabólica de Pdp3. A baixa taxa de crescimento específico, o decréscimo no consumo de glicose e o aumento da tolerância contra EROs apresentados pelo mutante W21A também podem ser observados para a cepa *Δpdp3*. Estes resultados estão de acordo com os de Gilbert e colaboradores que demonstraram que todas as três mutações (F18, W21 e F48) abolem independentemente a interação entre Pdp3 e um peptídeo de histona H3K36me3, sugerindo que Pdp3 necessita da gaiola aromática conservada para reconhecer o nucleossomo e se ligar à cromatina. Como o mutante Pdp3 W21A^{+} apresentou o mesmo fenótipo da cepa *Δpdp3*, conclui-se que a gaiola hidrofóbica de Pdp3-PWWP é essencial para sua função metabólica.

Pdp3 é um membro do complexo NuA3 que apresenta uma atividade histona acetiltransferase envolvida na transcrição do DNA. A maioria dos genes controlados por este complexo está envolvida na replicação do DNA (GILBERT et al., 2014). O complexo NuA3 existe em duas formas diferentes: NuA3a e NuA3b. NuA3a usa o domínio PHD de Yng1 para interagir com a lisina 4 na histona 3 trimetilada (H3K4me3) em regiões promotoras de genes transcricionalmente ativos. Sas3 então acetila a lisina 14 da histona 3 (H3K14), levando à iniciação da transcrição em um subconjunto de genes. Por outro lado, a enzima Set2 é responsável pela trimetilação da lisina 36 na histona 3. A interação entre Pdp3 e H3K36me3, que é promovida pelo domínio PWWP de Pdp3, recruta Sas3 e outras subunidades do complexo NuA3b para as regiões codificadoras de genes transcritos. Embora a função do complexo NuA3b não

seja totalmente compreendida, sabe-se que Sas3 pode acetilar histonas ou proteínas não-histonas facilitando o alongamento da transcrição (GILBERT et al., 2014). Foi observado que o fenótipo metabólico induzido pela superexpressão de Pdp3 é dependente da metilação específica de H3K36 realizada por Set2. Além disso, Pdp3 também depende do complexo NuA3b, indicando que uma mutação em outras subunidades do complexo afeta a reprogramação metabólica. A superexpressão de Pdp3 em *Δsas3* não teve efeito sobre os fenótipos metabólicos medidos, quando comparados com a cepa *Δsas3*. Portanto, os resultados sugerem que, sob condições respiratórias, o complexo NuA3b é responsável por mediar a alteração metabólica induzida por Pdp3.

Ao superexpressar Pdp3, em metabolismo respiratório, foi observado uma mudança no metabolismo em direção à fermentação, similar a superexpressão do oncogene humano NSD3s. A forma quimérica de Pdp3, substituindo o seu domínio PWWP pelo de NSD3s, apresentou as mesmas características funcionais tanto de superexpressão de Pdp3 quanto de NSD3s, ambas em metabolismo respiratório. Estes dados sugerem que NSD3s e Pdp3 desempenham papéis semelhantes no metabolismo energético, mudando do metabolismo respiratório para o fermentativo. Cluntun e colaboradores demonstraram que a acetilação de histonas é detectada pelo fluxo de glicose de maneira dose-dependente, o que é uma possível função do efeito Warburg (CLUNTUN et al., 2015). Esses resultados corroboram nosso trabalho, uma vez que Pdp3 faz parte de um complexo histona acetil-transferase.

A NSD3s humana e a Pdp3 de levedura estão envolvidas na regulação da expressão gênica e são reportadas neste trabalho como capazes de causar uma mudança metabólica do metabolismo aeróbico (respiração) para anaeróbico (fermentação). As alterações fenotípicas observadas nas linhagens com diferentes perfis de expressão de NSD3s e Pdp3 no modelo de levedura são muito semelhantes e concordam bem com a mudança metabólica de uma célula com características saudáveis para uma com características tumorais. Esses resultados indicam que o padrão de expressão gênica é importante para a transformação maligna dos fenótipos metabólicos celulares, de acordo com relatos anteriores. Em resumo, NSD3s e Pdp3 parecem desempenhar papéis semelhantes no metabolismo celular e as células que superexpressam ambas as proteínas, sob condições que simulam a respiração,

parecem se comportar metabolicamente como uma célula com características tumorais. A gaiola hidrofóbica do domínio PWWP é essencial para a função de Pdp3. O domínio PWWP de NSD3s foi capaz de substituir funcionalmente o domínio PWWP da proteína de levedura Pdp3. Uma vez que, o remodelamento da cromatina e a disfunção metabólica estão ganhando considerável atenção nos estudos sobre o câncer, pesquisas futuras acerca dos domínios PWWP de Pdp3 e NSD3s podem contribuir para o planejamento de novas drogas anticâncer.

6.2 METABOLÔMICA

Como foi observado, a superexpressão de NSD3s ou Pdp3 reprogramou o metabolismo da levedura. A superexpressão de NSD3s aumentou o conteúdo de alanina, piruvato, aspartato, valina e glutamato, enquanto diminuiu os de histidina, arginina, prolina e homoarginina. Além disso, a superexpressão de Pdp3 levou a um aumento de alanina, fosfocolina e aspartato, ao mesmo tempo em que diminuiu os níveis de histidina, treonina, prolina, arginina e homoarginina.

A diminuição na concentração de histidina, tanto em $NSD3s^{+}$ quanto em $Pdp3^{+}$, foi observada devido ao fato de que este aminoácido é uma exigência nutricional para a cepa BY4741. A superexpressão de NSD3s ou Pdp3 levou a uma diminuição nos níveis de arginina, uma alteração metabólica comumente encontrada no câncer. As células tumorais utilizam intensamente arginina para processos anabólicos (QIU et al., 2014); desse modo, os níveis de arginina diminuem mais rapidamente do que o de outros aminoácidos nas células em crescimento, mostrando que a arginina não é usada apenas para a síntese de proteínas (WHEATLEY, 2005). A síntese endógena de arginina não é suficiente para atender às necessidades de proliferação de células tumorais (QIU et al., 2014). Portanto, a arginina é necessária para as células cancerígenas e tem sido associada ao desenvolvimento de tumores (DELAGE et al., 2010; WHEATLEY, 2005). A diminuição dos níveis de arginina está relacionada a uma desregulação da ASS1 (Argininosuccinato Sintase 1) (Figura 19) em vários tipos de câncer, como o carcinoma hepatocelular (DELAGE et al., 2010), o melanoma maligno (DELAGE et al., 2010; QIU et al., 2014), mesotelioma maligno de pleura (DELAGE et al., 2010), próstata (DELAGE et al., 2010; QIU et al., 2014), câncer renal (DELAGE et al., 2010), linfoma (QIU et al., 2014) e glioma (QIU et al., 2014).

Os lipídios são os principais componentes estruturais das membranas celulares, mas também funcionam como fonte de energia e sinalização nos processos de crescimento celular, inflamação e imunidade. O aumento da biossíntese lipídica é uma característica das células tumorais, satisfazendo as necessidades na produção de membrana para a proliferação (MORI et al., 2016). As células tumorais apresentam um metabolismo alterado de colinas e lipídios (MORI et al., 2016), com um aumento nos níveis de fosfocolina e colina total (fosfocolina, glicerofosfocolina e colina) (ACKERSTAFF; GLUNDE; BHUJWALLA, 2003; GLUNDE et al., 2015; LOENING et al., 2005; MORI et al., 2016; NATTER; KOHLWEIN, 2013; STEWART et al., 2012). A síntese de fosfocolina é realizada a partir da colina pela ação da CK (Colina Quinase) (Figura 19) (ACKERSTAFF; GLUNDE; BHUJWALLA, 2003; GLUNDE et al., 2015; NATTER; KOHLWEIN, 2013; STEWART et al., 2012). Esta enzima é superexpressa em determinados tipos de tumores, tais como cérebro (ELKHALED et al., 2014), mama (JACOBS et al., 2004), próstata (KURHANEWICZ et al., 2002) e endométrio (TROUSIL et al., 2014), e é considerada a principal causa do aumento de fosfocolina e de colina total (GLUNDE et al., 2015; MORI et al., 2016; NATTER; KOHLWEIN, 2013; STEWART et al., 2012). O aumento dos níveis de fosfocolina também pode ser explicado pela maior taxa de transporte de colina (ACKERSTAFF; GLUNDE; BHUJWALLA, 2003; NATTER; KOHLWEIN, 2013). Aqui, um aumento nos níveis de fosfocolina foi observado em função da superexpressão de Pdp3. O aumento na concentração de fosfocolina pode estar associado a uma alteração na expressão ou atividade da colina quinase, como observado em células tumorais.

Valina, assim como isoleucina e leucina, são aminoácidos de cadeia ramificada (BCAA) que funcionam como importantes sinais nutricionais, e seu catabolismo participa de diversos processos patológicos e fisiológicos. Os pacientes com câncer de mama apresentam aumento dos níveis plasmáticos de BCAA, assim como a enzima BCAT1 (*Branched-Chain Amino Acid Transaminase 1*), que participa do catabolismo do BCAA (Figura 19). Já foi demonstrado que esta enzima promove o crescimento celular (ZHANG; HAN, 2017). Os níveis de valina são elevados nos cânceres de endométrio (TROUSIL et al., 2014) e mama (ZHANG; HAN, 2017). Os níveis intracelulares de valina aumentam com a superexpressão de NSD3s,

confirmando o resultado demonstrado no item 5.1, no qual a cepa superexpressando NSD3s apresentou taxa de crescimento maior do que a controle.

As células tumorais exibem alto consumo de glutamina, que é usado como principal substrato para a anaplerose (YANG; VENNETI; NAGRATH, 2017b). A via da glutaminólise (Figura 19) é responsável pela conversão da glutamina nos metabólitos do ciclo do TCA (YANG; VENNETI; NAGRATH, 2017b). O primeiro passo na glutaminólise é a conversão de glutamina em glutamato, que é catalisada pela enzima GLS (Figura 19). Esta enzima é altamente expressa em células tumorais, favorecendo a formação e consequentemente acúmulo de glutamato. A atividade aumentada de GLS está relacionada ao aumento do crescimento e proliferação tumoral (DEBERARDINIS et al., 2008a; DEBERARDINIS; CHENG, 2010). O excesso de glutamato pode ser redirecionado para a síntese de aminoácidos, proteínas e lipídios, como observado em células tumorais (DEBERARDINIS; CHENG, 2010). A cepa NSD3s^{+} apresentou níveis elevados de glutamato e maior taxa de crescimento específico quando comparados a controle.

Aspartato, alanina e fosfoserina são os principais aminoácidos não essenciais (NEAAs) receptores de nitrogênio da glutamina (YANG; VENNETI; NAGRATH, 2017b). As células em proliferação preferencialmente metabolizam o glutamato para produzir aminoácidos não essenciais; a maioria do aspartato intracelular vem da glutaminólise (YANG; VENNETI; NAGRATH, 2017b). Uma alta taxa de secreção de alanina é observada nas células proliferativas. As células tumorais têm um excesso de nitrogênio intracelular que se origina do metabolismo de glutamina, que deve ser excretado como alanina ou amônia. A alanina é produzida a partir da reação do glutamato com piruvato (ALBERS et al., 2008) (Figura 19). As mitocôndrias das células tumorais geram alanina na presença de piruvato levando à síntese de citrato a partir do glutamato, permitindo a biossíntese de membranas celulares (ALBERS et al., 2008). Altos níveis de alanina foram observados em vários tipos de tumores, como próstata (ALBERS et al., 2008; TESSEM et al., 2008) e endométrio (TROUSIL et al., 2014). Foi observado um aumento nos níveis de alanina e aspartato na superexpressão de NSD3s e Pdp3, o que pode estar relacionado ao aumento do metabolismo de glutamina. Este aumento beneficiaria a produção de proteínas, bem

como a síntese de ácidos graxos e triglicerídeos, como observado em células tumorais (ALBERS et al., 2008; TESSEM et al., 2008).

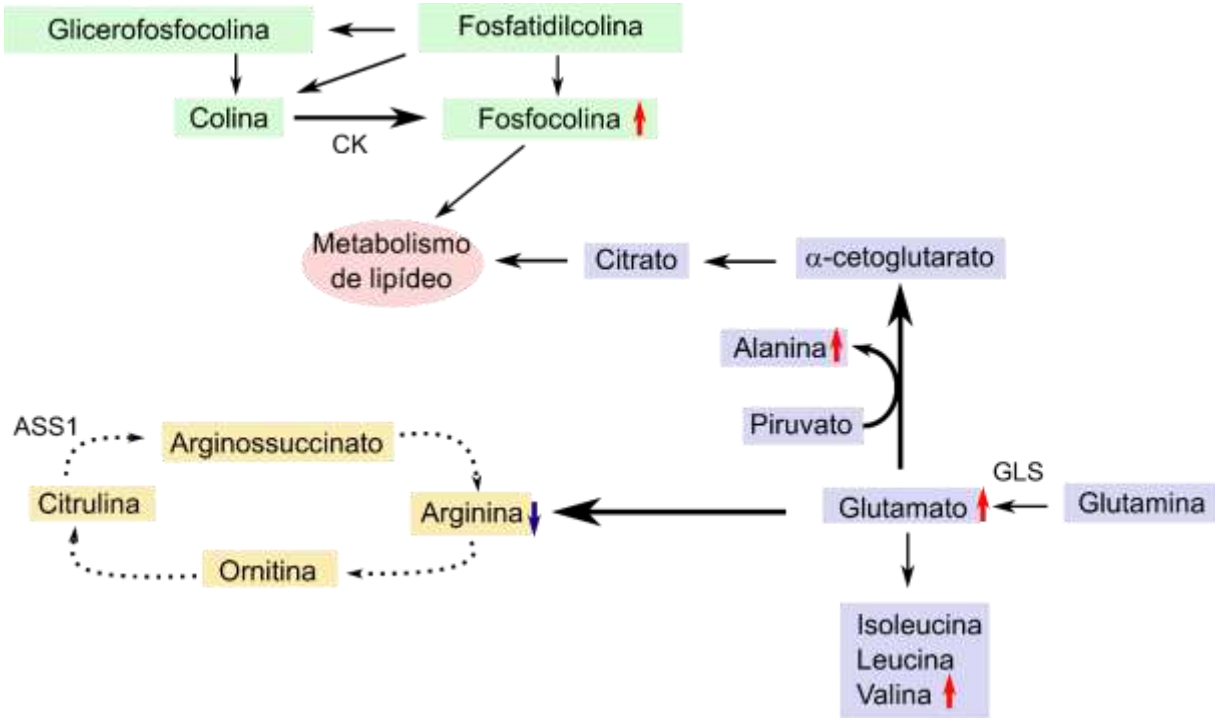

Figura 19. Vias metabólicas dos principais metabólitos detectados na superexpressão de NSD3s ou Pdp3. Os principais metabólitos detectados pertencem à glutaminólise (azul), metabolismo de colinas (verde) e síntese de arginina (amarelo). As setas azuis representam diminuição e a setas vermelhas representam aumento.

O perfil metabólico da NSD3s^{+} e Pdp3^{+} é similar; no entanto, este não é idêntico, indicando que cada proteína atua regulando um núcleo comum de vias metabólicas, além de um conjunto de outras reações específicas. O aumento de aspartato e alanina, juntamente com uma diminuição nos níveis de arginina, observada para as células que superexpressam NS3s e Pdp3 sugere um aumento na taxa de glutaminólise (Figura 19). Este efeito é característico das alterações metabólicas encontradas na tumorigênese, na qual as células tumorais adaptam suas vias à produção de macromoléculas necessárias para sustentar o crescimento e a sobrevivência. Além disso, NSD3s^{+} mostrou um aumento no conteúdo de glutamato, sugerindo aumento da glutaminólise. Também foi observado um aumento nos níveis de valina e fosfocolina por conta da superexpressão de NSD3s e Pdp3, respectivamente, sugerindo que vias como a biossíntese de proteínas e lipídios podem ser diferencialmente reguladas em resposta a cada proteína (Figura 19).

A amplificação de NSD3 é encontrada em diferentes tipos de câncer, como leucemia (ALBERT; HELIN, 2010; SALOURA et al., 2017; ZHOU et al., 2010), mama (ALBERT; HELIN, 2010; IRISH et al., 2016; SALOURA et al., 2017; YANG et al., 2010; ZHOU et al., 2010), bexiga (SALOURA et al., 2017; ZHOU et al., 2010), pulmão (SALOURA et al., 2017; ZHOU et al., 2010), endométrio (JONES; LIN, 2017), ovário (JONES; LIN, 2017) e cabeça e pescoço (SALOURA et al., 2016, 2017; ZHOU et al., 2010). A superexpressão de NSD3s levou a uma variação principalmente nos níveis de arginina, alanina, glutamato e valina. Essas alterações metabólicas já foram observadas em vários tipos de câncer, incluindo alguns onde a superexpressão de NSD3s foi observada (BELKIĆ; BELKIĆ, 2017; CONDE et al., 2015; GLUNDE et al., 2016; HU; SUN, 2018; JACOBS et al., 2004; MASSARI et al., 2016; SUMAN et al., 2018; TIAN et al., 2017; TROUSIL et al., 2014; ZHANG; HAN, 2017). No futuro, o desenho de novas drogas envolvendo inibidores dessas vias metabólicas; ou uma dieta regulando a ingestão de precursores ou os próprios metabólitos podem ser a chave para diminuir a progressão de tumores oriundos da amplificação de NSD3s.

6.3 PERSPECTIVAS

Tanto NSD3s quanto a isoforma curta de Pdp3 apresentam um único domínio conhecido como PWWP. A estrutura tridimensional do domínio PWWP de NSD3s e Pdp3 ainda é desconhecida. Portanto, torna-se necessária a investigação estrutural destas proteínas, a fim de compreender em detalhes seus mecanismos de ação, bem como aprofundar os estudos de suas funções biológicas identificando seus parceiros moleculares. No futuro, este conhecimento poderá ser empregado no desenvolvimento racional de drogas capazes de inibir a atividade transformante da oncoproteína NSD3, podendo ser utilizado como um novo tratamento anticâncer. Alguns resultados referentes ao presente projeto já foram obtidos por nosso grupo de pesquisa.

Com a finalidade de determinar a estrutura tridimensional desses domínios, a sequência de DNA que codifica o domínio PWWP de NSD3s (259-402) e Pdp3 (2-150) foram clonados no vetor de expressão bacteriano RP1B (PETI; PAGE, 2007).

A construção His_6GST-$NSD3_{259-402}$, que compreende o domínio PWWP de NSD3s, foi expressa em *E. coli* BL21 DE3 em meio mínimo M9 (isotopicamente enriquecida com ^{15}N) a 18 ºC, induzida com 1 mM de IPTG (isopropil-b-D-galactosídeo) por 18h. A proteína foi inicialmente purificada através de cromatografia por afinidade a níquel. Posteriormente, a cauda de purificação/solubilidade His_6GST foi clivada por incubação com a protease TEV (*Tobacco Etch Virus nuclear-inclusion-a endopeptidase)* (razão molar de 1:5, 16h, temperatura ambiente). Em seguida, $NSD3_{259-402}$ foi submetida a uma segunda etapa de cromatografia de afinidade a níquel e, por fim, a cromatografia de filtração em gel (Figura 20).

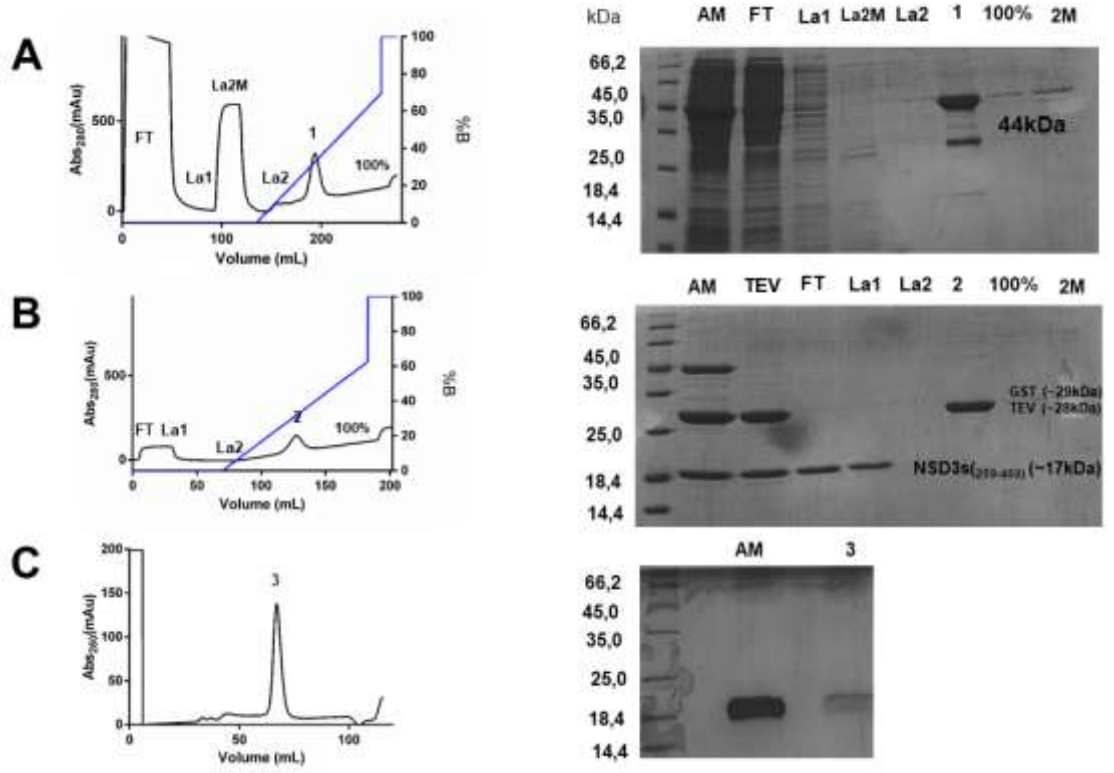

Figura 20. Purificação de NSD3s-PWWP. (A) Primeira cromatografia de afinidade a níquel. **(B)** Segunda cromatografia de afinidade a níquel, após clivagem com a protease TEV. **(C)** Terceira etapa de purificação, cromatografia de filtração em gel (tampão fosfato de sódio 20 mM (pH 6,5) NaCl 50 mM).

Na primeira etapa de purificação por afinidade a níquel, a construção His_6GST-$NSD3_{259-402}$ eluiu em uma concentração ~160 mM de imidazol (pico 1), o que é correspondente a uma banda de ~44 kDa no gel de SDS PAGE (Figura 19, poço 1). Observa-se que após 16h a proteína foi clivada da sua cauda de His_6GST (Figura 19B, poço TEV). Após a segunda etapa cromatográfica, a proteína eluiu com alto grau

de pureza diretamente no *flow through* (poço FT) e no lavado (poço la1). A eluição foi confirmada pelo aparecimento de uma banda em ~17 kDa no gel de SDS PAGE (Figura 20B). Na mesma purificação, observa-se a separação da cauda His_6GST e da protease TEV (poço 2) da amostra de interesse (Figura 20B). Para finalizar, a proteína foi submetida a cromatografia por filtração em gel, onde observa-se um único pico de eluição compatível com o monômero de $NSD3_{259-402}$ (Figura 20C).

Em seguida, a proteína purificada foi submetida a experimentos de RMN uni- e bidimensionais.

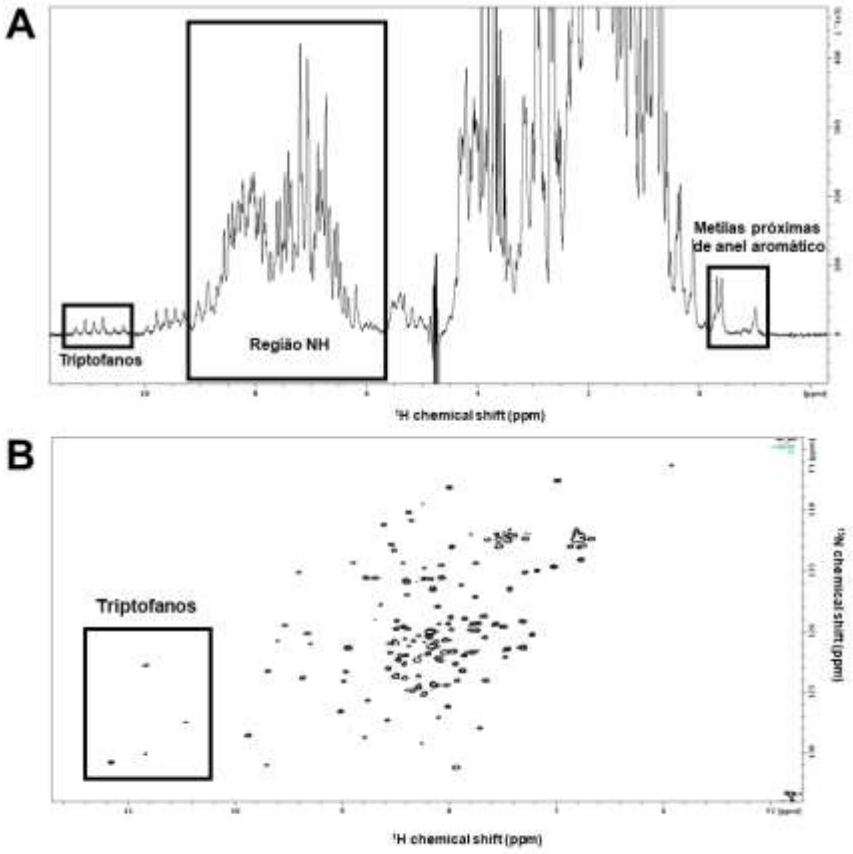

Figura 21. Espectros de RMN adquiridos para NSD3s-PWWP. (A) Espectro 1D ^{1}H RMN. **(B)** Espectro 2D [^{1}H, ^{15}N] HSQC.

A Figura 21A mostra o espectro 1D ^{1}H RMN adquirido para o domínio PWWP de NSD3s. O espectro mostra sinais de hidrogênio amídicos bem dispersos (6-9 ppm) e sinais de metilas próximas a anéis aromáticos (abaixo de zero ppm), o que é caraterístico de proteínas enoveladas. A Figura 21B mostra o espectro 2D [^{1}H, ^{15}N] HSQC adquirido para $NSD3_{259-402}$, onde observa-se a presença de linhas finas,

intensas e bem distribuídas. Ainda, é possível observar a presença de 4 sinais de RMN atribuídos aos 4 resíduos de triptofano presentes na sequência da proteína, 2 deles no motivo Pro-Trp-Trp-Pro, caraterístico desse domínio. Em função da qualidade dos espectros obtidos, o próximo passo será a produção de uma amostra de proteína duplamente enriquecida com ^{15}N e ^{13}C para a aquisição de espectros de 3D RMN (^{1}H, ^{15}N, ^{13}C) para o assinalamento das ressonâncias e determinação estrutural do domínio PWWP de NSD3s. O mesmo procedimento será realizado para a construção His_6-$Pdp3_{2-150}$. Após a determinação das duas estruturas 3D será possível a comparação das estruturas tridimensionais do domínio PWWP de NSD3s e Pdp3. Em seguida, será caracterizada a dinâmica interna dos domínios PWWP de NSD3s e Pdp3. Para finalizar, será determinada a interação *in vitro* com ligantes através da identificação dos resíduos que participam diretamente da ligação dos domínios PWWP de Pdp3 e NSD3s com diferentes sequências de DNA e peptídeos de histona.

7 CONCLUSÕES

- A superexpressão de NSD3s e Ppd3 em células de *S. cerevisiae* leva a uma alteração de fenótipo, apresentando características semelhantes a de uma célula tumoral.
- NSD3s e Pdp3 apresentam funções metabólicas semelhantes.
- O domínio PWWP de NSD3s é capaz de substituir funcionalmente o domínio PWWP de Pdp3.
- A integridade da gaiola hidrofóbica do domínio PWWP de Pdp3 é essencial para a sua função metabólica.
- A função metabólica de Pdp3 depende da trimetilação em H3K36 realizada pela enzima Set2.
- Os resultados indicam que a função metabólica de Pdp3 é mediada exclusivamente pelo complexo NuA3b.
- A superexpressão de NSD3s ou Pdp3 na levedura promoveu um provável aumento da glutaminólise, indicado por um aumento nos níveis de alanina e aspartato acompanhado por uma diminuição nos níveis de arginina.
- A hipótese do aumento da glutaminólise é confirmada pelo aumento dos níveis de glutamato observado em células NSD3s^{+}.
- A superexpressão de NSD3s ou Pdp3 levou a adaptações metabólicas adicionais, incluindo um possível aumento na biossíntese de proteínas e lipídios, que são específicos para cada proteína.

8 BIBLIOGRAFIA

ABBOTT, D. A. et al. Catalase overexpression reduces lactic acid-induced oxidative stress in Saccharomyces cerevisiae. **Applied and environmental microbiology**, v. 75, n. 8, p. 2320–5, abr. 2009.

ACKERSTAFF, E.; GLUNDE, K.; BHUJWALLA, Z. M. Choline phospholipid metabolism: A target in cancer cells? **Journal of Cellular Biochemistry**, v. 90, n. 3, p. 525–533, 2003.

AIROLDI ET AL. NMR analysis of budding yeast metabolomics: a rapid method for sample preparation. **Molecular BioSyst**, v. 11, n. 2, p. 1–5, 2015.

ALBERS, M. J. et al. Hyperpolarized 13C Lactate, Pyruvate, and Alanine: Noninvasive Biomarkers for Prostate Cancer Detection and Grading. **Cancer Research**, v. 68, n. 20, p. 8607–8615, out. 2008.

ALBERT, M.; HELIN, K. Histone methyltransferases in cancer. **Seminars in Cell & Developmental Biology**, v. 21, n. 2, p. 209–220, 2010.

ALVAREZ-VENEGAS, R.; AVRAMOVA, Z. Evolution of the PWWP-domain encoding genes in the plant and animal lineages. **BMC Evolutionary Biology**, v. 12, n. 1, p. 101, 2012.

BACCOLO, G. et al. Mitochondrial Metabolism and Aging in Yeast. In: [s.l: s.n.]. p. 1–33.

BATTAGLIA, A.; CAREY, J. C.; SOUTH, S. T. Wolf-Hirschhorn syndrome: A review and update. **American journal of medical genetics. Part C, Seminars in medical genetics**, v. 169, n. 3, p. 216–23, set. 2015.

BELKIĆ, K.; BELKIĆ, D. The Challenge of Ovarian Cancer: Steps Toward Early Detection Through Advanced Signal Processing in Magnetic Resonance Spectroscopy. **The Israel Medical Association journal : IMAJ**, v. 19, n. 8, p. 517–525, ago. 2017.

BENEDETTI, R. et al. Epigenetic-based therapy: From single- to multi-target approaches. **The international journal of biochemistry & cell biology**, v. 69, p. 121–31, dez. 2015.

BENNETT, R. L. et al. The Role of Nuclear Receptor–Binding SET Domain Family Histone Lysine Methyltransferases in Cancer. **Cold Spring Harbor Perspectives in Medicine**, v. 7, n. 6, p. a026708, jun. 2017.

BOTSTEIN, D.; FINK, G. R. Yeast : An Experimental Organism for 21st Century Biology. v. 189, n. November, p. 695–704, 2011.

BURNS, J.; MANDA, G. Metabolic Pathways of the Warburg Effect in Health and Disease: Perspectives of Choice, Chain or Chance. **International Journal of Molecular Sciences**, v. 18, n. 12, p. 2755, 19 dez. 2017.

CARLSON, M. Glucose repression in yeast. **Current Opinion in Microbiology**, v. 2, n. 2, p. 202–207, 1999.

CHEN, X. et al. Anticancer strategies based on the metabolic profile of tumor cells: therapeutic targeting of the Warburg effect. **Acta Pharmacologica Sinica**, v. 37, n. 8, p. 1013–1019, 4 ago. 2016.

CHEN, Z. et al. Involvement of the Warburg effect in non-tumor diseases processes. **Journal of Cellular Physiology**, v. 233, n. 4, p. 2839–2849, abr. 2018.

CHENG, C. et al. Lipid metabolism reprogramming and its potential targets in cancer. **Cancer Communications**, v. 38, n. 1, p. 27, 21 dez. 2018.

CLUNTUN, A. A. et al. The rate of glycolysis quantitatively mediates specific histone acetylation sites. **Cancer & Metabolism**, v. 3, n. 1, p. 10, 2015.

CONDE, V. R. et al. The progression from a lower to a higher invasive stage of bladder cancer is associated with severe alterations in glucose and pyruvate metabolism. **Experimental Cell Research**, v. 335, n. 1, p. 91–98, jul. 2015.

CRABTREE, H. G. The carbohydrate metabolism of certain pathological overgrowths. **Biochemical Journal**, v. 22, n. 5, p. 1289–1298, 1928.

CRABTREE, H. G. Observations on the carbohydrate metabolism of tumours. **The Biochemical journal**, v. 23, n. 3, p. 536–45, 1929.

DASTIDAR, R. G. et al. The nuclear localization of SWI / SNF proteins is subjected to oxygen regulation. **Cell & Bioscience**, v. 2, n. 1, p. 1, 2012.

DE CARVALHO, M. D. C.; DE MESQUITA, J. F. Structural modeling and in silico analysis of human superoxide dismutase 2. **PloS one**, v. 8, n. 6, p. e65558, 2013.

DE DEKEN, R. The Crabtree Effects: A Regulatory System in Yeast. **J Gen Microbiol**, v. 44, n. 1, p. 149–156, 1966.

DEBERARDINIS, R. J. et al. The Biology of Cancer: Metabolic Reprogramming Fuels Cell Growth and Proliferation. **Cell Metabolism**, v. 7, n. 1, p. 11–20, 2008a.

DEBERARDINIS, R. J. et al. Brick by brick: metabolism and tumor cell growth. **Current**

opinion in genetics & development, v. 18, n. 1, p. 54–61, fev. 2008b.

DEBERARDINIS, R. J.; CHENG, T. Q's next: the diverse functions of glutamine in metabolism, cell biology and cancer. **Oncogene**, v. 29, n. 3, p. 313–24, 21 jan. 2010.

DELAGE, B. et al. Arginine deprivation and argininosuccinate synthetase expression in the treatment of cancer. **International Journal of Cancer**, v. 126, n. 12, p. 2762–2772, 2010.

DERISI, J. L.; IYER, V. R.; BROWN, P. O. Exploring the metabolic and genetic control of gene expression on a genomic scale. **Science (New York, N.Y.)**, v. 278, n. 5338, p. 680–6, 1997.

DEVIT, M. J.; WADDLE, J. A.; JOHNSTON, M. Regulated Nuclear Translocation of the Migl Glucose Repressor. v. 8, n. August, p. 1603–1618, 1997.

DIAZ-RUIZ, R. et al. Biochimica et Biophysica Acta Tumor cell energy metabolism and its common features with yeast metabolism. **BBA - Reviews on Cancer**, v. 1796, n. 2, p. 252–265, 2009.

DIAZ-RUIZ, R.; RIGOULET, M.; DEVIN, A. The Warburg and Crabtree effects: On the origin of cancer cell energy metabolism and of yeast glucose repression. **Biochimica et Biophysica Acta (BBA) - Bioenergetics**, v. 1807, n. 6, p. 568–576, 2011a.

DIAZ-RUIZ, R.; RIGOULET, M.; DEVIN, A. The Warburg and Crabtree effects: On the origin of cancer cell energy metabolism and of yeast glucose repression. **Biochimica et Biophysica Acta (BBA) - Bioenergetics**, v. 1807, n. 6, p. 568–576, jun. 2011b.

ELEUTHERIO, E. et al. Oxidative stress and aging: Learning from yeast lessons. **Fungal Biology**, dez. 2017.

ELKHALED, A. et al. Characterization of metabolites in infiltrating gliomas using ex vivo 1 H high-resolution magic angle spinning spectroscopy. **NMR in Biomedicine**, v. 27, n. 5, p. 578–593, maio 2014.

FINICLE, B. T.; JAYASHANKAR, V.; EDINGER, A. L. Nutrient scavenging in cancer. **Nature reviews. Cancer**, 10 ago. 2018.

FLORES, C. L. et al. Carbohydrate and energy-yielding metabolism in non-conventional yeasts. **FEMS microbiology reviews**, v. 24, n. 4, p. 507–29, out. 2000.

FRANÇA, M. B.; PANEK, A. D.; ELEUTHERIO, E. C. A. Oxidative stress and its effects during dehydration. **Comparative Biochemistry and Physiology Part A: Molecular & Integrative Physiology**, v. 146, n. 4, p. 621–631, abr. 2007.

FU, Y. et al. The reverse Warburg effect is likely to be an Achilles' heel of cancer that can be exploited for cancer therapy. **Oncotarget**, v. 8, n. 34, 22 ago. 2017.

GANCEDO, C.; FLORES, C.-L. Moonlighting proteins in yeasts. **Microbiology and molecular biology reviews : MMBR**, v. 72, n. 1, p. 197–210, table of contents, mar. 2008.

GENTRIC, G.; MIEULET, V.; MECHTA-GRIGORIOU, F. Heterogeneity in Cancer Metabolism: New Concepts in an Old Field. **Antioxidants & Redox Signaling**, v. 26, n. 9, p. 462–485, 20 mar. 2017.

GILBERT, T. M. et al. A PWWP Domain-Containing Protein Targets the NuA3 Acetyltransferase Complex via Histone H3 Lysine 36 trimethylation to Coordinate Transcriptional Elongation at Coding Regions. **Molecular & Cellular Proteomics**, v. 13, n. 11, p. 2883–2895, 2014.

GLUNDE, K. et al. Choline metabolism-based molecular diagnosis of cancer: an update. **Expert Review of Molecular Diagnostics**, v. 15, n. 6, p. 735–747, abr. 2015.

GLUNDE, K. et al. update. v. 15, n. 6, p. 735–747, 2016.

GUARAGNELLA, N. et al. The expanding role of yeast in cancer research and diagnosis: insights into the function of the oncosuppressors p53 and BRCA1/2. p. 1–15, 2013.

HAJJI, N. et al. The bitter side of epigenetics: variability and resistance to chemotherapy. **Epigenomics**, p. epi-2017-0112, 22 jun. 2018.

HAN, X. et al. The role of histone lysine methyltransferase NSD3 in cancer. **OncoTargets and Therapy**, v. Volume 11, p. 3847–3852, jul. 2018.

HANAHAN, D.; WEINBERG, R. A. The hallmarks of cancer. **Cell**, v. 100, n. 1, p. 57–70, 7 jan. 2000.

HANAHAN, D.; WEINBERG, R. A. Hallmarks of Cancer: The Next Generation. **Cell**, v. 144, n. 5, p. 646–674, mar. 2011.

HAWKINS, L. J.; AL-ATTAR, R.; STOREY, K. B. Transcriptional regulation of metabolism in disease: From transcription factors to epigenetics. **PeerJ**, v. 6, p. e5062, 15 jun. 2018.

HE, C. et al. The methyltransferase NSD3 has chromatin-binding motifs, PHD5-C5HCH, that are distinct from other NSD (nuclear receptor SET domain) family members in their histone H3 recognition. **Journal of Biological Chemistry**, v. 288, n.

7, p. 4692–4703, 2013.

HERRERO, E. et al. Redox control and oxidative stress in yeast cells. **Biochimica et Biophysica Acta (BBA) - General Subjects**, v. 1780, n. 11, p. 1217–1235, 2008.

HIMMS-HAGEN, J. Glycerol metabolism in yeast. **Canadian journal of biochemistry**, v. 46, p. 1107–14, 1968.

HU, J.-M.; SUN, H.-T. Serum proton NMR metabolomics analysis of human lung cancer following microwave ablation. **Radiation Oncology**, v. 13, n. 1, p. 40, 12 dez. 2018.

HUEN, M. S. Y. et al. Regulation of Chromatin Architecture by the PWWP Domain-Containing DNA Damage-Responsive Factor EXPAND1/MUM1. **Molecular Cell**, v. 37, n. 6, p. 854–864, mar. 2010.

INCA. **Estimativa | 2016 Incidência de Câncer no Brasil**. [s.l: s.n.].

INCA. **Estimativa 2018: incidência de câncer no Brasil**. [s.l: s.n.].

IRISH, J. C. et al. Amplification of WHSC1L1 regulates expression and estrogen-independent activation of ERα in SUM-44 breast cancer cells and is associated with ERα over-expression in breast cancer. **Molecular Oncology**, v. 10, n. 6, p. 850–865, jun. 2016.

JACOBS, M. A. et al. Proton magnetic resonance spectroscopic imaging of human breast cancer: A preliminary study. **Journal of Magnetic Resonance Imaging**, v. 19, n. 1, p. 68–75, jan. 2004.

JIMENEZ-LOPEZ, J. C. et al. The maize ALDH protein superfamily: linking structural features to functional specificities. **BMC structural biology**, v. 10, p. 43, jan. 2010.

JONES, D.; LIN, D. Amplification of the NSD3-BRD4-CHD8 pathway in pelvic high-grade serous carcinomas of tubo-ovarian and endometrial origin. **Molecular and Clinical Oncology**, 8 jun. 2017.

JOSE, C.; BELLANCE, N.; ROSSIGNOL, R. Choosing between glycolysis and oxidative phosphorylation: A tumor's dilemma? **Biochimica et Biophysica Acta (BBA) - Bioenergetics**, v. 1807, n. 6, p. 552–561, 2011.

KACHROO, A. H. et al. Systematic humanization of yeast genes reveals conserved functions and genetic modularity. **Science**, v. 348, n. 6237, p. 921–925, 2015.

KIM, J. H. et al. The glucose signaling network in yeast. **Biochimica et Biophysica Acta - General Subjects**, v. 1830, n. 11, p. 5204–5210, 2013.

KONUMA, T. et al. Structural Mechanism of the Oxygenase JMJD6 Recognition by the Extraterminal (ET) Domain of BRD4. **Scientific Reports**, v. 7, n. 1, p. 16272, 24 dez. 2017.

KURHANEWICZ, J. et al. Combined magnetic resonance imaging and spectroscopic imaging approach to molecular imaging of prostate cancer. **Journal of Magnetic Resonance Imaging**, v. 16, n. 4, p. 451–463, out. 2002.

LI, Z. et al. The OncoPPi network of cancer-focused protein–protein interactions to inform biological insights and therapeutic strategies. **Nature Communications**, v. 8, p. 14356, 16 fev. 2017.

LINDSEY A. TORRE; FREDDIE BRAY; REBECCA L. SIEGEL; JACQUES FERLAY; JOANNIE LORTET-TIEULENT; AHMEDIN JEMAL, D. Global Cancer Statistics , 2012. **CA: A Cancer Journal for Clinicians**, v. 65, n. 2, p. 87–108, 2015.

LIU, Z. et al. Silencing of histone methyltransferase NSD3 reduces cell viability in osteosarcoma with induction of apoptosis. **Oncology Reports**, v. 38, n. 5, p. 2796–2802, nov. 2017.

LOENING, N. M. et al. Quantification of phosphocholine and glycerophosphocholine with31P edited1H NMR spectroscopy. **NMR in Biomedicine**, v. 18, n. 7, p. 413–420, nov. 2005.

LÓPEZ-LÁZARO, M. The warburg effect: why and how do cancer cells activate glycolysis in the presence of oxygen? **Anti-cancer agents in medicinal chemistry**, v. 8, n. 3, p. 305–312, 2008.

LUCIO-ETEROVIC, A. K.; CARPENTER, P. B. An open and shut case for the role of NSD proteins as oncogenes. **Transcription**, v. 2, n. 4, p. 158–161, 2011.

LUO, J. et al. An mRNA Gene Expression–Based Signature to Identify FGFR1-Amplified Estrogen Receptor–Positive Breast Tumors. **The Journal of Molecular Diagnostics**, v. 19, n. 1, p. 147–161, jan. 2017.

MAHMOOD, S. F. et al. PPAPDC1B and WHSC1L1 Are Common Drivers of the 8p11-12 Amplicon, Not Only in Breast Tumors But also in Pancreatic Adenocarcinomas and Lung Tumors. **The American journal of pathology**, v. 183, n. 5, p. 1–11, 2013.

MALINA, C.; LARSSON, C.; NIELSEN, J. Yeast mitochondria: an overview of mitochondrial biology and the potential of mitochondrial systems biology. **FEMS Yeast**

Research, v. 18, n. 5, 1 ago. 2018.

MANNARINO, C. et al. Requirement of glutathione for Sod1 activation during. n. August 2010, p. 19–25, 2011.

MANNARINO, S. C. et al. Glutathione is necessary to ensure benefits of calorie restriction during ageing in Saccharomyces cerevisiae. **Mechanisms of Ageing and Development**, v. 129, n. 12, p. 700–705, 2008.

MARTIN, B. J. E. et al. Histone H3K4 and H3K36 Methylation Independently Recruit the NuA3 Histone Acetyltransferase in Saccharomyces cerevisiae. **Genetics**, v. 205, n. 3, p. 1113–1123, mar. 2017.

MASSARI, F. et al. Metabolic phenotype of bladder cancer. **Cancer Treatment Reviews**, v. 45, p. 46–57, abr. 2016.

MINO, T.; TAKEUCHI, O. NSD3 keeps IRF3 active. **The Journal of Experimental Medicine**, v. 214, n. 12, p. 3475–3476, 4 dez. 2017.

MOELANS, C. B. et al. Copy number changes at 8p11-12 predict adverse clinical outcome and chemo- and radiotherapy response in breast cancer. **Oncotarget**, v. 9, n. 24, 30 mar. 2018.

MORI, N. et al. The Tumor Microenvironment Modulates Choline and Lipid Metabolism. **Frontiers in Oncology**, v. 6, n. December, 2016.

MORISHITA, M.; DI LUCCIO, E. Cancers and the NSD family of histone lysine methyltransferases. **Biochimica et Biophysica Acta (BBA) - Reviews on Cancer**, v. 1816, n. 2, p. 158–163, 2011a.

MORISHITA, M.; DI LUCCIO, E. Structural insights into the regulation and the recognition of histone marks by the SET domain of NSD1. **Biochemical and Biophysical Research Communications**, v. 412, n. 2, p. 214–219, ago. 2011b.

MOSKOVITZ, J. et al. Methionine sulfoxide reductase (MsrA) is a regulator of antioxidant defense and lifespan in mammals. **Proceedings of the National Academy of Sciences of the United States of America**, v. 98, n. 23, p. 12920–5, 6 nov. 2001.

NATTER, K.; KOHLWEIN, S. D. **Yeast and cancer cells - Common principles in lipid metabolismBiochimica et Biophysica Acta - Molecular and Cell Biology of Lipids**Elsevier B.V., , 2013.

NEBBIOSO, A. et al. Cancer epigenetics: Moving forward. **PLOS Genetics**, v. 14, n.

6, p. e1007362, 7 jun. 2018.

NEVOIGT, E.; STAHL, U. Osmoregulation and glycerol metabolism in the yeast Saccharomyces cerevisiae. **FEMS Microbiology Reviews**, v. 21, n. 3, p. 231–241, 1997.

NOTREDAME, C.; HIGGINS, D. G.; HERINGA, J. T-coffee: a novel method for fast and accurate multiple sequence alignment. **Journal of Molecular Biology**, v. 302, n. 1, p. 205–217, 2000.

OCAÑA, M. C. et al. Metabolism within the tumor microenvironment and its implication on cancer progression: An ongoing therapeutic target. **Medicinal Research Reviews**, 22 maio 2018.

PAPPAS, J. G. The clinical course of an overgrowth syndrome, from diagnosis in infancy through adulthood: the case of Beckwith-Wiedemann syndrome. **Current problems in pediatric and adolescent health care**, v. 45, n. 4, p. 112–7, abr. 2015.

PAVLIDES, S. et al. The reverse Warburg effect: Aerobic glycolysis in cancer associated fibroblasts and the tumor stroma. **Cell Cycle**, v. 8, n. 23, p. 3984–4001, 28 dez. 2009.

PETI, W.; PAGE, R. Strategies to maximize heterologous protein expression in Escherichia coli with minimal cost. **Protein Expression and PuriWcation**, v. 51, p. 1–10, 2007.

POTTER, M.; NEWPORT, E.; MORTEN, K. J. The Warburg effect: 80 years on. **Anon, 2017. The Warburg Effect and Mass Spectrometry-based Proteomic Analysis. Cancer Genomics & Proteomics, 14(4), pp.211–218. Available at: http://cgp.iiarjournals.org/content/14/4/211.abstract.Biochemical Society Transactions**, v. 44, n. 5, p. 1499–1505, 15 out. 2016.

QIN, S.; MIN, J. Structure and function of the nucleosome-binding PWWP domain. **Trends in biochemical sciences**, v. 39, n. 11, p. 536–47, nov. 2014.

QIU, F. et al. Arginine Starvation Impairs Mitochondrial Respiratory Function in ASS1-Deficient Breast Cancer Cells. **Science Signaling**, v. 7, n. 319, p. ra31-ra31, 1 abr. 2014.

RAMADAN, Z. et al. Metabolic profiling using principal component analysis, discriminant partial least squares, and genetic algorithms. **Talanta**, v. 68, n. 5, p. 1683–1691, 2006.

ROBINETTE, S. L. et al. Web Server Based Complex Mixture Analysis by. **Analytical**

Chemistry, v. 80, n. 10, p. 3606–3611, 2008.

RONA, G. B. **UMA NOVA VISÃO SOBRE A FUNÇÃO DA ORF YLR455W DE S. CEREVISIAE, SIMILAR AO PRÓ ONCOGENE HUMANO WHSC1L1/NSD3.** Universidade Federal do Rio de Janeiro – UFRJ, Rio de Janeiro. Instituto de Química.: Dissertação, 2014.

RONA, G. B. et al. The PWWP domain of the human oncogene WHSC1L1/NSD3 induces a metabolic shift toward fermentation. **Oncotarget**, v. 8, n. 33, 15 ago. 2017.

RONA, G. B.; ELEUTHERIO, E. C. A.; PINHEIRO, A. S. PWWP domains and their modes of sensing DNA and histone methylated lysines. **Biophysical Reviews**, v. 8, n. 1, p. 63–74, 14 mar. 2016.

ROY, A.; KUCUKURAL, A.; ZHANG, Y. Function Prediction. **Nat Protoc**, v. 5, n. 4, p. 725–738, 2011.

SALOURA, V. et al. WHSC1L1 drives cell cycle progression through transcriptional regulation of CDC6 and CDK2 in squamous cell carcinoma of the head and neck. **Oncotarget**, v. 7, n. 27, 5 jul. 2016.

SALOURA, V. et al. WHSC1L1-mediated EGFR mono-methylation enhances the cytoplasmic and nuclear oncogenic activity of EGFR in head and neck cancer. **Scientific Reports**, v. 7, p. 40664, 19 jan. 2017.

SAMANFAR, B. et al. Large-scale investigation of oxygen response mutants in Saccharomyces cerevisiae. **Molecular BioSystems**, v. 9, p. 1351–1359, 2013.

SANTIDRIAN, A. F. et al. Mitochondrial complex I activity and NAD + / NADH balance regulate breast cancer progression. **The Journal of Clinical Investigation**, v. 123, n. 3, p. 1068–1081, 2013.

SHAO, C. et al. Role of hypoxia-induced exosomes in tumor biology. **Molecular Cancer**, v. 17, n. 1, p. 120, 11 dez. 2018.

SHEN, C. et al. NSD3-Short Is an Adaptor Protein that Couples BRD4 to the CHD8 Chromatin Remodeler. **Molecular Cell**, v. 60, n. 6, p. 847–859, nov. 2015.

SHEN, M.; KANG, Y. Complex interplay between tumor microenvironment and cancer therapy. **Frontiers of Medicine**, 10 ago. 2018.

SHETH, K. et al. The behavioral characteristics of Sotos syndrome. **American journal of medical genetics. Part A**, v. 167A, n. 12, p. 2945–56, dez. 2015.

SHIN, D.-G.; BAYARSAIHAN, D. A Novel Epi-drug Therapy Based on the Suppression of BET Family Epigenetic Readers. **The Yale journal of biology and medicine**, v. 90, n. 1, p. 63–71, 2017.

SLATER, L. M.; ALLEN, M. D.; BYCROFT, M. Structural variation in PWWP domains. **Journal of Molecular Biology**, v. 330, n. 3, p. 571–576, 2003.

SOGABE, Y. et al. Unveiling epigenetic regulation in cancer, aging and rejuvenation with in vivo reprogramming technology. **Cancer Science**, 10 jul. 2018.

SPRINGER, S. et al. Engineering targeted chromosomal amplifications in human breast epithelial cells. **Breast Cancer Research and Treatment**, v. 152, n. 2, p. 313–321, 23 jul. 2015.

STEC, I. et al. The PWWP domain: a potential protein–protein interaction domain in nuclear proteins influencing differentiation? **FEBS Letters**, v. 473, n. 1, p. 1–5, 2000.

STEELS, E. L.; LEARMONTH, R. P.; WATSON, K. Stress tolerance and membrane lipid unsaturation in Saccharomyces cerevisiae grown aerobically or anaerobically. **Microbiology**, v. 140, n. 3, p. 569–576, 1994.

STEWART, J. D. et al. Choline-releasing glycerophosphodiesterase EDI3 drives tumor cell migration and metastasis. **Proceedings of the National Academy of Sciences**, v. 109, n. 21, p. 8155–8160, 2012.

STRAHL, B. D. et al. Set2 is a nucleosomal histone H3-selective methyltransferase that mediates transcriptional repression. **Molecular and cellular biology**, v. 22, n. 5, p. 1298–306, mar. 2002.

SUMAN, S. et al. Metabolic fingerprinting in breast cancer stages through 1 H NMR spectroscopy-based metabolomic analysis of plasma. **Journal of Pharmaceutical and Biomedical Analysis**, v. 160, p. 38–45, out. 2018.

TAKECHI, S.; NAKAYAMA, T. Sas3 is a histone acetyltransferase and requires a zinc finger motif. **Biochemical and biophysical research communications**, v. 266, n. 2, p. 405–10, 20 dez. 1999.

TEKADE, R. K.; SUN, X. The Warburg effect and glucose-derived cancer theranostics. **Drug Discovery Today**, v. 22, n. 11, p. 1637–1653, nov. 2017.

TESSEM, M. et al. Evaluation of lactate and alanine as metabolic biomarkers of prostate cancer using 1 H HR-MAS spectroscopy of biopsy tissues. **Magnetic Resonance in Medicine**, v. 60, n. 3, p. 510–516, set. 2008.

THE UNIPROT CONSORTIUM. Update on activities at the Universal Protein Resource (UniProt) in 2013. **Nucleic acids research**, v. 41, n. Database issue, p. D43-7, jan. 2013.

THEVELEIN, J. M. Signal transduction in yeast. **Yeast**, v. 10, n. 13, p. 1753–1790, dez. 1994.

TIAN, Y. et al. Systematic analyses of glutamine and glutamate metabolisms across different cancer types. **Chinese Journal of Cancer**, v. 36, n. 1, p. 88, 7 dez. 2017.

TIDWELL, T. R.; SØREIDE, K.; HAGLAND, H. R. Aging, Metabolism, and Cancer Development: from Peto's Paradox to the Warburg Effect. **Aging and Disease**, v. 8, n. 5, p. 662, 2017.

TOSATO, V. et al. Warburg effect and translocation-induced genomic instability : two yeast models for cancer cells. **Frontiers in oncology**, v. 2, n. January, p. 1–12, 2013.

TROUSIL, S. et al. Alterations of choline phospholipid metabolism in endometrial cancer are caused by choline kinase alpha overexpression and a hyperactivated deacylation pathway. **Cancer Research**, v. 74, n. 23, p. 6867–6877, 2014.

ULRICH, E. L. et al. BioMagResBank. **Nucleic acids research**, v. 36, n. November 2007, p. 402–408, 2008.

VERMEULEN, M. et al. Resource Quantitative Interaction Proteomics and Genome-wide Profiling of Epigenetic Histone Marks and Their Readers. **Cell**, v. 142, n. 6, p. 967–980, 2010.

VICENTE-MUÑOZ, S. et al. Comprehensive analysis of interacting proteins and genome-wide location studies of the Sas3-dependent NuA3 histone acetyltransferase complex. **FEBS open bio**, v. 4, p. 996–1006, jan. 2014.

VÖLKEL, P.; ANGRAND, P. The control of histone lysine methylation in epigenetic regulation. **Biochimie**, v. 89, n. 1, p. 1–20, jan. 2007.

VOUGIOUKLAKIS, T. et al. The NSD family of protein methyltransferases in human cancer. **Epigenomics**, v. 7, n. 5, p. 863–874, ago. 2015.

WANG, C. et al. The methyltransferase NSD3 promotes antiviral innate immunity via direct lysine methylation of IRF3. **The Journal of Experimental Medicine**, v. 214, n. 12, p. 3597–3610, 4 dez. 2017.

WANG, J.; QIU, Z.; WU, Y. Ubiquitin Regulation: The Histone Modifying Enzyme's Story. **Cells**, v. 7, n. 9, 27 ago. 2018.

WANG, Y. et al. Regulation of Set9-Mediated H4K20 Methylation by a PWWP Domain Protein. **Molecular Cell**, v. 33, n. 4, p. 428–437, 2009.

WARBURG, O. On the Origin of Cancer Cells. **Science**, v. 123, n. 3191, p. 309–314, 1956a.

WARBURG, O. On the origin of cancer cells. **Science (New York, N.Y.)**, v. 123, n. 3191, p. 309–14, 24 fev. 1956b.

WHEATLEY, D. N. Arginine deprivation and metabolomics: Important aspects of intermediary metabolism in relation to the differential sensitivity of normal and tumour cells. **Seminars in Cancer Biology**, v. 15, n. 4, p. 247–253, 2005.

WISHART, D. S. et al. HMDB 3.0--The Human Metabolome Database in 2013. **Nucleic acids research**, v. 41, n. Database issue, p. D801-7, jan. 2013.

WU, H. et al. Structural and histone binding ability characterizations of human PWWP domains. **PLoS ONE**, v. 6, n. 6, 2011.

XIA, J.; WISHART, D. S. Using MetaboAnalyst 3.0 for Comprehensive Metabolomics Data Analysis. In: **Current Protocols in Bioinformatics**. Hoboken, NJ, USA: John Wiley & Sons, Inc., 2016. p. 14.10.1-14.10.91.

XU, X. D. et al. Warburg effect or reverse warburg effect? A review of cancer metabolism. **Oncology research and treatment**, v. 38, n. 3, p. 117–22, 2015.

YANG, L.; VENNETI, S.; NAGRATH, D. Glutaminolysis : A Hallmark of Cancer Metabolism. n. February, p. 163–194, 2017a.

YANG, L.; VENNETI, S.; NAGRATH, D. Glutaminolysis: A Hallmark of Cancer Metabolism. **Annual Review of Biomedical Engineering**, v. 19, n. 1, p. annurev-bioeng-071516-044546, 15 ago. 2017b.

YANG, Z.-Q. et al. Transforming Properties of 8p11-12 Amplified Genes in Human Breast Cancer. **Cancer Research**, v. 70, n. 21, p. 8487–8497, 1 nov. 2010.

YI, K.; JU, Y. S. Patterns and mechanisms of structural variations in human cancer. **Experimental & Molecular Medicine**, v. 50, n. 8, p. 98, 7 ago. 2018.

YU, L. et al. The Glycolytic Switch in Tumors: How 1. Fu Y, Liu S, Yin S, Niu W, Xiong W, Tan M, et al. The reverse Warburg effect is likely to be an Achilles’ heel of cancer that can be exploited for cancer therapy. Oncotarget [Internet]. 2017 Aug 22;8(34). **Journal of Cancer**, v. 8, n. 17, p. 3430–3440, 2017.

ZHANG, L.; HAN, J. Branched-chain amino acid transaminase 1 (BCAT1) promotes the growth of breast cancer cells through improving mTOR-mediated mitochondrial biogenesis and function. **Biochemical and Biophysical Research Communications**, v. 486, n. 2, p. 224–231, 2017.

ZHANG, Q. et al. Structural Mechanism of Transcriptional Regulator NSD3 Recognition by the ET Domain of BRD4. **Structure**, v. 24, n. 7, p. 1201–1208, jul. 2016.

ZHANG, Y.; SKOLNICK, J. TM-align: a protein structure alignment algorithm based on the TM-score. **Nucleic acids research**, v. 33, n. 7, p. 2302–9, jan. 2005.

ZHONG, J.-T.; ZHOU, S.-H. Warburg effect, hexokinase-II, and radioresistance of laryngeal carcinoma. **Oncotarget**, v. 8, n. 8, 21 fev. 2017.

ZHOU, W.; LIOTTA, L. A.; PETRICOIN, E. F. The Warburg Effect and Mass Spectrometry-based Proteomic Analysis. **Cancer Genomics & Proteomics**, v. 14, n. 4, p. 211–218, 23 jun. 2017.

ZHOU, Z. et al. The NSD3L histone methyltransferase regulates cell cycle and cell invasion in breast cancer cells. **Biochemical and biophysical research communications**, v. 398, n. 3, p. 565–70, 30 jul. 2010.

Germana Breves Rona

Curriculum Vitae

Setembro/2018

Nome civil

Nome Germana Breves Rona

Dados pessoais

Nascimento 11/12/1985 - Rio de Janeiro/RJ - Brasil
CPF 058.228.047-80

Formação acadêmica/titulação

2014 Doutorado em Bioquímica.
Universidade Federal do Rio de Janeiro, UFRJ, Rio De Janeiro, Brasil
Orientador: Elis Cristina Araújo Eleutherio
Co-orientador: Anderson de Sa Pinheiro
Bolsista do(a): Coordenação de Aperfeiçoamento de Pessoal de Nível Superior

2013 - 2014 Mestrado em Bioquímica.
Universidade Federal do Rio de Janeiro, UFRJ, Rio De Janeiro, Brasil
Título: UMA NOVA VISÃO SOBRE A FUNÇÃO DA ORF YLR455W DE SACCHAROMYCES CEREVISIAE, SIMILAR AO PRÓ ONCOGENE HUMANO WHSC1L1/NSD3., Ano de obtenção: 2014
Orientador: Elis Cristina Araújo Eleutherio
Co-orientador: Anderson de Sa Pinheiro
Bolsista do(a): Coordenação de Aperfeiçoamento de Pessoal de Nível Superior

2006 - 2013 Graduação em Química.
Universidade Federal do Rio de Janeiro, UFRJ, Rio De Janeiro, Brasil
Título: Produção de 1,3-propanodiol a partir de glicerol por rota biotecnológica
Orientador: Rodrigo Volcan Almeida e Ségio Cantú Mannarino

2001 - 2003 Ensino Médio (2o grau) .
Colégio Teresiano, CT, Brasil

1992 - 2000 Ensino Fundamental (1o grau) .
Colégio Teresiano, CT, Brasil

Formação complementar

2015 Extensão universitária em DOCÊNCIA NO ENSINO FUNDAMENTAL E MÉDIO. (Carga horária: 690h).
AVM EDUCACIONAL LTDA., AE_PPROV, Rio De Janeiro, Brasil

2008 - 2008 Curso de curta duração em Recuperação de Áreas Degradadas. (Carga horária: 8h).
Empresa brasileira de Pesquisa agropecuária -solos, EMBRAPA-SOLOS, Brasil

2006 - 2006 Curso de curta duração em Processos bioquimicos. (Carga horária: 10h).
Universidade Federal do Rio de Janeiro, UFRJ, Rio De Janeiro, Brasil

2006 - 2006 Curso de curta duração em Segurança no laboratório e na industria. (Carga horária: 10h).

Atuação profissional

1. Universidade Federal do Rio de Janeiro - UFRJ

Vínculo institucional

2014 - Atual Vínculo: Bolsista , Enquadramento funcional: Aluna de Doutorado , Carga horária: 40, Regime: Dedicação exclusiva
Outras informações:
Orientadora: Prof. Dra. Elis Cristina Araujo Eleutherio

2014 - Atual Vínculo: Representante Estudantil , Enquadramento funcional: Representante Discente, Regime: Parcial
Outras informações:
Representante Discente do Programa de Pós-Graduação em Bioquímica do Instituto de Química da UFRJ.

2013 - 2014 Vínculo: Bolsista , Enquadramento funcional: Aluna de Mestrado , Carga horária: 40, Regime: Dedicação exclusiva
Outras informações:
Orientadora: Prof. Dra. Elis Cristina Araujo Eleutherio.

2012 - 2013 Vínculo: Bolsista , Enquadramento funcional: Iniciação Cientifica , Carga horária: 20, Regime: Parcial
Outras informações:
Orientador: Elis Cristina Araujo Eleutherio.

2011 - 2012 Vínculo: Projeto final de curso , Enquadramento funcional: Projeto final de curso , Carga horária: 20, Regime: Parcial
Outras informações:
Projeto: Produção de 1,3-propanodiol em E. coli: Engenharia metabólica e otimizaçãoOrientador: Rodrigo Volcan Almeida. Sérgio Cantú

2011 - 2012 Vínculo: Monitoria , Enquadramento funcional: Monitora de bioquímica , Carga horária: 8, Regime: Parcial
Outras informações:
Bioquíca I e II

2009 - 2010 Vínculo: Bolsista cnpq , Enquadramento funcional: Aluna de Iniciação Cientifica , Carga horária: 20, Regime: Parcial
Outras informações:
Projeto: Papel da Sod1 na longevidade de S. cerevisiae Orientador: Elis Cristina Araujo Eleutherio.

2007 - 2009 Vínculo: Bolsista cnpq , Enquadramento funcional: aluna de iniciação cientifica , Carga horária: 20, Regime: Parcial
Outras informações:
Projeto: ALTERAÇÃO DAS PROPRIEDADES QUÍMICAS DOS SOLOS PELO USO DE RESÍDUOS INDUSTRIAIS/DOMÉSTICOS Orientador: Daniel Vidal Pérez Sarai Maria de Alcantara

2. Empresa Brasileira de Pesquisa em Agropecuária - solos - EMBRAPA SOLOS

Vínculo institucional

2007 - 2009 Vínculo: Bolsista cnpq , Enquadramento funcional: estagiária , Carga horária: 20, Regime: Parcial

Producão

Produção bibliográfica

Artigos completos publicados em periódicos

1. ELEUTHERIO, E. C. A.; BRASIL, A. A.; **RONA, GERMANA**; MAGALHAES, R. S. S.
Trehalose: As Sweet as Effective in Biomedical Research and Biotechnology. Advances in Biotechnology & Microbiology. , v.8, p.1 - , 2018.

2. ELEUTHERIO, ELIS; DE ARAUJO BRASIL, ALINE; FRANÇA, MAURO BRAGA; SEIXAS DE ALMEIDA, DIEGO; **BREVES RONA, GERMANA**; SILVA MAGALHÃES, RAYNE STFHANY
Oxidative Stress and Aging: Learning from Yeast Lessons. Fungal Biology. , v.xx, p.xx - , 2017.

3. **RONA, G. B.**; ELEUTHERIO, ELIS; PINHEIRO, A. S.
PWWP domains and their modes of sensing DNA and histone methylated lysines. Biophysical Reviews. , p.1 - 12, 2016.

4. **RONA, GERMANA B.**; ALMEIDA, DIEGO S. G.; PINHEIRO, ANDERSON S.; ELEUTHERIO, ELIS C. A.
The PWWP domain of the human oncogene WHSC1L1/NSD3 induces a metabolic shift toward fermentation. Oncotarget. , v.xx, p.1-12 - , 2016.

5. **RONA, GERMANA**; HERDEIRO, RICARDO; MATHIAS, CRISTIANE JULIANO; TORRES, FERNANDO ARARIPE; PEREIRA, MARCOS DIAS; ELEUTHERIO, ELIS
CTT1 overexpression increases life span of calorie-restricted Saccharomyces cerevisiae deficient in Sod1. Biogerontology. , v.x, p.1 - 9, 2015.

6. Pérez, D. V.; de ALCANTARA, S.; RONA, G. B.; BETTIOL, W.; POLIDORO, J. C.
Chemical changes in an Oxisol cultivated with maize (Zea mays, L.) after six years disposal of sewage sludge. INTERNATIONAL JOURNAL OF ENVIRONMENTAL ENGINEERING (PRINT). , v.4, p.352 - 371, 2012.

Trabalhos publicados em anais de eventos (completo)

1. RONA, G. B.; Santos, F. A.; Gonçalves, F. S.; de ALCANTARA, S.; Pérez, D. V.; MELO, L.
EFEITO DA APLICAÇÃO CONTINUADA DE BIOSÓLIDO NA COMPARTIMENTALIZAÇÃO DE METAIS EM SOLO CULTIVADO COM BANANA (MUSA SPP). In: IV simposio internacional de meio ambiente, 2009, Rio de Janeiro.
IV simposio internacional de meio ambiente. , 2009. v.unico. p.469 - 472

2. Santos, F. A.; Gonçalves, F. S.; RONA, G. B.; de ALCANTARA, S.; Pérez, D. V.; MORICONI, W.
EFEITO RESIDUAL DA APLICAÇÃO DE BIOSÓLIDO NA CULTURA DO MILHO. In: IV simposio internacional de meio ambiente, 2009, Rio de Janeiro.
IV simposio internacional de meio ambiente. , 2009. v.unico. p.465 - 468

3. Gonçalves, F. S.; Santos, F. A.; RONA, G. B.; Pérez, D. V.; de ALCANTARA, S.; Wadt,P.G.S
INFLUÊNCIA DA APLICAÇÃO DO LODO DE CALEIRO E DE DECANTADOR EM ARGISSOLO VERMELHO-AMARELO DO ACRE In: IV Simpósio Internacional de Meio Ambiente, 2009, Rio de Janeiro.
IV Simpósio Internacional de Meio Ambiente. , 2009. v.unico. p.459 - 464

Trabalhos publicados em anais de eventos (resumo)

1. ELEUTHERIO, E. C. A.; **RONA, G. B.**; ALMEIDA, D. S. G.; PINHEIRO, A. S.

PWWP domain of the human oncogene WHSC1L1/NSD3 and the protein PDP3 of S. cerevisiae induce a metabolic shift toward fermentation In: PYFF6, 2016, Lisboa.
programme and Abstract Book of PYFF6. , 2016.

2. **RONA, G. B.**; ALMEIDA, D. S. G.; ELEUTHERIO, E. C. A.; PINHEIRO, A. S.
THE PWWP-CONTAINING PROTEIN PDP3 REGULATES ENERGETIC METABOLISM IN SACCHAROMYCES CEREVISIAE In: 23rd Congress of the International Union for Biochemistry and Molecular Biology – IUBMB and 44th Annual Meeting of SBBq, 2015, Foz do Iguaçu.
23rd Congress of the International Union for Biochemistry and Molecular Biology – IUBMB and 44th Annual Meeting of SBBq. , 2015.

3. ELEUTHERIO, E. C. A.; **RONA, G. B.**; PINHEIRO, A. S.; ALMEIDA, D. S. G.
The PWWP-containing protein Pdp3 regulates energetic metabolism in Saccharomyces cerevisiae In: 27th International Conference on Yeast Genetics and Molecular Biology, 2015, Trento.
27th International Conferenceon Yeast Genetics and Molecular Biology. , 2015.

4. **RONA, G. B.**; PINHEIRO, A. S.; ELEUTHERIO, E. C. A.
New Insights into the Function of YLR455W, a WHSC1L1/NSD3 Orthologue in Saccharomyces cerevisiae In: Chem Rio 2014 Symposium, 2014, Rio de Janeiro.
Chem Rio 2014 Symposium. , 2014.

5. **RONA, G. B.**; ELEUTHERIO, E. C. A.; PINHEIRO, A. S.
New Insights into the Function of YLR455W, a WHSC1L1/NSD3 Orthologue in Yeast In: XLIII Annual Meeting of the Brazilian Society for Biochemistry and Molecular Biology (SBBq), 2014, Foz do Iguaçu.
XLIII Annual Meeting of the Brazilian Society for Biochemistry and Molecular Biology (SBBq). , 2014.

6. BRASIL, A. A.; MAHTIAS, C. J.; RONA, G. B.; PEREIRA, M. D.; ELEUTHERIO, E. C. A.
Ageing biology using Saccharomyces cerevisiae as experimental model the role of Sod1 In: 16th Biennial Meeting of the Society for Free Radical Research International (SFRRI 2012), 2012, Londres.
Program and Abstracts - SFRRI 2012. , 2012. v.1. p.12 - 12

7. RONA, G. B.; HERDEIRO, R. S.; MAHTIAS, C. J.; ELEUTHERIO, E. C. A.
Aging Biology using Saccharomyces cerevisiae as experimental model - the role of sod1 In: XL Annual Meeting of the Brazilian Biochemistry and Molecular Biology Society (SBBq), 2011, Foz do Iguaçu.
XL Annual Meeting of the Brazilian Biochemistry and Molecular Biology Society (SBBq). , 2011.

8. RONA, G. B.; HERDEIRO, R. S.; PEREIRA, M. D.; ELEUTHERIO, E. C. A.
Sod1 is necessary to life span extension of calorie-restricted Saccharomyces cerevisiae In: The 25th international conference on yeast genetics and molecular biology, 2011, Olsztyn.
25th international conference on yeast genetics and molecular biology: Cell death, aging and human disease. , 2011. p.57 - 57

9. de ALCANTARA, S.; Pérez, D. V.; Santos, F. A.; TAGOMORI, I. S.; RONA, G. B.; PEREIRA, N. R.
Geoquímica de solos do estado do Mato Grosso do Sul In: XV Congreso Cientifico Internacional, 2010, Havana.
XV Congress CNIC 2010. , 2010.

10. Pérez, D. V.; de ALCANTARA, S.; Santos, F. A.; RONA, G. B.; BETTIOL, W.
. Efecto uso del biosólido em la acumulación de metales trazas em suelo cultivado con maíz (Zea mays, l.) In: : I CONGRESO IBEROAMERICANO DE QUIMICA, BIOQUIMICA E INGENIERIA QUIMICA, 2009, Havana.
I CONGRESO IBEROAMERICANO DE QUIMICA, BIOQUIMICA E INGENIERIA QUIMICA. , 2009.

11. Pérez, D. V.; de ALCANTARA, S.; RONA, G. B.; BETTIOL, W.; MORICONI, W.; FEITOSA, F. P.; ALMEIDA, M. R.
Efeito da aplicação de lodo de esgoto na acumulação de Fe, Mn, Zn, Cu, Ni, Pb e Cr em solo In: V Congreso Iberoamericano de FÍísica y Quimica ambiental, 2008, Mar del Plata.
Las fronteras de la física y química ambiental en Iberoamérica: Libro de Actas del V congreso iberoamericano de física y química ambiental. , 2008. v.único. p.54 - 54

Trabalhos publicados em anais de eventos (resumo expandido)

1. Pérez, D. V.; de ALCANTARA, S.; RONA, G. B.; BETTIOL, W.; MORICONI, W.
Efeito Residual da Aplicação de Biossólido In: FertBio, 2008, Londrina.
FertBio desafios para uso do solo com eficiencia e qualidade ambiental. , 2008.

2. de ALCANTARA, S.; MELO, L.; Pérez, D. V.; MENEGUELLI, N. A.; FEITOSA, F. P.; JORGE, G. S. A.; **RONA, G. B.**
Uso del Biosólido para fines agrícolas en utisol cultivado con plátano (musa spp) In: III Simpósio Internacional de Medio Ambiente, 2008, La Habana.
cd de resumos. , 2008.

Produção técnica

Demais produções técnicas

1. RONA, G. B.; Santos, F. A.; CRUZ, F. R.; PEREIRA, F. A.; ESPINDULA, L.
IV Simpósio Internacional de Meio Ambiente, 2009. (Outra produção técnica)

2. NASCIMENTO, A. R.; COSTA, A. C. S.; BARRETO, A. L.; CORTEZ, B.; CRUZ, F. R.; PEREIRA, F. A.; BARBOSA, G. F. C.; RONA, G. B.; ESPINDULA, L.; AGUIAR, P. F.; SANCA, R. N.
IV Simpósio Internacional de Meio Ambiente, 2009. (Outra produção técnica)

Orientações e Supervisões

Orientações e supervisões

Orientações e supervisões concluídas

Trabalhos de conclusão de curso de graduação

1. Natália Pinto de Almeida. **Investigação da função do domínio PWWP da proteína Pdp3 no metabolismo celular em Saccharomyce cerevisiae**. 2017. Curso (Química) - Universidade Federal do Rio de Janeiro

2. Diego Seixas Gomes de Ameida. **Estudo Metabólico da Proteína Pdp3 de Saccharomyces cerevisiae, cujo domínio PWWP se assemelha ao do oncogene humano NSD3**. 2015. Curso (Química) - Universidade Federal do Rio de Janeiro

Iniciação científica

1. Daniel Costa. **Determinação da estruta da Pdp3**. 2017. Iniciação científica - Instituto Federal do Rio de Janeiro

Orientações e supervisões em andamento

Trabalhos de conclusão de curso de graduação

1. Nathalia Lins. **Determinação da estrutura da oncoproteína NSD3**. 2018. Curso (Química) -

www.impactjournals.com/oncotarget/ Oncotarget, 2017, Vol. 8, (No. 33), pp: 54068-54081

Research Paper

The PWWP domain of the human oncogene WHSC1L1/NSD3 induces a metabolic shift toward fermentation

Germana B. Rona[1], Diego S. G. Almeida[1], Anderson S. Pinheiro[1] and Elis C. A. Eleutherio[1]

[1]Department of Biochemistry, Institute of Chemistry, Federal University of Rio de Janeiro, 21941-909, Rio de Janeiro, RJ, Brazil

Correspondence to: Germana B. Rona, **email:** rona.germana@gmail.com

Keywords: *PWWP, NSD3, Pdp3, Saccharomyces cerevisiae, cancer*

Received: *October 29, 2015* ***Accepted:*** *July 26, 2016* ***Published:*** *August 12, 2016*

ABSTRACT

WHSC1L1/NSD3, one of the most aggressive human oncogenes, has two isoforms derived from alternative splicing. Overexpression of long or short NSD3 is capable of transforming a healthy into a cancer cell. NSD3s, the short isoform, contains only a PWWP domain, a histone methyl-lysine reader involved in epigenetic regulation of gene expression. With the aim of understanding the NSD3s PWWP domain role in tumorigenesis, we used *Saccharomyces cerevisiae* as an experimental model. We identified the yeast protein Pdp3 that contains a PWWP domain that closely resembles NSD3s PWWP. Our results indicate that the yeast protein Pdp3 and human NSD3s seem to play similar roles in energy metabolism, leading to a metabolic shift toward fermentation. The swapping domain experiments suggested that the PWWP domain of NSD3s functionally substitutes that of yeast Pdp3, whose W21 is essential for its metabolic function.

INTRODUCTION

Emerging evidence indicates that cancer is primarily a metabolic disease involving disturbances in energy production through respiration and fermentation [1]. Even though very specific processes underlie cell malignant transformation, a large number of unspecific factors are able to initiate the disease, including radiation, chemicals, viruses, inflammation, etc. The apparent contradiction that such unspecific processes are able to cause the disease through a very specific and common mechanism was pointed out by Albert Szent-Györgyi, and considered the "oncogenic paradox" [2]. In addition, the mutation rate for most genes, including those considered essential for manifesting the hallmarks of cancer [3] is low, which makes it unlikely that the numerous pathogenic mutations found in cancer cells would occur sporadically within a normal human lifespan [4].

Although compelling evidence shows that genomic instability is present to some degree in all tumor cells [5], it is unclear how this phenotype relates to the origin of the disease. Even though no specific gene mutation or chromosomal abnormality is common to all cancers, nearly all cancers express aerobic fermentation (Warburg effect), regardless of their tissue or cellular origin [6], which is a robust metabolic hallmark of most tumors. As reviewed by Thomas N. Seyfried [1], several reports correlate respiratory dysfunction and mitochondrial structural defects to abnormalities in DNA repair mechanisms and the upregulation of fermentation pathways [7, 8], leading to carcinogenesis. This evidence supports the idea that cancer is a disease of metabolic origins. In such cases, oncogene upregulation becomes essential for increased glucose and glutamine metabolism following respiratory impairment [9]. The synthesis of nucleotides and fatty acids, as well as the consumption of glucose and glutamine are prevalent among tumor cell lines. These activities, especially glutamine intake, are used as reducing power and anaplerosis. Cancer cells metabolism is modified to simplify the uptake of nutrients into the biomass requirements to proliferation and cell growth. Recent studies show that several signaling pathways implicated in cell proliferation regulate metabolic pathways that incorporate nutrients into biosynthetic pathways. Some mutations enable cancer cells to acquire and metabolize nutrients in a way that favors proliferation rather than efficient ATP production [10, 11].

Gene amplification is a major mechanism for oncogene activation in human cancers [12–14], resulting in gene overexpression at both the RNA and protein levels [15]. Amplification of the short arm of human chromosome 8 has been reported in 10–15% of breast cancers and harbors several candidate oncogenes [12, 13, 15–17]. The 8p11-12 amplicon has been associated with estrogen receptor-positive tumors and lobular histology [18]. Recent studies have identified the Wolf-Hirschhorn syndrome candidate 1-like 1 gene (WHSC1L1, also known as NSD3) as one of the major leader oncogene candidates from the 8p11-12 region in breast cancer [15].

NSD3 is the third member of the NSD (nuclear receptor SET domain- containing) family. All proteins from this family have been directly linked to multiple human diseases. A striking feature of the three NSD proteins is that they are highly similar within a region of about 700 amino acids spanning a catalytic SET domain together with a pre and post-SET (Enhancer of zeste) domain, two PWWP (proline-tryptophan-tryptophan-proline) domains, five PHD (plant homeodomain) fingers, and a NSD-specific Cys-His rich domain (C5HCH) [19]. However, the similar domain architecture of the three NSD members does not indicate a functional redundancy [20]. NSD3 has been identified as a frequently amplified gene in breast cancer cell lines and primary breast carcinoma [21]. NSD3 has two main isoforms, NSD3l (long NSD3,1437 amino acid) and NSD3s (short NSD3, 645 amino acid) [15, 21], derived from alternative splicing of exon 10 [22]. Both NSD3 protein isoforms contain a PWWP domain; however, the short isoform presents only a single one [15]. Yang and co-workers have shown that both isoforms are located in the nucleus and might act as oncoproteins as they exhibit transforming properties [15].

The PWWP domain is exclusively found in eukaryotes, ranging from lower eukaryotes, such as protozoa and yeast, to human. The human genome encodes more than twenty PWWP-containing proteins, which are always located in the nucleus and play a major role in cell division, growth and differentiation. They are implicated in various chromatin functions, including DNA modification, repair, and transcriptional regulation [23, 24]. The PWWP domain acts as a chromatin modification reader by recognizing both DNA and histone methylated lysines at the level of the nucleosome [25, 26]. Despite the significant progress in understanding the PWWP domain function, many questions are yet to be answered, including its role in tumorigenesis.

The budding yeast *Saccharomyces cerevisiae* has been extensively used as a model for genetic analysis of various complex pathways and processes, including cell division, secretion, transcription and receptor-mediated signal transduction [27]. Due to genetic and metabolic similarities between *S. cerevisiae* and cancer cells, this microorganism has often been used as a tool for cancer research [28]. There are strong similarities between mammalian and yeast cell metabolism regulation by oncogenes/oncogene homologues. An interesting approach is the use of "tumorized yeasts" as a model for anti-cancer drug screening and for metabolism studies in order to determine how each one of these mutations would contribute to the profound metabolic alterations in cancer [29]. There are similarities between glucose catabolic repression of yeast oxidative metabolism and metabolic reprogramming of cancer cells, the Warburg effect [30]. Yeast cells growing on glucose and tumor cells show high cell proliferation and high glucose consumption rates and are both very sensitive to oxidative stress. Yeast cells engineered to express apoptosis-targeted proteins provide a powerful resource for the discovery of new genes responsible for modulation of cell-death pathways of humans and other higher organisms [27]. Like mammals, yeast undergoes apoptosis in response to oxidative stress and mitochondrial dysfunction. Escape from apoptosis and sustained cell growth are hallmarks of cancer [30–32]. Yeast is an attractive model to investigate the relations between programed cell death and mitochondrial dysfunction in both physiological and pathological conditions [33]. At least 60% of yeast genes have statistically robust human homologues or at least one conserved domain with human genes [30–32]. A substantial portion of conserved yeast and human genes perform much the same roles in both organisms, to an extent that the protein-coding DNA of a human gene can actually substitute that of yeast [27, 34]. However, if there are no direct yeast orthologous of human oncogenes/oncosuppressors, these genes can be heterologously expressed in yeast to study their function [35].

In light of these findings, the aim of this study was to evaluate the human NSD3s PWWP domain functionality in the *S. cerevisiae* experimental model.

RESULTS

Initially, we analyzed the effects of NSD3s overexpression on *S. cerevisae* energy metabolism, since overexpression of NSD3s was reported to transform a human healthy cell into a cell with tumorigenic characteristics [15]. Yeast strains were grown in glycerol, a carbon source that favors oxidative respiration, so the yeast metabolic phenotype could resemble that of a mammalian healthy cell. Figure 1A shows that the NSD3s$^+$ yeast strains displayed a specific growth rate (μ) higher than the control (WT). In addition, NSD3s$^+$ cells exhibited a decrease in oxygen consumption when compared to WT cells (Figure 1B), indicating that overexpression of NSD3s is capable of decreasing cell respiratory capacity leading to a faster proliferation.

It is well known that inhibition of the respiratory chain impairs the expression of antioxidant enzymes, which causes the cell to be more sensitive to reactive oxygen species (ROS) and results in oxidative damage

[36–38]. Downregulation of oxidative metabolism occurs both in the Warburg effect (tumor cells) and during catabolic repression (yeast). In such conditions, cells do not develop an efficient antioxidant defense against ROS, which are able to damage all major cellular building blocks, including DNA, lipids and proteins. These damages can lead to cell death, accelerate the aging process and the development of age-related diseases [39, 40]. Figure 2A shows that NSD3s$^+$ yeast cells were less viable than the control when submitted to oxidative stress conditions. In addition, NSD3s$^+$ mutant cells showed an increase of more than 50% in the levels of lipid peroxidation after one hour of hydrogen peroxide (20 mM) exposure (Figure 2B).

To examine the heterologous expression of NSD3s in yeast, we used an anti-his tag antibody, since the construct contains an N-terminal six-histidine tag. We performed a western blotting analysis and found that the short isoform of NSD3 was successfully expressed in yeast (Supplementary Figure S1).

Next, we screened protein databases for yeast proteins containing a PWWP domain. Among them, we selected Pdp3, which has a single PWWP domain with 25% sequence identity to that of NSD3s (Figure 3A). Pdp3 is primarily located in the nucleus, but undergoes cytoplasmic shuttling in response to stress conditions such as hypoxia [41]. According to the Uniprot database [42], the PWWP domain of Pdp3 comprises amino acids 7–68 [43]; however, Gilbert and co-workers demonstrated that Pdp3 residues 1–150 are required for the recognition of histone 3 trimethylated lysine 36 (H3K36me3). These data suggested that Pdp3, and likely other PWWP-containing proteins, requires a C-terminal α-helical region for its aromatic cage stability and function [43]. We constructed a structural model for the PWWP domains of NSD3s and Pdp3 extending beyond the predicted PWWP domain

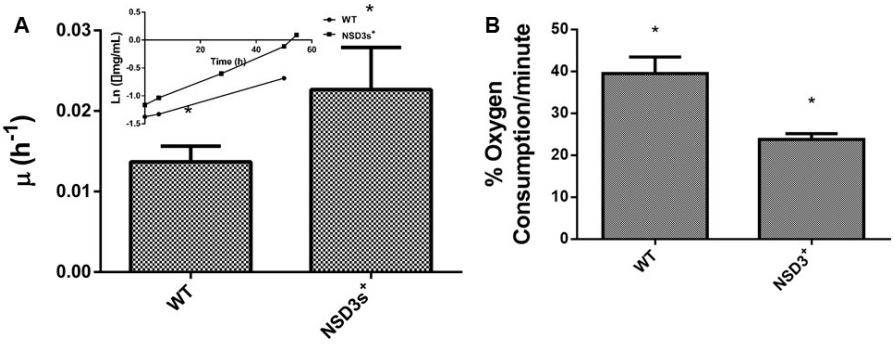

Figure 1: Effect of NSD3s overexpression on yeast growth rate and oxidative metabolism. WT strain and the mutant overexpressing human NSD3s (NSD3s$^+$ strain) were grown in drop out glycerol 4% until the middle of exponential growth phase. (**A**) For specific growth rate measurements, the absorbance at 570 nm were taken at regular intervals until cells reached stationary phase. The inset shows the growth rate. (**B**) A Clark electrode measured the oxygen consumption for ten minutes. The results represent the mean ± standard deviation of at least three independent experiments and *mean different results at WT vs NSD3s$^+$ *$p < 0.05$.

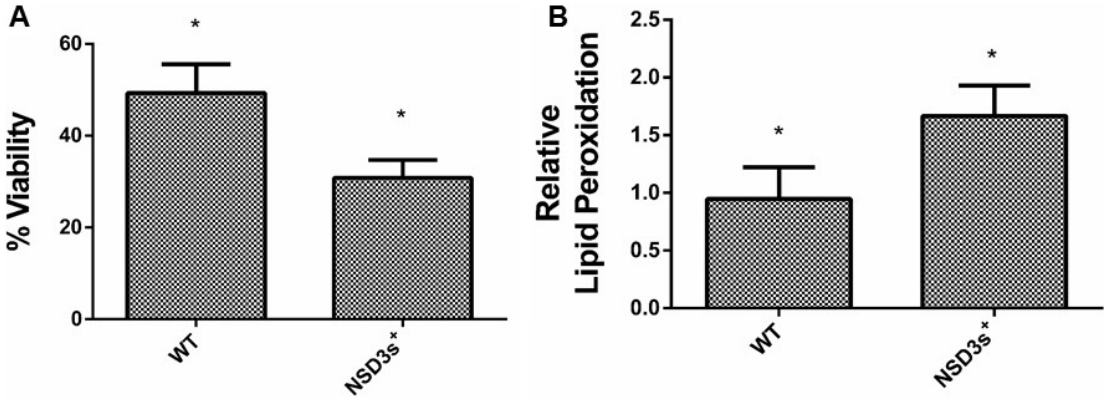

Figure 2: NSD3s overexpression increases yeast sensitivity to oxidative stress. WT strain and the mutant overexpressing human NSD3s (NSD3s$^+$ strain) were grown in drop out glycerol 4% until the middle of exponential growth phase. Oxidative damages were analyzed after stress with 20 mM H_2O_2/1 h/28°C/160 rpm. (**A**) Cellular viability was measured by standard dilution following plating on solid YPD medium for 72 h. Colony-forming units were counted and expressed as the percentage of cell viability, calculated by the (number of cells after stress/number of cells before stress) * 100. (**B**) The levels of lipid peroxidation were determined by the TBARS method and results were expressed as a ratio between the level of lipid peroxidation of stressed cells and control situation (before stress). The results represent the mean ± standard deviation of at least three independent experiments and *mean different results at WT vs NSD3s$^+$ *$p < 0.05$.

(Figure 3B and 3C, respectively) using the I-Tasser server [44] for *ab initio* modelling. One can observe that both structures are composed of a N-terminal β-barrel responsible for recognizing and binding histone methylated lysines [15] and a C-terminal α-helical substructure. An alignment between the NSD3s and Pdp3 PWWP structures was performed using TM-Align [45]. TM-score was used to assess the topological similarity between the two protein structures, while root mean square deviation (RMSD) measured the average distance between the backbone atoms of the superimposed proteins. Such parameters were used to analyze the topology and the structural similarity of the models [46, 47]. The RMSD values between the Pdp3 and NSD3s PWWP models was ~3.8Å for the full-length proteins, including the C-terminal α-helical region, and ~2.3Å when just the PWWP domain suggested by Uniprot (UniProt #Q06188 residues 7–68 (Pdp3) and UniProt # Q9BZ95 residues 270–333 (NSD3s)) was taken into consideration. This RMSD difference is consistent with similar 3D structures [44]. The TM-score was ~0.5 when aligning full-length Pdp3 and NSD3s PWWP domains and 0.65 when just the PWWP domain predicted by Uniprot was considered. It is known that a TM-score between 0.5~1.0 suggests a highly similar fold [48]. Despite the low sequence similarity between the PWWP domains of NSD3s and Pdp3, our bioinformatics analysis indicated that these structures are highly similar in 3D conformation and thus possibly hold a functional relationship.

PWWP domains employ an aromatic cage to interact with specific trimethylated histones. The aromatic residues are conserved within the PWWP domain of Pdp3 at positions F18, W21, and F48 [43]. Therefore, we asked whether the PWWP domain aromatic cage stability was important for its metabolic function. To answer that question, we deleted the Pdp3 protein from *S. cerevisiae* (Δ*pdp3*) and transformed this mutant with a plasmid expressing Pdp3 harboring the tryptophan to alanine at position twenty one (W21A) mutation. Yeast strains were grown in glucose, a carbon source that favors fermentative metabolism, so the metabolic phenotype resembles that of a tumorigenic cell. We reasoned that both Δ*pdp3* and W21A^{+} would present similar characteristics when compared to the control. Both yeast strains showed lower specific growth rate compared to the control (Figure 4A). In addition, WT cells displayed glucose consumption rates significantly higher than the mutants (Figure 4B). In relation to ROS sensibility, both *Pdp3* deficiency and expression of the *Pdp3* W21A mutant enhanced tolerance against ROS (Figure 5). After peroxide stress, the Δ*pdp3* and W21A^{+} survival rates were higher than the WT. Moreover, lipid peroxidation levels were decreased in Δ*pdp3* and W21A^{+} compared to WT (Figure 5B).

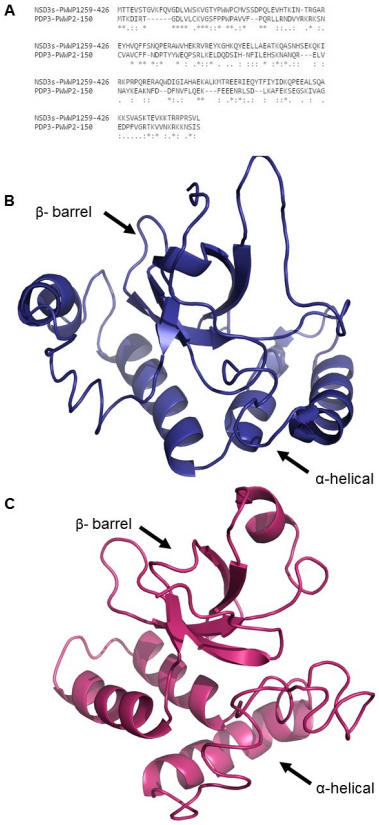

Figure 3: Primary sequence alignment and 3D structural models of NSD3s and Pdp3 PWWP domains. (**A**) Sequence alignment between the PWWP domains of NSD3s and Pdp3. (**B**) 3D structural model of NSD3s PWWP. (**C**) 3D structural model of Pdp3 PWWP.

Subsequently, we analyzed the effect of Pdp3 overexpression on the same metabolic phenotypes. We noticed that overexpression of Pdp3 induced an effect on cell metabolism similar to that of NSD3s. When grown in glycerol, yeast cells exhibited increased specific growth rate (Figure 6A), decreased oxygen consumption rate (Figure 6B) and higher sensitivity to ROS than the WT (Figure 7). Figure 7A shows that Pdp3^{+} yeast cells were less viable than the control when submitted to oxidative stress conditions. In addition, Pdp3^{+} mutant cells showed an increase in the levels of lipid peroxidation after one hour of hydrogen peroxide (20 mM) exposure (Figure 7B). To confirm that the PWWP domain regulates the metabolic shift through a mechanism depend on the ability of Pdp3 to bind methylated chromatin, Pdp3 was overexpressed in a Δ*set2* strain. The *S. cerevisiae* Set2 protein is a histone (H3) methyltransferase highly selective for lysine 36 (H3K36) [48]. As shown in Figure 8, Pdp3 overexpression did not cause any change in the metabolic behavior of the Δset2 strain. Both Δset2 and Δ*set2*(Pdp3)$^{+}$ strains exhibited the same growth (Figure 8A) and oxygen consumption rates (Figure 8B). In addition, tolerance to oxidative stress remained unchanged (Figure 8C and 8D). These results corroborate those obtained with the W21A^{+} mutant strain, suggesting that the effect of Pdp3 in the metabolic shift depends on the ability of its PWWP domain to recognize and bind to methylated H3K36. As previously shown, binding of Pdp3 to H3K36me3 recruits the NuA3b complex to coding regions of actively transcribed genes. Sas3, a subunit of the NuA3b complex, is a histone acetyltransferase that specifically acetylates H4, H3, and H2A [49]. However, the complete role of the NuA3b complex and the acetylation target of Sas3 remain unclear [43]. To verify if the metabolic function of Pdp3 is dependent on the NuA3b complex, Pdp3 was overexpressed in a Δ*sas3* strain. Pdp3 overexpression did not lead to any change in the Δ*sas3* metabolic behavior (Figure 9), suggesting that, under respiratory conditions, the NuA3b complex is responsible for mediating the metabolic shift induced by Pdp3.

Finally, a chimeric form of Pdp3 carrying the NSD3 PWWP1 domain was constructed to analyze if

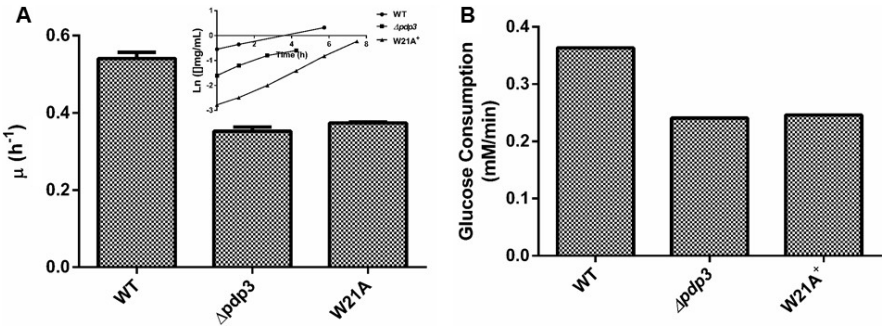

Figure 4: Pdp3 deficiency or W21A mutation shifts metabolism from fermentative to oxidative. WT, Δ*pdp3* and W21A^{+} strains were grown in drop out glucose 2% until the middle of exponential growth phase. (**A**) For specific growth rate measurements, the absorbance at 570 nm were taken at regular intervals until cells reached stationary phase. The inset shows the growth rate. (**B**) Glucose consumption rates were calculated by determining residual glucose level over the time. The results represent the mean ± standard deviation of at least three independent experiments and * or **mean different results at WT vs Δ*pdp3* *$p < 0.05$ and WT vs W21A^{+} **$p < 0,05$.

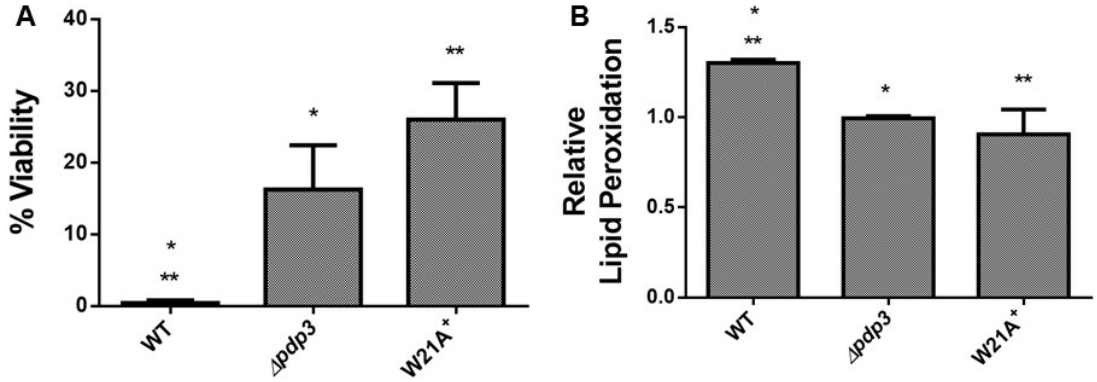

Figure 5: Effect of Pdp3 deficiency or W21A mutation on tolerance to oxidative stress. WT, Δ*pdp3* and W21A^{+} strains were grown in drop out glucose 2% until the middle of exponential growth phase. Oxidative damages were analyzed after stress with 3 mM H_2O_2/1 h/28°C/160 rpm. (**A**) Cellular viability was measured by standard dilution plate counts and expressed as the percentage of the colony-forming units before and after stress. (**B**) The levels of lipid peroxidation were determined by the TBARS method and the results were expressed as a ratio between the level of lipid peroxidation of stressed cells and control situation (before stress). The results represent the mean ± standard deviation of at least three independent experiments and * or **mean different results at WT vs Δ*pdp3* *$p < 0.05$ and WT vs W21A^{+} **$p < 0,05$.

the PWWP1 domain of NSD3s would be capable of functionally substituting that of Pdp3. When grown in glycerol, the chimera-expressing cells showed a higher specific growth rate (Figure 6A), a lower oxygen consumption (Figure 6B) and increased ROS sensitivity (Figure 7) than the WT, confirming that the PWWP domain of the human NSD3s protein is able to replace that of yeast Pdp3 in respiratory metabolism.

DISCUSSION

The work presented here explores the metabolic function of the PWWP domain of the short isoform of NSD3, a human oncogene, and Pdp3, a PWWP-containing protein from *S. cerevisiae*. Using glycerol (respiratory metabolism fermentative) and glucose as the sole carbon sources we were able to mimic the metabolic profile of a cell with healthy and a tumorigenic characteristics, in order to evaluate their metabolic similarity.

Glucose is the main carbon source consumed by *S. cerevisiae*, but yeast also makes use of other carbon sources [50, 51]. Inoculation of yeast into a glucose-rich medium is followed by rapid growth driven by fermentation and subsequent production of ethanol [52]. Gene expression analysis has discovered that many genes are differentially transcribed in response to different

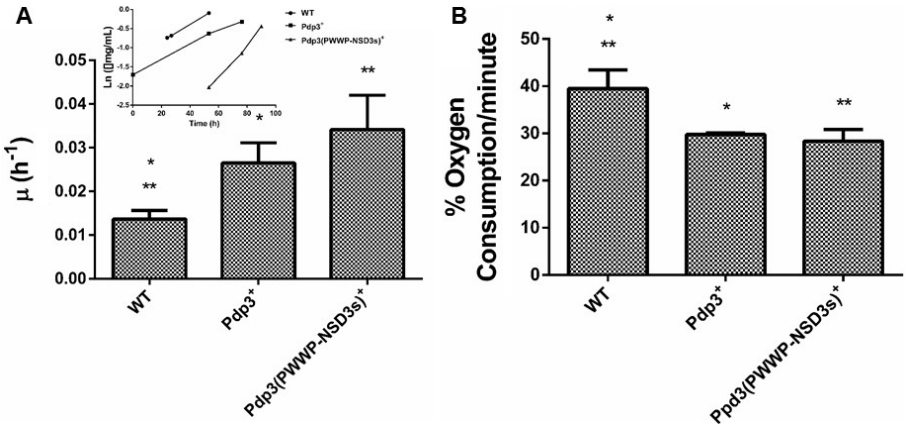

Figure 6: The PWWP domain of NSD3s functionally substitutes that of Pdp3. WT strain and the mutant overexpressing Pdp3 ($Pdp3^+$ strain), as well as the mutant expressing the Pdp3 chimera carrying the PWWP domain of NSD3s (Pdp3 $(PWWP\text{-}NSD3s)^+$) were grown in drop out glycerol 4% until the middle of exponential growth phase. (**A**) For specific growth rate measurements, the absorbance at 570 nm were taken at regular intervals until cells reached stationary phase. The inset shows the growth rate. (**B**) A Clark electrode measured the oxygen consumption for 10 min. The results represent the mean ± standard deviation of at least three independent experiments and * or **mean different results at WT vs $Pdp3^+$ *$p < 0.05$ and WT vs Pdp3 $(PWWP\text{-}NSD3s)^+$ **$p < 0{,}05$.

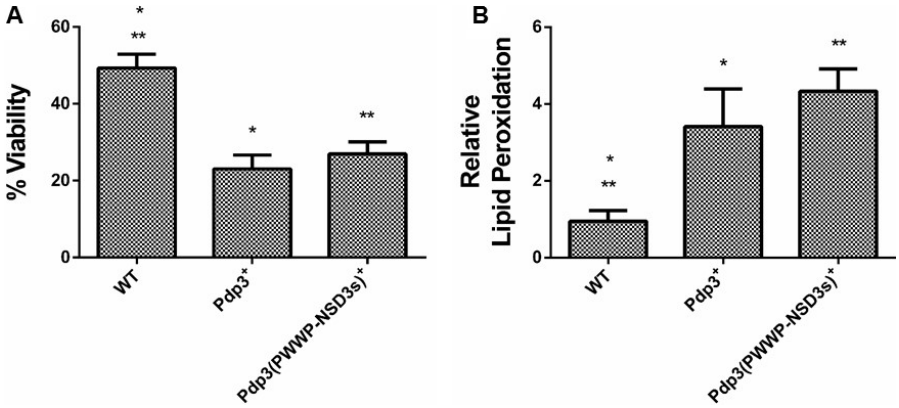

Figure 7: Effect of Pdp3 and Pdp3 (PWWP-NSD3s) chimera overexpression on tolerance to oxidative stress. WT strain and the mutant overexpressing Pdp3 ($Pdp3^+$ strain), as well as the mutant expressing the Pdp3 chimera carrying the PWWP domain of NSD3s (Pdp3 $(PWWP\text{-}NSD3s)^+$) were grown in drop out glycerol 4% until the middle of exponential growth phase. Oxidative damages were analyzed after stress with 20 mM H_2O_2/1 h/28°C/160 rpm. (**A**) Cellular viability was measured by standard dilution plate counts and expressed as the percentage of the colony-forming units before and after stress. (**B**) Oxidative damages were analyzed after stress with 20 mM H_2O_2/1 h/28°C/160 rpm. Lipid peroxidation levels were determined by the TBARS method and the results were expressed as a ratio between the level of lipid peroxidation of stressed cells and control situation (before stress). The results represent the mean ± standard deviation of at least three independent experiments and *or **mean different results at WT vs $PDP3^+$ *$p < 0.05$ and WT vs Pdp3 $(PWWP\text{-}NSD3s)^+$ **$p < 0{,}05$.

glucose levels. A set of genes are inducible by glucose, encoding low-affinity glucose transporters, glycolytic enzymes, and ribosomal proteins. Another ensemble of genes is repressed by glucose, including those involved in utilization of alternative carbon sources, gluconeogenesis, respiration, and peroxisomal functions [50–53]. Genes involved in the glucose catabolic repression pathway are of two types: genes required for repression, such as *HXK2* and *MIG1*, and genes required for derepression, as *SNF1* [53, 54].

Replacing glucose by glycerol as the carbon source forces yeast to obtain energy through respiration. When respiratory metabolism is adopted by yeast, glycerol is phosphorylated by glycerol kinase (Gut1) generating glycerol 3-phosphate. Then, glycerol 3-phosphate is oxidized to dihydroxyacetone phosphate (DHAP) by glycerol phosphate ubiquinone oxidoreductase (Gut2) located on the surface of the inner mitochondrial membrane. Electrons from this oxidation are transferred to ubiquinone, entering the respiratory chain [55, 56]. DHAP enters the glycolytic pathway, generating NADH (cytoplasm) and pyruvate, which goes to the respiratory chain. Glycerol-3-phosphate dehydrogenase (Gdp1/2) helps the re-oxidation of cytoplasmic NADH [57].

Healthy cells use mitochondrial oxidative phosphorylation for energy production [58], while tumor cells exhibit a significant increase in glycolysis and in the expression of glycolytic enzymes, converting most of glucose into L-lactate even under normal oxygen levels [11, 59]. This phenomenon is known as the Warburg effect and represents a metabolic hallmark of tumor cells, settling the idea that cancer is also a disease of metabolic characteristics [60]. It was shown that some cancer cells can reversibly switch between fermentation and respiration, depending on the absence or presence of glucose and environmental conditions [61]. This property represents an advantage of cancer cells *in vivo*, since it can adapt its metabolism to heterogeneous microenvironments for fast-growing conditions in malignant solid tumors [62]. In this study, we showed that NSD3s, an isoform of the human oncoprotein NSD3 [15], is capable of shifting cell metabolism from aerobic (respiration) to anaerobic (fermentation). This hypothesis was confirmed by the increase of the specific growth rate and decrease in

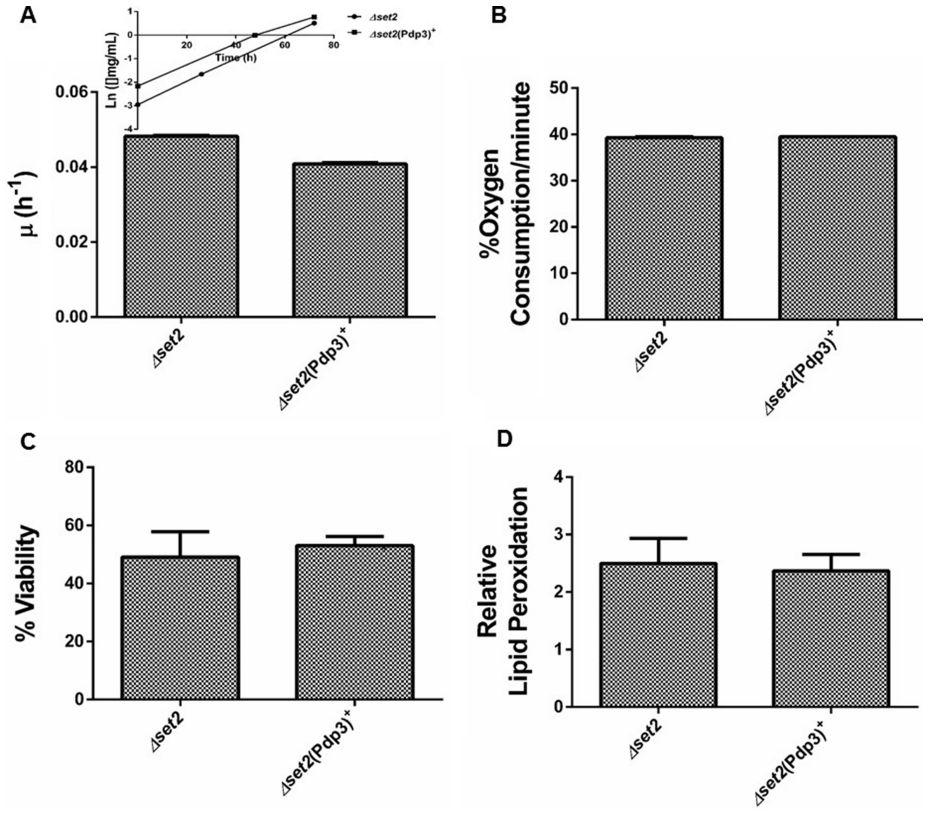

Figure 8: Set2 is essential for the Pdp3 recognition of H3K36me3. Δ*set2* strain and the mutant overexpressing Pdp3 (Δ*set2* (Pdp3)$^{+}$) were grown in drop out glycerol 4% until the middle of exponential growth phase. (**A**) For specific growth rate measurements, the absorbance at 570 nm were taken at regular intervals until cells reached stationary phase. The inset shows the growth rate. (**B**) A Clark electrode measured the oxygen consumption for 10 min. Oxidative damages were analyzed after stress with 20 mM H_2O_2/1 h/28°C/160 rpm. (**C**) Cellular viability was measured by standard dilution plate counts and expressed as the percentage of the colony-forming units before and after stress. (**D**) The levels of lipid peroxidation were determined by the TBARS method and results were expressed as a ratio between the level of lipid peroxidation of stressed cells and control situation (before stress). The results represent the mean ± standard deviation of at least three independent experiments.

oxygen consumption, leading to a lower tolerance against ROS in yeast. In mammalian cells, NSD3 overexpression induced the formation of expanding colonies in insulin-free medium. These cells were able to grow continuously in the absence of insulin-like growth factors, displayed the highest proliferation rate, and formed three-dimensional colonies in soft agar [15]. Based on the number of altered phenotypes acquired by NSD3-overexpressing mammalian cells, Yang and co-workers concluded that NSD3 is an important transforming oncogene from the 8p11-12 region [15]. Taken together, our results suggest that yeast cells overexpressing NSD3s display a metabolic phenotype similar to tumorigenic cells, under conditions that stimulate respiration.

NSD3s encodes a 645-amino acid protein containing one single PWWP domain [15, 62]. The PWWP domain is found in an extensive diversity of proteins playing a role in cell division, growth and differentiation. Several of these proteins are linked to cancer and certain diseases [63] or act as growth factors. *S. cerevisiae* harbors one PWWP-containing protein, Pdp3, which does not contain any other domain [64]. Pdp3 is a member of the NuA3 complex that shows a histone acetyltransferase activity involved in DNA transcription. The majority of genes controlled by this complex are involved in DNA replication [43]. The NuA3 complex exists in two different forms: NuA3a and NuA3b. NuA3a uses the plant homeodomain (PHD) finger of Yng1 to interact with histone 3 trimethylated lysine 4 (H3K4me3) at promoter regions of actively transcribed genes. Sas3 then acetylates histone 3 lysine 14 (H3K14), leading to transcription initiation at a subset of genes. On the other hand, Set2 trimethylates H3K36 (Figure 10A). The interaction between Pdp3 and H3K36me3 (Figure 10B), which is recognized by the PWWP domain of Pdp3 (Figure 10B), recruits Sas3 and other subunits of the NuA3b complex (Figure 10C) to the coding regions of actively transcribed genes. Although the function of NuA3b is not fully understood, Sas3 may acetylate

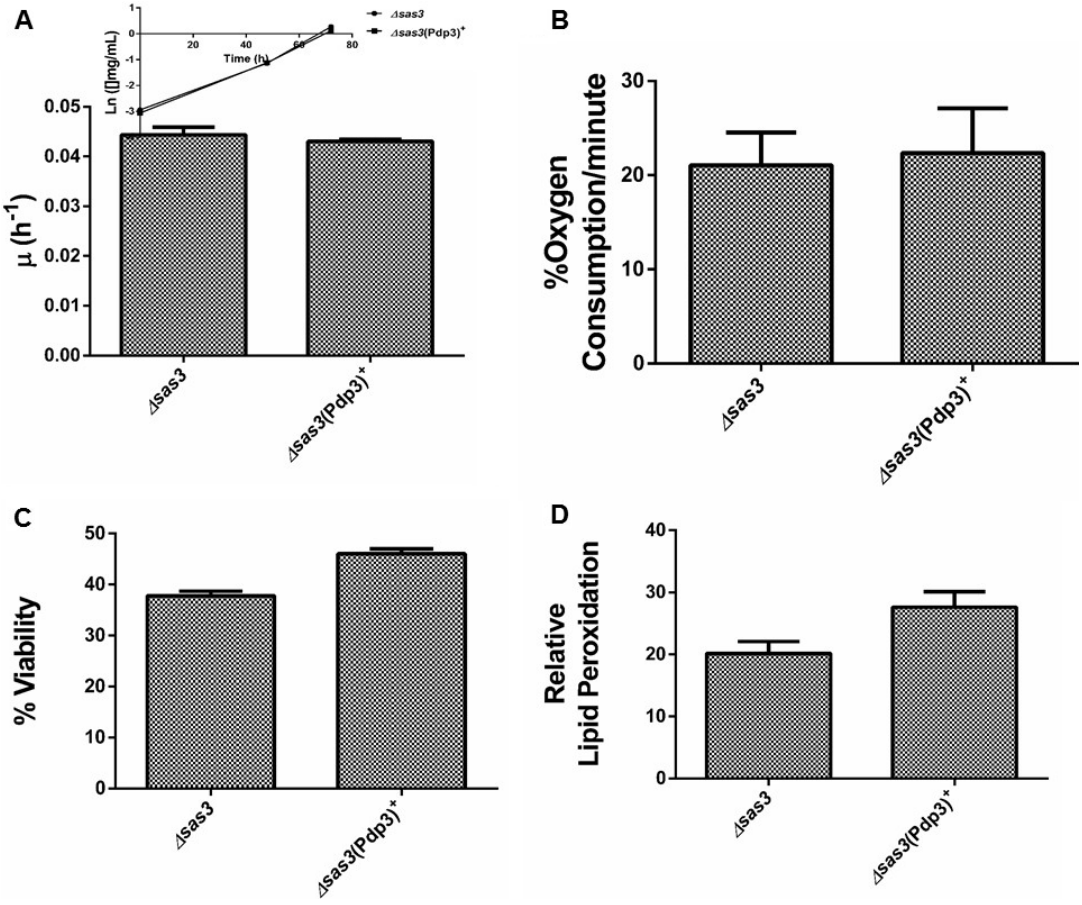

Figure 9: Sas3 is essential for the metabolic shift induced by Pdp3. Δ*sas3* strain and the mutant overexpressing Pdp3 (Δ*sas3* (Pdp3)$^{+}$) were grown in drop out glycerol 4% until the middle of exponential growth phase. (**A**) For specific growth rate measurements, the absorbance at 570 nm were taken at regular intervals until cells reached stationary phase. The inset shows the growth rate. (**B**) A Clark electrode measured the oxygen consumption for 10 min. Oxidative damages were analyzed after stress with 20 mM H_2O_2/1 h/28°C/160 rpm. (**C**) Cellular viability was measured by standard dilution plate counts and expressed as the percentage of the colony-forming units before and after stress. (**D**) The levels of lipid peroxidation were determined by the TBARS method and results were expressed as a ratio between the level of lipid peroxidation of stressed cells and control situation (before stress). The results represent the mean ± standard deviation of at least three independent experiments.

histones or non-histone (Figure 10C) proteins to facilitate transcription elongation [43]. Pdp3 depends on the ability of its PWWP domain to bind methylated chromatin (H3K36me3) in a respiratory metabolism. Our results indicate that the metabolic phenotype induced by Pdp3 overexpression is dependent on the specific methylation of H3K36, which is accomplished by Set2. Furthermore, we demonstrated that Pdp3 also depends on the NuA3b complex, indicating that a mutation in other subunits of the complex impacts metabolic reprogramming. Overexpression of Pdp3 in null Sas3 had no effect on the metabolic phenotypes measured, when compared with Δ*sas3*. Therefore, our results suggest that, under respiratory conditions, the NuA3b complex is responsible for mediating the metabolic shift induced by Pdp3.

A conserved aromatic cage within the Pdp3 PWWP domain is required for H3K36me3 binding. The aromatic residues are conserved in the PWWP domain of Pdp3 at positions F18, W21, and F48 [43]. We found that the integrity of the hydrophobic cage is essential for the Pdp3 metabolic function. The low specific growth rate, decreased glucose consumption, and increased tolerance against ROS displayed by the W21A mutant strain can also be observed for Δ*pdp3*. These results are in accordance with those of Gilbert and co-workers that demonstrated that all three mutations (F18, W21, and F48) independently abolish the interaction between Pdp3 and a H3K36me3 peptide, suggesting that Pdp3 requires a conserved aromatic cage to bind chromatin. Since the Pdp3 W21A^{+} mutant showed the same phenotype as the Δ*pdp3* strain, we concluded that the hydrophobic cage of Pdp3 PWWP is essential for its metabolic function. While overexpression of NSD3s was able to transform a healthy into a tumorigenic cell, knockdown of NSD3 in 8p11-12–amplified breast cancer cells resulted in loss of growth and survival [15]. Therefore, the absence of Pdp3 was beneficial to cells grown in glucose (fermentative metabolism).

We then concluded that overexpression of Pdp3 was capable of inducing a shift in metabolism toward

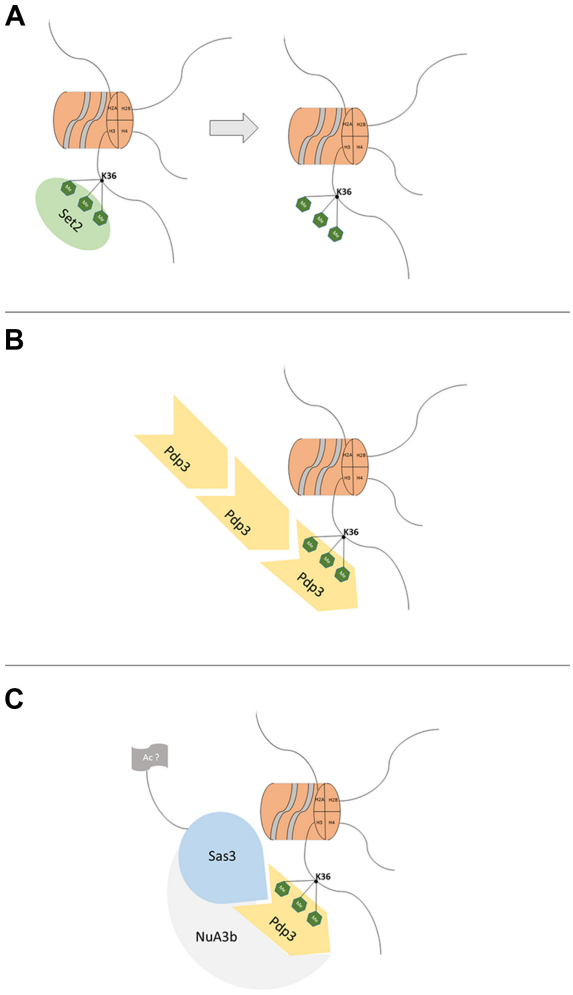

Figure 10: A model for the mechanism of action of Pdp3. (**A**) The Set2 histone methyltransferase trimethylates (green hexagon) histone H3 lysine 36 (black line). (**B**) Pdp3 recognizes and binds to H3K36me3. (**C**) After binding, Pdp3 recruits Sas3 and other subunits of the NuA3b complex, then Sas3 may acetylate (grey flag) histones or nonhistone proteins to facilitate transcription elongation [43].

fermentation, similar to overexpression of the human oncogene NSD3. The chimeric form of Pdp3, replacing its PWWP domain by that of NSD3s, functionally substitutes the yeast protein Pdp3. These data suggested that NSD3s and Pdp3 play similar roles in energy metabolism, shifting from aerobic to anaerobic metabolism. Cluntun and co-workers demonstrated that histone acetylation is sensed by glucose flux in a dose-dependent manner, which is a possible function of the Warburg effect [65]. These results corroborate our work, since Pdp3 is part of a histone acetyltransferase complex.

Human NSD3s and yeast Pdp3 are both involved in regulation of gene expression and are reported in this work as capable of causing a metabolic shift from aerobic (respiration) to anaerobic (fermentation) metabolism. The phenotypical changes observed in the strains with different profiles of expression of NSD3s and Pdp3 in the yeast model are very similar and agree well with the metabolic shift from a healthy to a carcinogenic cell. These results indicate that the pattern of gene expression is important to the malignant transformation of cell metabolic phenotypes, in accordance with previous reports. In summary, NSD3s and Pdp3 seem to play similar roles in cell metabolism and cells overexpressing both proteins, under conditions that simulate respiration, appear to metabolically behave like a tumorigenic cell. The hydrophobic cage is essential for Pdp3 function. We suggest that the PWWP domain of NSD3s functionally substitutes that of the yeast protein Pdp3. Given that chromatin remodeling and metabolic dysfunction are gaining considerable attention in cancer studies, future researches on the PWWP domains of Pdp3 and NSD3s may contribute to the design of new anti-cancer drugs.

MATERIALS AND METHODS

S. cerevisiae strains and growth conditions

WT strain BY4741 (*MATa; his3; leu2; met15; ura3*) and its isogenic mutants Δ*pdp3*, Δ*set2 and* Δ*sas3* harboring the *PDP3, SET2 and SAS3* genes interrupted by *KanMX4* were acquired from Euroscarf, Frankfurt, Germany. Stocks of both strains were maintained on solid 2% YPD (1% yeast extract, 2% glucose, 2% peptone and 2% agar) in appropriate conditions. For null mutants, the medium also contained 0.02% geneticine. *pECUh6NSD3S* (Enzimax, USA) and p*ECUh6PDP3* (Genscript, USA) 2 μ plasmids, containing *URA3* as selectable marker and harboring the NSD3s and *PDP3* genes, respectively, under control of the *CUP1* promoter, were used to transform WT strain using the lithium acetate protocol [66]. Similarly, the Pdp3 W21A and the Pdp3 chimera carrying the PWWP domain of NSD3s, acquired from Genscript, USA, were expressed in Δ*pdp3* using the same vector. The Pdp3 (PWWP-NSD3s) chimera (DNA sequence: ATGACAACGGAAGTG
TCCACTGGTGTTAAGTTTCAGGTTGGCGATCTTGT
GTGGTCCAAGGTGGGAACCTATCCTTGGTGGCCTT
GTATGGTTTCAAGTGATCCCCAGCTTGAGGTTCAT
ACTAAAATTAACACAAGAGGTGCCCGAGAATATC
ATGTCCAGTTTTTTAGCAACCAGCCAGAGAGGGC
GTGGGTTCATGAAAAACGGGTACGAGAGTATAAA
GGTCATAAACAGTATGAAGAATTACTGGCTGAGG
CAACCAAACAAGCCAGCAATCACTCTGAGAAACA
AAAGATTCGGAAACCCCGACCTCAGAGAGAACG
TGCTCAGTGGGATATTGGCATTGCCCATGCAGAGA
AAGCATTGAAAATGACTAGAGAAGAAAGAATAG
AACAGTATACTTTTATTTACATTGATAAACAGCCTG
AAGAGGCTTTATCCCAAGCAAAAAAGAGTGTTGC
CTCCAAAACCGAAGTTAAAAAAACCCGACGACC
AAGATCTGTGCTGATCAAAGAAGATCCGGAAGAT
AACCAGAAATCAAATGAAGAAGAAAGCAAACCG
AACATCAAACCGTCCAAAAAAAAGAGACCCACA
GCTAATTCGGGAGGAAAATCAAACAGTGGCAATA
AAAAGAAAGTTAAATTAGACTATTCCAGAAGAGT
AGAAATTTCACAGTTATTTCGCCGCAGGATTCAA
AGAAATCTAATCCAGAGAGAAACACCTCCTACTG
AGCATGAGATCAAGGAAACTCATGAACTATTAAA
TAGAATATATGAGAATTCTGACACCAAACGGCCCT
TTTTTGATTTGAAGGCCCTACGCGAAAGCAAATTA
CACAAGCTACTGAAAGCAATTGTTAATGATCCTGA
CTTAGGCGAATTTCACCCACTTTGTAAAGAAATTT
TACTGTCCTGGGCAGACCTAATCACAGAACTGAA
GAAAGAAAAGTTGCAAGCGCTACCTACGCCTTGA
was constructed replacing the PWWP domain of Pdp3 (residues 2-150; UniProt #Q06188) (DNA sequence: ACAAAAGATATTAGAACAGGCGATTTAGTGTTATG
CAAAGTTGGCTCGTTTCCACCTTGGCCAGCTGTA
GTATTTCCACAGCGTTTGCTGCGAAACGATGTATA
TAGAAAGAGAAAATCCAATTGTGTTGCTGTTTGTT
TTTTCAACGATCCAACTTATTATTGGGAACAACCC
AGTAGATTAAAGGAGCTAGATCAAGACAGCATTC
ACAATTTCATATTAGAACATAGTAAAAATGCAAAC
CAAAGGGAATTGGTCAATGCTTATAAGGAAGCAA
AAAATTTTGATGATTTCAACGTATTTTTACAAGAA
AAGTTTGAAGAAGAAAACAGGTTAAGTGATCTAA
AAGCGTTTGAGAAAAGTGAAGGTTCTAAAATCGT
TGCCGGAGAAGATCCCTTTGTAGGTCGAACAAAA
GTAGTGAATAAAAGAAAAAAAAATTCAATATCC)
by the PWWP1 domain of NSD3s (residues 259-426;UniProt #Q9BZ95-3) (DNA sequence: ATGACAACGGAAGTGTCCACTGGTGTTAAGTTTC
AGGTTGGCGATCTTGTGTGGTCCAAGGTGGGAAC
CTATCCTTGGTGGCCTTGTATGGTTTCAAGTGATCC
CCAGCTTGAGGTTCATACTAAAATTAACACAAGA
GGTGCCCGAGAATATCATGTCCAGTTTTTTAGCAA
CCAGCCAGAGAGGGCGTGGGTTCATGAAAAACG
GGTACGAGAGTATAAAGGTCATAAACAGTATGAA
GAATTACTGGCTGAGGCAACCAAACAAGCCAGCA
ATCACTCTGAGAAACAAAAGATTCGGAAACCCCG
ACCTCAGAGAGAACGTGCTCAGTGGGATATTGGC
ATTGCCCATGCAGAGAAAGCATTGAAAATGACTA

GAGAAGAAAGAATAGAACAGTATACTTTTATTTAC ATTGATAAACAGCCTGAAGAGGCTTTATCCCAAG CAAAAAAGAGTGTTGCCTCCAAAACCGAAGTTA AAAAAACCCGACGACCAAGATCTGTGCT). WT and Δ*pdp3* strains were also transformed with the pECUh6 vector, as a control. Transformants were selected in *drop out* medium (0.67% yeast nitrogen base without amino acids, 0.2% of *drop out* mixture and 2% agar) supplemented with 2% glucose. For all experiments, cells were grown up to mid-exponential phase (0.8 mg dry weight/ml) in liquid *drop out* medium, with or without uracil, and with 2% glucose or 4% glycerol, at 28°C and 160 rpm, with the ratio/flask volume medium of 5:1. The *CUP1*-regulated expression was induced with 50 μM $CuSO_4$ [67].

Bioinformatics analysis

The sequences of NSD3s (UniProt #Q9BZ95-3) and Pdp3 (UniProt #Q06188) PWWP domains were retrieved from the UniProt database [42]. The sequences were aligned using T-coffee [68]. ITasser was used for the *ab initio* modelling of the NSD3s and Pdp3 PWWP domains [44]. The TM-scores and root mean square deviations (RMSDs) of the mutant structures with respect to the wild-type structure were calculated using TM-Align [45].

Specific growth rate (μ)

The specific growth rate (μ) during the exponential phase was determined from a linear regression fit of the semilog plot of cell growth.

Oxygen consumption

Oxygen consumption was followed at 25°C in cell suspensions at 10 mg dry weight/mL incubated in 100 mM glucose and 50 mM Tris–HCl (pH 4.5) using a computer-interfaced Clark electrode operating in an air-tight chamber with continuous stirring [71, 72]. Addition of 2 mM CN^- completely abolished the oxygen consumption of WT cells (both when CN^- is added in the middle of the curve or when cells are previously incubated for 20 min), confirming that oxygen consumption was solely due to mitochondrial activity (Supplementary Figure S2). The rate of oxygen consumption was calculated from the slope of the curves. The percentage of oxygen consumption rate (%oxygen consumption/minute) was calculated from the maximum oxygen consumption trace of dithionite, which was used as a positive control (100%) and the fitting of each measurement curve. Each measurement was performed three times independently, and the oxygen consumption rate was expressed as the mean value ± standard deviation.

Glucose consumption

Cell suspensions were centrifuged, the supernatant was discarded and the pellet was resuspended in 50 mM phosphate buffer pH 6.0, 20 mM glucose, at a final cell concentration of 3 mg dry weight/mL. Over the time, samples were collected, centrifuged and the cell-free supernatants were used for glucose consumption determination. The concentration of glucose in the supernatant was measured by HPLC (Shimadzu) equipped with a refractive index detector. An Aminex HPX-87H column (7.8 mm ID × 30 cm, BioRad, USA) was used for separation. The HPLC apparatus operated with a mobile phase of 0.004 mM sulfuric acid at a flow rate of 0.6 mL/min [71, 72].

Oxidative stress, cell viability and lipid peroxidation

Cells at the first exponential phase growing on drop out medium glucose 2% or glycerol 4% were directly stressed (3 mM or 20 mM H_2O_2 [73], respectively, during 1 h at 28°C/160 rpm). Cell viability was determined by standard dilution plate counts on solid YPD medium. Viability was expressed as the percentage of colony forming units of stressed cells related to the control [69, 74, 75]. Lipid oxidation was measured by TBARS (thiobarbituric acid reactive species) method, which detects malondialdehyde, a final product of lipid peroxidation. Briefly, cells were centrifuged and washed with cold distilled water. The cell pellets were resuspended in 0.5 ml of 10% TCA (w/v) followed by addition of 1.5 g of glass beads. The samples were lysed by 6 cycles of 20 s agitation on a vortex followed by 20 s on ice. Extracts were centrifuged and the supernatant mixed with 0.1 ml of 0.1 M EDTA and 0.6 ml of 1% (w/v) thiobarbituric acid prepared in 0.05 M NaOH. The reaction mixture was incubated in a boiling water bath for 15 min and, after cooling, the absorbance was measured at 532 nm [76–78].

Statistical analysis

Data were expressed as mean values ± SD of at least three independent experiments. Values were compared by Student's *t* -test, which denotes homogeneity between experimental groups at $p < 0.05$.

ACKNOWLEDGMENTS

I would like to thank Dr. Roberto Salgado Amado and Dr.Claudio Akio Masuda for the contribution to this paper.

CONFLICTS OF INTEREST

The authors declare that they have no conflicts of interest.

GRANT SUPPORT

This work was supported by grants from FAPERJ, CAPES and CNPq.

REFERENCES

1. Seyfried TN, Flores RE, Poff AM, D'Agostino DP. Cancer as a metabolic disease: implications for novel therapeutics. Carcinogenesis. 2014; 35:515–27.
2. Szent-Györgyi A. The living state and cancer. Proc Natl Acad Sci USA. 74:2844–7.
3. Hanahan D, Weinberg RA. The hallmarks of cancer. Cell. 2000; 100:57–70.
4. Loeb LA. A mutator phenotype in cancer. Cancer Res. 2001; 61:3230–9.
5. Salk JJ, Fox EJ, Loeb LA. Mutational heterogeneity in human cancers: origin and consequences. Annu Rev Pathol. 2010; 5:51–75.
6. Seyfried TN, Shelton LM. Cancer as a metabolic disease. Nutr Metab (Lond). 2010; 7:7.
7. Phillips D, Aponte AM, French SA, Chess DJ, Balaban RS. Succinyl-CoA synthetase is a phosphate target for the activation of mitochondrial metabolism. Biochemistry. 2009; 48:7140–9.
8. Hochedlinger K, Blelloch R, Brennan C, Yamada Y, Kim M, Chin L, Jaenisch R. Reprogramming of a melanoma genome by nuclear transplantation. Genes Dev. 2004; 18:1875–85.
9. Hall A, Meyle KD, Lange MK, Klima M, Sanderhoff M, Dahl C, Abildgaard C,Thorup K, Moghimi SM, Jensen PB, Bartek J, Guldberg P, Christensen C. Dysfunctional oxidative phosphorylation makes malignant melanoma cells addicted to glycolysis driven by the (V600E)BRAF oncogene. Oncotarget. 2013; 4:584–99. doi: 10.18632/oncotarget.965.
10. Vander Heiden MG, Cantley LC, Thompson CB. Understanding the Warburg effect: the metabolic requirements of cell proliferation. Science. 2009; 324:1029–33.
11. DeBerardinis RJ, Sayed N, Ditsworth D, Thompson CB. Brick by brick: metabolism and tumor cell growth. Curr Opin Genet Dev. 2008; 18:54–61.
12. Yang ZQ, Streicher KL, Ray ME, Abrams J, Ethier SP. Multiple interacting oncogenes on the 8p11-p12 amplicon in human breast cancer. Cancer Res. 2006; 66:11632–43.
13. Bernard-Pierrot I, Gruel N, Stransky N, Vincent-Salomon A, Reyal F, Raynal V, Vallot C, Pierron G, Radvanyi F, Delattre O. Characterization of the recurrent 8p11-12 amplicon identifies PPAPDC1B, a phosphatase protein, as a new therapeutic target in breast cancer. Cancer Res. 2008; 68:7165–75.
14. Yang ZQ, Albertson D, Ethier SP. Genomic organization of the 8p11-p12 amplicon in three breast cancer cell lines. Cancer Genet Cytogenet. 2004; 155:57–62.
15. Yang ZQ, Liu G, Bollig-Fischer A, Giroux CN, Ethier SP. Transforming Properties of 8p11-12 Amplified Genes in Human Breast Cancer Transforming Properties of 8p11-12 Amplified Genes in Human Breast Cancer. 2010; 8487–97.
16. Gelsi-Boyer V. Comprehensive Profiling of 8p11-12 Amplification in Breast Cancer. Mol Cancer Res. 2005; 3:655–67.
17. Mahmood SF, Gruel N, Nicolle R, Chapeaublanc E, Delattre O, Radvanyi F, Bernard-Pierrot I. PPAPDC1B and WHSC1L1 Are Common Drivers of the 8p11-12 Amplicon, Not Only in Breast Tumors But also in Pancreatic Adenocarcinomas and Lung Tumors. Am J Pathol. 2013; 183:1–11.
18. Ray ME, Yang ZQ, Albertson D, Kleer CG, Washburn JG, Macoska JA, Ethier SP. Genomic and expression analysis of the 8p11-12 amplicon in human breast cancer cell lines. Cancer Res. 2004; 64:40–7.
19. Li Y, Trojer P, Xu C, Cheung P, Kuo A, Drury WJ, Qiao Q, Neubert TA, Xu RM, Gozani O, Reinberg D. Nature of the Substrate The Target of the NSD Family of Histone Lysine Methyltransferases Depends on the Nature of the Substrate. J Biol Chem. 2009; 284:34283-95.
20. He C, Li F, Zhang J, Wu J, Shi Y. The Methyltransferase NSD3 Has Chromatin-binding Motifs, PHD5-C5HCH, That Are Distinct from Other NSD (Nuclear Receptor SET Domain) Family Members in Their Histone H3. J Biol Chem. 2013; 288:4692–703.
21. Vougiouklakis T, Hamamoto R, Nakamura Y, Saloura V. The NSD family of protein methyltransferases in human cancer. Epigenomics. 2015; 1–12.
22. Stec I, Ommen GB Van, Dunnen JT Den. Closely Resembles WHSC1 and Maps to a Duplicated Region Shared with 4p16. 3. Genomics. 2001; 76:5–8.
23. Wu H, Zeng H, Lam R, Tempel W, Amaya MF, Xu C, Dombrovski L, Qiu W, Wang Y, Min J. Structural and Histone Binding Ability Characterizations of Human PWWP Domains. PLos One. 2011; 6.
24. Qin S, Min J. Structure and function of the nucleosome-binding PWWP domain. Trends Biochem Sci. 2014; 39:536–47.
25. Wang Y, Reddy B, Thompson J, Wang H, Noma KI, Yates JR, Jia S. Regulation of Set9-Mediated H4K20 Methylation by a PWWP Domain Protein. Mol Cell. 2009; 33:428–37.
26. Maurer-Stroh S, Dickens NJ, Hughes-Davies L, Kouzarides T, Eisenhaber F, Ponting CP. The Tudor domain "Royal Family": Tudor, plant Agenet, Chromo, PWWP and MBT domains. Trends Biochem Sci. 2003; 28:69–74.
27. Botstein D, Fink GR. Yeast : An Experimental Organism for 21st Century Biology. Genetics. 2011; 189:695–704.
28. Tosato V, Grüning NM, Breitenbach M, Arnak R, Ralser M, Bruschi CV. Warburg effect and translocation-induced genomic instability: two yeast models for cancer cells. Front Oncol. 2012; 2:212.
29. Diaz-Ruiz R, Rigoulet M, Devin A. The Warburg and Crabtree effects: On the origin of cancer cell energy metabolism and of yeast glucose repression. Biochim Biophys Acta - Bioenerg. 2011; 1807:568–76.
30. Khurana V, Lindquist S. Modelling neurodegeneration in Saccharomyces cerevisiae: why cook with baker's yeast? Nat Rev Neurosci. 2010; 11:436–49.

31. Carmona-Gutierrez D, Ruckenstuhl C, Bauer MA, Eisenberg T, Büttner S, Madeo F. Cell death in yeast: growing applications of a dying buddy. Cell Death Differ. 2010; 17:733–4.
32. Guaragnella N, Zdralević M, Antonacci L, Passarella S, Marra E, Giannattasio S. The role of mitochondria in yeast programmed cell death. Front Oncol. 2012; 2:70.
33. Guaragnella N, Zdralević M, Lattanzio P, Marzulli D, Pracheil T, Liu Z, Passarella S, Marra E, Giannattasio S. Yeast growth in raffinose results in resistance to acetic-acid induced programmed cell death mostly due to the activation of the mitochondrial retrograde pathway. Biochim Biophys Acta. 2013; 1833:2765–74.
34. Kachroo AH, Laurent JM, Yellman CM, Meyer AG, Wilke CO, Marcotte EM. Systematic humanization of yeast genes reveals conserved functions and genetic modularity. Science. 2015; 348:921–5.
35. Guaragnella N, Palermo V, Galli A, Moro L, Mazzoni C, Giannattasio S. The expanding role of yeast in cancer research and diagnosis: insights into the function of the oncosuppressors p53 and BRCA1/2. FEMS Yeast Res. 2014; 2–16.
36. Ruckenstuhl C, Bu S, Carmona-gutierrez D, Eisenberg T, Kroemer G, Sigrist SJ, Fröhlich KU, Madeo F. The Warburg Effect Suppresses Oxidative Stress Induced Apoptosis in a Yeast Model for Cancer. PLoS One. 2009; 4:2–7.
37. González-Siso MI, García-Leiro A, Tarrío N, Cerdán ME. Sugar metabolism, redox balance and oxidative stress response in the respiratory yeast Kluyveromyces lactis. Microb Cell Fact. 2009; 8:46.
38. Jamieson DJ. Oxidative stress responses of the yeast Saccharomyces cerevisiae. Yeast. 1998; 14:1511–27.
39. Abbott DA, Suir E, Duong GH, de Hulster E, Pronk JT, van Maris AJA. Catalase overexpression reduces lactic acid-induced oxidative stress in Saccharomyces cerevisiae. Appl Environ Microbiol. 2009; 75:2320–5.
40. Moskovitz J, Bar-Noy S, Williams WM, Requena J, Berlett BS, Stadtman ER. Methionine sulfoxide reductase (MsrA) is a regulator of antioxidant defense and lifespan in mammals. Proc Natl Acad Sci U S A. 2001; 98:12920–5.
41. Dastidar RG, Hooda J, Shah A, Cao TM, Henke RM, Zhang L. The nuclear localization of SWI/SNF proteins is subjected to oxygen regulation. Cell Biosci. 2012; 2:1.
42. The UniProt Consortium. Update on activities at the Universal Protein Resource (UniProt) in 2013. Nucleic Acids Res. 2013; 41:D43–7.
43. Gilbert TM, McDaniel SL, Byrum SD, Cades JA, Dancy BCR, Wade H, Tackett AJ, Strahl BD, Taverna SD. A PWWP Domain-Containing Protein Targets the NuA3 Acetyltransferase Complex via Histone H3 Lysine 36 trimethylation to Coordinate Transcriptional Elongation at Coding Regions. Mol Cell Proteomics. 2014; 13:2883–95.
44. Roy A, Kucukural A, Zhang Y. I-TASSER: a unified platform for automated protein structure and function prediction. Nat Protoc. 2011; 5:725–38.
45. Zhang Y. TM-align: a protein structure alignment algorithm based on the TM-score. Nucleic Acids Res. 2005; 33:2302–9.
46. de Carvalho MDC, De Mesquita JF. Structural modeling and in silico analysis of human superoxide dismutase 2. PLoS One. 2013; 8:e65558.
47. Jimenez-Lopez JC, Gachomo EW, Seufferheld MJ, Kotchoni SO. The maize ALDH protein superfamily: linking structural features to functional specificities. BMC Struct Biol. 2010; 10:43.
48. Strahl BD, Grant PA, Briggs SD, Sun ZW, Bone JR, Caldwell JA, Mollah S, Cook RG, Shabanowitz J, Hunt DF, Allis CD. Set2 is a nucleosomal histone H3-selective methyltransferase that mediates transcriptional repression. Mol Cell Biol. 2002; 22:1298–306.
49. Takechi S, Nakayama T. Sas3 is a histone acetyltransferase and requires a zinc finger motif. Biochem Biophys Res Commun. 1999; 266:405–10.
50. Carlson M. Glucose repression in yeast. Current Opinion in Microbiology. 1999; 2:202–7.
51. Kim JH, Roy A, Jouandot D, Cho KH. The glucose signaling network in yeast. Biochim Biophys Acta - Gen Subj. 2013; 1830:5204–10.
52. DeRisi JL, Iyer VR, Brown PO. Exploring the metabolic and genetic control of gene expression on a genomic scale. Science. 1997; 278:680–6.
53. Thevelein JM. Signal transduction in yeast. Yeast. 1994; 10:1753–90.
54. Devit MJ, Waddle JA, Johnston M. Regulated Nuclear Translocation of the Migl Glucose Repressor. Mol Biol Cell. 1997; 8:1603–18.
55. Flores CL, Rodríguez C, Petit T, Gancedo C. Carbohydrate and energy-yielding metabolism in non-conventional yeasts. FEMS Microbiol Rev. 2000; 24:507–29.
56. Nevoigt E, Stahl U. Osmoregulation and glycerol metabolism in the yeast Saccharomyces cerevisiae. FEMS Microbiol Rev. 1997; 21:231–41.
57. Herrero E, Ros J, Bellí G, Cabiscol E. Redox control and oxidative stress in yeast cells. Biochim Biophys Acta - Gen Subj. 2008; 1780:1217–35.
58. Santidrian AF, Matsuno-yagi A, Ritland M, Seo BB, Leboeuf SE, Gay LJ, Yagi T, Felding-Habermann B. Mitochondrial complex I activity and NAD +/NADH balance regulate breast cancer progression. J Clin Invest. 2013; 123:1068–81.
59. López-Lázaro M. The warburg effect: why and how do cancer cells activate glycolysis in the presence of oxygen? Anticancer Agents Med Chem. 2008; 8:305–12.
60. Warburg O. On the Origin of Cancer Cells. Science. 1956; 123:309–14.
61. Jose C, Bellance N, Rossignol R. Choosing between glycolysis and oxidative phosphorylation: A tumor's dilemma? Biochim Biophys Acta - Bioenerg. 2011; 1807:552–61.
62. Zhou Z, Thomsen R, Kahns S, Nielsen AL. The NSD3L histone methyltransferase regulates cell cycle and cell

invasion in breast cancer cells. Biochem Biophys Res Commun. 2010; 398:565–70.

63. Slater LM, Allen MD, Bycroft M. Structural variation in PWWP domains. J Mol Biol. 2003; 330:571–6.

64. Stec I, Nagl SB, van Ommen GJB, den Dunnen JT. The PWWP domain: a potential protein–protein interaction domain in nuclear proteins influencing differentiation? FEBS Lett. 2000; 473:1–5.

65. Cluntun AA, Huang H, Dai L, Liu X, Zhao Y, Locasale JW. The rate of glycolysis quantitatively mediates specific histone acetylation sites. Cancer Metab. 2015; 3:10.

66. Gietz D, St Jean A, Woods RA, Schiestl RH. Improved method for high efficiency transformation of intact yeast cells. Nucleic Acids Res. 1992; 20:1425.

67. Pereira MD, Herdeiro RS, Fernandes PN, Eleutherio ECA, Panek AD. Targets of oxidative stress in yeast sod mutants. Biochim Biophys Acta. 2003; 1620:245–51.

68. Notredame C, Higgins DG, Heringa J. T-coffee: a novel method for fast and accurate multiple sequence alignment. J Mol Biol. 2000; 302:205–17.

69. Mannarino SC, Amorim MA, Pereira MD, Moradas-Ferreira P, Panek AD, Costa V, Eleutherio EC. Glutathione is necessary to ensure benefits of calorie restriction during ageing in Saccharomyces cerevisiae. Mech Ageing Dev. 2008; 129:700–5.

70. Bonawitz ND, Rodeheffer MS, Shadel GS. Defective mitochondrial gene expression results in reactive oxygen species-mediated inhibition of respiration and reduction of yeast life span. Mol Cell Biol. 2006; 26:4818–29.

71. Vilela L de F, de Araujo VPG, Paredes R de S, Bon EP da S, Torres FAG, Neves BC, Eleutherio EC. Enhanced xylose fermentation and ethanol production by engineered Saccharomyces cerevisiae strain. AMB Express. 2015; 5:16.

72. Liu X, Ai N, Zhang H, Lu M, Ji D, Yu F, Ji J. Quantification of glucose, xylose, arabinose, furfural, and HMF in corncob hydrolysate by HPLC-PDA–ELSD. Carbohydr Res. 2012; 353:111–4.

73. Horn A, Parrilha GL, Melo KV, Fernandes C, Horner M, Visentin Ldo C, Santos JA, Santos MS, Eleutherio EC, Pereira MD. An iron-based cytosolic catalase and superoxide dismutase mimic complex. Inorg Chem. 2010; 49:1274–6.

74. Mannarino C, Vilela LF, Brasil AA, Aranha JN, Moradas-ferreira P, Pereira MD, Costa V, Eleutherio EC. Requirement of glutathione for Sod1 activation during. 2011; 2010:19–25.

75. Rona G, Herdeiro R, Mathias CJ, Torres FA, Pereira MD, Eleutherio E. CTT1 overexpression increases life span of calorie-restricted Saccharomyces cerevisiae deficient in Sod1. Biogerontology. 2015; 1:1–21.

76. Mariani D, Mathias CJ, da Silva CG, Herdeiro R da S, Pereira R, Panek AD, Eleutherio EC, Pereira MD. Involvement of glutathione transferases, Gtt1and Gtt2, with oxidative stress response generated by H2O2 during growth of Saccharomyces cerevisiae. Redox Rep. 2008; 13:246–54.

77. Steels EL, Learmonth RP, Watson K. Stress tolerance and membrane lipid unsaturation in Saccharomyces cerevisiae grown aerobically or anaerobically. Microbiology. 1994; 140:569–76.

78. de Sá RA, de Castro FA, Eleutherio ECA, de Souza RM, da Silva JFM, Pereira MD. Brazilian propolis protects Saccharomyces cerevisiae cells against oxidative stress. Braz J Microbiol. 2013; 44:993–1000.

Biophys Rev (2016) 8:63–74
DOI 10.1007/s12551-015-0190-6

REVIEW

PWWP domains and their modes of sensing DNA and histone methylated lysines

Germana B. Rona[1] · **Elis C. A. Eleutherio**[1] · **Anderson S. Pinheiro**[1]

Received: 15 September 2015 / Accepted: 14 December 2015 / Published online: 14 January 2016

Abstract Chromatin plays an important role in gene transcription control, cell cycle progression, recombination, DNA replication and repair. The fundamental unit of chromatin, the nucleosome, is formed by a DNA duplex wrapped around an octamer of histones. Histones are susceptible to various post-translational modifications, covalent alterations that change the chromatin status. Lysine methylation is one of the major post-translational modifications involved in the regulation of chromatin function. The PWWP domain is a member of the Royal superfamily that functions as a chromatin methylation reader by recognizing both DNA and histone methylated lysines. The PWWP domain three-dimensional structure is based on an N-terminal hydrophobic β-barrel responsible for histone methyl-lysine binding, and a C-terminal α-helical domain. In this review, we set out to discuss the most recent literature on PWWP domains, focusing on their structural features and the mechanisms by which they specifically recognize DNA and histone methylated lysines at the level of the nucleosome.

Keywords Epigenetics · Histone · Lysine · Methylation · PWWP Domain

Chromatin and histones

The eukaryotic genome is highly packed in a dynamic polymer called chromatin. In addition to its structural role, allowing DNA compaction within the nucleus, chromatin regulates a number of essential cellular processes, including gene transcription, cell cycle progression, DNA recombination, replication and repair (Luger et al. 2012). The basic unit of chromatin is the nucleosome, which is composed of 147 base pairs of DNA wrapped around an octamer of histones formed by a tetramer of H3-H4 and two dimers of H2A-H2B (Arents et al. 1991; Luger et al. 1997; Kornberg and Lorck 1999).

Histones undergo numerous post-translational modifications (PTMs), including lysine acetylation, lysine/arginine methylation, serine/threonine/tyrosine/histidine phosphorylation, proline isomerization, arginine deimination, lysine ubiquitination, ADP-ribosylation, sumoylation, crotonylation, propionylation, butyrylation, formylation, hydroxylation, and serine/threonine O-GlcNAcylation (Arnaudo and Garcia 2013; Andreoli and Del Rio 2014; Rothbart and Strahl 2014). Most covalent modifications are present in the intrinsically disordered N- and C-terminal tails of histones; however, some are found in their globular, folded domains (Andreoli and Del Rio 2014; Rothbart and Strahl 2014). Histone PTMs occur with high substrate specificity resulting in different outcomes in terms of chromatin structure and function (Andreoli and Del Rio 2014; Rothbart and Strahl 2014).

Since 1964, when Vincent Allfrey first described histone acetylation and methylation (Allfrey et al. 1964), much research has been focused on the correlation between histone PTMs and chromatin-dependent functions, namely transcriptional regulation. Significant advance in this field came from the discovery of proteins that incorporate, remove, and recognize PTMs in histones, acting as "writers", "erasers", and "readers" of the covalent marks, respectively. The first direct link between histone PTMs and transcriptional regulation was provided by the concomitant identification of a transcription-associated histone acetyl transferase, p55/GCN5 (Brownell et al. 1996), and a histone deacetylase, HDAC1/Rpd3

✉ Anderson S. Pinheiro
pinheiro@iq.ufrj.br

[1] Department of Biochemistry, Institute of Chemistry, Federal University of Rio de Janeiro, Rio de Janeiro 21941-909, Brazil

(Taunton et al. 1996). One major landmark was the proposal of the histone code hypothesis by Strahl and Allis (2000). Although the existence of such a code has been the subject of much debate in the literature (Henikoff 2005; Rando 2012), important concepts were introduced with it. Firstly, distinct PTMs may work individually or in combination to give rise to different biological outcomes. Therefore, two distinct PTMs may work together in a synergistic or antagonistic fashion (Strahl and Allis 2000; Cheung et al. 2000). Secondly, histone PTMs may have a direct effect on chromatin structure, altering histone–histone and histone–DNA interactions, most likely due to charge neutralization as in lysine acetylation (Shogren-Knaak et al. 2006). Finally, histone PTMs may work as specific docking sites for protein readers that selectively bind to chromatin and direct downstream events (Turner et al. 1992; Ruthenburg et al. 2011). The identification of the bromodomain as an acetyl-lysine reader module further confirmed this idea and suggested the existence of other effector proteins capable of reading histone PTMs (Dhalluin et al. 1999).

Lysine methylation

Lysine methylation is one of the major PTMs involved in the regulation of chromatin function. Depending on the specific site of methylation, the outcomes may vary significantly. Methylation of histone lysines H3K4, H3K36, and H3K79 are hallmarks of actively transcribed chromatin, while those of H3K9, H3K27, and H4K20 are silenced chromatin marks (Völkel and Angrand 2007; Wozniak and Strahl 2014). The degree of lysine methylation is also a form of transcriptional regulation and histones can be mono-, di- or trimethylated (Völkel and Angrand 2007; Wozniak and Strahl 2014). H3K4me3 is associated with active transcription, H3K9me3, H3K27me3 and H4K20me3 are involved in chromatin repression, while H3K4me1 is a known gene enhancer (Heintzman et al. 2007; Wozniak and Strahl 2014).

Methylation of specific lysines on histones is accomplished by histone lysine methyltranferases (HKMTs). These enzymes either contain a catalytic SET domain, homologous to the suppressor of variegation 3–9 from *Drosophila melanogaster*, or belong to the Dot1/DOT1L protein family (Völkel and Angrand 2007). Despite its stability, lysine methylation is a reversible process and can be removed by enzymes of the lysine-specific demethylase (KDM) family or enzymes carrying Jumonji (JmjC) domains (Völkel and Angrand 2007). In addition to KMTs and KDMs, a number of other protein domains are capable of binding and recognizing histone methylated lysines, acting as readers of the methylation marks. They are present in several chromatin modifying, remodeling and adaptor proteins (Taverna et al. 2007).

The royal superfamily

Among chromatin readers, we highlight the Royal superfamily, which includes Tudor, Chromo (chromatin-binding), MBT (malignant brain tumor), and PWWP domains. They are involved in several chromatin roles by identifying histone methylated lysines/arginines (Maurer-Stroh et al. 2003). This family seems to be a product of divergent evolution as they share a common ancestor structurally characterized by three conserved β-strands. These domains employ conserved aromatic residues to compose a hydrophobic cavity accountable for methyl-histone binding (Adams-Cioaba and Min 2009; Gayatri and Bedfort 2014).

The PWWP domain

The PWWP domain was first described as a structural motif in WHSC1, a HKMT involved in the Wolf–Hirschhorn syndrome (Stec et al. 1998). The Pro-Trp-Trp-Pro sequence motif is conserved in eukaryotes and the protein domains that encompass it usually contain about 90–130 amino acids. Despite conservation, some variations on the Pro-Trp-Trp-Pro sequence motif may occur. For example, the PWWP domains of the DNA methyltransferases DNMT3a/b contain SWWP motifs (Qiu et al. 2002), while that of the hepatoma-derived growth factor (HDGF) comprises a PHWP motif (Sue et al. 2004) (Fig. 1). Recently, the first position of the Pro-Trp-Trp-Pro sequence motif has been shown to regulate the PWWP domain stability and oligomerization (Hung et al. 2015). PWWP domains that contain a proline as the first amino acid residue of the Pro-Trp-Trp-Pro motif are more stable, less dynamic, and less prone to aggregation than those that display an alanine at the same position (Hung et al. 2015).

The PWWP domain is exclusively found in eukaryotes, ranging from lower eukaryotes such as protozoa and yeast to men. The human genome encodes more than 20 PWWP-containing proteins, which are located in the nucleus and play a major role in cell division, growth, and differentiation. They are implicated in various chromatin functions, including DNA modification, repair, and transcriptional regulation (Wu et al. 2011; Qin and Min 2014).

Protein-protein interactions modulate the PWWP domain function

Stec and co-workers (2000) suggested that the PWWP domain may work as a protein–protein interaction site, influencing both chromatin remodeling and transcription. In fact, the DNA methyltransferase DNMT3a directly interacts with SAL-like 3 (SALL3) through its PWWP domain. SALL3 binding decreases DNMT3a interaction with chromatin,

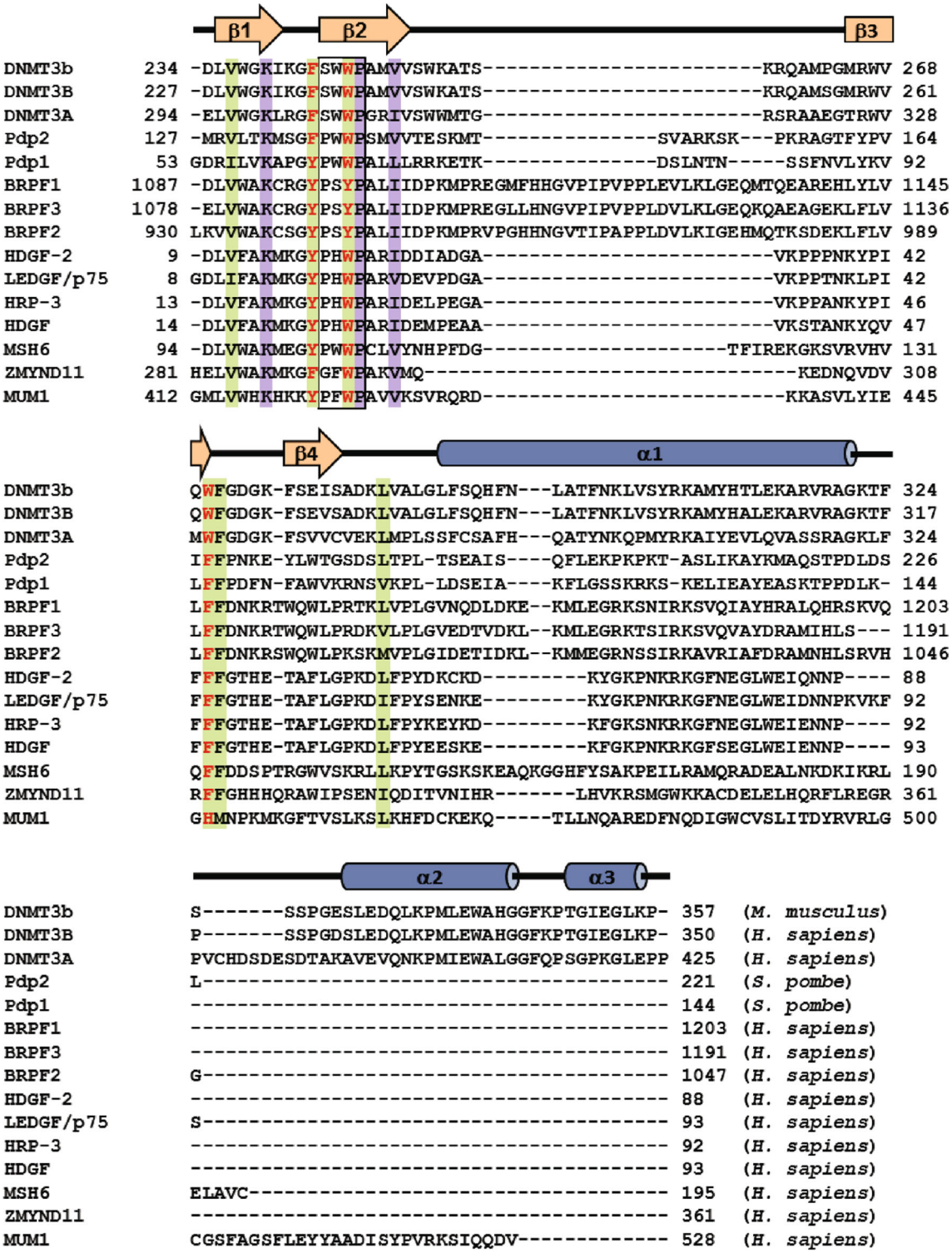

Fig. 1 Sequence alignment of PWWP domains. Primary sequence alignment of PWWP domains with previously determined three-dimensional structures. The experimental secondary structure of mouse DNMT3b PWWP (1KHC) is depicted on *top* of the figure. The Pro-Trp-Trp-Pro sequence motif is highlighted by the *black box*. Purple boxes mark highly conserved residues, while *green boxes* mark similar residues. The aromatic cage residues that directly participate in histone methylated lysine binding and recognition are colored *red*. Sequence alignment was performed with ClustalW2

inhibiting DNMT3a-mediated CpG island methylation (Shikauchi et al. 2009). The PWWP domain of DNMT3b interacts with the zinc-finger and homeobox protein ZHX1, leading to an increase in DNMT3b transcriptional repression

(Kim et al. 2007). In addition, DNMT3b PWWP was also shown to interact with the small ubiquitin-related modifier (SUMO) E3 ligase PIAS1 (Park et al. 2008). The lens epithelium-derived growth factor LEDGF/p75, also known as PSIP1 (PC4 and SFRS1 interacting protein 1), is a transcriptional coactivator that tethers the HIV-1 integrase to active host chromatin. LEDGF/p75 interacts with the methylation-associated transcriptional modulator MeCP2 both in vitro and in human cancer cells (Leoh et al. 2012). This interaction is mediated by its N-terminal PWWP-CR1 domain and regulates MeCP2 transcriptional activity (Leoh et al. 2012). Furthermore, LEDGF/p75 PWWP was shown to interact with the transcriptional activator TOX4 and the splicing cofactor NOVA1 (Morchikh et al. 2013). These proteins seem to play a role in the regulation of LEDGF/p75 interaction with chromatin, controlling processes such as virus replication, DNA repair, and transcription (Morchikh et al. 2013). Despite the large number of binding partners, the molecular mechanisms underlying the modulation of the PWWP domain activity by protein ligands still remain to be elucidated.

Structural features of PWWP domains

To date, several three-dimensional structures of PWWP domains have been reported, including those of DNMT3a, DNMT3b, Pdp1, Pdp2, HDGF, HDGF2, HDGF-related protein 3 (HRP-3), Bromo and plant homeodomain (PHD) finger–containing protein 1 (BRPF1), BRPF2, BRPF3, LEDGF/p75, Mutated melanoma-associated antigen 1 (MUM1), MutS homolog 6 (MSH6), and Zinc finger MYND domain-containing protein 11 (ZMNYD11) (Qiu et al. 2002; Slater et al. 2003; Sue et al. 2004, 2007; Nameki et al. 2005; Lukasik et al. 2006; Laguri et al. 2008; Vezzoli et al. 2010; Wu et al. 2011; Eidahl et al. 2013; van Nuland et al. 2013; Wang et al. 2014; Wen et al. 2014). Table 1 summarizes the structural data currently available in the literature. The PWWP domain adopts a similar fold in all PWWP-containing proteins. This fold can be divided into two distinct substructural motifs: an N-terminal β−barrel substructure and a C-terminal helical substructure (Fig. 2) (Qiu et al. 2002). The N-terminal β−barrel is the most conserved feature of the PWWP domain and it consists of five antiparallel β-strands (β1−β5). The Pro-Trp-Trp-Pro motif is located at the interface of the two substructures, positioned at the end of the β−β arch that connects strands β1 and β2 (β1-β2 arch) and the beginning of β2 (Fig. 2). The first proline residue usually forms a β-bulge, while the second proline induces a bend in strand β2. In addition, the side chains of the two tryptophan residues are oppositely oriented and partially solvent exposed (Fig. 2) (Qiu et al. 2002. The β2−β3 loop is the less conserved part of the β−barrel, both in terms of amino acid composition and length, allowing for the insertion of different secondary structural elements (Qiu et al. 2002, 2012; Slater et al. 2003; Nameki et al. 2005; Vezzoli et al. 2010; Wu et al. 2011).

In contrast to the β-barrel, the C-terminal helical substructure is strikingly variable and may contain two to six α-helices (Fig. 3). The PWWP domains of DNMT3a/b contain a bundle of five α-helices (Qiu et al. 2002; Wu et al. 2011). On the other hand, those of BRPF1, HDGF, HDGF2, and Pdp1 are composed of two α-helices connected by a loop (Lukasik et al. 2006; Vezzoli et al. 2010; Wu et al. 2011; Qiu et al. 2012). Recently, the structure of the PWWP domain from LEDGF/p75 revealed a C-terminal region with less helical content than its counterparts. LEDGF/p75 PWWP contains a shorter helix α3, which leads to a longer connecting loop (Eidahl et al. 2013; van Nuland et al. 2013). Despite the lack of sequence conservation, one α-helix is virtually identical in all PWWP structures determined so far (Fig. 3). This common α-helix is packed against the β-barrel. The stability of the PWWP domain arises from intramolecular hydrogen bonds and polar interactions. These interactions occur not only between residues located in the same substructure but also between residues on different substructures, such as those present in the β1−β2 arch and β3−β4 loop and the ones in the helical region (Qiu et al. 2002, 2012; Slater et al. 2003; Nameki et al. 2005; Vezzoli et al. 2010; Wu et al. 2011).

The PWWP domain uses a basic surface to nonspecifically interact with DNA

The PWWP domain contains a significant amount of basic residues (lysines and arginines), which raises its isoelectric point to more than 9. This creates a positively charged surface that functions as a favorable interface for DNA binding. Qiu and co-workers (2002) demonstrated for the first time that the PWWP domain of DNMT3b directly binds DNA in vitro. In addition, mutations on the PWWP domains of DNMT3a and DNMT3b abolish their interaction with heterochromatin and inhibit their ability to methylate DNA (Chen et al. 2004; Ge et al. 2004). From that time until now, numerous PWWP domains have been shown to exhibit DNA-binding activity, including those of LEDGF/p75 (Singh et al. 2006; Eidahl et al. 2013; van Nuland et al. 2013), HDGF (Lukasik et al. 2006; Yang and Everett 2007), MSH6 (Laguri et al. 2008), DNMT3a (Purdy et al. 2010), Pdp1 (Qiu et al. 2012), and the Bromo-ZnF-PWWP domain of human ZMNYD11 (Wang et al. 2014). For most proteins, DNA binding occurs in a nonspecific manner, without sequence selectivity. The PWWP domain of DNMT3b binds to a 234-bp element of the pericentric chromatin as well as random genomic sequences (Chen et al. 2004). This interaction is efficiently inhibited by sheared salmon sperm

Table 1 Three-dimensional structures of PWWP domains currently available in the literature

Protein	PDBid	Organism	Structure determination	DNA interaction	Histone methyl-lysine interaction	Reference
DNA methyltrasferase 3 beta (DNMT3b) apo	1KHC	Mouse	X-ray crystallography	Nonspecific		Qiu et al. 2002
SPBC215.07c (Pdp2) apo	1H3Z	*Schizosaccharomyces pombe*	Solution NMR			Slater et al. 2003
Hepatoma derived growth factor (HDGF) apo	1RI0	Human	Solution NMR	Heparin		Sue et al. 2004
	2B8A	Human	Solution NMR	Nonspecific		Lukasik et al. 2006
Hepatoma derived growth factor (HDGF) domain-swapped dimer	2NLU	Human	Solution NMR	Heparin		Sue et al. 2007
HDGF-related protein 3 (HRP-3) apo	1N27	Human	Solution NMR			Nameki et al. 2005
MutS Homolog 6 (MSH6) apo	2GF1	Human	Solution NMR			Laguri et al. 2008
Bromo and plant homeodomain (PHD) finger–containing protein 1 (BRPF1) apo	2X35	Human	X-ray crystallography		H3K36me3	Vezzoli et al. 2010
	3L42	Human	X-ray crystallography		H3K36me2, H3K36me3, H3K79me2, H3K79me3	Wu et al. 2011
BRPF1:H3K36me3 peptide complex	2X4W	Human	X-ray crystallography		H3K36me3	Vezzoli et al. 2010
	2X4X	Human	X-ray crystallography		H3K36me3	Vezzoli et al. 2010
	2X4Y	Human	X-ray crystallography		H3K36me3	Vezzoli et al. 2010
	3MO8	Human	X-ray crystallography		H3K36me3	Wu et al. 2011
Bromo and plant homeodomain (PHD) finger–containing protein 2 (BRPF2) apo	3LYI	Human	X-ray crystallography		H3K36me2, H3K79me2, H3K79me3	Wu et al. 2011
Bromo and plant homeodomain (PHD) finger–containing protein 3 (BRPF3) apo	3PFS	Human	X-ray crystallography			Wu et al. 2011
Hepatoma derived growth factor 2 (HDGF2) apo	3EAE	Human	X-ray crystallography		H3K36me2	Wu et al. 2011
Mutated-melanoma associated antigen 1 (MUM1) apo	3PMI	Human	X-ray crystallography		H3K36me2, H3K36me3	Wu et al. 2011
DNA methyltrasferase 3 alpha (DNMT3a): Bis-Tris complex	3LLR	Human	X-ray crystallography		H3K36me3	Wu et al. 2011
DNMT3b:Bis-Tris complex	3QKJ	Human	X-ray crystallography			Wu et al. 2011
HDGF2:H4K20me3 peptide complex	3QBY	Human	X-ray crystallography		H3K36me2	Wu et al. 2011
HDGF2:H3K79me3 peptide complex	3QJ6	Human	X-ray crystallography		H3K36me2	Wu et al. 2011
Pdp1 apo	2L89	*Schizosaccharomyces pombe*	Solution NMR	Nonspecific	H4K20me	Qiu et al. 2012
Lens epithelium-derived growth factor (LEDGF/p75) apo	2M16	Human	Solution NMR	Nonspecific	H3K36me3	Eidahl et al. 2013
	3ZEH	Human	Solution NMR	Nonspecific	H3K36me3	Van Nuland et al. 2013
Zinc finger MYND domain-containing protein 11 (ZMNYD11) Bromo-ZnF-PWWP apo	4NS5	Human	X-ray crystallography	Nonspecific	H3K36me3	Wang et al. 2014
	4N4G	Human	X-ray crystallography		H3.3K36me3	Wen et al. 2014
ZMNYD11 Bromo-ZnF-PWWP:H3.1K36me3 peptide complex	4N4H	Human	X-ray crystallography		H3.3K36me3	Wen et al. 2014
ZMNYD11 Bromo-ZnF-PWWP:H3.3K36me3 peptide complex	4N4I	Human	X-ray crystallography		H3.3K36me3	Wen et al. 2014

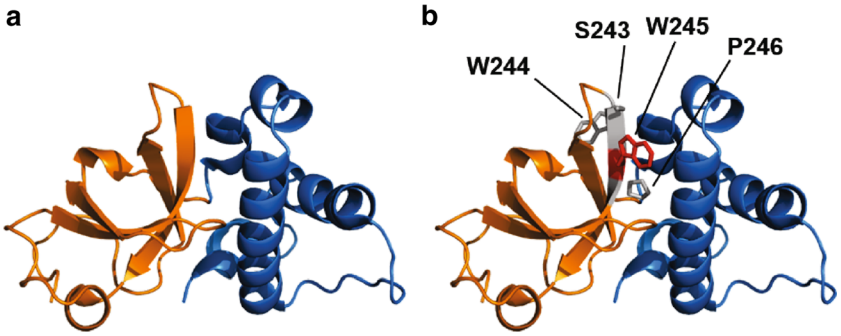

Fig. 2 The PWWP domain fold. Ribbon diagram of mouse DNMT3b PWWP domain three-dimensional structure (1KHC). **a** The PWWP domain fold can be subdivided into two distinct substructural motifs. The N-terminal β-barrel is represented in *orange*, while the C-terminal helical bundle is colored *blue*. **b** The Pro-Trp-Tro-Pro sequence motif is positioned in the beginning of strand β2 and displayed in *sticks*. Residue W245 of mouse DNMT3b PWWP is engaged in direct binding to histone methyl-lysines and is *red*, while other residues (S243, W244, 9246) are *gray*

DNA, indicating that DNMT3b PWWP is a nonspecific DNA-binding module (Chen et al. 2004). The PWWP domain of HDGF is unable to discriminate between A/T and C/G-rich sequences (Lukasik et al. 2006). NMR titration experiments showed that HDGF PWWP binds to a 15-bp oligonucleotide containing the CACC sequence and a mutant of this DNA, confirming the lack of sequence specificity (Lukasik et al. 2006). The PWWP domain of MSH6 binds to a double-stranded 35-bp oligonucleotide without any preference for G/T mismatches or nicked DNA (Laguri et al. 2008). Moreover, the PWWP domain of DNMT3a exhibits no clear preference for hemimethylated, double-methylated, or CpG-containing double-stranded DNA sequences (Purdy et al. 2010). Finally, consistent with previous results, the PWWP domains of *Schizosaccharomyces pombe* Pdp1, as well as the human proteins LEDGF/p75 and ZMNYD11 were shown to bind DNA nonspecifically (Qiu et al. 2012; van Nuland et al. 2013; Eidahl et al. 2013; Wang et al. 2014). In contrast to these data, Yang and Everett (2007) have shown that the PWWP domain of HGDF is able to specifically recognize a 37-bp DNA element common to the promoter of SMYD1, arguing about the specificity of interaction between PWWP domains and DNA. DNA binding by PWWP domains occurs with a wide range of affinities, with K_d values varying from low nanomolar to high micromolar. DNA-binding affinity and stoichiometry are directly linked to DNA size, suggesting that multiple binding events may occur (Lukasik et al. 2006; Qiu et al. 2012; Eidahl et al. 2013; van Nuland et al. 2013).

NMR titration experiments revealed the DNA-binding interface of numerous PWWP-containing proteins, such as

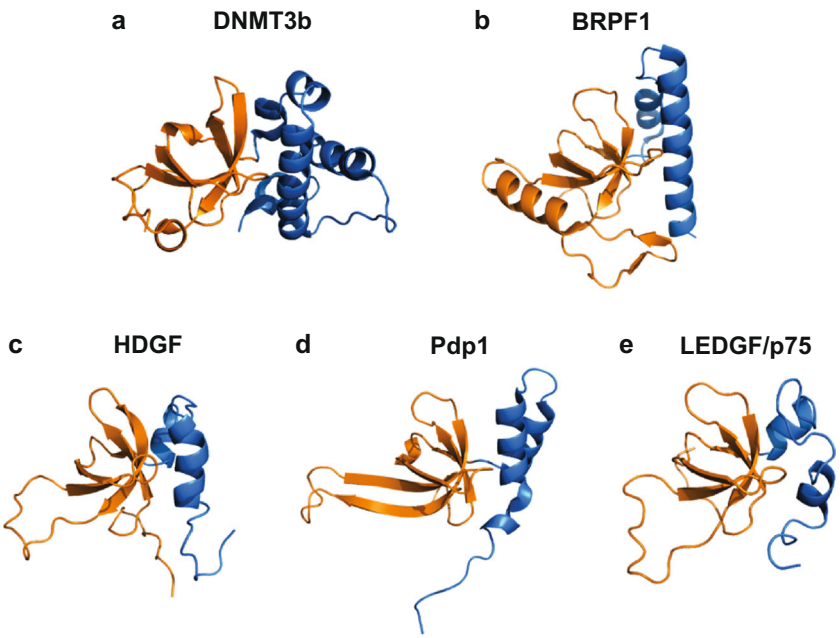

Fig. 3 Structural diversity of the PWWP domain C-terminal helical bundle. The PWWP domain C-terminal substructure may contain two to six helices. **a** Ribbon diagram of mouse DNMT3b PWWP (1KHC) displaying its five α-helical bundle. **b** Ribbon diagram of human BRPF1 PWWP (2X35). **c** Ribbon diagram of human HDGF PWWP (1RI0). **d** Ribbon diagram of yeast Pdp1 PWWP (2L89). **e** Ribbon diagram of human LEDGF/p75 PWWP (2M16). The C-terminal substructures of BRPF1, HDGF, Pdp1, and LEDGF/p75 PWWP domains are composed of two α-helices connected by a loop. All C-terminal helical bundles are *blue*

HDGF (Lukasik et al. 2006), Pdp1 (Qiu et al. 2012), and LEDGF/p75 (Eidahl et al. 2013; van Nuland et al. 2013). Several protein resonances are shifted upon addition of DNA, indicating a DNA-binding event that happens in the fast exchange regime. Most of the shifted resonances localize to a single side of the PWWP domain structure. These resonances correspond to residues located in the β1-β2 arch and Pro-Trp-Trp-Pro motif, as well as strand β2 and the helical turns in the C-terminal region. This putative DNA-binding site superimposes well with a highly positively charged surface formed by lysine and arginine residues exposed to the solvent (Fig. 4) (Lukasik et al. 2006; Qiu et al. 2012; Eidahl et al. 2013; van Nuland et al. 2013). This suggests that the PWWP–DNA interaction occurs mostly through electrostatic contacts with the phosphate backbone of the DNA, and thus agrees well with a nonspecific binding mode (Lukasik et al. 2006; Qiu et al. 2012; Eidahl et al. 2013; van Nuland et al. 2013).

The PWWP domain acts as a histone methyl-lysine reader through a conserved aromatic cage

Structural and sequence similarities between the PWWP domain and other members of the Royal superfamily suggested a possible role in the recognition of modified histone residues. It was only in 2009 that Wang and co-workers found out that the PWWP domain of the yeast protein Pdp1 directly binds to histone 4 lysine 20 monomethylation (H4K20me1) and that this interaction is crucial for the histone methyltransferase Set9 chromatin association (Wang et al. 2009). These results first established a functional role for the PWWP domain as a methyl-lysine reader motif involved in epigenetic regulation. After the discovery that Pdp1 PWWP recognizes H4K20me1, many other PWWP domains were shown to exhibit methylated histone-binding activity, including those of BRPF1 (Vezzoli et al. 2010; Wu et al. 2011), DNMT3a (Dhayalan et al. 2010), BRPF2 (Wu et al. 2011), HDGF2 (Wu et al. 2011), WHSC1 (Wu et al. 2011), WHSC1L1 (Wu et al. 2011), LEDGF/p75 (Pradeepa et al. 2012; Eidahl et al. 2013; van Nuland et al. 2013), Ioc4 (Maltby et al. 2012; Smolle et al. 2012), ZMYND11 (Wen et al. 2014; Wang et al. 2014; Guo et al. 2014), and Pdp3 (Gilbert et al. 2014).

A high-throughput mass spectrometry screening identified the PWWP domain as a histone 3 lysine 36 trimethylation-binding module (Vermeulen et al. 2010). With the exception of Pdp1, all other PWWP domains specifically recognize H3K36me3, suggesting a functional role for this domain as a putative H3K36me3 sensor. This histone trimethylation mark is associated with the coordination of important cellular events such as transcription elongation, mRNA splicing, and expression of developmental genes (Kolasinska-Zwierz et al. 2009; Nimura et al. 2009). Interestingly, in vitro binding of purified PWWP domains to methylated histone peptides occur with very low affinities, with K_d values in the low millimolar range (Vezzoli et al. 2010; Dhayalan et al. 2010; Wu et al. 2011; Qiu et al. 2012; Eidahl et al. 2013; van Nuland et al. 2013; Wen et al. 2014; Wang et al. 2014).

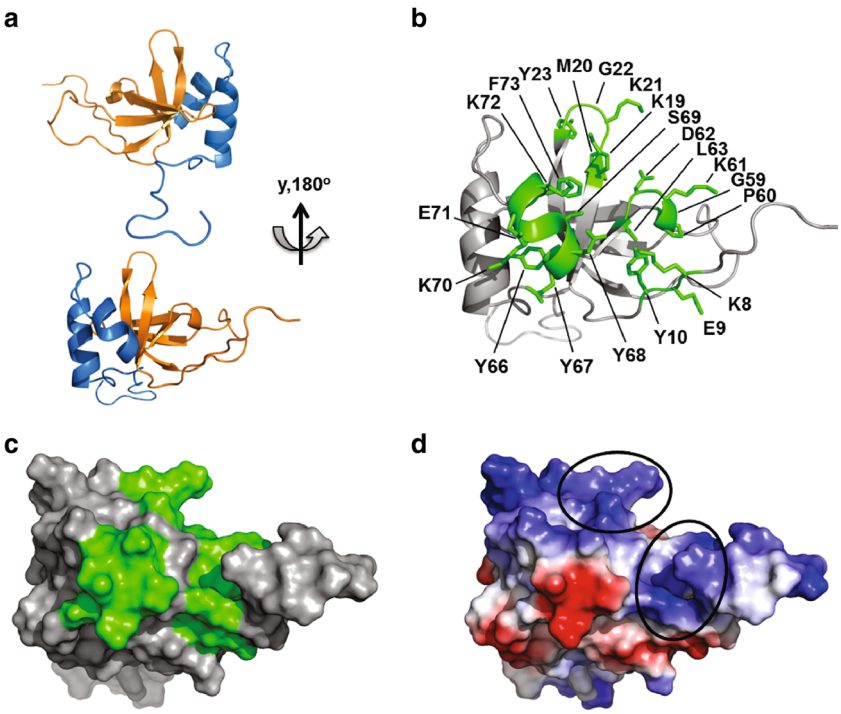

Fig. 4 The PWWP domain DNA-binding interface. **a** Ribbon diagram of human HDGF PWWP three-dimensional structure (2B8A). The N-terminal β-barrel is colored *orange*, while the C-terminal helical bundle is *blue*. The HDGF PWWP structure is first represented in the same orientation as Fig. 2 and then rotated 180° about the *y* axis. **b** The HDGF PWWP–DNA interface. Residues that directly engage in DNA binding are *green* and labeled. **c** Surface representation of the HDGF PWWP structure (2B8A) highlighting the residues that compose the DNA-binding interface (*green*). **d** Electrostatics distribution of the HDGF PWWP structure showing that the DNA-binding surface is positively charged

Structural analysis revealed that the PWWP domain binds to histone methyl-lysines through a hydrophobic cavity composed of three aromatic residues located in the β1−β2 arch, Pro-Trp-Trp-Pro motif and strand β3 (Vezzoli et al. 2010; Wu et al. 2011; Qiu et al. 2012; Eidahl et al. 2013; van Nuland et al. 2013; Wen et al. 2014; Wang et al. 2014). These amino acids side chains are perpendicularly oriented to one another, forming an aromatic cage that accommodates the trimethyl ammonium group (Fig. 5). Mutations of the residues that compose the aromatic cage abolish methylated histone peptide binding (Wang et al. 2009, 2014; Vezzoli et al. 2010; Maltby et al. 2012; Smolle et al. 2012; Wen et al. 2014; Gilbert et al. 2014; Guo et al. 2014). Moreover, this aromatic cage is a common molecular architecture found in members of the Royal superfamily. Sequence alignment shows that the aromatic cage residues are conserved among several PWWP domains, indicating a common binding mode to methylated histone tails (Vezzoli et al. 2010; Wu et al. 2011; Qiu et al. 2012; Eidahl et al. 2013; van Nuland et al. 2013; Wen et al. 2014; Wang et al. 2014) (Fig. 1). However, some PWWP domains contain a truncated version of the aromatic cage, lacking one of the three aromatic residues, and thus are unable to bind histone methyl-lysines (Gong et al. 2012).

In addition to the aromatic cage, the β2−β3 loop directly participates in histone interaction as it forms one of the walls of the binding pocket (Wu et al. 2011; Qiu et al. 2012). The β2−β3 loop is the region that differs mostly among PWWP domains. These structural differences suggest that the β2−β3 loop may be implicated in determining ligand binding specificity. It is worth noting that the methyl-lysine binding pocket is located in a different position than the DNA binding site. Therefore, PWWP domains employ distinct but contiguous interfaces for binding histones and DNA (Qiu et al. 2012; van Nuland et al. 2013).

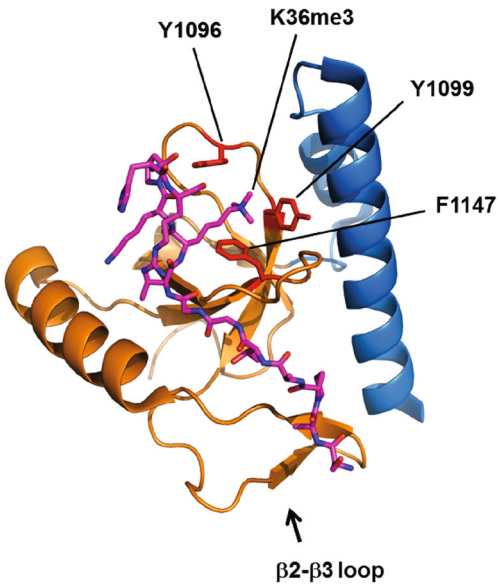

Fig. 5 The PWWP domain histone methyl-lysine-binding aromatic cage. Ribbon diagram of human BRPF1:H3K36me3 peptide complex three-dimensional structure (2X4W). The N-terminal β-barrel is in *orange*, while the C-terminal helical bundle is *blue*. The H3K36me3-containing histone peptide is displayed in *sticks* and colored *magenta*. The residues that compose the BRPF1 PWWP aromatic cage (Y1096, Y1099, and F1147) responsible for binding H3K36me3 are represented in *sticks* and colored *red*

The PWWP domain simultaneously binds DNA and histone methyl-lysines within the context of the nucleosome

The observation that the PWWP domain binds histones and DNA in separate regions raised the possibility that this domain may simultaneously interact with methylated histone tails and nucleosomal DNA. A GST-pull down assay demonstrated that the PWWP domain of the *S. pombe* protein Pdp1 directly interacts with isolated yeast nucleosomes (Wang et al. 2009). In addition, the PWWP domain of DNMT3a is able to pull down native nucleosomes purified from human cells (Dhayalan et al. 2010). Direct nucleosomal binding has been shown to a variety of PWWP-containing proteins, including Pdp1 (Wang et al. 2009; Qiu et al. 2012), DNMT3a (Dhayalan et al. 2010), Ioc4 (Maltby et al. 2012; Smolle et al. 2012), LEDGF/p75 (Eidahl et al. 2013; van Nuland et al. 2013), and ZMNYD11 (Guo et al. 2014). In all cases, nucleosomal interaction is enhanced by histone methylation. The PWWP domain of Pdp1 interacts with nucleosomes purified from wild-type yeast cells, but not with those from strains carrying the histone methyltransferase Set9 deletion or the H4K20R mutation, indicating that Pdp1 PWWP specifically recognizes H4K20me (Wang et al. 2009). Similarly, the PWWP domain of DNMT3a specifically interacts with nucleosomes harboring the H3K36me3 mark (Dhayalan et al. 2010).

The understanding of the PWWP domain binding specificity to nucleosomes has been greatly facilitated by the use of methyl-lysine analogues. In this approach, nucleosomes are reconstituted from recombinant expressed histones containing a specific K to C mutation (i.e., K36C) and further chemically modified to mimic the methylation state (i. e. $H3K_C36me3$). The PWWP domain of Pdp1 preferentially binds to recombinant reconstituted nucleosomes carrying the $H4K_C20me3$ analogue (Qiu et al. 2012). Furthermore, the PWWP domains of Ioc4 (Smolle et al. 2012) and LEDGF/p75 (Eidahl et al. 2013; van Nuland et al. 2013) exhibit higher affinity for $H3K_C36me3$-containing than unmethylated nucleosomes. In vitro binding experiments using purified nucleosomes containing methyl-lysine analogues have shown that the PWWP domain affinity is higher for intact nucleosomes than for either isolated histone peptides or DNA. Qiu and co-workers (2012) demonstrated that the PWWP domain of Pdp1 interacts with H4K20me3 peptide and DNA with K_d values of ~6.0 mM and

~4.2 μM, respectively. Although the interactions with the histone peptide and DNA are rather weak, Pdp1 PWWP displays enhanced binding to nucleosomes containing the H4K$_C$20me3 methylation analogue. Moreover, Eidahl and co-workers (2013) found that GST-fused LEDGF/p75 PWWP binds to H3K$_C$36me3-containing nucleosomes (K_d ~48 nM) much more strongly than to isolated H3K36me3 peptide (K_d ~2.7 mM) and DNA (K_d ~1.5 μM). Similarly, van Nuland and co-workers (2013) revealed a respective four and two orders of magnitude enhancement in LEDGF/p75 PWWP binding affinity to H3K$_C$36me3 nucleosomes (K_d ~ 1.5 μM) relative to H3K36me3 peptide (K_d ~17 mM) and DNA (K_d ~150 μM). This affinity enhancement toward nucleosomes is probably due to concerted binding of the PWWP domain to both histone methyl-lysines and DNA.

On the basis of structural data, an atomic model for the PWWP domain-nucleosome complex has been constructed (Fig. 6) (Qiu et al. 2012; Eidahl et al. 2013; van Nuland et al. 2013). In this model, the PWWP domain contacts the two DNA duplexes wrapped around the histone core at two different binding interfaces. Each interface shows a high degree of electrostatic complementarity with the phosphate backbone of the nucleosomal DNA. In addition, the methylated histone tail emerges from between the two DNA duplexes and interacts with the PWWP domain aromatic cage located in the middle of the two DNA-binding sites (Fig. 6). The current model suggests that the hydrophobic pocket and the basic surfaces act synergistically to ensure high-affinity binding of the PWWP domain to nucleosomes (Qiu et al. 2012; Eidahl et al. 2013; van Nuland et al. 2013).

Conclusions

In conclusion, the PWWP domain, a member of the Royal superfamily, functions as a histone methyl-lysine reader, most likely H3K36me3, through a conserved aromatic cage present in its N-terminal β-barrel substructure. In addition, most PWWP domains employ basic interfaces to nonspecifically bind DNA. Nucleosomal DNA interaction results in an increase in binding affinity to histone methyl-lysines. Concerted binding to methylated histone tails and DNA leads to specific recognition of

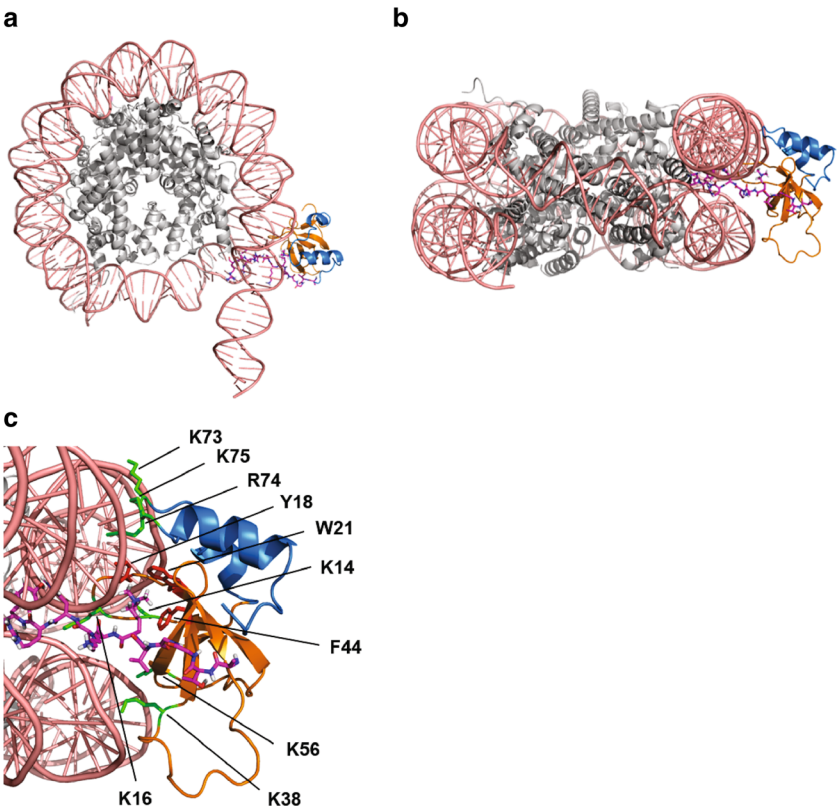

Fig. 6 Structural model of the LEDGF/p75 PWWP-nucleosome complex. (**a**) Ribbon diagram of the data-driven structural model of the LEDGF/p75 PWWP domain in complex with the nucleosome (3ZH1). Histones are colored *gray*, while nucleosomal DNA is shown in salmon. The N-terminal β-barrel of the LEDGF/p75 PWWP domain is colored *orange*, and the C-terminal helical bundle is colored *blue*. Histone H3 residues 31–42, harboring the K36 trimehthylation mark, are displayed in *sticks* and colored *magenta* (**b**) Same as in a rotated 180° about the *x* axis. (**c**) A zoom in on the LEDGF/p75 PWWP domain interaction with the nucleosomal particle. The aromatic cage residues Y18, W21, F44, which are directly engaged in H3K36me3 binding, are represented in *sticks* and colored *red*. In addition, residues K16, K38, K56, K73, R74, K75, which nonspecifically bind DNA, are represented in *sticks* and colored *green*

H3K36me3-containing nucleosomes. A similar mode of interaction may be used to recognize other histone PTMs located close to the nucleosomal core.

Acknowledgments This work was supported by grants from Fundação Carlos Chagas Filho de Amparo à Pesquisa do Estado do Rio de Janeiro (FAPERJ), Conselho Nacional de Desenvolvimento Científico e Tecnológico (CNPq), and by a Brazil Initiative Collaboration grant from Brown University to A.S.P. G.B.R is recipient of a Coordenação de Aperfeiçoamento de Pessoal de Nível Superior (CAPES) graduate fellowship.

Compliance with ethical standards

Conflict of interest Germana B. Rona declares that she has no conflict of interest.

Elis C. A. Eleutherio declares that she has no conflict of interest.

Anderson S. Pinheiro declares that he has no conflict of interest.

Ethical approval This article does not contain any studies with human participants or animals performed by any of the authors.

References

Adams-Cioaba MA, Min J (2009) Structure and function of histone methylation binding proteins. Biochem Cell Biol 87:93–105. doi:10.1139/O08-129

Allfrey VG, Faulkner R, Mirsky AE (1964) Acetylation and methylation of histones and their possible role in the regulation of RNA synthesis. Proc Natl Acad Sci U S A 51:786–794. doi:10.1073/pnas.51.5.786

Andreoli F, Del Rio A (2014) Physicochemical modifications of histones and their impact on epigenomics. Drug Discov Today 19:1372–1379. doi:10.1016/j.drudis.2014.05.005

Arents G, Bulringame RW, Wang BC, Love WE, Moudrianakis EN (1991) The nucleosomal core histone octamer at 3.1 Å resolution: a tripartite protein assembly and a left-handed superhelix. Proc Natl Acad Sci U S A 88:10148–10152

Arnaudo AM, Garcia BA (2013) Proteomic characterization of novel histone post-translational modifications. Epigenetics Chromatin 6:24. doi:10.1186/1756-8935-6-24

Brownell JE, Zhou J, Ranalli T, Kobayashi R, Edmondson DG, Roth SY, Allis CD (1996) Tetrahymena histone acetyltransferase A: a homolog to yeast Gcn5p linking histone acetylation to gene activation. Cell 84:843–851. doi:10.1016/S0092-8674(00)81063-6

Chen T, Tsujimoto N, Li E (2004) The PWWP domain of Dnmt3a and Dnmt3b is required for DNA methylation to the major satellite repeats at pericentric heterochromatin. Mol Cell Biol 24:9048–9058. doi:10.1128/MCB.24.20.9048-9058.2004

Cheung P, Allis CD, Sassone-Corsi P (2000) Signaling to chromatin through histone modifications. Cell 103:263–271. doi:10.1016/S0092-8674(00)00118-5

Dhalluin C, Carlson JE, Zeng L, He C, Aggarwal AK, Zhou MM (1999) Structure and ligand of a histone acetyltransferase bromodomain. Nature 399:491–496. doi:10.1038/20974

Dhayalan A, Rajavelu A, Rathert P, Tamas R, Jurkowska RZ, Ragozin S, Jeltsch A (2010) The Dnmt3a PWWP domain reads histone 3 lysine 36 trimethylation and guides DNA methylation. J Biol Chem 285:26114–26120. doi:10.1074/jbc.M109.089433

Eidahl JO, Crowe BL, North JA, McKee CJ, Shriabai N, Feng L, Plumb M, Graham RL, Gorelick RJ, Hess S, Poirier MG, Foster MP, Kvaratskhelia M (2013) Structural basis for high-affinity binding of LEDGF PWWP to mononucleosomes. Nucleic Acids Res 41:3924–3936. doi:10.1093/nar/gkt074

Gayatri S, Bedfort MT (2014) Readers of histone methylarginine marks. Biochim Biophys Acta 1839:702–710. doi:10.1016/j.bbagrm.2014.02.015

Ge YZ, Pu MT, Gowher H, Wu HP, Ding JP, Jeltsch A, Xu GL (2004) Chromatin targeting of the de novo DNA methyltransferases by the PWWP domain. J Biol Chem 279:25447–25454. doi:10.1074/jbc.M312296200

Gilbert TM, McDaniel SL, Byrun SD, Cades JA, Dancy BC, Wade H, Tackett AJ, Strahl BD, Taverna SD (2014) A PWWP domain-containing protein targets the NuA3 acetyltransferase complex via histone H3 lysine 36 trimethylation to coordinate transcriptional elongation at coding regions. Mol Cell Proteomics 13:2883–2895. doi:10.1074/mcp.M114.038224

Gong W, Zhou T, Mo J, Perrett S, Wang J, Feng Y (2012) Structural insight into recognition of methylated histone tails by the retinoblastoma-binding protein 1. J Biol Chem 287:8531–8540. doi:10.1074/jbc.M111.299149

Guo R, Zheng L, Park JW, Lv R, Chen H, Jiao F, Xu W, Mu S, Wen H, Qiu J, Wang Z, Yang P, Wu F, Hiu J, Fu X, Shi X, Shi YG, Xing Y, Lan F, Shi Y (2014) BS69/ZMYND11 reads and connects histone H3.3 lysine 36 trimethylation-decorated chromatin to regulated pre-mRNA processing. Mol Cell 56:298–310. doi:10.1016/j.molcel.2014.08.022

Heintzman ND, Stuart RK, Hon G, Fu Y, Ching CW, Hawkins RD, Barrera LO, Van Calcar S, Qu C, Ching KA, Wang W, Weng Z, Green RD, Crawford GE, Ren B (2007) Distinctive and predictive chromatin signatures of transcriptional promoters and enhancers in the human genome. Nat Genet 39:311–318. doi:10.1038/ng1966

Henikoff S (2005) Histone modifications: combinatorial complexity or cumulative simplicity? Proc Natl Acad Sci U S A 102:5308–5309. doi:10.1073/pnas.0501853102

Hung YL, Lee HJ, Jiang I, Lin SC, Lo WC, Lin YJ, Sue SC (2015) The first residue of the PWWP motif modulates HATH domain binding, stability, and protein-protein interaction. Biochemistry 54:4063–4074. doi:10.1021/acs.biochem.5b00454

Kim SH, Park J, Choi MC, Kim HP, Park JH, Jung Y, Lee JH, Oh DY, Im SA, Bang YJ, Kim TY (2007) Zinc-fingers and homeoboxes 1 (ZHX1) binds DNA methyltranferase (DNMT) 3b to enhance DNMT3b-mediated transcriptional repression. Biochem Biophys Res Commun 355:318–323. doi:10.1016/j.bbrc.2007.01.187

Kolasinska-Zwierz P, Down T, Latorre I, Liu T, Liu XS, Ahringer J (2009) Differential chromatin marking of introns and expressed exons by H3K36me3. Nat Genet 41:376–381. doi:10.1038/ng.322

Kornberg RD, Lorck Y (1999) Twenty-five years of the nucleosome, fundamental particle of the eukaryote chromosome. Cell 98:285–294. doi:10.1016/S0092-8674(00)81958-3

Laguri C, Duband-Goulet I, Friedich N, Axt M, Belin P, Callebaut I, Gilquin B, Zinn-Justin S, Couprie J (2008) Human mismatch repair protein MSH6 contains a PWWP domain that targets double stranded DNA. Biochemistry 47:6199–6207. doi:10.1021/bi7024639

Leoh LS, van Heertum B, De Rijck J, Filippova M, Rios-Colon L, Basu A, Martinez SR, Tungteakkhun SS, Filppov V, Christ F, De Leon M, Debyser Z, Casiano CA (2012) The stress oncoprotein LEDGF/p75 interacts with the methyl CpG binding protein MeCP2 and influences its transcriptional activity. Mol Cancer Res 10:378–391. doi:10.1158/1541-7789.MCR-11-0314

Luger K, Mader AW, Richmond RK, Sargent DF, Richmond TJ (1997) Crystal structure of the nucleosome core particle at 2.8 Å resolution. Nature 398:251–260. doi:10.1038/38444

Luger K, Dechassa ML, Tremethick DJ (2012) New insights into nucleosome and chromatin structure: an ordered state or a disordered affair? Nat Rev Mol Cell Biol 13:436–447. doi:10.1038/nrm3382

Lukasik SM, Cierpicki T, Borloz M, Grembecka J, Everett A, Bushweller JH (2006) High resolution structure of the HDGF PWWP domain: a potential DNA binding domain. Protein Sci 15:314–232. doi:10.1110/ps.051751706

Maltby VE, Martin BJ, Shchulze JM, Johnson I, Hentrich T, Sharma A, Kobor MS, Howe L (2012) Histone H3 lysine 36 methylation targets the Isw1b remodeling complex to chromatin. Mol Cell Biol 32:3479–3485. doi:10.1128/MCB.00389-12

Maurer-Stroh S, Dickens NJ, Hughes-Davies L, Kouzarides T, Eisenhaber F, Ponting CP (2003) The Tudor domain 'Royal Family': Tudor, plant Agenet, Chromo, PWWP and MBT domains. Trends Biochem Sci 28:69–74. doi:10.1016/S0968-0004(03)00004-5

Morchikh M, Naughtin M, Di Nunzio F, Xavier J, Charneau P, Jacob Y, Lavigne M (2013) TOX4 and NOVA1 proteins are partners of LEDGF PWWP domain and affect HIV-1 replication. PLos ONE 8:e81217. doi:10.1371/journal.pone.0081217

Nameki N, Tochio N, Koshiba S, Inoue M, Yabuki T, Aoki M, Seki E, Matsuda T, Fujikura Y, Saito M, Ikari M, Watanabe M, Terada T, Shirozu M, Yoshida M, Hirota H, Tanaka A, Hayashizaki Y, Güntert P, Kigawa T, Yokoyama S (2005) Solution structure of the new PWWP domain of the hepatoma-derived growth factor family. Protein Sci 14:756–764. doi:10.1110/ps.04975305

Nimura K, Ura K, Shiratori H, Ikawa M, Okabe M, Schwartz RJ, Kaneda Y (2009) A histone H3 lysine 36 trimethyltransferase links Nkx2-5 to Wolf-Hirschhorn syndrome. Nature 460:287–291. doi:10.1038/nature08086

Park J, Kim TY, Jung Y, Song SH, Kim SH, Oh DY, Im SA, Bang YJ (2008) DNA methyltransferase 3B mutant in ICF syndrome interacts non-covalently with SUMO-1. J Mol Med 86:1269–1277. doi:10.1007/s00109-008-0392-5

Pradeepa MM, Sutherland HG, Ule J, Grimes GR, Bickmore WA (2012) Psip1/Ledgf p52 binds methylated histone H3K36 and splicing factors and contributes to the regulation of alternative splicing. PLoS Genet 8:e1002717. doi:10.1371/journal.pgen.1002717

Purdy MM, Holz-Schietinger C, Reich NO (2010) Identification of a second DNA binding site in human DNA methyltransferase 3A by substrate inhibition and domain selection. Arch Biochem Biophys 498:13–22. doi:10.1016/j.abb.2010.03.007

Qin S, Min J (2014) Structure and function of the nucleosome-binding PWWP domain. Trends Biochem Sci 39:536–547. doi:10.1016/j.tibs.2014.09.001

Qiu C, Sawada K, Zhang X, Cheng X (2002) The PWWP domain of mammalian DNA methyltransferase Dnmt3b defines a new family of DNA-binding folds. Nat Struct Biol 9:217–224. doi:10.1038/nsb759

Qiu Y, Zhang W, Zhao C, Wang W, Zhang J, Zhang Z, Li G, Shi Y, Tu X, Wu J (2012) Solution structure of the Pdp1 PWWP domain reveals its unique binding sites for methylated H4K20 and DNA. Biochem J 442:527–538. doi:10.1042/BJ20111885

Rando OJ (2012) Combinatorial complexity in chromatin structure and function: revisiting the histone code. Curr Opin Genet Dev 22:148–155. doi:10.1016/j.gde.2012.02.013

Rothbart SB, Strahl BD (2014) Interpreting the language of histone and DNA modifications. Biochim Biophys Acta 1839:627–643. doi:10.1016/j.bbagrm.2014.03.001

Ruthenburg AJ, Li H, Milne TA, Dewell S, McGinty RK, Yuen M, Ueberheide B, Dou Y, Muir TW, Patel DJ, Allis CD (2011) Recognition of mononucleosomal histone modification pattern by BPTF via multivalent interactions. Cell 145:692–706. doi:10.1016/j.cell.2011.03.053

Shikauchi Y, Saiura A, Kubo T, Niwa Y, Yamamaoto J, Murase Y, Yoshikawa H (2009) SALL3 interacts with DNMT3A and shows the ability to inhibit CpG island methylation in hepatocellular carcinoma. Mol Cell Biol 29:1944–1958. doi:10.1128/MCB.00840-08

Shogren-Knaak M, Ishii H, Sun JM, Pazin MJ, Davie JR, Peterson CL (2006) Histone H4-K16 acetylation controls chromatin structure and protein interactions. Science 311:844–847. doi:10.1126/science.1124000

Singh DP, Kubo E, Takamura Y, Shinohara T, Kumar A, Chylack LT Jr, Fatma N (2006) DNA binding domains and nuclear localization signal of LEDGF: contribution of two helix-turn-helix (HTH)-like domains and a stretch of 58 amino acids of the N-terminal to the trans-activation potential of LEDGF. J Mol Biol 355:379–394. doi:10.1016/j.jmb.2005.10.054

Slater LM, Allen MD, Bycroft M (2003) Structural variation in PWWP domains. J Mol Biol 330:571–576. doi:10.1016/S0022-2836(03)00470-4

Smolle M, Venkatesh S, Gogol MM, Li H, Zhang Y, Florens L, Washburn MP, Workman JL (2012) Chromatin remodelers Isw1 and Chd1 maintain chromatin structure during transcription by preventing histone exchange. Nat Struct Mol Biol 19:884–892. doi:10.1038/nsmb.2312

Stec I, Wright TJ, van Ommen GJ, de Boer PA, van Haeringen A, Moorman AF, Altherr MR, den Dunnen JT (1998) WHSC1, a 90 kb SET domain-containing gene, expressed in early development and homologous to a Drosophila dysmorphy gene maps in the Wolf-Hirschhorn syndrome critical region and is fused to IgH in t(4;14) multiple myeloma. Hum Mol Genet 7:1071–1082. doi:10.1093/hmg/7.7.1071

Stec I, Nagl SB, van Ommen GJ, den Dummen JT (2000) The PWWP domain: a potential protein-protein interaction domain in nuclear proteins influencing differentiation? FEBS Lett 473:1–5. doi:10.1016/S0014-5793(00)01449-6

Strahl BD, Allis CD (2000) The language of covalent histone modifications. Nature 403:41–45. doi:10.1038/47412

Sue SC, Chen JY, Lee SC, Wu W, Huang T (2004) Solution structure and heparin interaction of human hepatoma-derived growth factor. J Mol Biol 343:1365–1377. doi:10.1016/j.jmb.2004.09.014

Sue SC, Lee WT, Tien SC, Lee SC, Yu JG, Wu WJ, Wu WG, Huang TH (2007) PWWP module of human hepatoma-derived growth factor forms a domain-swapped dimer with much higher affinity for heparin. J Mol Biol 367:456–472. doi:10.1016/j.jmb.2007.01.010

Taunton J, Hassig CA, Schreiber SL (1996) A mammalian histone deacetylase related to the yeast transcriptional regulator Rpd3p. Science 272:408–411. doi:10.1126/science.272.5260.408

Taverna SD, Li H, Ruthenburg AJ, Allis CD, Patel DJ (2007) How chromatin-binding modules interpret histone modifications: lessons from professional pocket pickers. Nat Struct Mol Biol 14:1025–1040. doi:10.1038/nsmb1338

Turner BM, Birley AJ, Lavender J (1992) Histone H4 isoforms acetylated at specific lysine residues define individual chromosomes and chromatin domains in Drosophila polytene nuclei. Cell 69:375–384. doi:10.1016/0092-8674(92)90417-B

Van Nuland R, van Schaik FM, Simonis M, van Heesch S, Cuppen E, Boelens R, Timmers HM, van Ingen H (2013) Nucleosomal DNA binding drives the recognition of H3K36-methylated nucleosomes by the PSIP1-PWWP domain. Epigenetics Chromatin 6:1–12. doi:10.1186/1756-8935-6-12

Vermeulen M, Eberl HC, Matarase F, Marks H, Denissov S, Butter F, Lee KK, Olsen JV, Hyman AA, Stunnenberg HG, Mann M (2010) Quantitative interaction proteomics and genome-wide profiling of epigenetic histone marks and their readers. Cell 142:967–980. doi:10.1016/j.cell.2010.08.020

Vezzoli A, Bonadies N, Aleen MD, Freund SM, Santiveri CM, Kvinlaug BT, Huntly BJ, Göttgens B, Bycroft M (2010) Molecular basis of histone H3K36me3 recognition by the PWWP domain of BRPF1. Nat Struct Mol Biol 17:617–619. doi:10.1038/nsmb.1797

Völkel P, Angrand PO (2007) The control of histone lysine methylation in epigenetic regulation. Biochimie 89:1–20. doi:10.1016/j.biochi.2006.07.009

Wang Y, Reddy B, Thompson J, Wang H, Noma K, Yates JR III, Jia S (2009) Regulation of Set9-mediated H4K20 methylation by a

PWWP domain protein. Mol Cell 33:428–437. doi:10.1016/j.molcel.2009.02.002

Wang J, Qin S, Li F, Li S, Zhang W, Peng J, Zhang Z, Gong Q, Wu J, Shi Y (2014) Crystal structure of human BS69 Bromo-ZnF-PWWP reveals its role in H3K36me3 nucleosome binding. Cell Res 24:890–893. doi:10.1038/cr.2014.38

Wen H, Li Y, Xi Y, Jiang S, Stratton S, Peng D, Tanaka K, Ren Y, Xia Z, Wu J, Li B, Barton MC, Li W, Haitao L, Shi X (2014) ZMYND11 links histone H3.3K36me3 to transcription elongation and tumour suppression. Nature 508:263–268. doi:10.1038/nature13045

Wozniak GC, Strahl BD (2014) Hitting the 'mark': interpreting lysine methylation in the context of active transcription. Biochim Biophys Acta 1839:1353–1361. doi:10.1016/j.bbagrm.2014.03.002

Wu H, Zeng H, Lam R, Tempel W, Amaya MF, Xu C, Dombrovski L, Qiu W, Wang Y, Min J (2011) Structural and histone binding ability characterizations of human PWWP domains. PLos ONE 6:e18919. doi:10.1371/journal.pone.0018919

Yang J, Everett AD (2007) Hepatoma derived growth factor binds DNA through the N-terminal PWWP domain. BMC Mol Biol 8:101. doi:10.1186/1471-2199-8-101

Accepted Manuscript

Oxidative Stress and Aging: Learning from Yeast Lessons

Elis Eleutherio, Aline de Araujo Brasil, Mauro Braga França, Diego Seixas de Almeida, Germana Breves Rona, Rayne Stfhany Silva Magalhães

PII: S1878-6146(17)30168-X

DOI: 10.1016/j.funbio.2017.12.003

Reference: FUNBIO 876

To appear in: *Fungal Biology*

Received Date: 25 August 2017

Revised Date: 4 December 2017

Accepted Date: 5 December 2017

Please cite this article as: Eleutherio, E., de Araujo Brasil, A., França, M.B., Seixas de Almeida, D., Breves Rona, G., Silva Magalhães, R.S., Oxidative Stress and Aging: Learning from Yeast Lessons, *Fungal Biology* (2018), doi: 10.1016/j.funbio.2017.12.003.

Oxidative Stress and Aging: Learning from Yeast Lessons

Elis Eleutherio*, Aline de Araujo Brasil, Mauro Braga França, Diego Seixas de Almeida, Germana Breves Rona and Rayne Stfhany Silva Magalhães

Institute of Chemistry, Federal University of Rio de Janeiro (UFRJ), 21941-909, Brazil

*Corresponding author

eliscael@iq.ufrj.br

Abstract

The yeast *Saccharomyces cerevisiae* has played a vital role in the understanding of the molecular basis of aging and the relationship of aging process with oxidative stress (non-homeostatic accumulation of Reactive Oxygen Species, ROS). The mammalian and yeast antioxidant responses are similar and over 25% of human-degenerative disease related genes have close homologues in yeast. The reduced genetic redundancy of yeast facilitates visualization of the effect of a deleted or mutated gene. By manipulating growth conditions, yeast cells can survive only fermenting (low ROS levels) or respiring (increased ROS levels), which facilitates the elucidation of the mechanisms involved with acquisition of tolerance to oxidative stress. Furthermore, the yeast databases are the most complete of all eukaryotic models. In this work, we highlight the value of *S. cerevisiae* as a model to investigate the oxidative stress response and its potential impact on aging and age-related diseases.

Keywords: *Saccharomyces cerevisiae*, lifespan, Reactive Oxygen Species (ROS), cancer, neurodegenerative diseases

1. Introduction

Oxygen is required for aerobic life but may also play a crucial role in the aging process. According to the oxidative stress theory of aging, aging and age-associated diseases are associated with the damage caused by reactive oxygen species, ROS, to cellular constituents (Finkel & Holbrook 2000).

The majority of ROS production occurs in the electron transport chain (ETC) of the mitochondria (Sheu *et al.* 2006). In this process, one molecule of oxygen receives four electrons being reduced to water; however, throughout the process, some of the electrons leak prematurely from electrons carriers to oxygen yielding ROS (Murphy 2009). As electrons are sequentially transferred from complex I or complex II to complex III and then to complex IV, protons are translocated from the mitochondrial matrix to intermembrane space creating an electrochemical gradient, which is used as energy to ATP synthesis by ATP synthase. During this transport, electrons can be directly transferred to oxygen to generate superoxide (single-electron transfer) or hydrogen peroxide (pair-electron transfer), mainly at complex I, II and III, which use ubiquinone as acceptor (Brand 2016). Superoxide remains within the compartment in which is generated, because it is unable to cross membranes. Superoxide is rapidly converted to hydrogen peroxide by the enzyme superoxide dismutase (SOD) (Herrero *et al.* 2008). Superoxide can also undergo spontaneous dismutation, although at a slower rate (Abreu & Cabelli 2010). Contrary to superoxide, peroxide can cross membranes and be fully reduced to water by catalases or peroxidases. Alternatively, peroxide can be partially reduced to hydroxyl radical, the most reactive and dangerous radical, a reaction which requires the presence of reduced iron or cupper (Herrero *et al.* 2008). Hydroxyl

radical can also be generated when superoxide reacts with nitric oxide, producing another highly reactive and dangerous radical, nitrogen dioxide (Sheu *et al.* 2006).

The oxygen consumption rate depends on the organism and its physiological condition. Human body extracts around 2,500 calories from food by consuming around one hundred millions molecules of oxygen per cell per minute (Wagner *et al.* 2011). It is estimated that 0.01% of all oxygen consumed is converted to ROS in the skeletal muscle during exercise (at rest, this percentage is 10-fold higher); thus, 10^4 - 10^5 molecules of ROS are formed per cell each minute (Goncalves *et al.* 2015). In face of these high ROS production rates, which increase the risk of hydroxyl radical formation, against which there is no defense, the cellular antioxidant system is very efficient: i) the proportion between antioxidant enzyme and its substrate is inverted (there is much more catalyst than substrate); ii) the rate of the antioxidant enzyme-catalysed reaction is only limited by diffusion (kcat/Km in the order of 10^8 to 10^9 M^{-1} s^{-1}) (Chelikani *et al.* 2004; Abreu & Cabelli 2010).

The efficient and sophisticated antioxidant defense system counteracts and regulates overall ROS levels to maintain physiological homeostasis (Fig. 1A). Lowering ROS levels below the homeostatic set point impairs the physiological role of ROS in some cellular processes, such as induction of antioxidant defense, cell proliferation, and host defense. On the other hand, increased ROS levels are also detrimental. ROS are able to damage all the cell building blocks, such as DNA, lipids, and proteins, leading to membrane damage, loss of organelle functions, reduction in metabolic efficiency, chromatid breaks and mutations (Schieber & Chandel 2014). Fig. 1B outlines the impact of ROS levels on cellular physiology.

According to oxidative stress theory of aging, first proposed in 1954, aging is correlated to the accumulation of cellular damages triggered by ROS produced by normal cell metabolism (Harman 2006). Therefore, throughout the aging process, antioxidants decreased, increasing oxidative damage and, consequently, the chance of disease and death. Oxidative stress has been implicated in the progression of age-related diseases, such as Alzheimer's disease (AD), Parkinson's disease (PD) and amyotrophic lateral sclerosis (ALS) (Barnham *et al.* 2004). Several data support the oxidative stress theory of aging (Harman 2006; Viña *et al.* 2013). In 2011, a review was published which summarized the main data obtained from different studies that evaluated the oxidative stress indexes in healthy individuals related to age (Del Valle 2011). In those studies, hundreds of volunteers from diverse nationalities were analyzed, and healthy individuals were divided according to their ages, confirming the oxidative stress theory of aging. However, some studies presented conflicting and contradictory results concerning the level of some antioxidants found in older people. In the last years, genetically modified animals were obtained to test the oxidative stress theory of aging. Some studies found that the overexpression of antioxidant enzymes extends lifespan, corroborating the theory, but other works put it in doubt by showing that increased ROS levels increase longevity (López-Otín *et al.* 2013; Viña *et al.* 2013). Taken into consideration the role of ROS in the response to stress condition, which is crucial for cell survival, it is possible to harmonize both interpretations (Reczek & Chandel 2015). Mild concentrations of ROS are necessary to induce antioxidant defense, increasing cell protection and longevity. However, if the level of ROS exceeds the protective capacity of the antioxidants, oxidative damage will take place, accelerating aging and increasing the chance of diseases.

The molecular mechanisms of the oxidative stress response and the role of ROS in the biology of aging and in the development of age-related diseases have not yet been fully understood. The use of simple models such as the microorganism *Saccharomyces cerevisiae* has helped with the elucidation of these questions. Studies using this yeast have already contributed to the understanding of basic cellular and molecular processes. In 1996, *S. cerevisiae* had its genome fully sequenced and published. Since then, the extensive functional characterization of its genome (around 90%) along with the huge genetic conservation with humans have triggered a series of new works which humanized the yeast (Khurana & Lindquist 2010; Engel *et al.* 2013; Kachroo *et al.* 2015). Corroborating this evidence is the fact that between 2001 and 2016, five Nobel Prize winners (in Table 1) have used yeast as experimental model. Thus, in addition of being used in ancient biotechnological processes, such as alcoholic fermentation and backing, yeasts are currently explored for the production of therapeutic products, such as human hormones (insulin, insulin analogues, somatotropin, glucagon), vaccines (hepatitis B virus surface antigen and virus-like particles of protein L1 of human papillomavirus), human growth factors (IGF1, NGF, EGF) and human blood proteins (hemoglobin, factors VIII and XIII, antithrombin III, serum albumin albumin) (Ferrer-Miralles *et al.* 2009).

S. cerevisiae has some interesting characteristics that explain its extensive use as an experimental eukaryotic cell model or as a platform to produce recombinant proteins. Besides being non-pathogenic and classified as GRAS (Generally Recognized as Safe) by Food and Drug Administration (FDA), it has a short generation time (1.5-3 h) and grows in a highly reproducible and genetically stable way. In addition, it is amenable to genetic modifications by recombinant DNA technology or classical genetic

manipulations. Other advantages for choosing *S. cerevisiae* as model are: (i) the ease in obtaining mutants from commercial collections of yeast strains for studies of functional genomics, subcellular protein localization, ant protein-protein interaction; (ii) the availability of public databases, such as Saccharomyces Genome Database (SGD), which organize and permanently actualize data obtained from omics studies, such as transcriptomics, proteomics, metabolomics, interactomics (protein–protein interactions), and locasomics (protein localization) (Laurent *et al.* 2016).

Studies of budding yeast have made immense contributions to our understanding of the aging process and age related-diseases (Kaeberlein 2010). It is possible to study both chronological and replicative ageing using *S. cerevisiae* (Oliveira *et al.* 2017). Chronological aging is defined by how long a cell can survive in a non-dividing state. Throughout aging, cellular and molecular damages accumulate. Chronological lifespan is measured by culturing cells in non-proliferating conditions and then determining viability over time. Replicative ageing is defined by the number of daughter cells produced by a mother cell before senescence. Damages are asymmetrically inherited by the mother cell and removed from the daughter cell. Replicative lifespan (RLS) is measured by physical removal of daughter cells, which are easily distinguished from mother cells.

Several pathways involved in degenerative diseases are conserved in yeast, such as protein folding and degradation, autophagy, vesicular trafficking, lysosomal and peroxisomal role, and apoptosis (Tenreiro & Outeiro 2010). Moreover, 17% of the *S. cerevisiae* genes (approximately 1000 genes) are members of orthologous genes families associated with several human diseases (Botstein & Fink 2011).

The oxidative stress response of *S. cerevisiae* is similar to that of mammals, including the sites of ROS formation in the ETC and the main antioxidant enzymes (Herrero *et al.* 2008). Yeast lacks complex I, but has three rotenone-insensitive NADH-ubiquinone oxidoreductase, Ndi1, Nde1, and Nde2, located at the mitochondrial inner membrane space. Mitochondrial matrix NADH is oxidized by the internal Ndi1, while Nde1 and Nde2, with their active sites facing the mitochondrial intermembrane space, oxide the external NADH. Like complex I of mammals, Nde1 and Nde2 are important sources of ROS in the *S. cerevisiae* ETC (Fang & Beattie 2003).

By manipulating growth conditions, yeast cells can survive only fermenting or respiring (Kayikci & Nielsen 2015). At high concentrations of glucose (above 70 mM), *S. cerevisiae* can only undergo fermentation; therefore, ROS levels are reduced. As consequence, intracellular antioxidant defense system is repressed and cells are highly sensitive to oxidative stress. However, yeast cells can adapt to severe oxidative stress if exposed to external antioxidants or moderate concentrations of oxidants (Fernandes *et al.* 2007). Thus, this strategy helps to processes involved with acquisition of tolerance to oxidative stress and its correlation with degenerative processes. In other experimental models, such as mammal cells, which depend on respiration to obtain energy, the correlation ROS-aging is more difficult to analyze.

S. cerevisiae is only able to respire when growing in non-repressor carbon sources, such as glycerol and ethanol. Thus by plating yeast cells in media containing glucose or glycerol, we are able to determine the frequency of respire-deficient mutant cells, known as petite (Mannarino *et al.* 2008). Petites are unable to respire because they possess some mitochondrial dysfunction, a process highly implicated with degenerative diseases (J.Barnham *et al.* 2004; López-Otín *et al.* 2013). On the other

hand, since *S. cerevisiae* is not exclusively dependent on respiration to survive, mutations that result in mitochondrial dysfunction can be investigated in this model organism (de Carvalho *et al.* 2017).

This review focuses on the contribution of yeast in understanding the binomial oxidative stress-molecular mechanisms involved in age-related pathologies, such as neurodegenerative diseases and cancer.

2. Neurodegenerative diseases

2.1 Cellular processes and aggregation in yeast models

Protein misfolding and aggregation are widely recognized as key features of age-related illness, specifically neurodegenerative diseases (Hartl *et al.* 2011; Saez & Vilchez 2014). In recent years, the budding yeast *S. cerevisisae* has provided important general insights for deciphering the basis of neurodegeneration, underlying protein misfolding (Shrestha & Megeney 2015). Furthermore, yeast models of neurodegeneration have identified cellular factors that modulate aggregation and subsequent toxicity of proteins associated with PD (Outeiro 2003), AD (Vandebroek *et al.* 2005; Caine *et al.* 2007), Huntington´s Disease (HD) (Krobitsch & Lindquist 2000; Willingham 2003) and ALS (Johnson *et al.* 2009; Bastow *et al.* 2016). These proteins include fibrillar α-synuclein (α-Syn), which accumulates in proteinaceous inclusions, known as Lewy bodies observed in familial and sporadic cases of PD (Spillantini *et al.* 1997). The AD pathological hallmarks include the formation of extracellular plaques structures containing amyloid-β (Aβ) as well as intracellular buildup of neurofibrillary tangles of hyperphosphorylated tau protein (Fruhmann *et al.* 2017). Likewise, HD is characterized by the presence of intracellular cytotoxic aggregation of huntingtin protein

(Htt) containing polyglutamine (polyQ) expansions (Ross & Poirier 2004; Novak & Tabrizi 2010). The accumulation of cytoplasmic aggregates of Cu,Zn-superoxide dismutase (Sod1), the RNA-binding proteins TDP-43 and FUS, has been implicated in ALS affected patients (Rosen *et al.* 1993; Neumann *et al.* 2006; Vance *et al.* 2009). The abnormal structures formed by these different protein species have also been implicated in impairing the proteasomal functionality as well as the expression of proteins involved in proteostasis (Tyedmers *et al.* 2010; Shrestha & Megeney 2015). Because the protein misfolding, quality control, and degradation machineries as well as oxidative stress response are remarkably well conversed across eucaryotes (Tenreiro *et al.* 2013; Oliveira *et al.* 2017), yeast has emerged as a robust and tractable organism to model proteostasis and oxidative modifications in neurodegenerative diseases.

The mechanisms underlying α-Syn dysfunction in PD as well as in other disorders termed synucleophaties have been successfully studied in yeast models based on the heterologous expression of human α-Syn (Outeiro 2003). The first study conducted in yeast models of PD showed that α-Syn toxicity led to the formation of intracellular inclusions and the expression of α-Syn resulted in dose-dependent cytotoxicity (Outeiro 2003). In this study, the intracellular localization was investigated in yeast cells by expressing the fluorescently labeled wild type (WT) and mutant A53T α-Syn. Both WT and A53T α-Syn were directed to the plasma membrane at lower expression levels, and they were able to accumulate into cytoplasmic inclusions upon increased expression levels. Moreover, α-Syn expression in yeast established dysfunction in several cellular processes promoting lipid accumulation and affecting vesicular trafficking as well as the proteostasis machinery (Outeiro 2003; Lázaro *et al.* 2017). Extensive evidences on the involvement of the protein quality control systems, response to mitochondrial damages

and regulation of vacuolar transport in neurodegeneration came from studies of mutations in several genes associated with PD (eg. DJ-1, Parkin, Pink1, ATP13A2) as well as using yeast humanized models (Menezes *et al.* 2015). Hsp31, Hsp32, Hsp33, and Hsp34 are examples of Heat shock proteins highly conserved in yeast which belong to DJ-1 family. It was found that human DJ-1 and the yeast orthologues physically interacted with α-Syn, ameliorating the α-Syn induced toxicity and reducing α-Syn aggregation in yeast cells (Zondler *et al.* 2014). Human Parkin expressed in yeast has promoted chronological longevity and oxidative stress resistance, which appeared to be dependent on mitochondrial function (Pereira *et al.* 2015a). Yeast models were also used to confirm the relevance of Pink1-dependent phosphorylation of ubiquitin, in the activation of Parkin (Koyano *et al.* 2014). *YPK9* gene is the yeast orthologue of lysosomal P-type ATPase ATP13A2, and the mutated protein can cause early-onset PD (Gitler *et al.* 2009). Studies performed in yeast cells showed *YPK9* suppressed the α-Syn toxicity and that this benefit depends on the vacuolar localization and ATPase activity of Vps35. In addition, the enhanced α-Syn toxicity in *vps35*Δ yeast strain corroborated the increase in α-Syn inclusion accumulation in the vacuole (Dhungel *et al.* 2015).

The uses of AD humanized yeast models have provided powerful new approaches to help understand the molecular mechanisms underlying tau and Aβ toxicity. Using *S. cerevisiae* to study the mechanisms and phenotypical influence of expression of alpha-synuclein as well as the coexpression of protein tau, Zabrocki *et al*. 2005 showed that both proteins are synergistically toxic in yeast cells, as observed by inhibition of proliferation (Zabrocki *et al.* 2005). It has been shown that the human phosphorylated Tau-3R and 4R isoforms expressed in yeast assumed a pathological

conformation and aggregated (Vandebroek *et al.* 2005). In addition to post-translational modifications and oligomerization/aggregation, oxidative stress is also involved in AD pathogenesis; however, the interaction between them are still unclear. In yeast, oxidative stress and mitochondrial dysfunction, produced by the addition of Fe^{2+} ions, enhanced human tau aggregation independent of phosphorylation (Vanhelmont *et al.* 2010). Although Aβ aggregation is associated with the formation of extracellular amyloid plaques in AD patients, Aβ species also accumulate inside the cell, including intracellular multivesicular bodies (Almeida 2006), lysosomes, or other vesicular compartments (Nixon 2007; D'Angelo *et al.* 2013). The creation of the first yeast model to study AD in yeast cells by the expression of GFP-fused Aβ served as an important basis to investigate the toxic effects of Aβ on these cellular processes in yeast cells (Caine *et al.* 2007). Further, by using a By4741 based yeast system expressing Aβ-link-GFP construct, D'Angelo *et al*. 2013 established a system in which Aβ enters the secretory pathway and goes to the plasma membrane becoming toxic to the cells (D'Angelo *et al.* 2013). Using this model, the authors were able to define intracellular traffic pathways as a necessary process for the generation of toxic species in yeast cells.

Yeast models to study HD have recapitulated the polyQ length-dependent aggregation and toxicity by expressing different versions of human Htt protein. Moreover, many other mechanisms involved in the mutant Htt-induced toxicity have been identified from yeast models, such as the modulation of specific molecular chaperones (eg. Hsp104, Sis1 and Ssa1/2), the propagation of endogenous prions, and the autophagic clearance of polyQ protein in yeast (Krobitsch & Lindquist 2000; Meriin *et al.* 2002). It has also been successfully established that aggregation of mutant Htt in

yeast affects endocytosis, cell cycle progression, proteolysis and mitochondrial function (Meriin *et al.* 2007; Bocharova *et al.* 2008; Duennwald & Lindquist 2008; Tauber *et al.* 2011; Kochneva-Pervukhova *et al.* 2012). Recently, the beneficial effect of the protein refolding machinery in inhibiting the aggregation of the mutant Htt 103Q was demonstrated as result of the activation of trehalose synthetic enzyme, trehalose-6-phosphate synthase 1 and Hsp104 in heat shocked *S. cerevisiae* cells (Saleh *et al.* 2014).

Since oxidative modifications to proteins increase during aging, it had been proposed that oxidation of Sod1 mutants associated to the familial form of ALS (FALS) may trigger their misfolding and aggregation (Dal Vechio *et al.* 2014; Petrov *et al.* 2016). By using chronologically aged yeast cells, it was shown that the expression of A4V mutation on human Sod1 as well as the absence of the antioxidant glutathione (GSH) affected human Sod1 activation and increased oxidative damage compared to the WT isoform. This study indicated GSH as a prominent target in the molecular mechanism of FALS during aging (Brasil *et al.* 2013). In addition, studies using a yeast background to investigate FALS found that pathogenic mutations in TDP-43 protein promote its aggregation and toxicity (Johnson *et al.* 2009). The inclusions readily formed by TDP-43 protein in yeast models showed similar effects in higher eukaryotic models (Figley & Gitler 2013) and were structurally identical to aggregates in degenerating neurons of patients with ALS (Johnson *et al.* 2008). Such studies suggest the yeast model remains an ideal platform to study the cellular processes of several aggregation-prone proteins that characterize neurodegeneration.

2.2. Mitochondrial Dysfunction, Oxidative Biomarkers and Antioxidant Molecules

A large number of studies demonstrate that mitochondrial dysfunction and oxidative stress are hallmarks of PD (Sharma *et al.* 2006; Vila *et al.* 2008; Federico *et al.* 2012). As mentioned before, the accumulation of α-syn protein is one of the main causes of PD. *In vitro* experiments showed that α-syn reversibly blocks the largest flow channel of metabolites in and out of mitochondria (VDAC), located on the mitochondrial outer membrane (Rostovtseva *et al.* 2015). The same work, using a yeast model for PD, demonstrated that the α-syn toxicity is VDAC dependent. On the other hand, the autosomal recessive form of PD is associated with mutations in the Parkin protein, an E3 ubiquitin ligase. Parkin and Pink1 are associated with mitochondrial autophagy process in response to stress (Shiba-Fukushima *et al.* 2017). Pereira et al (2015) used a yeast model to study the human Parkin protein, and noted that Parkin was able to increase the chronological lifespan and resistance to oxidative stress of yeast cells. In response to stress with hydrogen peroxide, the Parkin protein, initially expressed in the cytosol, is translocated to the mitochondria, promoting greater degradation.

In AD, the Aβ accumulates intra and mainly extracellularly, as a result of amyloid precursor protein (APP) cleavage (Deyts *et al.* 2016). In 2011, a yeast model was created for studying amyloid toxicity, and in order to establish the relationship between Aβ toxicity, endocytosis and risk factors of AD (Treusch *et al.* 2011). Yeast cells were transfected with a multicopy plasmid containing Aβ1-42 amino acid sequence (driven to the secretory pathway) whose expression was controlled by the galactose-inducible promoter. This construction allowed identification of a series of Aβ toxicity modifiers, involved either in endocytosis or cytoskeleton. Using a similar model, Chen and Petranovic (2015) observed that yeast cells which produce Aβ constitutively, and directed to the secretory pathway, have decreased growth and respiratory rates,

increased oxidative stress, and markers of mitochondrial dysfunction. More recently, França, Lima and Eleutherio (2017) demonstrated that mitochondrial dysfunction and, consequently, ROS increase occurs due to a change in the activities of complexes III and IV in the electron transport chain (ETC). Furthermore, to minimize the increase in intracellular oxidation, a series of cellular responses are triggered. One of these responses was the signaling transmitted to the nucleus to regulate the increase of the expression of enzymes like aconitase (Aco1), catalases (Cta1 and Ctt1) and superoxide dismutases (Sod1 and Sod2). In the mitochondria, Cta1 and Sod2 demonstrated to operate jointly in the maintenance of redox homeostasis and mitochondria integrity.

The Sod1 isoform of superoxide dismutase also plays an important role in ALS. Martins and English (2014) used yeast cells as a model for non-dividing motor neurons and observed that the protein misfolding mechanisms that give rise to sporadic ALS (SALS) are triggered by oxidative damage in the wild-type Sod1. Recently, Bastow et al. (2016) used yeast to demonstrate that the toxic effect of Sod1 instability promotes senescence because it avoids vacuole acidification and impairs metabolic regulation, and not because it is related to loss of mitochondrial function or ROS increase.

Despite the advances made in the research on neurodegenerative disorders, they have no cure and therapeutics needs information about the mechanisms involved in the process, which are still poor elucidated. The neurotoxicity exhibited in a series of disorders is associated with increased levels of oligomers and fibers in the brain. Hence, a number of compounds have been studied in order to find toxicity suppressors by disaggregation and/or oxidative stress reduction, and yeast has proven to be an excellent model for this type of analysis.

Polyphenols represent the most abundant class of antioxidants in the human diet,

being widely found in different types of foods. Therefore, in the past several years, a great number of studies have demonstrated their beneficial effects on neurodegenerative disorders such as AD and PD (Moosavi *et al.* 2016). Recently, a family of 21 polyphenolic compounds, consisting of those found naturally in leaves of salvia, and some of their analogues, were synthesized and subsequently screened for their activity against the Aβ peptide in yeast cells, which found that they were able to revert the toxicity generated by the peptide (Porzoor *et al.* 2015). The same work observed that 14 of these compounds were able to significantly decrease fluorescence in yeast cells transformed with Aβ fused to GFP. In another work, polyphenols from *Corema Album* leaves were able to reduce the formation of α-syn inclusions, ROS levels, and consequently, cytotoxicity in yeast cells (Macedo *et al.* 2015).

3. Mitochondrial Dysfunction in Cancer and Yeast Cells

Mutations in mtDNA and impairment of mitochondrial function arise as an inevitable consequence of aging and oxidative stress. Mutations in nuclear and mitochondrial genes involved in the oxidative phosphorylation (OXPHOS) were reported to play a significant role in the development of tumorigenesis (Chandra & Singh 2011), and mitochondrial dysfunction is being considered an important hallmark of cancer cells (Modica-napolitano & Singh 2004; Rossignol *et al.* 2009). The damage to mitochondrial function and structure can be caused by ROS generated during respiration. The progressive loss of mitochondria respiratory capacity has been linked to the metabolic and genetic transformation observed in cancer cells (Seyfried 2015).

Mitochondrial DNA mutations and changes in their content have been increasingly identified in various types of cancer and correlated to malignancy (Chandra

& Singh 2011). Mutations in mtDNA D-loop region have been reported as an independent molecular prognostic indicator in breast cancer (Mantripragada *et al.* 2008).

mtDNA is small, lacks introns, has a limited DNA repair capability, lacks protective histones and relies on a single control region (D-loop) to control replication and transcription of its genes (Chandra & Singh 2011). As mitochondrial biomolecules are directly exposed to ROS generated during cell respiration, mitochondria are highly susceptible to oxidative damage. ROS generated during the ETC can damage mitochondrial lipids (e.g., lipid peroxidation), causing changes in membrane fluidity and permeability; can oxidize proteins, causing loss of function and metabolic burden to the cell; and direct damage mtDNA, which causes progressive defects in the expression of the OXPHOS components coded by mtDNA. ROS damage to mtDNA can also impair the replicative capacity of mtDNA or even interfere with fusion and fission events that are necessary for mitochondrial remodelling. The cumulative generation of ROS progressively damages mitochondrial structure and function; as a consequence, the respiratory capacity of the cell becomes impaired (Van *et al.* 2003).

Given the importance of mtDNA for the proper expression and constitution of the OXPHOS system, any mutations in its genetic content will have a huge impact on the respiratory capacity of the cell. To keep the energetic level and produce metabolic intermediates to maintain its proper metabolic function the cell must express adaptive responses to mitochondrial dysfunction. These responses include genetic and metabolic adaptations that act to rearrange primary biochemical pathways and intracellular responses to maintain cell viability in the presence of a respiratory dysfunction (Singh 2004; Seyfried 2015).

The progressive oxidative damage is a well-known effect of aging, but the specific oxidative damage to mitochondria has been gaining increase attention by the scientific community and is being considered by some authors one of the most important factors in the malignant metabolic transformation of the cell observed in cancers (Seyfried 2015). *S. cerevisiae* is an interesting model to study cancer as a mitochondrial metabolic disease, because this yeast is able to survive without functional mitochondria and even in the total absence of mtDNA, enabling study about the effects of respiratory impairment on the genomic and metabolic profile of the cell. Yeast cells that contain wild-type mtDNA (referred to as *rho*$^{+}$) are able to perform the OXPHOS and metabolize non-fermentable carbon sources. If there are mutations in mtDNA (*rho*$^{-}$ cell) or a complete loss of mtDNA (*rho*^{0} cell), the cells are unable to express functional mtDNA-encoded subunits of the ETC and/or OXPHOS, thus they become respiratory-deficient and are unable to metabolize non-fermentable carbon sources (Dirick *et al.* 2014). These cells, usually referred to as *petite*, because of their small colony size, are only capable of growing on fermentable carbon sources (such as glucose), which are a substrate for glycolysis. The *petite* phenotype can arise as a consequence of mtDNA (cytoplasmic *petite*) or nDNA (nuclear *petite*) mutations that compromise the OXPHOS system. The relative simplicity in identifying and isolating *petite* mutants in *S. cerevisiae* allowed researchers to study the effects of mtDNA depletion and respiratory damage on the metabolic and gene expression profile of the cell (Merz & Westermann 2009), helping identify fundamental gene-products that are essential for mitochondrial function. The investigation of mitochondrial processes in yeast provided important data for the comprehension of mitochondrial dynamics in human cells (Kuzmenko *et al.* 2016), mostly because of the similarity between human and yeast mtDNA biochemistry (Smith

& Snyder 2006). For example, the first gene encoding a mtDNA polymerase was discovered in yeast (MIP1) (Foury 1989).

S. cerevisiae has been used as a model organism to investigate not only mitochondrial dynamics, function and oxidative stress, but also the dynamics of the metabolic adaptation to mitochondrial damage. *S. cerevisiae* studies showed that there is a causal relationship between mtDNA damage and genomic instability in the nucleus (Rasmussen *et al.* 2003; Doudican *et al.* 2005). These studies provide important data to support that mitochondrial oxidative damage caused by ROS, associated with respiratory impairment, can cause genomic instability and direct mutations in the nucleus. The question raised by using yeast model in these experiments is whether mitochondrial damage can act as a driver cause in the malignant metabolic and genetic transformation observed in cancer cells. As ROS can damage mitochondria structure over time, could ROS play a central role in cancer development? This issue has been investigated and growing evidence supports direct damage by ROS to mtDNA is important for tumorigenic profile development (Sabharwal & Schumacker 2014).

To cope with respiratory function impairment caused by progressive loss of mitochondrial function due to oxidative damage, the cell must be able to perform an adaptive response to reorganize cellular metabolism in order to obtain metabolite intermediates in the presence of an impaired TCA, ETC or OXPHOS. The first well characterized pathway that signals mitochondrial dysfunction to the nucleus in order to express and adaptive response was studied in *S. cerevisiae* and is referred to as retrograde pathway (RTG) (Ronald A Butow 2004; Da Cunha *et al.* 2015). Basically, the yeast protein Rtg2p senses variations in homeostatic signals from mitochondria that are related to respiratory dysfunction, which causes a cascade of events that culminates

with translocation of the heterodimeric complex Rtg1-Rtg3p to the nucleus and activation of gene expression in response to the mitochondrial dysfunction. Some of the genes controlled by RTG response are required for activation of anaplerotic pathways and glyoxylate cycle, which provides precursors for the biosynthesis of tricarboxylic acid (TCA) cycle intermediates from acetate, even in the presence of a truncated TCA cycle due to mitochondrial dysfunction (Jazwinski 2013). The retrograde pathway was also found to play a significant role in extending yeast chronological lifespan (Hashim *et al.* 2014) and promoting nuclear genome stability (Borghouts *et al.* 2004). The retrograde pathway is well known and characterized in the yeast model human cells also have a pathway that signals mitochondrial dysfunction and stress signals to the nucleus to express adaptive responses to respiratory impairment. One important effector of this response in human cells is the transcription factor NFκ-B, considered to have evolved from RTG-dependent retrograde pathway (Srinivasan *et al.* 2010), and is responsible for a wide spectrum of signalling, genetic and metabolic adaptations to stress, organelle dysfunction and aging (Hoesel & Schmid 2013; Jing & Lee 2014). Bioinformatics analysis has found a structural homology between mammalian Myc-Max heterodimer and yeast Rtg1-Rtg3 complex, which is responsible for the activation of gene expression in yeast retrograde pathway. The transcription factor c-Myc was found to be activated in human cells upon activation of the retrograde response. NFκ-B has two binding sites for Myc, a transcription factor found to be activated upon retrograde response, suggesting communication of these factors in the retrograde response pathway in human cells (Jazwinski 2013). RTG pathway in yeast also plays an important role in oxidative response. Mutant cells, with an impaired RTG pathway, decrease in important

antioxidant enzymes, such as catalase and glutathione peroxidase, making them more vulnerable to oxidative stress (Da Cunha *et al.* 2015).

ROS damage to mitochondria gradually increases with aging. As a consequence, the respiratory function of the cell is progressively impaired. In order to cope with the loss of respiratory function, the cell activates a retrograde pathway that signals the mitochondrial damage to the nucleus, activating the expression of a transient metabolic response to allow the cell to deal with the impaired respiration until the mitochondrial damage is repaired by other pathways, such as the mitocheckpoint (Singh *et al.* 2009). If the mitochondria function is restored, the cell returns to its homeostatic metabolic state. If mitochondria damage is severe and cannot be repaired, the retrograde response is persistent, which leads to a progressive shift in the metabolic profile of the cell and causes genome instability in yeast (Doudican *et al.* 2005). In human cells, this process culminates with the development of the tumour metabolic profile, resistance to apoptosis, upregulation of oncogenes and nuclear genome instability (Singh 2004).

S. cerevisiae has a variety of genes that are homologous to the proto-oncogenes of human cells, which allows the use of the yeast model to study how such genes control essential processes in the cell. For example, the glucose-induced repression of oxidative metabolism in yeast, referred to as catabolite repression or Crabtree effect, is regulated by oncogene homologues, such as RAS and SCH9 (Guaragnella *et al.* 2014). The yeast Crabtree effect and the Warburg effect of cancer cells are similar in terms of the metabolic outcome (Diaz-ruiz *et al.* 2009; Diaz-Ruiz *et al.* 2011; Natter & Kohlwein 2013). In both cell types, there is a downregulation of oxidative metabolism and an enhancement of fermentation, despite the presence of oxygen. These changes cause a rearrangement of the oxidative profile of the cell. While the Warburg effect is considered

an irreversible phenotype of cancer cells, *S. cerevisiae* Crabtree effect is a reversible phenotype, as the catabolic repression depends on high glucose concentration. These metabolic similarities indicate that *S. cerevisiae* is a useful model to study cancer cell metabolism and screen for metabolic-targeted drugs for anti-tumour therapy.

The yeast genes RAS1 and RAS2 are homologous to the RAS proto-oncogenes of the mammalian cells and were the first ones to be implicated in yeast longevity (Tamanoi 2011). The convergence of the RAS pathway and the RTG pathway, through the regulatory function of Mks1p (Sekito 2002), controls stress resistance and life span in yeast (Shama *et al.* 1998; Jazwinski 1999). The SCH9 gene of *S. cerevisiae* codes for a protein kinase with a catalytic domain, which is very similar to that of the human Akt1, a known oncogene that promotes cellular growth and activates proliferation and survival pathways in cancer (Carpten *et al.* 2007). Sch9p plays an important role in glucose signalling in yeast (Diaz-Ruiz *et al.* 2011), regulating the expression of ETC genes (Lavoie & Whiteway 2008), and is a central component that controls the metabolic shift from TCA cycle and respiration (oxidative metabolism) to Glycolysis (Wei *et al.* 2009).

In the absence of orthologs, *S. cerevisiae* usually have an analogous pathway, or the human gene can be studied by heterologous expression and the resulting phenotype can be evaluated (Tosato *et al.* 2012). The well-known p53 protein, which controls some cellular processes related to cellular growth and apoptosis (Farnebo *et al.* 2010) and is frequently found mutated in cancer cells, does not have a direct homologous in yeast. However, the effect of its expression in yeast can provide relevant information about the role performed by this protein in regulating fundamental cellular processes conserved among yeast and human cells. Yeast has been used to screen for toxic mutations of p53 (Inga & Resnick 2001; Šmardová *et al.* 2005), to identify intracellular location and

dynamics of this protein (Abdelmoula-Souissi *et al.* 2011) and even to find functional homologous proteins that are able to metabolically interact with p53 (Facchin *et al.* 2003).

3.1 Anti-Cancer Drugs

The causes of cancer are related to point mutations, activation of oncogene, inactivation of tumor suppressors and epigenetic changes (Wiedemann & Morgan 1992; Gao Guangxun , Chen Liang 2014). Epigenetic modifications throughout aging lead the cells to cancer transformation, changing essential epigenetics process, such as DNA methylation and histone modifications, which are essential for normal cellular development (Fraga *et al.* 2007). Growth signaling in *S. cerevisiae* and in higher eukaryotes may impact oxidative stress and age-related diseases, like cancer, stimulating DNA replication stress, which leads to DNA damage and genome instability (Dayan *et al.* 2017). Targeted therapy is applied in cancer drug design to interfere in a specific site (usually a protein) that plays an important role in tumor growth and progression (Sawyers 2004).

Chemical genetics is the intervention in biological systems using small molecules, this technique employs protein-bindings, high-throughput screening and phenotypic methods, and have been developed in the pharmaceutical field (Spring 2005). Chemical genetics will lead to better development of studies in new anti-tumor drugs (Spring 2005). Currently, model organisms, with the biochemistry of cancer-like tumor cells, have been used to study the effect and design of new antitumor drugs (Gao Guangxun , Chen Liang 2014). In this context, *S. cerevisiae* is a widely known and used model organism in the investigation of cellular processes due to yeast conserved genome and

cellular biology (Khurana & Lindquist 2010). The current trend in cancer treatment research is development of drugs with defined molecular targets (Sangmalee *et al.* 2012).

The antitumor effect of some anticancer drugs is due to the production of ROS (Lu 2005). β-Lapachone (β-lap) is a known natural products isolated from *Tabebuia impetiginosa* and is a naphthoquinone that holds anticancer activities (Hussain & Green 2017). *S. cerevisiae* was used to investigate the mechanisms by which β-lap acts against cancer. Unlike other quinone drugs, β-lap cannot inactivate enzymes involved in cancer, like topisomerase II. Toxicity caused by β-lap in yeast cell is mainly due to oxidative and environmental stresses, and it leads to cell death like necrosis process. This compound has already entered in phase I and II clinical trials against cancer (Ramos-Pérez *et al.* 2014). Quercetin has powerful anticancer effects but presents some limitations like it poor water solubility. However, 3,7-dihydroxy-2-[4-(2-chloro-1,4-naphthoquinone-3-yloxy)-3-hydroxyphenyl]-5-hydroxychromen-4-one (CHNQ) is a quercetin derivative naphthoquinone, which induces ROS production and autophagy in yeast cells. CHNQ can be suggested as chemotherapeutic drug, because it can guide tumor cell to death (Enayat *et al.* 2016).

S. cerevisiae has been used to investigate drugs that act on DNA topoisomerases, which are important targets of anticancer therapeutics (Harbury *et al.* 1992; Sangmalee *et al.* 2012). Topoisomerases can be divided in type I (Top1) and type II (Top2) enzymes. Top1 cleaves a single strand of a DNA double-strand to allow passage of a second strand between the DNA break, which is reattached. Camptothecin is a Top1 inhibitor indicated as a antitumor drug and has been tested in the budding yeast (Nitiss & Wang 1988; Reid *et al.* 1998). Top2 is highly conserved, is essential

during mitosis, and responsible for cleaving and rejoin duplex DNA (Reid *et al.* 1998). Top2 enzymes are also important in cell growth and proliferation, with an increased expression. Many drugs have been tested in *S. cerevisiae*. Salvacine is a diterpenoid with a quinone moiety synthetized from a natural product isolated from *Salvia prionitis lance.* When tested in *S. cerevisiae*, Salvacine targeted topoisomerase II, inducing intracellular ROS production and generating double-strand DNA breaks (Lu 2005). Top2 poisons are drugs capable of increasing breaking complexes top2-DNA, converting the enzyme in a cellular toxin, which leads to cell death (Hammonds *et al.* 1998; McClendon & Osheroff 2007). Etoposide, amsacrine, and doxorubicin can inhibit the link of the cleaved strand (Froelich-Ammon & Osheroff 1995; Hammonds *et al.* 1998; Van Hille & Hill 1998). The other Top2 poison activity tested in *S. cerevisiae* include Daunorubicin, Genistein, Actinomycin D, Distamycin A, TOP 53, Cisplatin, Camptothecin, mitoxantrone, Vinorelbine, Cytosine arabinoside, Podophyllotoxin, Epipodophyllotoxin, Colchicine, Suramin, Irinotecan, Azatoxin, Etopophos (Van Hille & Hill 1998), Ellipticine (Reid *et al.* 1998; Van Hille & Hill 1998), and bisdioxopiperazine compounds (Reid *et al.* 1998; Van Hille & Hill 1998).

Inhibition of histone deacetylase and DNA methyltransferase, using drugs with epigenetic modulating activity, has become a therapeutic target against cancer and aging (Khan *et al.* 2016). SIR2 encodes an NAD^+-dependent histone deacetylase in charge of the hypoacetylated state of histones in chromatin silencing (Imai *et al.* 2000; Moazed 2001). In yeast, Sir2p act in transcriptional regulation, cell cycle progression, DNA-damage repair, stress response, and aging (Gartenberg 2000; Rodriguez & Fraga 2010). Sirtuins have a high level of conservation of the catalytic domain (Grozinger *et al.* 2001). Splitomicin inhibits Sir2p activity (Bedalov *et al.* 2001; Hirao *et al.* 2003) and

can be a drug candidate in other deacetylases for treating cancer. Acetylation or deacetylation leads to a cromatin remodeling, which drives the availability and transcriptional ability of a gene. Mistarget of enzymes can lead to a pathological gene silencing that appears in cancer. Histone deacetylases inhibitors are a promising candidate to desing of new antitumor drugs (Wolffe 2001). A3 and sirtinol were the most powerful inhibitors of human SIR2 tested in *S. cerevisiae* (Grozinger *et al.* 2001).

Methylthioadenosine phosphorylase (MTAP), an important enzyme in the methionine salvage pathway, is silenced in a variety of human cancers (Subhi *et al.* 2003; Kadariya *et al.* 2011). All human tissues express MTAP, so it is important to investigate compounds that are capable of inhibiting the growth of MTAP deficient cells (Kadariya *et al.* 2011). *S. cerevisiae* was used to screen compounds that were able to inhibit the growth of cells lacking MTAP, which showed that compounds containing a 1,3,4-thiadiazine ring enhanced growth inhibition in yeast and human cells deleted in MTAP (Kadariya *et al.* 2011). MTA is a by-product of polyamine metabolism. The limiting enzyme in polyamine synthesis is ornithine decarboxylase (ODC), and overexpression of ODC can be observed in different kinds of cancers (Subhi *et al.* 2003). 4-methylthio-2-oxobutanoic acid (MTOB), an Intermediary of MTAP pathway, is suggested as a negative regulator of polyamine metabolism, which justifies MTAP as a tumor suppressor (Subhi *et al.* 2003).

When *S. cerevisiae* does not have direct orthologous with human cells, these genes can be expressed in heterologous form to study their functions and mechanisms (Guaragnella *et al.* 2014). *S. cerevisiae* has been used to identify PARP inhibitors. Inhibition of PARP1 and PARP2 (Poly(ADP-ribose) polymerases) activity has potential anticancer drug activity (Perkins *et al.* 2001). These enzymes are activated in oxidative

stress (Hocsak *et al.* 2017) involved in the DNA repair pathways DNA replication and error-repair is a critical component of cancer cell survival (Dziadkowiec *et al.* 2016). Cells with BRCA-1 and BRCA-2 mutations harbor a defect in homologous repair and seem to be highly vulnerable to the effects of PARP inhibition. Therefore, inhibition of PARP presents a potential anticancer drug activity (Dziadkowiec *et al.* 2016). *S. cerevisiae* has been used to screen and identify active inhibitors of mammalian PARF in biochemical assay and in yeast cell extracts (Perkins *et al.* 2001). Thiochromenone and benzothiazinone are new inhibitors that appears to have more selectivity to PARP1; on the other hand, phthalazine seems to be more selective to PARP2 (Perkins *et al.* 2001). Some available PARF inhibitors are already in phase III trial, and showed antitumor efficacy (Dziadkowiec *et al.* 2016).

S. cerevisiae can be used to study the mechanism of a drug action. Antitumor drugs that damage DNA are considered to interfere in chromosomal DNA replication; however, the molecular mechanisms are not known (Wang *et al.* 2001). It was shown in *S. cerevisiae* that Adozelesin, an anticancer drug, blocks replication fork progression and inhibits the activity of replication origin (Wang *et al.* 2001). Another way to use *S. cerevisiae* is to analyze the cellular mechanism of antitumor drugs resistance. Cisplatin is a famous anticancer drug that forms platinum-DNA adducts (Perez *et al.* 1998) and induces ROS production by a process independent of DNA damage signaling in *S. cerevisiae* (Marullo *et al.* 2013). Unfortunately, some patients presents cellular resistance against cisplatin, which limits its therapeutic potential (Perez *et al.* 1998). Nitrogen permease regulator 2 (NPR2) is a yeast gene responsible for the inhibition of TORC1 activity, by regulating the synthesis and the intake of glutamine as a nitrogen source (Laxman *et al.* 2014). Cells lacking Npr2 have faster proliferative rate, and these

gene is a tumor suppressor (Laxman *et al.* 2014). Cells with deleted Npr2 are resistant to cisplatin and doxorubicin (Schenk *et al.* 2003). Ruthenium compounds belong to the most promising candidates of non-platinum metal complexes in cancer therapy, and include KP1019, a promising anticancer drug during cancer treatment. Research in *S. cerevisiae* demonstrated that K1019 targets histone proteins, interacting with histone 3 (H3), with important consequences for DNA damage responses and epigenetics (Singh *et al.* 2014).

Another way to use *S. cerevisiae* to study anticancer drugs is related to the delivery of nanoparticles (drugs) to tumor cells. Antitumor drugs, mainly composed of small interfering RNA (siRNA) and other nucleic acids, have some problems such as poor solubility and stability, unwanted toxicity, and inability to pass over cell membrane. Therefore, it is important to investigate the delivery of drugs to the target cells (Yoo *et al.* 2011). The lipid composition in cell membrane of *S. cerevisiae* is quite similar to the composition of mammal membranes (Weisman 2003; Armstrong 2010); therefore, the yeast vacuoles are a good system for drug delivery through the mammal membrane to targeted cells or tissues (Gujrati *et al.* 2016). Gujrat and co-workers, genetically engineered *S. cerevisiae* to produce vacuoles displaying human epidermal growth factor receptor 2 (HER2)-specific antibody. The vacuoles were charged with anticancer doxrubicin and then displayed to cancer cell culture. This system enhanced drug cellular entrance, which improved the drug delivery and avoided tumor growth (Gujrati *et al.* 2016). Studies in this area are increasing, pointing to *S. cerevisiae* as a potential candidate in nanoparticle delivery development.

4. Human Premature Aging

In addition to cancer and neurodegenerative disease, *S. cerevisiae* has been used to study human diseases related to aging and oxidative stress, as human premature aging. Progeroid syndromes are classified as monogenic syndrome because they are related to single mutations in genes from the DNA damage repair (mutations in RecQ helicases), Lamin A/C (LMNA) and Nucleotide Excise Repair (NER) (Martin & Oshima 2000). There are more than ten different syndromes related to progeroid, differentiated mainly by the mutated protein, including Werner (WS) and Bloom's syndromes (BS) (mutations in WRN and BLM, helicases from the RecQ-like DNA helicases family) (Myung *et al.* 2001) and *Xeroderma pigmentosum* (XP) (mutation in XPG endonuclease) (Moriel-Carretero *et al.* 2015; Kang *et al.* 2014).

Some of the characteristics on progeroid syndromes, such as predisposition to cancer in BS and WS and the appearance of neuronal degeneration in XP, as well as the premature aging, are directly linked to genomic instability and defects in the protective mechanisms against oxidative stress (Herrero *et al.* 2008; Moriel-Carretero *et al.* 2015). ROS can induce DNA damage as double/single strand break, interstrand cross-link, and genomic instability observed in premature aging phenotypes (Hasty 2003).

RecQ-like helicases are important, as the nucleotide excision repair (NER) system, to maintain genome integrity, sense DNA damage, and guarantee fork maintains the right replication process (Yoshimura *et al.* 2017). Beside this, DNA damage caused by exposition to UV are initially repaired by the NER system (Kang *et al.* 2014).

To better understand the importance of WRN, BLM and XPG to protect human cells and how mutations can lead to progeroid syndromes, it is fundamental to work with an experimental cell model, which lacks WRN, BLM, and XPG and mimics the disease phenotype. The difficulty to obtain mutant animal cell lines (Aggarwal & Brosh Jr. 2010) and the high degree of conservation of RecQ-like DNA helicases (Mirzaei *et al.* 2011) are the main reasons why *S. cerevisiae* has become an useful model to study the molecular mechanisms involved in progeroid syndromes (Chen & Brill 2014).

Sgs1 is the only RecQ-helicase in yeast homologue to human WRN and BLM (Madia *et al.* 2008). *S. cerevisiae* cells lacking *SGS1* have a short lifespan (Madia *et al.* 2008). Sgs1 and WRN interact with RPA (single-stranded DNA binding protein) as well as with Top3 (Schmidt *et al.* 2006; Levens *et al.* 2016).

The first yeast model to study progeroid syndrome was construct by expressing WRN and BLM in mutant cells *sgs1*. With this model, Aggarwal and Brosh showed that WRN is not able to rescue *sgs1* sensitivity to DNA damage, while BLM rescue the phenotype. This was the first time that an experiment showed that WRN and BLM are human RecQ-helicase with distinct functions (Aggarwal & Brosh 2009). Beyond the function, using the same mutant, Chen and Brill determinate that the activity of WRN is associated to N-terminus and this helicase has a coiled coil domain (Chen & Brill 2014). Using a double yeast mutant *sgs1top3*, Aggarwal & Brosh observed for the first time that WRN interact genetically with Top3, because WRN was able to restore phenotype in the double mutant (Aggarwal & Brosh 2009). Working with combination of different mutation in genes related to DNA damage in mutant yeast cells *sgs1*, followed by expression of WRN, Madia and co-workers showed that WRN suppressed certain phenotypes, which

indicates that the human RecQ helicase has some functional similarity to Sgs1(Madia *et al.* 2008).

To verify the relation between oxidative stress and progeroid syndrome, Madia and co-workers using *S. cerevisiae sgs1* cells showed that these cells treated with hydrogen peroxide had the lower chronological survival than the same mutant, without any kind of oxidative induction. The same was observed with cells treated with menadione. This result confirms that cells that lack Sgs1, in a model that mimics progeroid syndrome, have a rate of cell death higher that in control cell and are more sensitive to oxidative agents, confirmed that RecQ-helicases are essential to protect cells against oxidative stress (Madia *et al.* 2008).

S. cerevisiae is also useful to study XPG endonuclease, which are related to XS. As in WS and BS, *S. cerevisiae* has a homologue to XPG known as Rad2. The characterization and the role of XPG was only determined after the discovered of Rad2 (Kang *et al.* 2014). Patients with XS are extremely sensitive to UV; hence, they have high incidence of cancer (mainly skin cancer) (Moriel-Carretero *et al.* 2015). This was confirmed using yeast cells lacking RAD3 and treated with UV light, finding that these cells are more sensitive than a cell with no mutation. As UV light releases ROS, this also indicated that Rad and XPG are important to protect cells against oxidative stress (Herrera-Moyano *et al.* 2014).

Although *S. cerevisiae* has shown to be a very useful model to study progeroid syndromes, the literature still lacks works using yeast to better understand these syndromes. However, it is believed that in about ten years more researches will use yeast cell to gain new insight about cancer and aging related disease (Brosh & Bohr 2007), to development treatment to cure or prevent this disease.

5. Conclusions

Some works have focused on the mechanism by which *S. cerevisiae* acquires tolerance to oxidative stress, which has been linked to diseases, such as cancer, and to the aging process. Because of the universal response to this stress, further insight into the response of *S. cerevisiae* will improve our understanding of human defense mechanisms and, consequently, the necessary foundation for practical applications. Remarkable examples of the utility of this organism for the elucidation of the molecular mechanisms involved in human diseases are the application of fundamental knowledge of cell cycle regulation and autophagy uncovered in yeast towards research in cancer and neurodegenerative diseases. These studies won the medicine Nobel prizes in 2002 and 2016, respectively. *S. cerevisiae* is a very attractive organism to work with, given its tractability, susceptibility to genetic modifications and the high genetic conservation with humans. For studies that aim to investigate the relation between oxidative stress and age-related diseases, the great advantage of *S. cerevisiae,* compared with other experimental models, is its capacity to grow using fermentative or oxidative metabolism. Thus, by shifting cells from the reduced environment of fermentation to a more oxidant condition, it is easy to verify the effect of oxidative stress on the molecular mechanisms of age-related diseases. Researchers have been humanizing yeast by expressing human proteins in yeast or even by humanizing entire pathways. The use of these 'humanized yeast systems' together with the metabolic versatility of this yeast should help identify disease-related cellular events and novel pharmacological agents to interfere with these processes.

Acknowledgements

This review was supported by grants from FAPERJ, CAPES and CNPq. It was also facilitated by grants in support of the International Symposium on Fungal Stress (ISFUS)-2017 meeting from CAPES (PAEP 88887.126652/2017-00) and (FAPEG – 201710267000110).

References

Abdelmoula-Souissi S, Delahodde A, Bolotin-Fukuhara M, Gargouri A, Mokdad-Gargouri R, 2011. Cellular localization of human p53 expressed in the yeast saccharomyces cerevisiae: Effect of NLSI deletion. *Apoptosis* **16**: 746–756.

Abreu IA, Cabelli DE, 2010. Superoxide dismutases-a review of the metal-associated mechanistic variations. *Biochimica et Biophysica Acta - Proteins and Proteomics* **1804**: 263–274.

Aggarwal M, Brosh RM, 2009. WRN helicase defective in the premature aging disorder Werner syndrome genetically interacts with topoisomerase 3 and restores the top3 slow growth phenotype of sgs1 top3. *Aging* **1**: 219–233.

Aggarwal M, Brosh Jr. RM, 2010. Genetic Studies of Human DNA Repair Proteins Using Yeast as a Model System. *Journal of Visualized Experiments*: 1–5. https://doi.org/10.3791/1639

Almeida CG, 2006. beta-Amyloid Accumulation Impairs Multivesicular Body Sorting by Inhibiting the Ubiquitin-Proteasome System. *Journal of Neuroscience* **26**: 4277–4288.

Armstrong J, 2010. Yeast vacuoles: More than a model lysosome. *Trends in Cell Biology* **20**: 580–585.

Barnham K, Masters C, Bush A, 2004. Neurodegenerative diseases and oxidative stress. *Nature Reviews Drug Discovery* **3**: 205–214.

Bastow EL, Peswani AR, Tarrant DSJ, Pentland DR, Chen X, Morgan A, Staniforth GL, Tullet JM, Rowe ML, Howard MJ, Tuite MF, Gourlay CW, 2016. New links between SOD1 and metabolic dysfunction from a yeast model of Amyotrophic Lateral Sclerosis (ALS). *Journal of Cell Science* **129**: 4118–4129.

Bedalov A, Gatbonton T, Irvine WP, Gottschling DE, Simon JA, 2001. Identification of a small molecule inhibitor of Sir2p. *Proceedings of the National Academy of Sciences of the United States of America* **98**: 15113–8.

Bocharova NA, Sokolov SS, Knorre DA, Skulachev VP, Severin FF, 2008. Unexpected link between anaphase promoting complex and the toxicity of expanded polyglutamines expressed in yeast. *Cell Cycle* **7**: 3943–3946.

Borghouts C, Benguria A, Wawryn J, Jazwinski SM, 2004. Rtg2 Protein Links Metabolism and Genome Stability in Yeast Longevity. *Genetics* **166**: 765–777.

Botstein D, Fink GR, 2011. Yeast: An experimental organism for 21st century biology. *Genetics* **189**: 695–704.

Brand MD, 2016. Mitochondrial generation of superoxide and hydrogen peroxide as the source of mitochondrial redox signaling. *Free Radical Biology and Medicine* **100**: 14–31.

Brasil AA, Belati A, Mannarino SC, Panek AD, Eleutherio ECA, Pereira MD, 2013. The involvement of GSH in the activation of human Sod1 linked to FALS in chronologically aged yeast cells. *FEMS Yeast Research* **13**: 433–440.

Brosh RM, Bohr VA, 2007. Human premature aging, DNA repair and RecQ helicases. *Nucleic Acids Research* **35**: 7527–7544.

Caine J, Sankovich S, Antony H, Waddington L, Macreadie P, Varghese J, Macreadie I, 2007. Alzheimer's Aβ fused to green fluorescent protein induces growth stress and a heat shock response. *FEMS Yeast Research* **7**: 1230–1236.

Carpten JD, Faber AL, Horn C, Donoho GP, Briggs SL, Robbins CM, Hostetter G, Boguslawski S, Moses TY, Savage S, Uhlik M, Lin A, Du J, Qian Y, Zeckner DJ, Tucker-Kellogg G, Touchman J, Patel K, Mousses S, Bittner M, Schevitz R, Lai MT, Blanchard KL, Thomas JE, 2007. A transforming mutation in the pleckstrin homology domain of AKT1 in cancer. *Nature* **448**: 439–444.

De Carvalho MDC, De Mesquita JF, Eleutherio ECA, 2017. In Vivo Characterization of I91T Sod2 Polymorphism of Saccharomyces cerevisiae. *Journal of Cellular Biochemistry* **118**: 1078–1086.

Chandra D, Singh KK, 2011. Genetic insights into OXPHOS defect and its role in cancer. *Biochimica et Biophysica Acta - Bioenergetics* **1807**: 620–625.

Chelikani P, Fita I, Loewen PC, 2004. Diversity of structures and properties among catalases. *Cellular and Molecular Life Sciences* **61**: 192–208.

Chen C-F, Brill SJ, 2014. Multimerization domains are associated with apparent strand exchange activity in BLM and WRN DNA helicases. *DNA repair* **22**: 137–46.

Chen X, Petranovic D, 2015. Amyloid-ß peptide-induced cytotoxicity and mitochondrial dysfunction in yeast. *FEMS Yeast Research* **15**: fov061.

Da Cunha FM, Torelli NQ, Kowaltowski AJ, 2015. Mitochondrial Retrograde Signaling: Triggers, Pathways, and Outcomes. *Oxidative Medicine and Cellular Longevity*. http://dx.doi.org/10.1155/2015/482582

D'Angelo F, Vignaud H, Di Martino J, Salin B, Devin A, Cullin C, Marchal C, 2013. A yeast model for amyloid- aggregation exemplifies the role of membrane trafficking and PICALM in cytotoxicity. *Disease Models & Mechanisms* **6**: 206–216.

Dal Vechio FH, Cerqueira F, Augusto O, Lopes R, Demasi M, 2014. Peptides that activate the 20S proteasome by gate opening increased oxidized protein removal and reduced protein aggregation. *Free Radical Biology and Medicine* **67**: 304–313.

Dayan IE, Arga KY, Ulgen KO, 2017. Multiomics Approach to Novel Therapeutic Targets for Cancer and Aging-Related Diseases: Role of Sld7 in Yeast Aging Network. *OMICS: A Journal of Integrative Biology* **21**: 100–113.

Deyts C, Thinakaran G, Parent AT, 2016. APP Receptor? To Be or Not To Be. *Trends in pharmacological sciences*. https://doi.org/10.1016/j.tips.2016.01.005

Dhungel N, Eleuteri S, Li L bo, Kramer NJ, Chartron JW, Spencer B, Kosberg K, Fields JA, Stafa K, Adame A, Lashuel H, Frydman J, Shen K, Masliah E, Gitler AD, 2015. Parkinson's Disease Genes VPS35 and EIF4G1 Interact Genetically and Converge on alpha-Synuclein. *Neuron* **85**: 76–88.

Diaz-Ruiz R, Rigoulet M, Devin A, 2011. The Warburg and Crabtree effects: On the origin of cancer cell energy metabolism and of yeast glucose repression. *Biochimica et Biophysica Acta - Bioenergetics* **1807**: 568–576.

Diaz-ruiz R, Uribe-carvajal S, Devin A, Rigoulet M, 2009. Biochimica et Biophysica Acta Tumor cell energy metabolism and its common features with yeast metabolism. *BBA - Reviews on Cancer* **1796**: 252–265.

Dirick L, Bendris W, Loubiere V, Gostan T, Gueydon E, Schwob E, 2014. Metabolic and Environmental Conditions Determine Nuclear Genomic Instability in Budding Yeast Lacking Mitochondrial DNA. *G3: Genes| Genomes| Genetics* **4**: 411–423.

Doudican NA, Doudican NA, Song B, Song B, Shadel GS, Shadel GS, Doetsch PW, Doetsch PW, 2005. Oxidative DNA Damage Causes Mitochondrial Genomic Instability in. *Society* **25**: 5196–5204.

Duennwald ML, Lindquist S, 2008. Impaired ERAD and ER stress are early and specific events in polyglutamine toxicity. *Genes and Development* **22**: 3308–3319.

Dziadkowiec KN, Gąsiorowska E, Nowak-Markwitz E, Jankowska A, 2016. PARP inhibitors: review of mechanisms of action and BRCA1/2 mutation targeting. *Menopausal Review* **4**: 215–219.

Enayat S, Şeyma Ceyhan M, Taşkoparan B, Stefek M, Banerjee S, 2016. CHNQ, a novel 2-Chloro-1,4-naphthoquinone derivative of quercetin, induces oxidative stress and autophagy both in vitro and in vivo. *Archives of Biochemistry and Biophysics* **596**: 84–98.

Engel SR, Dietrich FS, Fisk DG, Binkley G, Balakrishnan R, Costanzo MC, Dwight SS, Hitz BC, Karra K, Nash RS, Weng S, Wong ED, Lloyd P, Skrzypek MS, Miyasato SR, Simison M, Cherry JM, 2013. The Reference Genome Sequence of Saccharomyces cerevisiae: Then and Now. *G3: Genes| Genomes| Genetics* **4**: 389–398.

Facchin S, Lopreiato R, Ruzzene M, Marin O, Sartori G, Götz C, Montenarh M, Carignani G, Pinna LA, 2003. Functional homology between yeast piD261/Bud32 and human PRPK: Both phosphorylate p53 and PRPK partially complements piD261/Bud32 deficiency. *FEBS Letters* **549**: 63–66.

Fang J, Beattie DS, 2003. External alternative NADH dehydrogenase of Saccharomyces cerevisiae: A potential source of superoxide. *Free Radical Biology and Medicine* **34**: 478–488.

Farnebo M, Bykov VJN, Wiman KG, 2010. Biochemical and Biophysical Research Communications The p53 tumor suppressor : A master regulator of diverse cellular processes and therapeutic target in cancer. *Biochemical and Biophysical Research Communications* **396**: 85–89.

Federico A, Cardaioli E, Da Pozzo P, Formichi P, Gallus GN, Radi E, 2012. Mitochondria, oxidative stress and neurodegeneration. *Journal of the neurological sciences* **322**: 254–62.

Fernandes PN, Mannarino SC, Silva CG, Pereira MD, Panek AD, Eleutherio ECA, 2007. Oxidative stress response in eukaryotes: effect of glutathione, superoxide dismutase and catalase on adaptation to peroxide and menadione stresses in Saccharomyces cerevisiae. *Redox report : communications in free radical research* **12**: 236–244.

Ferrer-Miralles N, Domingo-Espín J, Corchero J, Vázquez E, Villaverde A, 2009. Microbial factories for recombinant pharmaceuticals. *Microbial Cell Factories* **8**: 17.

Figley MD, Gitler AD, 2013. Yeast genetic screen reveals novel therapeutic strategy for ALS. *Rare Diseases* **1**: e24420.

Finkel T, Holbrook NJ, 2000. Oxidants, oxidative stress and the biology of ageing. *Nature* **408**: 239–247.

Foury F, 1989. Cloning and sequencing of the nuclear gene MIP1 encoding the catalytic subunit of the yeast mitochondrial DNA polymerase. *The Journal of biological chemistry* **264**: 20552–60.

Fraga MF, Agrelo R, Esteller M, 2007. Cross-talk between aging and cancer: The epigenetic language. *Annals of the New York Academy of Sciences* **1100**: 60–74.

França MB, Lima KC, Eleutherio ECA, 2017. Oxidative Stress and Amyloid Toxicity: Insights From Yeast. *Journal of Cellular Biochemistry* **118**: 1442–1452.

Froelich-Ammon SJ, Osheroff N, 1995. Topoisomerase poisons: Harnessing the dark side of enzyme mechanism. *Journal of Biological Chemistry* **270**: 21429–21432.

Fruhmann G, Seynnaeve D, Zheng J, Ven K, Molenberghs S, Wilms T, Liu B, Winderickx J, Franssens V, 2017. Yeast buddies helping to unravel the complexity of neurodegenerative disorders. *Mechanisms of Ageing and Development* **161**: 288–305.

Gao Guangxun , Chen Liang HC, 2014. Anti-cancer Drug Discovery: Update and Comparisons in Yeast, Drosophila, and Zebrafish. *Curr Mol Pharmacol* **7**: 44–51.

Gartenberg MR, 2000. The Sir proteins of Saccharomyces cerevisiae: Mediators of transcriptional silencing and much more. *Current Opinion in Microbiology* **3**: 132–137.

Gitler AD, Chesi A, Geddie ML, Strathearn KE, Hamamichi S, Hill KJ, Caldwell KA, Caldwell GA, Cooper AA, Rochet J-C, Lindquist S, 2009. α-Synuclein is part of a diverse and highly conserved interaction network that includes PARK9 and manganese toxicity. *Nature Genetics* **41**: 308–315.

Goncalves RLS, Quinlan CL, Perevoshchikova I V., Hey-Mogensen M, Brand MD, 2015. Sites of superoxide and hydrogen peroxide production by muscle mitochondria assessed ex vivo under conditions mimicking rest and exercise. *Journal of Biological Chemistry* **290**: 209–227.

Grozinger CM, Chao ED, Blackwell HE, Moazed D, Schreiber SL, 2001. Identification of a Class of Small Molecule Inhibitors of the Sirtuin Family of NAD-dependent Deacetylases by Phenotypic Screening. *Journal of Biological Chemistry* **276**: 38837–38843.

Guaragnella N, Palermo V, Galli A, Moro L, Mazzoni C, Giannattasio S, 2014. The expanding role of yeast in cancer research and diagnosis: Insights into the function of the oncosuppressors p53 and BRCA1/2. *FEMS Yeast Research* **14**: 2–16.

Gujrati V, Lee M, Ko Y-J, Lee S, Kim D, Kim H, Kang S, Lee S, Kim J, Jeon H, Kim SC, Jun Y, Jon S, 2016. Bioengineered yeast-derived vacuoles with enhanced tissue-penetrating ability for targeted cancer therapy. *Proceedings of the National Academy of Sciences* **113**: 710–715.

Hammonds TR, Maxwell A, Jenkins JR, 1998. Use of a rapid throughput in vivo screen to investigate inhibitors of eukaryotic topoisomerase II enzymes. *Antimicrobial Agents and Chemotherapy* **42**: 889–894.

Harbury P, Wasserman R, Wang JC, 1992. Amsacrine and Etoposide Hypersensitivity of Yeast Cells Overexpressing DNA Topoisomerase II. *Cancer Research* **52**: 4467–4472.

Harman D, 2006. Free radical theory of aging: An update - Increasing the functional life span. In: *Annals of the New York Academy of Sciences*. pp. 10–21.

Hartl FU, Bracher A, Hayer-Hartl M, 2011. Molecular chaperones in protein folding and proteostasis. *Nature* **475**: 324–332.

Hashim Z, Mukai Y, Bamba T, Fukusaki E, 2014. Metabolic Profiling of Retrograde Pathway Transcription Factors Rtg1 and Rtg3 Knockout Yeast. *Metabolites* **4**: 580–598.

Hasty P, 2003. Aging and Genome Maintenance: Lessons from the Mouse? *Science* **299**: 1355–1359.

Herrera-Moyano E, Moriel-Carretero M, Montelone BA, Aguilera A, 2014. The rem Mutations in the ATP-Binding Groove of the Rad3/XPD Helicase Lead to Xeroderma pigmentosum-Cockayne Syndrome-Like Phenotypes. *PLoS Genetics* **10**. https://doi.org/10.1371/journal.pgen.1004859

Herrero E, Ros J, Bellí G, Cabiscol E, 2008. Redox control and oxidative stress in yeast cells. *Biochimica et Biophysica Acta (BBA) - General Subjects* **1780**: 1217–1235.

Van Hille B, Hill BT, 1998. Yeast cells expressing differential levels of human or yeast DNA topoisomerase II: A potent tool for identification and characterization of topoisomerase II-targeting antitumour agents. *Cancer Chemotherapy and Pharmacology* **42**: 345–356.

Hirao M, Posakony J, Nelson M, Hruby H, Jung M, Simon JA, Bedalov A, 2003. Identification of Selective Inhibitors of NAD+-dependent Deacetylases Using Phenotypic Screens in Yeast. *Journal of Biological Chemistry* **278**: 52773–52782.

Hocsak E, Szabo V, Kalman N, Antus C, Cseh A, Sumegi K, Eros K, Hegedus Z, Gallyas F, Sumegi B, Racz B, 2017. PARP inhibition protects mitochondria and reduces ROS production via PARP-1-ATF4-MKP-1-MAPK retrograde pathway. *Free Radical Biology and Medicine* **108**: 770–784.

Hoesel B, Schmid JA, 2013. The complexity of NF- κ B signaling in inflammation and cancer. *Molecular Cancer* **12**: 1.

Hussain H, Green IR, 2017. Lapachol and lapachone analogs: A journey of two decades of patent research (1997-2016). *Expert Opinion on Therapeutic Patents* **3776**: 13543776.2017.1339792.

Imai S, Armstrong CM, Kaeberlein M, Guarente L, 2000. Transcriptional silencing and longevity protein Sir2 is an NAD-dependent histone deacetylase. *Nature* **403**: 795–800.

Inga A, Resnick MA, 2001. Novel human p53 mutations that are toxic to yeast can enhance transactivation of specific promoters and reactivate tumor p53 mutants. *Oncogene* **20**: 3409–19.

J.Barnham K, L.Masters C, Bush AI, 2004. Neurodegenerative diseases and oxidative stress. *Biomedicine & Pharmacotherapy* **58**: 39–46.

Jazwinski SM, 1999. The RAS genes: A homeostatic device in Saccharomyces cerevisiae longevity. *Neurobiology of Aging* **20**: 471–478.

Jazwinski SM, 2013. The retrograde response: When mitochondrial quality control is not enough. *Biochimica et Biophysica Acta - Molecular Cell Research* **1833**: 400–409.

Jing H, Lee S, 2014. NF-κB in cellular senescence and cancer treatment. *Molecules and cells* **37**: 189–195.

Johnson BS, McCaffery JM, Lindquist S, Gitler AD, 2008. A yeast TDP-43 proteinopathy model: Exploring the molecular determinants of TDP-43 aggregation and cellular toxicity. *Proceedings of the National Academy of Sciences* **105**: 6439–6444.

Johnson BS, Snead D, Lee JJ, McCaffery JM, Shorter J, Gitler AD, 2009. TDP-43 is intrinsically aggregation-prone, and amyotrophic lateral sclerosis-linked mutations accelerate aggregation and increase toxicity. *Journal of Biological Chemistry* **284**: 20329–20339.

Kachroo AH, Laurent JM, Yellman CM, Meyer AG, Wilke CO, Marcotte EM, 2015. Evolution. Systematic humanization of yeast genes reveals conserved functions and genetic modularity. *Science* **348**: 921–925.

Kadariya Y, Tang B, Myers CB, Fukui J, Peterson JR, Kruger WD, 2011. Chemical Genetic Screening for Compounds That Preferentially Inhibit Growth of Methylthioadenosine Phosphorylase (MTAP)–Deficient Saccharomyces cerevisiae. *Journal of Biomolecular Screening* **16**: 44–52.

Kaeberlein M, 2010. Lessons on longevity from budding yeast. *Nature* **464**: 513–9.

Kang M-S, Yu S-L, Kim H-Y, Gorospe CM, Choi BH, Lee SH, Lee S-K, 2014. Yeast RAD2, a homolog of human XPG, plays a key role in the regulation of the cell cycle and actin dynamics. *Biology open* **3**: 29–41.

Kayikci Ö, Nielsen J, 2015. Glucose repression in Saccharomyces cerevisiae. *FEMS Yeast Research* **15**. doi: 10.1093/femsyr/fov068

Khan S, Shukla S, Sinha S, Meeran SM, 2016. Epigenetic targets in cancer and aging: dietary and therapeutic interventions. *Expert Opinion on Therapeutic Targets* **20**: 689–703.

Khurana V, Lindquist S, 2010. Modelling neurodegeneration in Saccharomyces cerevisiae: why cook with baker's yeast? *Nature reviews. Neuroscience* **11**: 436–449.

Kochneva-Pervukhova N V., Alexandrov AI, Ter-Avanesyan MD, 2012. Amyloid-mediated sequestration of essential proteins contributes to mutant huntingtin toxicity in yeast. *PLoS ONE* **7**.

Koyano F, Okatsu K, Kosako H, Tamura Y, Go E, Kimura M, Kimura Y, Tsuchiya H, Yoshihara H, Hirokawa T, Endo T, Fon EA, Trempe J-F, Saeki Y, Tanaka K, Matsuda N, 2014. Ubiquitin is phosphorylated by PINK1 to activate parkin. *Nature* **510**: 162–168.

Krobitsch S, Lindquist S, 2000. Aggregation of huntingtin in yeast varies with the length of the polyglutamine expansion and the expression of chaperone proteins. *Proceedings of the National Academy of Sciences* **97**: 1589–1594.

Kuzmenko A, Derbikova K, Salvatori R, Tankov S, 2016. Aim-less translation : loss of Saccharomyces cerevisiae mitochondrial translation initiation factor mIF3 / Aim23 leads to unbalanced protein synthesis. *Nature Publishing Group*: 1–9. https://doi.org/10.1038/srep18749

Laurent JM, Young JH, Kachroo AH, Marcotte EM, 2016. Efforts to make and apply humanized yeast. *Briefings in Functional Genomics* **15**: 155–163.

Lavoie H, Whiteway M, 2008. Increased respiration in the sch9Delta mutant is required for increasing chronological life span but not replicative life span. *Eukaryotic Cell* **7**: 1127–1135.

Laxman S, Sutter BM, Shi L, Tu BP, 2014. Npr2 inhibits TORC1 to prevent inappropriate utilization of glutamine for biosynthesis of nitrogen-containing metabolites. *Science Signaling* **7**: ra120–ra120.

Lázaro DF, Pavlou MAS, Outeiro TF, 2017. Cellular models as tools for the study of the role of alpha-synuclein in Parkinson's disease. *Experimental Neurology*. https://doi.org/10.1016/j.expneurol.2017.05.007

Levens D, Baranello L, Kouzine F, 2016. Controlling gene expression by DNA mechanics: emerging insights and challenges. *Biophysical Reviews* **8**: 259–268.

López-Otín C, Blasco MA, Partridge L, Serrano M, Kroemer G, 2013. The hallmarks of aging. *Cell* **153**: 1194–217.

Lu H-R, 2005. Reactive Oxygen Species Elicit Apoptosis by Concurrently Disrupting Topoisomerase II and DNA-Dependent Protein Kinase. *Molecular Pharmacology* **68**: 983–994.

Macedo D, Tavares L, McDougall GJ, Vicente Miranda H, Stewart D, Ferreira RB, Tenreiro S, Outeiro TF, Santos CN, 2015. (Poly)phenols protect from α-synuclein toxicity by reducing oxidative stress and promoting autophagy. *Human molecular genetics* **24**: 1717–32.

Madia F, Gattazzo C, Wei M, Fabrizio P, Burhans WC, Weinberger M, Galbani A, Smith JR, Nguyen C, Huey S, Comai L, Longo VD, 2008. Longevity mutation in SCH9 prevents recombination errors and premature genomic instability in a Werner/Bloom model system. *Journal of Cell Biology* **180**: 67–81.

Mannarino SC, Amorim M a., Pereira MD, Moradas-Ferreira P, Panek AD, Costa V, Eleutherio EC a, 2008. Glutathione is necessary to ensure benefits of calorie restriction during ageing in Saccharomyces cerevisiae. *Mechanisms of Ageing and Development* **129**: 700–705.

Mantripragada K, Caley M, Stephens P, Jones C, Kluwe L, Guha A, Mautner V, Upadhyaya M, 2008. Telomerase Activity is a Biomarker for High Grade Malignant Peripheral Nerve Sheath Tumors in Neurofibromatosis Type 1 Individuals. *Genes, chromosomes & cancer* **47**: 238–246.

Martin GM, Oshima J, 2000. Lessons from human progeroid syndromes. *Nature* **408**: 263–6.

Martins D, English AM, 2014. SOD1 oxidation and formation of soluble aggregates in yeast: relevance to sporadic ALS development. *Redox biology* **2**: 632–9.

Marullo R, Werner E, Degtyareva N, Moore B, Altavilla G, Ramalingam SS, Doetsch PW, 2013. Cisplatin induces a mitochondrial-ros response that contributes to

cytotoxicity depending on mitochondrial redox status and bioenergetic functions. *PLoS ONE* **8**: 1–15.

McClendon AK, Osheroff N, 2007. DNA topoisomerase II, genotoxicity, and cancer. *Mutation Research - Fundamental and Molecular Mechanisms of Mutagenesis* **623**: 83–97.

Menezes R, Tenreiro S, Macedo D, Santos C, Outeiro T, 2015. From the baker to the bedside: yeast models of Parkinson's disease. *Microbial Cell* **2**: 262–279.

Meriin AB, Zhang X, Alexandrov IM, Salnikova AB, Ter-Avanesian MD, Chernoff YO, Sherman MY, 2007. Endocytosis machinery is involved in aggregation of proteins with expanded polyglutamine domains. *The FASEB Journal* **21**: 1915–1925.

Meriin AB, Zhang X, He X, Newnam GP, Chernoff YO, Sherman MY, 2002. Huntingtin toxicity in yeast model depends on polyglutamine aggregation mediated by a prion-like protein Rnq1. *Journal of Cell Biology* **157**: 997–1004.

Merz S, Westermann B, 2009. Genome-wide deletion mutant analysis reveals genes required for respiratory growth, mitochondrial genome maintenance and mitochondrial protein synthesis in Saccharomyces cerevisiae. *Genome Biology* **10**: R95.

Mirzaei H, Syed S, Kennedy J, Schmidt KH, 2011. Sgs1 truncations induce genome rearrangements but suppress detrimental effects of BLM overexpression in Saccharomyces cerevisiae. *Journal of molecular biology* **405**: 877–91.

Moazed D, 2001. Enzymatic activities of Sir2 and chromatin silencing. *Current Opinion in Cell Biology* **13**: 232–238.

Modica-napolitano JS, Singh KK, 2004. Mitochondrial dysfunction in cancer. **4**: 755–762.

Moosavi F, Hosseini R, Saso L, Firuzi O, 2016. Modulation of neurotrophic signaling pathways by polyphenols. *Drug design, development and therapy* **10**: 23–42.

Moriel-Carretero M, Herrera-Moyano E, Aguilera A, 2015. A unified model for the molecular basis of Xeroderma pigmentosum -Cockayne Syndrome. *Rare Diseases* **3**: e1079362.

Murphy MP, 2009. How mitochondria produce reactive oxygen species. *Biochemical Journal* **417**: 1–13.

Myung K, Datta a, Chen C, Kolodner RD, 2001. SGS1, the Saccharomyces cerevisiae homologue of BLM and WRN, suppresses genome instability and homeologous recombination. *Nature genetics* **27**: 113–116.

Natter K, Kohlwein SD, 2013. Biochimica et Biophysica Acta Yeast and cancer cells – common principles in lipid metabolism. *BBA - Molecular and Cell Biology of Lipids* **1831**: 314–326.

Neumann M, Sampathu DM, Kwong LK, Truax AC, Micsenyi MC, Chou TT, Bruce J, Schuck T, Grossman M, Clark CM, McCluskey LF, Miller BL, Masliah E, Mackenzie IR, Feldman H, Feiden W, Kretzschmar HA, Trojanowski JQ, Lee VM-Y, 2006. Ubiquitinated TDP-43 in Frontotemporal Lobar Degeneration and Amyotrophic Lateral Sclerosis. *Science* **314**: 130–133.

Nitiss J, Wang JC, 1988. DNA topoisomerase-targeting antitumor drugs can be studied in yeast. *Proceedings of the National Academy of Sciences* **85**: 7501–7505.

Nixon RA, 2007. Autophagy, amyloidogenesis and Alzheimer disease. *Journal of Cell Science* **120**: 4081–4091.

Novak MJU, Tabrizi SJ, 2010. Huntington's disease. *BMJ (Clinical research ed.)* **340**: c3109.

Oliveira A V., Vilaça R, Santos CN, Costa V, Menezes R, 2017. Exploring the power of yeast to model aging and age-related neurodegenerative disorders. *Biogerontology* **18**: 3–34.

Outeiro TF, 2003. Yeast Cells Provide Insight into Alpha-Synuclein Biology and Pathobiology. *Science* **302**: 1772–1775.

Pereira C, Costa V, Martins LM, Saraiva L, 2015a. A yeast model of the Parkinson's disease-associated protein Parkin. *Experimental Cell Research* **333**: 73–79.

Pereira C, Costa V, Martins LM, Saraiva L, 2015b. A yeast model of the Parkinson's disease-associated protein Parkin. *Experimental cell research* **333**: 73–9.

Perez RP, Mehboobali N, Iqbal MP, Thatcher N, Crowther D, Fox B, 1998. Cellular and molecular determinants of cisplatin resistance. *European Journal of Cancer* **34**: 1535–1542.

Perkins E, Sun D, Nguyen A, Tulac S, Francesco M, Tavana H, Nguyen H, Tugendreich S, Barthmaier P, Couto J, Yeh E, Thode S, Jarnagin K, Jain A, Morgans D, Melese T, 2001. Novel Inhibitors of Poly (ADP-ribose) Polymerase / PARP1 and PARP2 Identified Using a Cell-based Screen in Yeast Novel Inhibitors of Poly (ADP-ribose) Polymerase / PARP1 and PARP2 Identified Using a Cell-based Screen in Yeast. *Cancer Research* **10**: 4175–4183.

Petrov D, Daura X, Zagrovic B, 2016. Effect of Oxidative Damage on the Stability and Dimerization of Superoxide Dismutase 1. *Biophysical Journal* **110**: 1499–1509.

Porzoor A, Alford B, Hügel H, Grando D, Caine J, Macreadie I, 2015. Anti-Amyloidogenic Properties of Some Phenolic Compounds. *Biomolecules* **5**: 505–527.

Ramos-Pérez C, Lorenzo-Castrillejo I, Quevedo O, García-Luis J, Matos-Perdomo E, Medina-Coello C, Estévez-Braun A, MacHín F, 2014. Yeast cytotoxic sensitivity to the antitumour agent ??-lapachone depends mainly on oxidative stress and is largely independent of microtubule- or topoisomerase-mediated DNA damage. *Biochemical Pharmacology* **92**: 206–219.

Rasmussen AK, Chatterjee A, Rasmussen LJ, Singh KK, 2003. Mitochondria-mediated nuclear mutator phenotype in Saccharomyces cerevisiae. *Nucleic Acids Research* **31**: 3909–3917.

Reczek CR, Chandel NS, 2015. ROS-dependent signal transduction. *Current Opinion in Cell Biology* **33**: 8–13.

Reid RJD, Benedetti P, Bjornsti M-A, 1998. Yeast as a model organism for studying the actions of DNA topoisomerase-targeted drugs. *Biochimica et Biophysica Acta (BBA) - Gene Structure and Expression* **1400**: 289–300.

Rodriguez RM, Fraga MF, 2010. Aging and cancer: are sirtuins the link? *Future oncology (London, England)* **6**: 905–15.

Ronald A Butow NGA, 2004. Mitochondrial Signalling: The Retrograde Response. *Molecular cell* **14**: 1–15.

Rosen DR, Siddique T, Patterson D, Figlewicz DA, Sapp P, Hentati A, Donaldson D, Goto J, O'Regan JP, Deng H-X, Rahmani Z, Krizus A, McKenna-Yasek D, Cayabyab A, Gaston SM, Berger R, Tanzi RE, Halperin JJ, Herzfeldt B, den Bergh R Van, Hung W-Y, Bird T, Deng G, Mulder DW, Smyth C, Laing NG, Soriano E, Pericak–Vance MA, Haines J, Rouleau GA, Gusella JS, Horvitz HR, Brown RH, 1993. Mutations in Cu/Zn superoxide dismutase gene are associated with familial amyotrophic lateral sclerosis. *Nature* **362**: 59–62.

Ross CA, Poirier MA, 2004. Protein aggregation and neurodegenerative disease. *Nature Medicine* **10**: S10–S17.

Rossignol R, Karbowski M, Arismendi-Morillo G, 2009. Electron microscopy morphology of the mitochondrial network in human cancer. *The International Journal of Biochemistry & Cell Biology* **41**: 2062–2068.

Rostovtseva TK, Gurnev PA, Protchenko O, Hoogerheide DP, Yap TL, Philpott CC, Lee JC, Bezrukov SM, 2015. α-Synuclein Shows High Affinity Interaction with Voltage-dependent Anion Channel, Suggesting Mechanisms of Mitochondrial Regulation

and Toxicity in Parkinson Disease. *The Journal of biological chemistry* **290**: 18467–77.

Sabharwal SS, Schumacker PT, 2014. Mitochondrial ROS in cancer : *Nature Publishing Group* **14**: 709–721.

Saez I, Vilchez D, 2014. The Mechanistic Links Between Proteasome Activity, Aging and Age-related Diseases. *Current genomics* **15**: 38–51.

Saleh AA, Gune US, Chaudhary RK, Turakhiya AP, Roy I, 2014. Roles of Hsp104 and trehalose in solubilisation of mutant huntingtin in heat shocked Saccharomyces cerevisiae cells. *Biochimica et Biophysica Acta - Molecular Cell Research* **1843**: 746–757.

Sangmalee S, Laorpaksa A, Sukrong S, 2012. A topoisomerase II poison screen of ethnomedicinal Thai plants using a yeast cell-based assay. *Journal of Ethnopharmacology* **142**: 432–437.

Sawyers C, 2004. Targeted cancer therapy. *Nature* **432**: 294–297.

Schenk PW, Brok M, Boersma AWM, Brandsma J a, Den Dulk H, Burger H, Stoter G, Brouwer J, Nooter K, 2003. Anticancer drug resistance induced by disruption of the Saccharomyces cerevisiae NPR2 gene: a novel component involved in cisplatin- and doxorubicin-provoked cell kill. *Molecular pharmacology* **64**: 259–268.

Schieber M, Chandel NS, 2014. ROS Function in Redox Signaling and Oxidative Stress. *Current Biology* **24**: R453–R462.

Schmidt KH, Wu J, Kolodner RD, 2006. Control of Translocations between Highly Diverged Genes by Sgs1, the Saccharomyces cerevisiae Homolog of the Bloom's Syndrome Protein. *Molecular and Cellular Biology* **26**: 5406–5420.

Sekito T, 2002. RTG-dependent Mitochondria-to-Nucleus Signaling Is Regulated by MKS1 and Is Linked to Formation of Yeast Prion [URE3]. *Molecular Biology of the Cell* **13**: 795–804.

Seyfried TN, 2015. Cancer as a mitochondrial metabolic disease. *Frontiers in Cell and Developmental Biology* **3**: 1–12.

Shama S, Kirchman PA, Jiang JC, Jazwinski SM, 1998. Role of RAS2 in recovery from chronic stress: effect on yeast life span. *Exp Cell Res* **245**: 368–378.

Sharma N, Brandis KA, Herrera SK, Johnson BE, Vaidya T, Shrestha R, Debburman SK, 2006. alpha-Synuclein budding yeast model: toxicity enhanced by impaired proteasome and oxidative stress. *Journal of molecular neuroscience : MN* **28**: 161–78.

Sheu SS, Nauduri D, Anders MW, 2006. Targeting antioxidants to mitochondria: A new therapeutic direction. *Biochimica et Biophysica Acta - Molecular Basis of Disease* **1762**: 256–265.

Shiba-Fukushima K, Ishikawa KI, Inoshita T, Izawa N, Takanashi M, Sato S, Onodera O, Akamatsu W, Okano H, Imai Y, Hattori N, 2017. Evidence that phosphorylated ubiquitin signaling is involved in the etiology of Parkinson's disease. *Human Molecular Genetics* **26**: 3172–3185.

Shrestha A, Megeney L a, 2015. Yeast proteinopathy models : a robust tool for deciphering the basis of neurodegeneration. *Microbial Cell* **2**: 1–8.

Singh KK, 2004. Mitochondria damage checkpoint in apoptosis and genome stability. *Fems Yeast Research* **5**: 127–132.

Singh K, Kulawiec M, Ayyasamy V, 2009. p53 regulates mtDNA copy number and mitocheckpoint pathway. *Journal of Carcinogenesis* **8**: 8.

Singh V, Kumar G, Mandal P, Reddy MA, Tomar RS, 2014. Anti-cancer drug KP1019 modulates epigenetics and induces DNA damage response in Saccharomyces cerevisiae. *FEBS Letters* **588**: 1044–1052.

Šmardová J, Šmarda J, Koptíková J, 2005. Functional analysis of p53 tumor suppressor in yeast. *Differentiation* **73**: 261–277.

Smith MG, Snyder M, 2006. Yeast as a Model for Human Disease. In: *Current Protocols in Human Genetics*. pp. 1230–1237.

Spillantini MG, Schmidt ML, Lee VM-Y, Trojanowski JQ, Jakes R, Goedert M, 1997. Alpha-synuclein in Lewy bodies. *Nature* **388**: 839–840.

Spring DR, 2005. Chemical genetics to chemical genomics: small molecules offer big insights. *Chemical Society Reviews* **34**: 472.

Srinivasan V, Kriete A, Sacan A, Michal Jazwinski S, 2010. Comparing the yeast retrograde response and NF-κB stress responses: Implications for aging. *Aging Cell* **9**: 933–941.

Subhi AL, Diegelman P, Porter CW, Tang B, Lu ZJ, Markham GD, Kruger WD, 2003. Methylthioadenosine Phosphorylase Regulates Ornithine Decarboxylase by Production of Downstream Metabolites. *Journal of Biological Chemistry* **278**: 49868–49873.

Tamanoi F, 2011. Ras signaling in yeast. *Genes & cancer* **2**: 210–5.

Tauber E, Miller-Fleming L, Mason RP, Kwan W, Clapp J, Butler NJ, Outeiro TF, Muchowski PJ, Giorgini F, 2011. Functional gene expression profiling in yeast implicates translational dysfunction in mutant huntingtin toxicity. *Journal of Biological Chemistry* **286**: 410–419.

Tenreiro S, Munder MC, Alberti S, Outeiro TF, 2013. Harnessing the power of yeast to unravel the molecular basis of neurodegeneration. *Journal of Neurochemistry* **127**: 438–452.

Tenreiro S, Outeiro TF, 2010. Simple is good: Yeast models of neurodegeneration. *FEMS Yeast Research* **10**: 970–979.

Tosato V, Grüning N-M, Breitenbach M, Arnak R, Ralser M, Bruschi C V, 2012. Warburg effect and translocation-induced genomic instability: two yeast models for cancer cells. *Frontiers in oncology* **2**: 212.

Treusch S, Hamamichi S, Goodman JL, Matlack KES, Chung CY, Baru V, Shulman JM, Parrado a., Bevis BJ, Valastyan JS, Han H, Lindhagen-Persson M, Reiman EM, Evans D a., Bennett D a., Olofsson a., DeJager PL, Tanzi RE, Caldwell K a., Caldwell G a., Lindquist S, 2011. Functional Links Between A Toxicity, Endocytic Trafficking, and Alzheimer's Disease Risk Factors in Yeast. *Science* **334**: 1241–1245.

Tyedmers J, Mogk A, Bukau B, 2010. Cellular strategies for controlling protein aggregation. *Nature Reviews Molecular Cell Biology* **11**: 777–788.

Del Valle LG, 2011. Oxidative stress in aging: Theoretical outcomes and clinical evidences in humans. *Biomedicine and Aging Pathology* **1**: 1–7.

Van RH, Hamilton ML, Richardson A, 2003. Oxidative damage to DNA and aging. *Exerc.Sport Sci.Rev.* **31**: 149–153.

Vance C, Rogelj B, Hortobagyi T, De Vos KJ, Nishimura AL, Sreedharan J, Hu X, Smith B, Ruddy D, Wright P, Ganesalingam J, Williams KL, Tripathi V, Al-Saraj S, Al-Chalabi A, Leigh PN, Blair IP, Nicholson G, de Belleroche J, Gallo J-M, Miller CC, Shaw CE, 2009. Mutations in FUS, an RNA Processing Protein, Cause Familial Amyotrophic Lateral Sclerosis Type 6. *Science* **323**: 1208–1211.

Vandebroek T, Vanhelmont T, Terwel D, Borghgraef P, Lemaire K, Snauwaert J, Wera S, Van Leuven F, Winderickx J, 2005. Identification and isolation of a hyperphosphorylated, conformationally changed intermediate of human protein tau expressed in yeast. *Biochemistry* **44**: 11466–11475.

Vanhelmont T, Vandebroek T, De Vos A, Terwel D, Lemaire K, Anandhakumar J, Franssens V, Swinnen E, Van Leuven F, Winderickx J, 2010. Serine-409

phosphorylation and oxidative damage define aggregation of human protein tau in yeast. *FEMS Yeast Research* **10**: 992–1005.

Vila M, Ramonet D, Perier C, 2008. Mitochondrial alterations in Parkinson's disease: new clues. *Journal of Neurochemistry* **107**: 317–328.

Viña J, Borras C, Abdelaziz KM, Garcia-Valles R, Gomez-Cabrera MC, 2013. The Free Radical Theory of Aging Revisited: The Cell Signaling Disruption Theory of Aging. *Antioxidants & Redox Signaling* **19**: 779–787.

Wagner BA, Venkataraman S, Buettner GR, 2011. The rate of oxygen utilization by cells. *Free Radical Biology and Medicine* **51**: 700–712.

Wang Y, Beerman TA, Kowalski D, 2001. Antitumor drug adozelesin differentially affects active and silent origins of DNA replication in yeast checkpoint kinase mutants. *Cancer Research* **61**: 3787–3794.

Wei M, Fabrizio P, Madia F, Hu J, Ge H, Li LM, Longo VD, 2009. Tor1/Sch9-Regulated Carbon Source Substitution Is as Effective as Calorie Restriction in Life Span Extension (SK Kim, Ed,). *PLoS Genetics* **5**: e1000467.

Weisman LS, 2003. Yeast Vacuole Inheritance and Dynamics. *Annual Review of Genetics* **37**: 435–460.

Wiedemann LM, Morgan GJ, 1992. How are cancer associated genes activated or inactivated? *European Journal of Cancer* **28**: 248–251.

Willingham S, 2003. Yeast Genes That Enhance the Toxicity of a Mutant Huntingtin Fragment or -Synuclein. *Science* **302**: 1769–1772.

Wolffe AP, 2001. Chromatin remodeling: why it is important in cancer. *Oncogene* **20**: 2988–2990.

Yoo J-W, Irvine DJ, Discher DE, Mitragotri S, 2011. Bio-inspired, bioengineered and biomimetic drug delivery carriers. *Nature Reviews Drug Discovery* **10**: 521–535.

Yoshimura A, Seki M, Enomoto T, 2017. The role of WRNIP1 in genome maintenance. *Cell Cycle* **16**: 515–521.

Zabrocki P, Pellens K, Vanhelmont T, Vandebroek T, Griffioen G, Wera S, Van Leuven F, Winderickx J, 2005. Characterization of alpha-synuclein aggregation and synergistic toxicity with protein tau in yeast. *FEBS Journal* **272**: 1386–1400.

Zondler L, Miller-Fleming L, Repici M, Gonçalves S, Tenreiro S, Rosado-Ramos R, Betzer C, Straatman KR, Jensen PH, Giorgini F, Outeiro TF, 2014. DJ-1

interactions with α-synuclein attenuate aggregation and cellular toxicity in models of Parkinson's disease. *Cell Death and Disease* **5**: e1350.

Figure legends

Fig 1 – (A) ROS production, as a result of normal metabolism, and antioxidant enzymes that counteract and regulate overall ROS levels to maintain physiological homeostasis. (B) Reduced ROS levels, which can be achieved by a low ROS production (for example, during fermentative metabolism), are detrimental due to impaired physiological process, such as the induction of antioxidant defense system. As a consequence, cells are more sensitive to increased levels of oxidants, accelerating aging and increasing the chances of diseases. On the other hand, increased ROS levels (oxidative stress) are also deleterious. An oxidative stress occurs when the production of ROS overcome the antioxidant defense, which can be achieved by an increase in ROS production, a decrease in the antioxidant activity, or both.

Table 1. Nobel prizes for yeast! Nobel Prizes awarded for Physiology or Medicine and Chemistry which used *S. cerevisiae* as eukaryotic cell model.

Year	Nobel prize in	Laureates	Rationale
1907	Chemistry	E. Buchner	“for his biochemical researches and his discovery of cell-free fermentation".
1929	Chemistry	A. Harden & H. von Euler-Chelpin	"for their investigations on the fermentation of sugar and fermentative enzymes"
1968	Physiology or Medicine	R. Holley, H. Khorana & M. Nirenberg	"for their interpretation of the genetic code and its function in protein synthesis". The first primary structural determination of a tRNA, that of yeast alanine tRNA by R. Holley’s group at Cornell University
1999	Physiology or Medicine	G. Blobel	"for the discovery that proteins have intrinsic signals that govern their transport and localization in the cell".
2001	Physiology or Medicine	L. Hartwell, P. Nurse & T.Hunt	Hartwell discovered genes that control the cell cycle in *S. cerevisiae*
2004	Chemistry	A. Ciechanover, A. Hershko & I. Rose	Ciechanover used yeast to elucidate the ubiquitin-mediated protein degradation
2006	Chemistry	R. Kornberg	"for his studies of the molecular basis of eukaryotic transcription".
2009	Physiology or Medicine	E. Blackburn, C. Greider & J. Szostak	Szostak studied the role of telomere elongation in yeast senescence
2013	Physiology or Medicine	J. Rothman, R. Schekman & T. Südhof	Schekman used yeast to study the mechanisms of vesicle traffic
2016	Physiology or Medicine	Y. Ohsumi	"for his discoveries of mechanisms for autophagy".

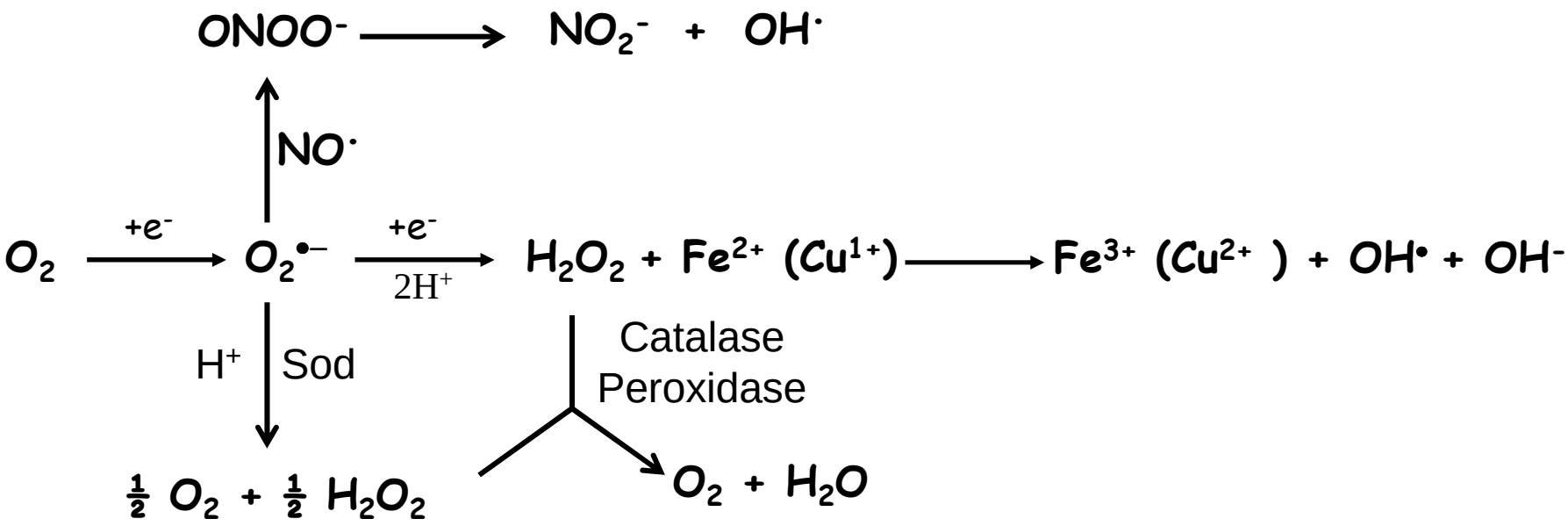

ROS production

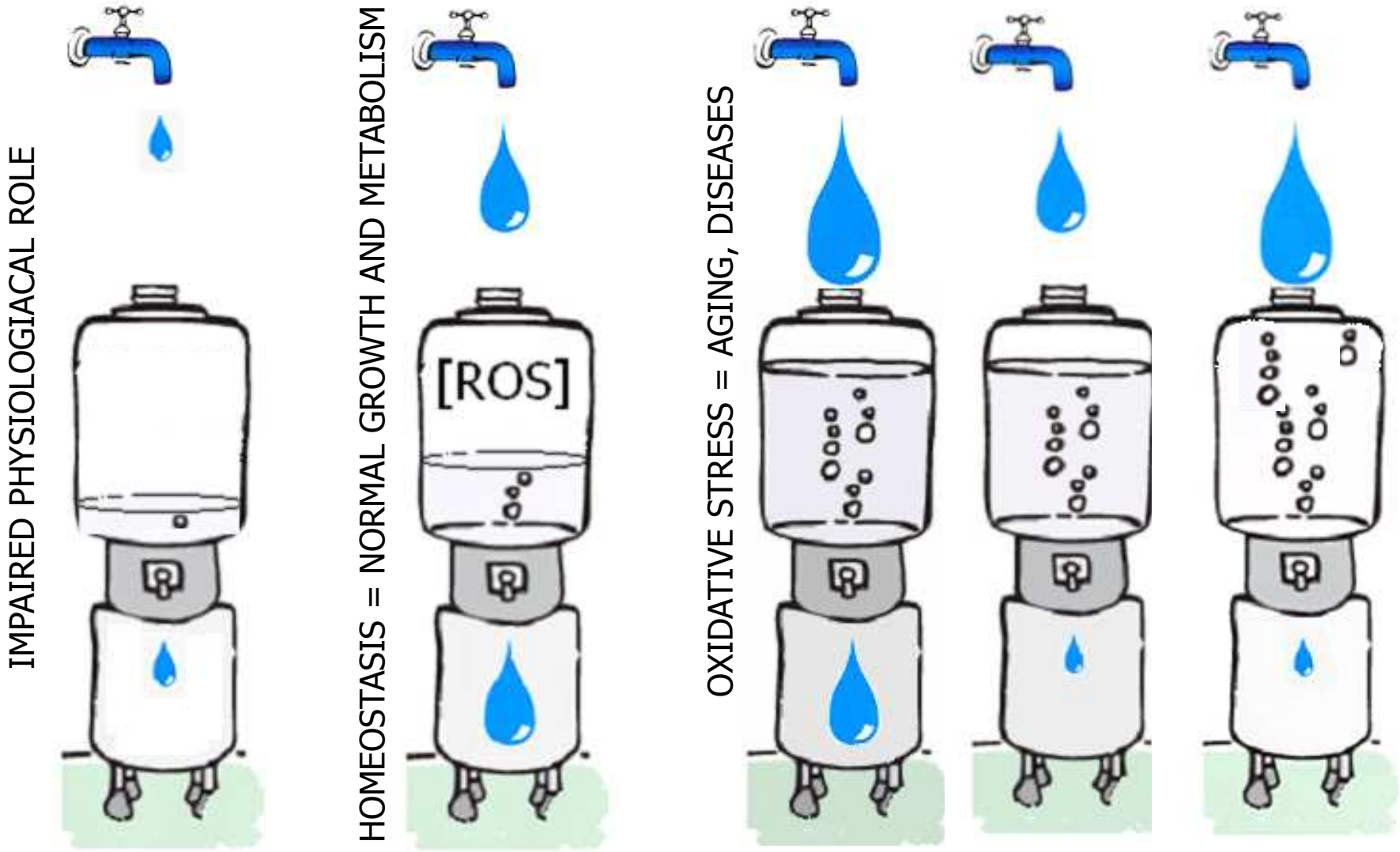

Antioxidant Defenses (ROS destruction)

Advances in
Biotechnology & Microbiology
ISSN 2474-7637

Juniper Publishers
key to the Researchers

Mini Review
Volume 8 Issue 4 - March 2018
DOI: 10.19080/AIBM.2018.08.555745

Adv Biotech & Micro

Trehalose: As Sweet as Effective in Biomedical Research and Biotechnology

Elis Cristina Araujo Eleutherio*, Aline Araújo Brasil, Germana Breves Rona and Rayne Stfhany Silva Magalhães

Institute of Chemistry, Federal University of Rio de Janeiro, Brazil

Submission: January 27, 2018**; Published:** March 20, 2018

***Corresponding author:** Elis Eleutherio, Departamento de Bioquímica - Universidade Federal do Rio de Janeiro. Av. Athos da Silveira Ramos, nº149, Bloco A-sala 547 CEP: 21941909 Centro de Tecnologia, Cidade Universitária, Rio de Janeiro-RJ, Brazil, Tel: +552139387260, Email: eliscael@iq.ufrj.br

Abstract

Since the trehalose discovery, this disaccharide has been reported to accumulate in anhydrobiotic organisms which are able to survive completely dry and dormant until living conditions improve. Trehalose has been widely studied to understand its function and abundance in nature due to its unique features, including the ability to sustain and preserve a wide array of biological molecules. In face of these physical and chemical properties, this sugar has been used in a variety of food, medical and cosmetic products as well as in many biomedical researches. Currently, there is a growing interest in the use of trehalose as a relevant therapeutic agent in neurodegenerative disorders such as Alzheimer's, Huntington's and Parkinson's diseases as well as in the modification of trehalose molecule into novel inhibitors of cancer cell migration and invasion. These current applications have proven possible because of the trehalose ability to enhance autophagic activity, respond against a variety of environmental stressors and stabilize protein folding mechanisms. This brief review highlights the promising biotechnological and biomedical applications of trehalose.

Keywords: Trehalose; Microorganisms; Biotechnology

Abbreviations: T6P: Trehalose-6-Phosphate; Tps1: Trehalose synthase; Ath1: Acid trehalase; HD: Huntington's disease; PD: Parkinson's disease; AD: Alzheimer´s Disease; ROS: Reactive Oxygen Species; PoliQ: Polyglutamine; LBD: Lewy body disease; APP: Amyloid Precursor Protein; ER: Endoplasmatic Reticulum; OTSA: Trehalose-6-phosphate synthase

Introduction

Trehalose is a non reducing disaccharide composed of two residues of glucose joined through 1,1-α,α-glycosidic linkage [1,2]. This sugar is found in bacteria, fungi, plants, insects, and invertebrates, but not in vertebrates [3,4]. Humans have the ability to hydrolyze but not to synthesize treahlose. The main functions of trehalose are to confer protection against stress and to serve as fuel reserve [5]. The first recorded information of trehalose was in cocoons of Larinus beetles in 1681, and in 1953, Leloir and Cabib elucidated for the first time the complete metabolic pathway of trehalose. Trehalose can be biosynthesized by five pathways. It can be produced by the trehalose-phosphate synthase/trehalose phosphatase pathway in yeast, bacteria, archaea, insects, and plants.

Archaea, like *Hyperthermophilic archeae, Pyrococcus horikoshii, Thermococcus litoralis, Thermoproteus tenax* can also convert glucose and UDP-glucose into trehalose using trehalose-synthesizing glycosyltransferase [6]. Through the TreY/TreZ pathway Sulfolobus and Mycobacterium can convert malto oligosaccharides into trehalose [2]. Malto oligosaccharides and maltose can also be converted to trehalose by the trehalose synthase pathway in some bacteria [7]. The fifth biosynthetic pathway converts glucose and glucose-1-phosphate in trehalose using trehalose phosphorylase in bacteria, yeast and fungi, for example *Bacillus stearothermophilus*, T*hermoanaerobacter brockii* and *Copelatus subterraneus* [6]. In face of the interesting properties of trehalose, its role and metabolism have been investigated since a long time. However, there are still questions to be answered. Recently, Arthrobacter was used as a model to analyze development switches caused by the environment. This is possible because of its resistance to stress, probably related to their pleomorphic behavior. Trehalose-6-phosphate synthase (otsA) of Arthrobacter is probably involved in cellular morphology, representing an adaptation of bacteria that survive in extreme environments [8].

The protective effect of trehalose on *Rhodobacter sphaeroides* has also been presented. It was shown that a trehalose matrix

is able to protect the centers reactions of photosynthetic protein complexes against dehydration, leading to a greater maintenance of its photochemical activity [9]. *Saccharomyces cerevisiae*, *Candida albicans*, and *Candida Tropicalis* were used as experimental models to show the ability of Trehalose-6-Phosphate (T6P) to inhibit trehalose synthase (Tps1) activity. In this way, T6P reduced the trehalose synthesis that is directly related to the virulence of some pathogens [10]. The protective effect of trehalose on *Aureobasidium subglaciale*, a fungus collected on soil contaminated with radiation and heavy metals, has already been demonstrated. In this study, a strain with three fold higher trehalose production, due to overexpression of Tps1 and the deletion of acid trehalase (Ath1), showed greater resistance against heavy-metal and radiation than the control strain. This data leads to the conclusion that there is a relationship between trehalose accumulation and the oxidative stress response in *Aureobasidium subglaciale* [11]. Subheading: Biotechnology Applications of Trehalose More than a decade after the liberation of the use of trehalose in humans by the United States and the European Union, which classified trehalose as safe, the studies about this sugar are increasingly focused on its beneficial properties for humans [12]. Those properties are mainly related to the trehalose structure, specifically on the interaction between the two molecules of glucose and its function as a kosmotrope [13]. These properties are important for the protective roles against stress, as oxidative stress, heating and starving. Furthermore, trehalose is synthetized in a wide range of organism, other than humans, which lack TPS enzyme, necessary for trehalose production [5]. Since trehalose is able to stabilize the structure of biomolecules (proteins, enzymes, DNA) and macrostructures (lipid bilayer) and to avoid protein aggregation during denaturating conditions, it has been intensively investigated for application in the treatment of infectious diseases, caused by pathogens whose virulence depend on trehalose synthesis, neurodegenerative diseases and cancer [10,14]. On the other hand, some groups are developing methodologies to introduce trehalose in different areas, as cosmetics (development of bath oils, moisturizers, due to its role as protection against dehydration); pharmaceutical applications (as component in medicines to treat high blood pressure, due to its role to protects against osmotic stress) [14]. Trehalose can be found in some methods to produce and preserve dried vegetables and fruits, in the production of Swiss cheeses and as sweetener [15,16]. One of the problems faced during therapeutic treatment, which use drugs that need to be delivered inside the organism, is how to introduce this component without side effects to the organism and with high rates of absorption. An alternative for oral delivery and parenteral methods is the use of biodegradable microneedles. Some studies are focused in the use of trehalose during the creation of these needles due to its capacity of interaction with the biomolecules, producing a sugar glass layer, and then, protecting the structure against composition alterations during its development before their use in humans [17].

Due to its cryoprotective and preservative role, trehalose can be found in solutions of organs transplantation, development of vaccines, antibodies, and during skin treatment with anti-inflammatory drugs, where trehalose is used to reduce the side effects, as cutaneous irritation [15,18].

Trehalose as a therapeutic candidate ready to enter clinical trials

Trehalose also displays a number of remarkable qualities including the ability to protect the integrity of cells against desiccation, heat, cold and oxidation(5). Moreover, trehalose may act as a chemical chaperone, preserving protein structure stability, protein folding as well as reducing aggregation of pathologically misfolded proteins [19,20]. Oxidative stress, aggregation and proteasomal dysfunction have been considered key mechanisms associated with neurodegenerative disorders, including Huntington's disease (HD) [21], Parkinson's disease (PD) [22] and Alzheimer´s disease (AD) [23,24]. It was recently reported the treatment with trehalose was able to counteract the increase in reactive oxygen species (ROS), ubiquitinated proteins, huntingtin and activated caspase-3 levels induced by the inhibitor of proteasome activity epoxomicin. The authors also pointed out the valuable effects of this disaccharide in proteinopathies, as an autophagy enhancer, chemical chaperone, antioxidant and an interesting therapeutic candidate for testing in HD patients [21].

By using *in vitro* and *in vivo* models of HD, other studies have shown the trehalose was able to inhibit polyglutamine (poliQ) mediated aggregation [25,26]. Recent studies demonstrate that trehalose protects dopaminergic neurons in the striato-nigral pathway from the pathological symptoms induced by MPTP (eg. vessel regression and ischemia) in mouse models of Parkinson´s disease [27]. Other study currently highlighted the ability of the autophagy enhancer, trehalose to protect against A53T α-synuclein mediated dopamine degeneration in a rat model of PD [28]. Trehalose intake has increased levels of chaperone molecules, such as Hsp 90 and SigmaR1 along with autophagy in brains of model mice of Lewy body disease (LBD). It has also been reported in this study that oral administration of trehalose suppressed the levels of detergent-insoluble α-synuclein in mice [29]. As such, in Alzheimer´s disease, trehalose promotes the cellular clearance of the phosphorylated pathogenic tau protein [30-32]. In addition, cell treatment with trehalose was capable to alter vesicular trafficking, thereby decreasing the degradation of Alzheimer-associated Amyloid Precursor Protein (APP) in endolysosomal compartments and the secretion of amyloid-β peptide [33]. The role of trehalose in reducing Aβ peptide aggregation is still unclear, however a very recent study concluded that trehalose affects the conformation of Aβ peptide to form α-helical structure, which may prevent the formation of β-sheets and thereby aggregation [34].

The autophagic effects of trehalose together with its anti-apoptotic property on tumor cells and lack of toxicity on

How to cite this article: Elis Cristina Araujo Eleutherio, Aline Araújo Brasil, Germana Breves Rona, Rayne Stfhany Silva Magalhães. Trehalose: As Sweet as Effective in Biomedical Research and Biotechnology. Adv Biotech & Micro. 2018; 8(4): 555745. DOI: 10.19080/AIBM.2018.08.555745.

normal cells has been recently used as a Potential neoadjuvant for antitumor drugs for treating several cancers [35]. Other medically property of trehalose include the suppression of the osteoarthritis (OA) [36], herpesviruses [37] and age-associated liver injuries [38] mainly through the elimination of oxidative stress, reduction of endoplasmatic reticulum (ER) stress and autophagic flux restoration [36].

Conclusion

Since trehalose's discovery, this disaccharide has been widely studied due to its interesting and unique properties. It was formerly focused on the better understanding of the pathways of synthesis and its role in the microorganisms that synthesized it. In the last decade, research involving trehalose has increased focusing on its application in the food, pharmaceutical, and cosmetics industry. Based on the results obtained so far using different models, and the advance of new research techniques, more studies are on the way to find more applications of this interesting and versatile sugar.

Acknowledgement

This review was supported by grants from FAPERJ, CAPES and CNPq.

References

1. Thammahong A, Puttikamonkul S, Perfect JR, Brennan RG, Cramer RA (2017) Central role of the trehalose biosynthesis pathway in the pathogenesis of human fungal infections: opportunities and challenges for therapeutic development. Microbiol Mol Biol Rev 81(2): e00053-e000116.
2. O Neill MK, Piligian BF, Olson CD, Woodruff PJ, Swarts BM (2017) Tailoring trehalose for biomedical and biotechnological applications. Pure Appl Chem 89(9): 1223-1249.
3. Singer MA, Lindquist S (1998) Thermotolerance in *Saccharomyces cerevisiae*: the Yin and Yang of trehalose. Trends Biotechnol 16(11): 460-468.
4. Benaroudj N, Lee DH, Goldberg AL (2001) Trehalose accumulation during cellular stress protects cells and cellular proteins from damage by oxygen radicals. J Biol Chem 276: 24261-24267.
5. Eleutherio E, Panek A, De Mesquita JF, Trevisol E, Magalhães R (2015) Revisiting yeast trehalose metabolism. Curr Genet 61(3): 263-274.
6. Walmagh M, Zhao R, Desmet T (2015) Trehalose analogues: latest insights in properties and biocatalytic production. Int J Mol Sci 16: 13729-13745.
7. Nishimoto T, Nakano M, Nakada T, Chaen H, Fukuda S, et al. (1996) Purification and properties of a novel enzyme, trehalose synthase, from Pimelobacter sp. R48. Biosci Biotechnol Biochem 60(4): 640-644.
8. Chen X, An L, Fan X, Ju F, Zhang B, et al. (2017) A trehalose biosynthetic enzyme doubles as an osmotic stress sensor to regulate bacterial morphogenesis. PLoS Genet 13: e1007062.
9. Knox PP, Lukashev EP, Seifullina NK, Gorokhov VV, Rubin AB (2017) Influence of trehalose on high-temperature stability of the photosynthetic reaction centers. Dokl Biochem Biophys 477(1): 368-371.
10. Magalhães RSS, De Lima KC, De Almeida DSG, De Mesquita JF, Eleutherio ECA (2017) Trehalose-6-Phosphate as a potential lead candidate for the development of tps1 inhibitors: insights from the trehalose biosynthesis pathway in diverse yeast species. Appl Biochem Biotechnol 181(3): 914-924.
11. Liu T, Zhu L, Zhang Z, Huang H, Zhang Z, et al. (2017) Protective role of trehalose during radiation and heavy metal stress in *Aureobasidium subglaciale* F134. Sci Rep 7(1): 17586.
12. Yang S, Lv X, Wang X, Wang J, Wang R, et al. (2017) Cell-surface displayed expression of trehalose synthase from pseudomonas putida atcc 47054 in pichia pastoris using pir1p as an anchor protein. Front Microbiol 8: 2583.
13. Cray JA, Russell JT, Timson DJ, Singhal RS, Hallsworth JE (2013) A universal measure of chaotropicity and kosmotropicity. Environ Microbiol 15(1): 287-296.
14. Jain NK, Roy I (2009) Effect of trehalose on protein structure. Protein Sci 18(1): 24-36.
15. Pawlicka kaczorowska J, Czaczyk K (2017) Effect of crude and pure glycerol on biomass production and trehalose accumulation by Propionibacterium freudenreichii ssp. Acta Biochim Pol 64(4): 621-629.
16. Yan X, Zhu L, Yu Y, Xu Q, Huang H, et al. (2018) In situ biocatalytic production of trehalose with auto-induction expression of trehalose synthase. J Agric Food Chem 66(6): 1444-1451.
17. Martin CJ, Allender CJ, Brain KR, Morrissey A, Birchall JC (2012) Low temperature fabrication of biodegradable sugar glass microneedles for transdermal drug delivery applications. J Control Release 158(1): 93-101.
18. Kayasuga Kariya Y, Iwanaga S, Fujisawa A, Lin LS, Suzuki S (2013) Dermal cell damage induced by topical application of non-steroidal anti-inflammatory drugs is suppressed by trehalose co-lyophilization in Ex Vivo analysis. J Vet Med Sci 75(12): 1619-1622.
19. Upagupta C, Carlisle RE, Dickhout JG (2017) Analysis of the potency of various low molecular weight chemical chaperones to prevent protein aggregation. Biochem Biophys Res Commun 486(1): 163-170.
20. Portbury SD, Hare DJ, Finkelstein DI, Adlard PA (2017) Trehalose improves traumatic brain injury-induced cognitive impairment. PLoS One 12(8): e0183683.
21. Fernandez-Estevez MA, Casarejos MJ, Sendon JL, Caldentey JG, Ruiz C, et al. (2014) Trehalose reverses cell malfunction in fibroblasts from normal and huntington's disease patients caused by proteosome inhibition. PLoS One 9(2): 1-9.
22. Liu Z, Zhou T, Ziegler AC, Dimitrion P, Zuo L (2017) Oxidative stress in neurodegenerative diseases: from molecular mechanisms to clinical applications. Oxid Med Cell Longev 2017: 2525967.
23. Hartl FU (2017) Protein misfolding diseases. Annu Rev Biochem 86: 21-26.
24. Hartl FU, Bracher A, Hayer-Hartl M (2011) Molecular chaperones in protein folding and proteostasis. Nature 475(7356): 324-332.
25. Sarkar S, Davies JE, Huang Z, Tunnacliffe A, Rubinsztein DC (2007) Trehalose, a Novel mTOR-independent Autophagy Enhancer, Accelerates the Clearance of Mutant Huntingtin and α-Synuclein. J Biol Chem 282: 5641-5652.
26. Tanaka M, Machida Y, Niu S, Ikeda T, Jana NR, et al. (2004) Trehalose alleviates polyglutamine-mediated pathology in a mouse model of Huntington disease. Nat Med 10(2): 148-154.
27. Sarkar S, Chigurupati S, Raymick J, Mann D, Bowyer JF, et al. (2014) Neuroprotective effect of the chemical chaperone, trehalose in a chronic MPTP-induced Parkinson's disease mouse model. Neurotoxicology 44: 250-262.

How to cite this article: Elis Cristina Araujo Eleutherio, Aline Araújo Brasil, Germana Breves Rona, Rayne Stfhany Silva Magalhães. Trehalose: As Sweet as Effective in Biomedical Research and Biotechnology. Adv Biotech & Micro. 2018; 8(4): 555745. DOI: 10.19080/AIBM.2018.08.555745.

28. He Q, Koprich JB, Wang Y, Yu WB, Xiao BG, et al. (2016) Treatment with Trehalose prevents behavioral and neurochemical deficits produced in an aav α-synuclein rat model of parkinson's disease. Mol Neurobiol 53(4): 2258-2268.

29. Tanji K, Miki Y, Maruyama A, Mimura J, Matsumiya T, et al. (2015) Trehalose intake induces chaperone molecules along with autophagy in a mouse model of Lewy body disease. Biochem Biophys Res Commun 465(4): 746-752.

30. Casarejos MJ, Solano RM, Gómez A, Perucho J, de Yébenes JG, et al. (2011) The accumulation of neurotoxic proteins, induced by proteasome inhibition, is reverted by trehalose, an enhancer of autophagy, in human neuroblastoma cells. Neurochem Int 58(4): 512-520.

31. Krüger U, Wang Y, Kumar S, Mandelkow EM (2012) Autophagic degradation of tau in primary neurons and its enhancement by trehalose. Neurobiol Aging 33(10): 2291-2305.

32. Schaeffer V, Lavenir I, Ozcelik S, Tolnay M, Winkler DT, et al. (2012) Stimulation of autophagy reduces neurodegeneration in a mouse model of human tauopathy. Brain 135: 2169-2177.

33. Tien NT, Karaca I, Tamboli IY, Walter J (2016) Trehalose alters subcellular trafficking and the metabolism of the Alzheimer-associated amyloid precursor protein. J Biol Chem 291(20): 10528-10540.

34. Khan SH, Kumar R (2017) Trehalose induced conformational changes in the amyloid-β peptide. Pathol Res Pract 213(6): 643-648.

35. El Magd M, Khamis A, Nasr Eldeen SK, Ibrahim WM, Salama AF (2017) Trehalose enhances the antitumor potential of methotrexate against mice bearing Ehrlich ascites carcinoma. Biomed Pharmacother 92: 870-878.

36. Tang Q, Zheng G, Feng Z, Chen Y, Lou Y, et al. (2017) Trehalose ameliorates oxidative stress-mediated mitochondrial dysfunction and ER stress via selective autophagy stimulation and autophagic flux restoration in osteoarthritis development. Cell Death Dis 8(10): e3081.

37. Meier JL, Grose C (2017) Variable effects of autophagy induction by trehalose on herpesviruses depending on conditions of infection. Yale J Biol Med 90(1): 25-33.

38. Pagliassotti MJ, Estrada AL, Hudson WM, Wei Y, Wang D, et al. (2017) Trehalose supplementation reduces hepatic endoplasmic reticulum stress and inflammatory signaling in old mice. J Nutr Biochem 45: 15-23.

DOI: 10.19080/AIBM.2018.08.555745

How to cite this article: Elis Cristina Araujo Eleutherio, Aline Araújo Brasil, Germana Breves Rona, Rayne Stfhany Silva Magalhães. Trehalose: As Sweet as Effective in Biomedical Research and Biotechnology. Adv Biotech & Micro. 2018; 8(4): 555745. DOI: 10.19080/AIBM.2018.08.555745.

From: **Gary Stein** <onbehalfof@manuscriptcentral.com>
Date: Seg, 16 de jul de 2018 09:13
Subject: Journal of Cellular Biochemistry - Major Revision on Manuscript ID JCB-18-0872
To: <pinheiro@iq.ufrj.br>, <asapinheiro@gmail.com>

16-Jul-2018

Dear Dr Pinheiro:

Manuscript ID JCB-18-0872 entitled "¹H NMR metabolomics reveals increased glutaminolysis upon overexpression of NSD3s or Pdp3 in Saccharomyces cerevisiae" which you submitted to the Journal of Cellular Biochemistry, has been reviewed. The comments of the reviewer(s) are included at the bottom of this letter.

There is interest in your manuscript, however before the paper could be found acceptable, it will be necessary for you to undertake revisions in accordance with the comments of the reviewer(s). Please include a cover letter that indicates what changes have been made.

To revise your manuscript, log into https://mc.manuscriptcentral.com/jcb-wiley and enter your Author Center, where you will find your manuscript title listed under "Manuscripts with Decisions." Under "Actions," click on "Create a Revision." Your manuscript number has been appended to denote a revision.

You will be unable to make your revisions on the originally submitted version of the manuscript. Instead, revise your manuscript using a word processing program and save it on your computer. When submitting your revised manuscript, you must respond to the comments made by the reviewer(s) in the space provided. Please document any changes you make to the original manuscript. In order to expedite the processing of the revised manuscript, please be as specific as possible in your response to the reviewer(s).

Please review the attached document listing the file requirements for your revision.

Once the revised manuscript is prepared, you can upload it and submit it through your Author Center.

You should submit a revision within 180 days.

If you feel that your paper could benefit from English language polishing, you may wish to consider having your paper professionally edited for English language by a service such as Wiley's at http://wileyeditingservices.com. Please note that while this service will greatly improve the readability of your paper, it does not guarantee acceptance of your paper by the journal.

IMPORTANT: Your original files are available to you when you upload your

revised manuscript. Please delete any redundant files before completing the submission.

Because we are trying to facilitate timely publication of manuscripts submitted to the Journal of Cellular Biochemistry, your revised manuscript should be uploaded as soon as possible. If it is not possible for you to submit your revision in a reasonable amount of time, we may have to consider your paper as a new submission.

PLEASE NOTE!
Effective immediately, papers accepted for publication in JCB will now publish online as Accepted Articles within 5-7 days after acceptance and will be indexed by PubMed within 48 hours of release into the public domain. Papers will be published in final format in print and this version will replace the Accepted Article (unedited) version online. PLEASE NOTE THAT ACCEPTED ARTICLE PUBLICATION MAKES IT INCUMBENT UPON THE AUTHORS TO SUBMIT THEIR REVISIONS WITH LITTLE OR NO ALTERATIONS NECESSARY.

Once again, thank you for submitting your manuscript to the Journal of Cellular Biochemistry and I look forward to receiving your revision.

Sincerely,
Dr Gary Stein
Executive Editor, Journal of Cellular Biochemistry
jcb@med.uvm.edu

Reviewer: 1

Comments to the Author
The authors concluded that the overexpression of NSD3s or Pdp3 induces the acquisition of a tumoural metabolic phenotype in yeast. The paper is clear and well written. My comments are minor:
The potential translation of the new data on metabolome in conditions of overexpressed NSD3s in breast cancer and other cancers should be added.
Área de anexos